Fall 2014

U-Pb Geochronology of the Miocene Peach Spring Tuff Supereruption And Precursor Cook Canyon Tuff, Western Arizona, USA

Marsha Izabella Lidzbarski
San Jose State University

DOI: https://doi.org/10.31979/etd.c2xh-zwh9

U-PB GEOCHRONOLOGY OF THE MIOCENE PEACH SPRING TUFF SUPERERUPTION AND PRECURSOR COOK CANYON TUFF, WESTERN ARIZONA, USA

A Thesis

Presented to

The Faculty of the Department of Geology

San José State University

In Partial Fulfillment

of the Requirements for the Degree

Master of Science

by

Marsha I. Lidzbarski

December 2014

The Designated Thesis Committee Approves the Thesis Titled

U-PB GEOCHRONOLOGY OF THE MIOCENE PEACH SPRING TUFF SUPERERUPTION AND PRECURSOR COOK CANYON TUFF, WESTERN ARIZONA, USA

by

Marsha I. Lidzbarski

APPROVED FOR THE DEPARTMENT OF GEOLOGY

SAN JOSÉ STATE UNIVERSITY

December 2014

Dr. Jonathan Miller	Department of Geology
Dr. Robert Miller	Department of Geology
Dr. Jorge Vazquez	United States Geological Survey

ABSTRACT

U-PB GEOCHRONOLOGY OF THE MIOCENE PEACH SPRING TUFF SUPERERUPTION AND PRECURSOR COOK CANYON TUFF, WESTERN ARIZONA, USA

by Marsha I. Lidzbarski

The 18.8 Ma Peach Spring Tuff, Arizona, is a >600 km^3 ignimbrite formed from the Miocene supereruption of Silver Creek caldera, Black Mountains, Arizona, and is an important Miocene stratigraphic bed in the southwestern United States. Peach Spring Tuff overlies the undated and less-voluminous Cook Canyon Tuff. Ion-microprobe and high-precision thermal ionization U-Pb dating of chemically abraded zircon crystals from Peach Spring Tuff and Cook Canyon Tuff reveal the crystallization history of both magma systems leading to eruption. A spread of U-Pb dates from ca. 18.1 to 22.0 Ma for Peach Spring Tuff relative to its $^{40}Ar/^{39}Ar$ age indicates variable Pb loss, with potential additional uncertainty due to complexities associated with $^{40}Ar/^{39}Ar$ dating. The youngest U-Pb crystallization date for Cook Canyon Tuff zircon crystals constrains the maximum eruption age to ca. 18.9 Ma, and indicates that eruption of the Cook Canyon Tuff preceded the Peach Spring Tuff eruption by no more than 2-3 x 10^5 years. The complex U-Pb zircon age spectra for both units indicate several 10^5 years of pre-eruptive magma residence, likely in a crystal mush state. When combined, the ages and trace elements for Peach Spring Tuff and Cook Canyon Tuff zircon crystals suggest that these two silicic magmas were derived from discrete but temporally and spatially overlapping magma systems.

ACKNOWLEDGEMENTS

Support for this research came from National Science Foundation grants EAR-0911728 and EAR-0409882

At this moment of accomplishment, I would like to gratefully acknowledge my adviser Professor Jonathan Miller, whose brilliance and ambitious spirit in regard to research successfully guided me through this can of worms. I would like to thank my committee members, Professor Robert Miller for his constructive reviews, timely edits, and campfire dance lessons, and Dr. Jorge Vazquez for his endless encouragement and motivation. He was once my professor, now he is my colleague and he will forever be my mentor. I would also like to thank the faculty, staff, and students of the San José State Geology Department for making my graduate experience an unforgettable one.

Most of the results described in this thesis would not have been possible without the close collaboration of a few laboratories. I owe a deep debt of gratitude to Roland Mundil for his time and invaluable assistance at the Berkeley Geochronology Center. I would also like to thank Charlie Bacon, Joe Wooden and Matt Coble for their assistance at the Stanford USGS Micro Analysis Center, with whose wealth of knowledge and pep talks, I was able to retain my sanity. I am most grateful to the collaborators of this research project, specifically Calvin Miller, Susanne McDowell, Charles Ferguson and Sarah Overton for their unparalleled enthusiasm, sharing their data, listening to my crazy ideas, and lending me their expertise and inspiration.

I deeply thank my family, especially my mother Maria, my sister Megan, and my brother Mark for their unconditional support, encouragement and endless patience. I sincerely thank Dr. Yan Xin and my friends in Connecticut, who, along with my family, were there at the start of this journey, and helped mold me into the responsible, successful adult I am today.

I cannot forget friends who went through hard times, cheered me on, made sure I remembered to eat, and who have shared as much anticipation for this day as I have. Thank you Esther, Danielle, Raquel, and my Changos. I expand my thanks to Trials Pub for treating me like family while I'm so far from my own and allowing me to us your establishment as my living room and writing headquarters. I especially thank Syrus and Thane (my emergency contact), without whose hugs, back-cracking ability, thinking juice, and unfailing support I would not have completed this work.

TABLE OF CONTENTS

LIST OF FIGURES

LIST OF TABLES

INTRODUCTION

Supereruptions, which produce >450 km^3 of erupted magma, commonly involve explosive phenomena that can have a catastrophic impact on the regional or global environment (Rampino et al., 1988; Rampino and Self, 1992; Sparks et al., 2005; Self, 2006). Large ignimbrite eruptions, though geographically widespread, are rare compared to the small eruptions that construct volcanoes (Glazner et al., 2004). The paucity of such events limits our understanding of how long it takes to build up the magma systems that produce them. Thus, supereruptions play a central role in ongoing debates about the nature of crustal magmatism and the magmatic processes involved in leading to the build-up of large magma bodies that can produce supereruptions.

One of the central controversies involves residence time, which is generally defined as the duration of storage of silicic magma in the upper crust prior to eruption (e.g., Halliday et al., 1989; Sparks et al., 1990; Mahood, 1990; Reid et al., 1997; Heumann et al. 2002; Vazquez and Reid, 2002; Schmitt et al., 2003; Miller and Wooden, 2004; Memeti et al., 2010; Cooper and Kent, 2014). Work on some of the more recent supereruptions (Long Valley, Yellowstone, Taupo, the SW Nevada Volcanic Field) provides some insight into the timescales and processes involved; geochronological studies suggest that at least some of these systems are long-lived, on the order of 10^5 to $>10^6$ years (e.g. Halliday et al., 1989; Mahood, 1990; Vazquez and Reid, 2002; Hildreth, 2004; Charlier et al., 2005; Simon and Reid, 2005; Bindeman et al., 2006; Reid, 2008;

Deering et al., 2011), but is this the case for all supereruptions? Does this time frame represent the period over which eruptible magma is stored, or does it correspond to a more protracted evolution of waxing and waning magma storage, perhaps punctuated by rare eruptions when appreciable quantities of melt have accumulated?

Large, composite batholiths may represent the unerupted equivalents of magma systems that ultimately form super volcanoes and so have increasingly received attention as natural laboratories for examining the build-up of large magma volumes in the crust. For example, zircon geochronology indicates that the Spirit Mountain batholith in the Colorado River Extensional Corridor of southern Nevada, western Arizona and southeastern California, underwent piecemeal construction spanning approximately 2 million years (Walker et al., 2007), and produced appreciable quantities of high-silica leucogranite, although no supereruptions have been linked to the Spirit Mountain batholith.

The lack of evidence for bodies of liquid on the order of 10^3 km in the present-day upper crust (Heumann et al., 2002) has generally been taken as evidence that residence times of many hundreds of thousands of years for eruptible magma are untenable (e.g., Reid et al., 1997; Heumann et al., 2002). More recently, a number of studies have invoked storage of large magma volumes in relatively immobile, near-solidus, crystal mushes (cf. Hildreth, 2004 and Bachmann and Bergantz, 2008 for summaries) that episodically undergo “magma defrosting” (Mahood, 1990) or rejuvenation by new inputs of hot magma and/or volatiles (e.g., Bachmann and

Bergantz, 2004; Burgisser and Bergantz, 2011, Deering et al., 2011; Huber et al., 2011; Cooper and Kent, 2014).

To help elucidate the timescales and processes by which large quantities of magma accumulate, are stored, modified in the upper crust and then erupted, I investigated the zircon geochemistry and geochronology of the >600 km^3 Peach Spring Tuff (Young and Brennan, 1974) as well as the underlying Cook Canyon Tuff (possibly related to the same caldera/magma system). This research is part of a larger NSF-funded study being undertaken by students and senior researchers at San José State University, Vanderbilt University, Stanford University, the Berkeley Geochronology Center, New Mexico Tech, the Arizona Geological Survey, and the US Geological Survey.

ZIRCON U-Pb DATING

The long-lived uranium-lead (U-Pb) radioactive decay system plays a central role in resolving the geochronology of magmatic systems. Pairing of two uranium decay series allows for more feasible and reliable age determinations. Concordance of these ages provides an internal "test" for closed-system behavior (Schmitz et al., 2003). Wide utilization of U-Pb in geochronology is possible because of the common occurrence of zircon in most metaluminous to peraluminous rocks. Zircon typically saturates early in most metaluminous to peraluminous melts (Watson and Harrison, 1983), and diffusivity of U and Pb in the zircon lattice is exceedingly slow, even at magmatic temperatures (Cherniak et al., 1997; Cherniak and Watson, 2001). Thus, zircon proves to be a robust igneous geochronometer and is capable of recording subsequent changes in chemical and thermal conditions during crystallization (Miller and Wooden, 2004; Bolhar et al., 2010; Claiborne et al., 2010). Because zircon preferentially incorporates uranium into its crystal structure, but largely excludes lead, nearly all of the lead measured in zircon analysis is derived from U decay.

In addition, because of the low solubility of zircon in common crustal melts (Watson and Harrison, 1983) and its durability in Earth's surface environments, zircon can survive the orogenic cycle, including: growth in magma and solidification, uplift, weathering, transport, and burial, metamorphic recrystallization in the solid state, and then subsequent partial melting. Zircon crystals show a wide variety of zoning patterns and reaction textures that reflect this complex history. The variations in morphology of magmatic crystals have also been correlated to magmatic conditions (Pupin, 1972; Parrish and Noble, 2003).

Challenges arise when dating igneous zircon, especially in volcanic rocks, because the history of any individual zircon is commonly complex, and results in the preservation of intragranular complexities that may be difficult to recognize and therefore difficult to date. The quest for accurate and precise measurements of the U and Pb isotopic compositions of complex zircons has led to the development of several analytical techniques: Thermal Ionization Mass Spectrometry (TIMS), Secondary Ion Mass Spectrometry (SIMS) and Laser Ablation Inductively Coupled Plasma Mass Spectrometry (LA-ICPMS). This thesis uses TIMS and SIMS in tandem to examine the age complexities of zircon in the Peach Spring and Cook Canyon Tuffs. Each has advantages and disadvantages.

TIMS was the first method to be developed and was therefore first to be applied to U-Pb dating of zircon. Modern TIMS analysis is still widely used and produces the most accurate and precise U-Pb dates. In preparation of samples for TIMS analysis, individual zircon crystals or aliquots of multiple crystals are dissolved completely and then commonly purified by a chemical separation process. The samples are spiked with a U-Pb tracer of known isotopic composition, which mixes and equilibrates with the U and Pb in the sample solution and allows for a very accurate and precise determination of the isotope ratios of the unknown.

In the earliest attempts to use zircon for radiometric dating by TIMS, it became clear that Pb loss commonly affects zircon crystals because the ages obtained by the two U-Pb systems were commonly in disagreement (Wetherill, 1956). This “discordance” presumably occurs because of leakage through crystals that have suffered extensive radiation damage during decay (Tilton, 1960; Wetherill, 1963). The earliest attempt to remedy the Pb loss problem was undertaken by Silver and Deutsch (1963) who found low-U zircons could be isolated from higher-U (and presumably more damaged) zircons by magnetic susceptibility. Additional refinements in magnetic separation and the development of techniques to mechanically remove the outer layers of zircon, which are presumably most susceptible to Pb loss by volume diffusion, produced greater concordancy (Krogh, 1982a,b). All of these techniques create a sample bias in the population of zircons that are to be selected for analysis and so potentially biases the age obtained. Mattinson (2005) developed a “chemical abrasion” technique utilizing a warm HF acid leach that appears to mitigate much of the Pb-loss problem, and also allows one to analyze crystals that might otherwise be selectively removed using the other methods. Modern techniques include a thermal annealing step that heals crystals after removal of the radiation damaged portions of the zircon in the chemical abrasion step (Mundil et al. 2004; Mattinson, 2005). Concentrations in routine TIMS isotope analysis are determined by isotope dilution using a U-Pb tracer solution, and it is therefore common to refer to this technique as “CA-ID-TIMS”. In the discussion that follows, this technique is referred to simply as CA-TIMS, with the understanding that the thermal annealing step is undertaken for all TIMS analysis, and that U, Pb concentrations are determined by isotope dilution.

SIMS analysis was developed after TIMS and was designed for measuring the chemical and isotopic composition of solid materials on a scale of a few 10^0 to 10^1 microns (Ireland and Williams, 2003). Sampling complex zircon crystals can pose a significant challenge to the TIMS method, because large volumes of the crystal (frequently an entire crystal) must be dissolved and thus a date obtained represents a volume-weighted average of domains within the zircon that may have different ages. This problem encountered in TIMS has typically been referred to as “inheritance,” where earlier formed zircon preserved in cores is overgrown by younger magmatic zircon. Like Pb loss, inheritance also produces age discordance. SIMS analysis has the advantage of being able to analyze much smaller volume domains in zircon crystals and can therefore be used to detect age differences in single crystals and even quite small age differences in zircons from ostensibly homogeneous zircon populations (Ireland and Williams, 2003).

Standard preparation for SIMS involves embedding the zircons in round epoxy mounts that are ground and polished to expose a cross-sectional view of the zircon crystal. The mounts are gold-coated and imaged with a Scanning Electron Microscope (SEM) equipped with a cathodoluminescence (CL) detector. CL imaging identifies growth domains and can reveal inclusions as well as adhering glass. Growth domains in zircon imaged in CL are related to varying abundance of uranium (U) and yttrium (Y). Dark bands correspond to areas enriched in U and Y, whereas brighter areas are deficient in these trace elements.

Several recent SIMS studies (e.g., Schmitt, 2010, Storm et al., 2010 and Storm et al. 2011) highlight the diversity of single crystal ages and find that growth of crystals is not always continuous. These studies used depth profiling to examine age variation in the crystals. With this technique, euhedral zircons are pressed into indium (Fig. 1) so their flat crystal faces are parallel to the “sputter surface,” and hence parallel to the width of the ion beam. In this way, only the outermost surface of the crystal, which may reflect last recrystallization in the melt, is sampled. The unpolished-exposed crystal face is analyzed first, followed by re-polishing and further analysis. The beam pit is shallow (4-6 µm); therefore, this technique allows crystallization ages to be resolved at order-of-magnitude higher spatial resolution compared to conventional spot analyses. The most significant results show that in addition to eruption age, other crystallization periods and even hiatuses (Storm et. al., 2011) can be recorded in the outer 25 µm of a zircon crystal. This information is not resolvable with conventional SIMS and TIMS analysis. Crystal-face analyses of un-polished zircon and age depth profiling provide a better assessment of whether crystals represent earlier magmatic episodes or were contemporaneous with the erupted melts.

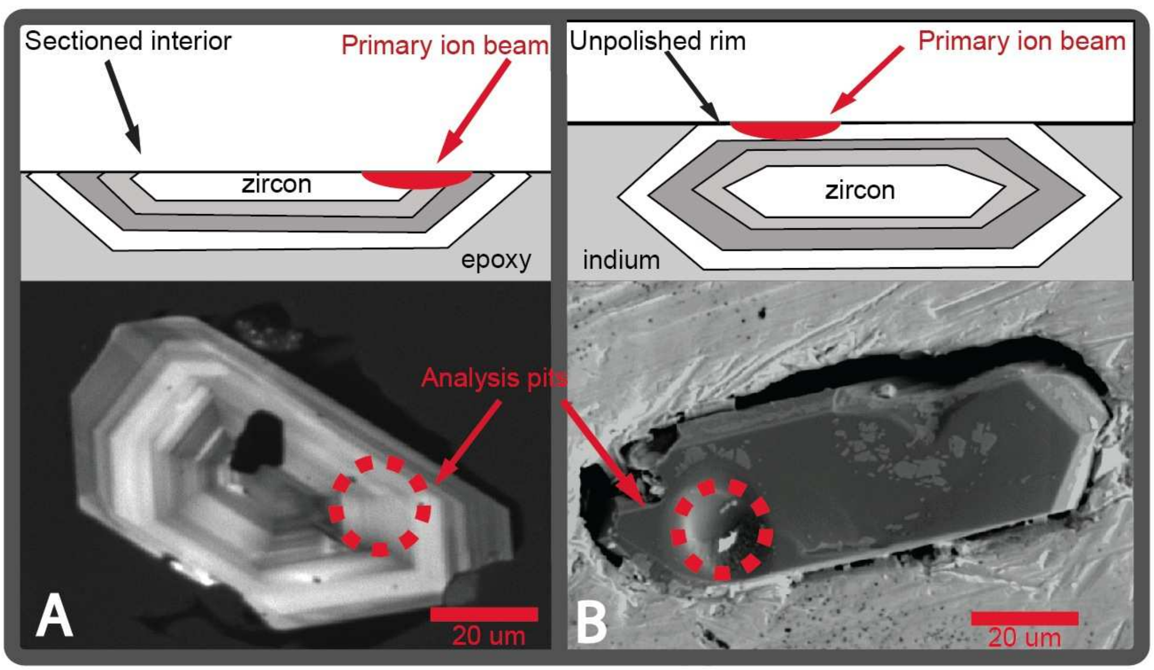

Figure 1. (A) Cathodoluminescence image of a sectioned zircon crystal mounted in epoxy, and (B) secondary electron image of an un-polished zircon crystal embedded in indium metal. The cartoons above each image depict the area sampled by the ion beam.

TIMS vs. SIMS summary

The long-lived viability of TIMS results from reasonable ionization efficiency, a simple mass spectrum, excellent signal to noise characteristics, relatively small order mass fractionation, negligible Pb and U contamination of samples by the instrument, and lack of reliance on mineral standards in the calibration process (Parrish and Noble, 2003). While many studies illustrate the power of TIMS, they are based on situations where the zircons are simple and composed of but one age component and where the effect of Pb loss has been effectively eliminated by application of air abrasion techniques (Parrish and Noble, 2003) or chemical abrasion (Mattinson, 2005).

Sampling complex crystals can pose a significant challenge to the TIMS method, but is the strength of the ion microprobe; therefore the strengths of the SHRIMP compliment those of ID-TIMS (Davis et al. 2003). Refinement of TIMS techniques via single crystal analysis and analysis of crystal fragments, combined with chemical abrasion and blank reduction have permitted crystal to crystal age comparisons and comparisons between distinct zones within crystals as in SIMS analysis (Barboni and Schoene, 2014), but with much higher precision (<<0.1%). Nevertheless, the volume domain sampled for even a crystal fragment is much larger than that for SIMS (one or several orders of magnitude), and so for work on complex, polychronic zircons, SIMS remains an important technique. An ideal approach to examining complex zircons would use both types of analysis, which is the approach taken here.

GEOLOGIC BACKGROUND AND SETTING

The ultimate resolution of the thermal history of voluminous magma chambers requires the combined approach of zircon characterization by imaging techniques such as SE (Secondary Electron) and CL, testing by SIMS for age homogeneity and single-crystal sample selection, and analysis by CA-TIMS for maximum precision and accuracy. This thesis research focuses on two ignimbrite eruptions exposed in the southwestern United States: 1) The early Miocene Peach Spring Tuff, a voluminous (>600 km^3), zoned ignimbrite (trachyte to high-SiO_2 rhyolite) that is exposed widely in eastern California, western Arizona, and southernmost Nevada (Fig. 2) (Young and Brennan, 1974; Glazner et al. 1986) and 2) the little-studied, and less voluminous, trachytic Cook Canyon Tuff that underlies the Peach Spring Tuff in many locations, where the two are exposed in western Arizona and southeastern California (Fig. 3) (Buesch and Valentine, 1986; Gaudio, 2003).

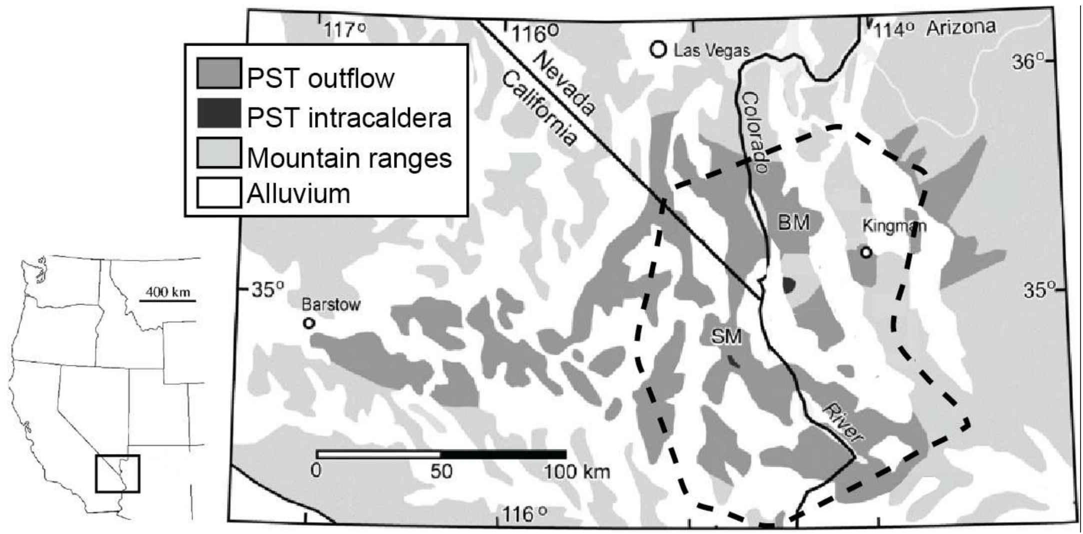

Figure 2. General distribution of Peach Spring Tuff (PST) and Cook Canyon Tuff (CCT). Shaded areas adapted and modified from Ferguson et al. (2013). Peach Spring Tuff intracaldera fill (black shading) in the Sacramento Mountains (SM) and Black mountains (BM) denote caldera fragments identified by Ferguson et al. (2013). Black dashed line encompasses known and suspected exposures of the Cook Canyon Tuff (modified from Buesch, 1993).

Figure 3. Miocene stratigraphy exposed in a highway road cut (I-40) at Kingman, Arizona showing the relationship of the Cook Canyon Tuff (CCT) to the Peach Spring Tuff (PST). The black dashed line marks the top of a paleosol (dark reddish layer) that separates the tuffs at this location.

Previous Work: Peach Spring and Cook Canyon Tuffs

The Peach Spring Tuff has been recognized regionally since the mid 1980s and is the only known supereruption-sized ignimbrite in the region (Glazner et al., 1986). It is densely welded and has a distinct sanidine-rich, quartz-poor mineralogy (Fig. 4A), and is mostly high silica rhyolite; it also has a distinctive heavy mineral assemblage characterized by abundant titanomagnetite and sphene (Fig. 4B) (Gusa et al., 1986). Although the source caldera of the Peach Spring Tuff was unknown until just recently, it is a widespread stratigraphic marker unit across the highly extended Colorado River Extensional Corridor (CREC), which extends from the west edge of the Colorado Plateau into the central Mojave Desert. It has thus been especially important in studies of the timing of regional extension (Glazner et al., 1986; Wells and Hillhouse, 1986; Nielson and Beratan, 1995; Miller et al., 1998).

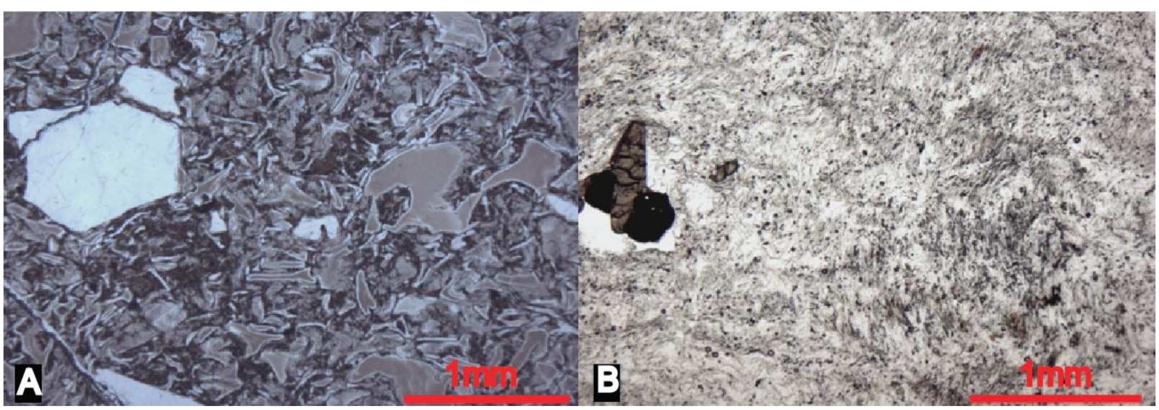

Figure 4. Photomicrographs of Peach Spring Tuff ignimbrite showing welded shard texture (A); (B) rhyolitic outflow pumice showing sphene intergrown with magnetite.

Early attempts to determine the age of the Peach Spring Tuff using K-Ar dating were generally unsuccessful, and produced conflicting dates because of appreciable excess Ar. In the 1990s, use of multi-crystal step heating and single-crystal fusion $^{40}Ar/^{39}Ar$ geochronology (Nielson et al., 1990; Miller et al., 1998) produced the first robust dates of the ignimbrite (ca. 18.5 Ma). More recently, *individual* $^{40}Ar/^{39}Ar$ analyses of sanidine (single crystal fusion and combined split) by Ferguson et al. (2013) yielded dates from 18.61 ± 0.07 Ma to 19.02 ± 0.13 Ma (errors are 1 sigma). The error-weighted averages (of *individual* analyses) for each sample, including intracaldera Peach Spring Tuff, range from 18.74 ± 0.07 to 18.82 ± 0.05 Ma. Combining these averages with that of Miller et al. (1998) gives the mean reported by Ferguson et al. (2013) of 18.78 ± 0.02 Ma, MSWD = 1.14 (Fig. 5). All dates reported in Ferguson et al. (2013) were calculated using a value of 28.20 Ma for the Fish Canyon Tuff sanidine fluence monitor (Kuiper et al., 2008). The Miller et al. (1998) date of 18.47 ± 0.07 Ma, recalculated to the same fluence monitor age becomes 18.74 ± 0.07 Ma (Fig. 5). A composite of U-Pb ion probe ages from multiple pumices found in lake deposits in distal Peach Spring Tuff from the central Mojave Desert also gave an age of ca. 18.7 Ma (Miller et al., 2010), in general agreement with the new Ar-Ar results.

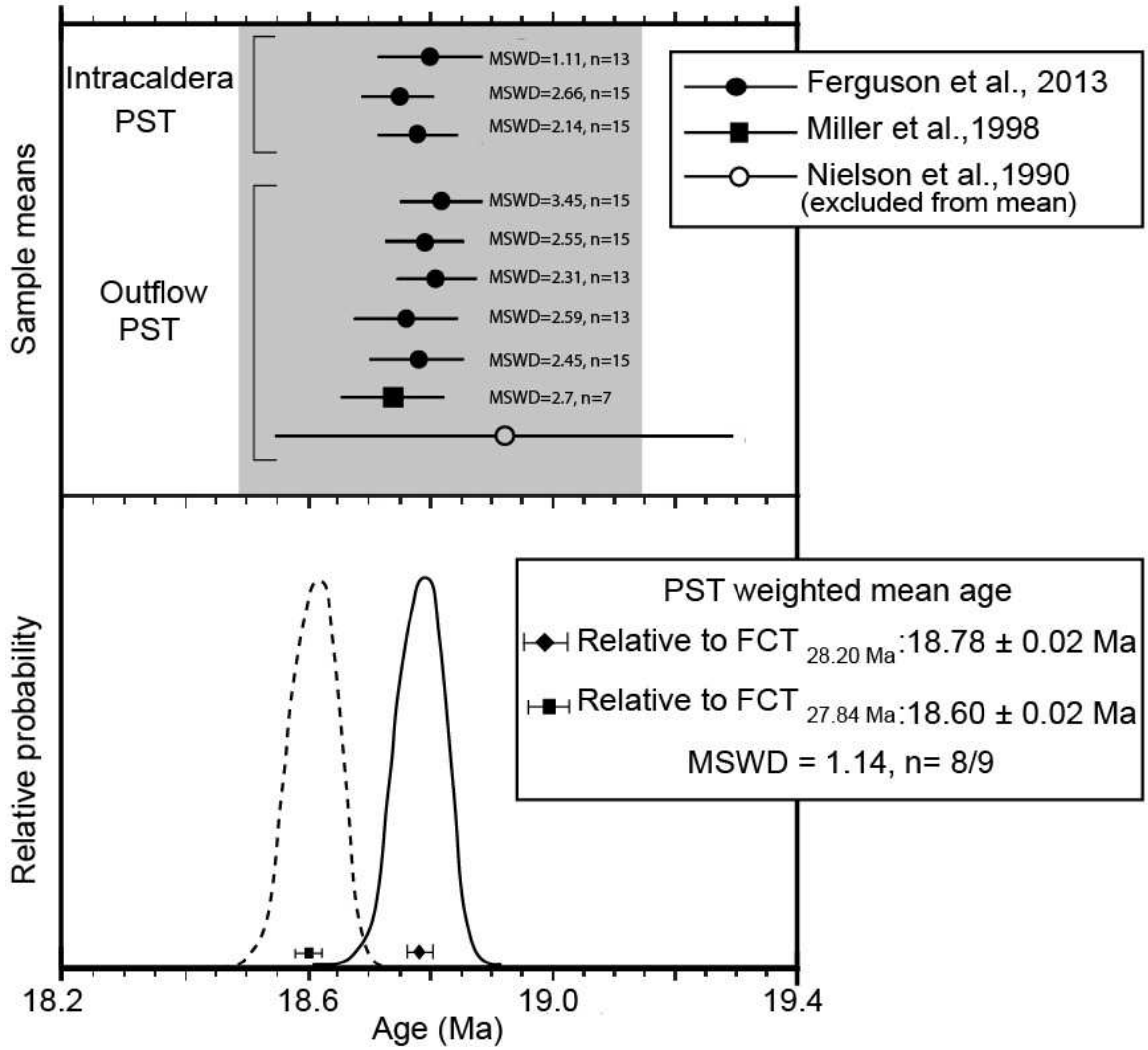

Figure 5. Summary of $^{40}Ar/^{39}Ar$ dates reported by Ferguson et al. (2013) from Peach Spring Tuff (PST) sanidine phenocrysts. Upper panel shows age determinations and 2σ errors from three separate studies. Each data point represents the weighted mean age obtained from multiple analyses in a given sample. Shading indicates the total range of ages captured by *individual analyses* in samples from Ferguson et al. (2013) and Miller et al. (1998). Lower panel shows age probability distribution (Deino and Pots, 1992) constructed from the sample means and uncertainties. Ages in the upper panel are relative to Fish Canyon Tuff sanidine at 28.20 Ma (Kuiper et al., 2008). Lower panel shows the difference between weighted mean age calculated by Ferguson et al. (2013) assuming 28.20 Ma for Fish Canyon sanidine and the weighted mean age assuming a younger age (27.84 Ma) as used or reported by other studies (e.g. Sampson and Alexander, 1987; Nielson et al., 1990; Miller at al., 1998; Channell et al., 2010; Mark et al., 2013; Phillips and Matchan, 2013,). The difference between the resulting means is approximately 200 kilo years.

As noted, the source caldera of the Peach Spring Tuff had been unknown until recently, despite detailed and extensive study of the Miocene geology by workers in the Colorado River Extensional Corridor in the 1980s and 1990s. Mapping undertaken by the Arizona Geological Survey (Pearthree et al., 2009; Ferguson et al., 2013) and the new $^{40}Ar/^{39}Ar$ geochronology (Ferguson et al., 2013) has now definitively identified a caldera on the west flank of the southern Black Mountains of Arizona as the source.

Ferguson et al. (2008, 2013) have named this the Silver Creek caldera and have recently located a second fragment of the caldera in the northern Sacramento Mountains (Fig. 2) (Ferguson et al., 2013). The discovery of the caldera and the identification of Peach Spring Tuff intracaldera fill and caldera-related intrusions by Ferguson et al. (2008) revived interest in the ignimbrite, and led to important new insights into this enigmatic supereruption (Pamukcu et al., 2013). The volcanic and intrusive units within and surrounding the caldera range in age from ~19 to ~17 Ma (McDowell et al., 2014)(Fig. 6). The Peach Spring Tuff conformably overlies a >1km thick section of feldspar-rich trachytic to trachydacitic and basaltic to trachyandesitic volcanics. In most areas, the top of this section is the Cook Canyon Tuff. The stratigraphically lowest unit, the Alcyone Trachyte, was dated at 19.01 ± 0.26 Ma (McDowell et al., 2014).

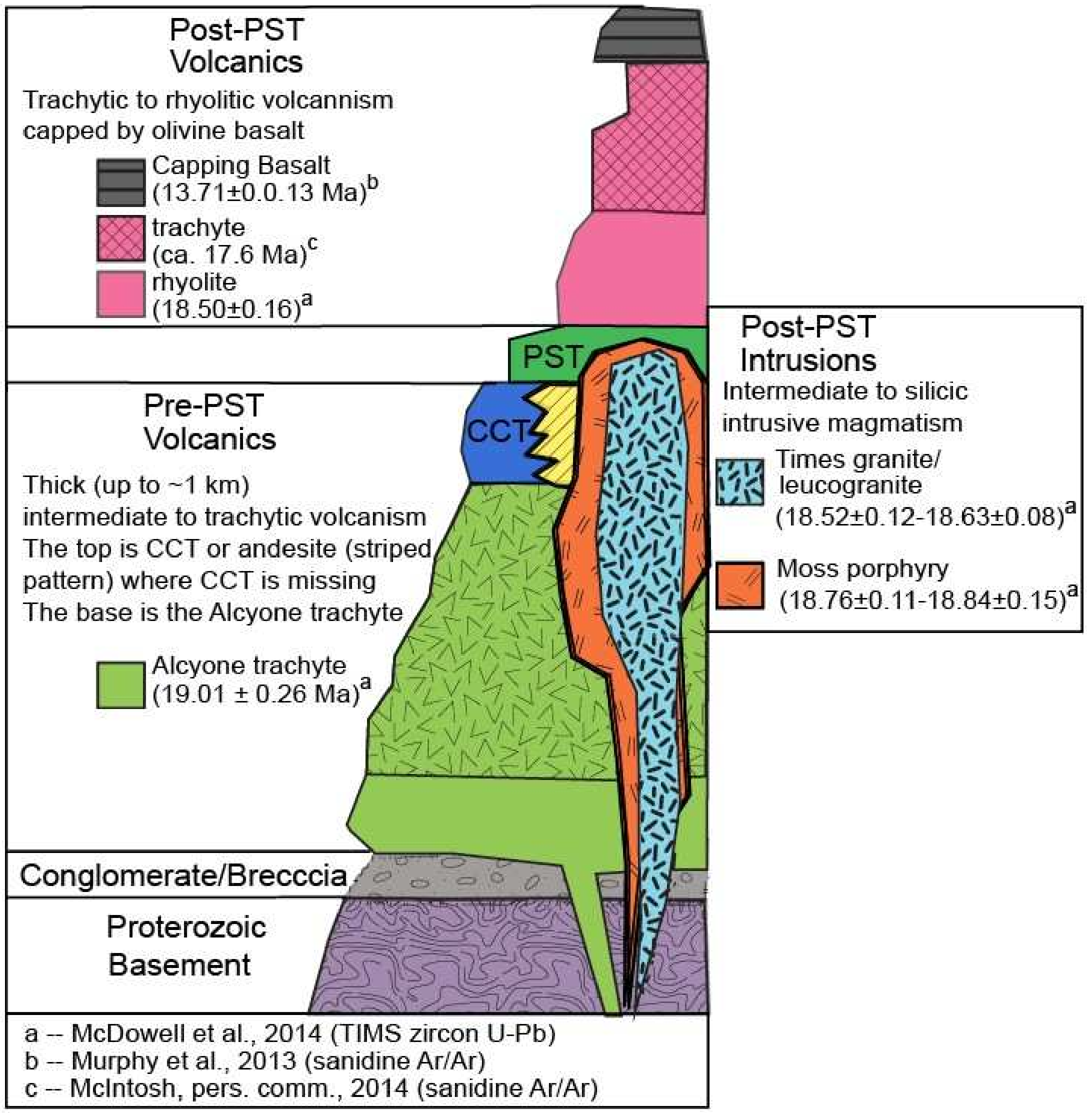

Figure 6. Generalized stratigraphy in the southern Black Mountains. Ages of pre- and post-Peach Spring Tuff units were determined in previous work (adapted and modified from Ransome, 1923; Ferguson et al, 2008; Ferguson et al., 2013; Murphy et al., 2013; McDowell et al., 2014).

The Cook Canyon Tuff is generally sanidine-poor and is thus poorly dated. Bill McIntosh (pers. comm., 2012) has obtained a single bulk step-heating plagioclase $^{40}Ar/^{39}Ar$ age for the Cook Canyon Tuff at Kingman Arizona of 19.28±0.05 Ma. A date of 18.5 ± 0.2 Ma on biotite (not recalculated using the Kuiper et al. 2008 Fish Canyon values) was obtained by Wilds (1997), and suggests that the Cook Canyon Tuff and Peach Spring Tuff erupted very close in time. The source of the Cook Canyon Tuff is still unknown, but based on its outcrop distribution likely lies somewhere in the vicinity of Kingman, Arizona and the California border. Gaudio (2003) speculated, based on geochemistry, that the Cook Canyon Tuff is related to the Peach Spring magma system, and that the higher degree of welding observed in the Cook Canyon Tuff in the southern Black Mountains indicated that this area was more proximal to the source caldera. As noted above, the Cook Canyon Tuff is separated by less than 2 meters of intervening strata at Kingman (Fig. 3), and the very limited geochronology that has so far been done shows overlap with the Peach Spring Tuff.

Growth of the Silver Creek magma system and eruption of the Peach Spring Tuff

There is little information known on the timescale over which the ignimbrite was assembled, and how much time a Peach Spring magma body existed prior to eruption. Integration of geochemical, textural, and modeling-based data provides substantial information on the compositional evolution of the Peach Spring magma preceding its eruption. These data show that the Peach Spring magma body was compositionally and thermally zoned with a basal trachytic cumulate (Pamukcu et al., 2013).

Pamukcu et al. (2013) have suggested that mafic magma injection may have unlocked and remobilized the basal cumulate mush body comprising the Peach Spring magma system and triggered an eruption. Mafic magmas injecting silicic magmas have been implicated as important in the development of many large magma bodies. Heat can help unlock crystal mush and produce eruptible magma and may also trigger overturn of the magma body; in addition, volatile over-pressurization can occur as the injected mafic magma cools and de-gasses, which may ultimately lead to eruption (e.g., Sparks et al., 1977; Pallister et al., 1992; Bachmann and Bergantz, 2003; Bindeman and Valley, 2003; Kennedy and Stix, 2007; Wark et al., 2007; Deering et al., 2011). Evidence for a mafic trigger in the Peach Spring Tuff is evident in high temperature overgrowths on resorbed zircon (Fig. 7), concave-down crystal size distributions, and the presence of mafic enclaves in the tuff (Pamukcu et al., 2013).

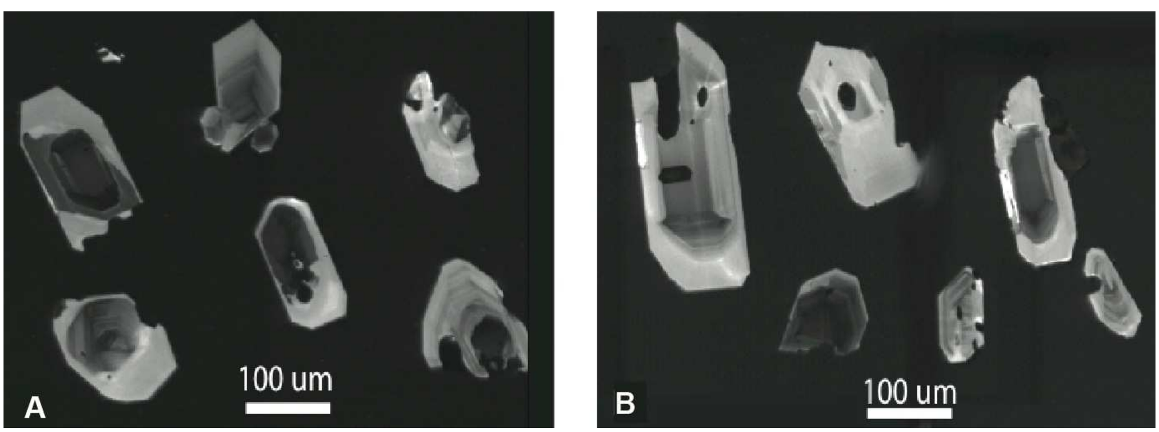

Figure 7. Cathodoluminescence images of bright overgrowths on Peach Spring Tuff zircon (A) and Cook Canyon Tuff zircon (B).

This previous work implies that the Peach Spring Tuff may have spent much of its existence as a nearly moribund crystal mush body that had enough sustained magma input over time to grow to appreciable (batholith size) before erupting. Growth of such a magma or mush body is best documented through detailed zircon geochronology. Hence, this study attempts to address the persistent question of whether or not an erupted batholithic volume of magma (the Peach Spring Tuff supereruption) implies a long integrated and piecemeal construction (as in the case of the very nearby and at least superficially similar (i.e. quartz monzonite to high silica granite) Spirit Mountain batholith through the integration of both high accuracy and high precision dating techniques (Mattinson, 2005) and trace element analysis of zircon.

The ultimate resolution of the thermal history of voluminous magma chambers requires careful assessment of the chronology of their growth and assembly, which is uniquely attainable through zircon, and possibly other minor accessory phases for which U-Pb methods can be used. Thorough characterization of the zircon population in terms of both age and texture requires the combining imaging techniques such as SE and CL, testing by SIMS for age homogeneity and single-crystal sample selection, and analysis by CA-ID-TIMS for maximum precision and accuracy.

The specific goals of this Master's research project were to:

1. assess the temporal and zircon geochemical record of the construction of the Peach Spring Tuff magma chamber.
2. better evaluate the petrogenetic links if any between the Cook Canyon

Tuff and Peach Spring Tuff using U-Pb dating and zircon geochemistry. It should be noted that a high-precision age on the Cook Canyon Tuff potentially places tight constraints on the possible growth time of the Peach Spring magma chamber and possibly on the storage time of eruptible Peach Spring magma if it can be determined that the two tuffs share the same source caldera.

3. contribute to the growing body of precise and accurate geochronological data that is necessary to understand the formation and duration of magma bodies that lead to supereruptions.
4. provide ages for comparison to post caldera intrusions and to test the hypothesis that these intrusions are potentially unerupted plutonic residue of the Peach Spring Tuff supereruption.

METHODS

Whole pumice samples from both the Peach Spring Tuff and Cook Canyon Tuff were collected in Spring 2011. The benefit of whole versus bulk tuff is that it limits xenocrystic contamination. In an attempt to encompass and adequately represent the compositional diversity of the Peach Spring Tuff, pumice clasts were collected from areas within the ignimbrite that might potentially represent compositional end-members of the ignimbrite thus containing zircon that grew at various times and in contrasting geochemical and perhaps thermal environments throughout the duration of the magmatic system. These areas include both proximal (Caliche Springs, AZ) and distal outcrops (Kingman, AZ). Proximal Peach Spring Tuff samples include pumice from the base and the top to check for magma chamber zoning. The two Cook Canyon Tuff pumices were collected from a single location from a pumice-rich outcrop along US I-40 in Kingman.

Sample Descriptions

TABLE 1. SAMPLE DESCRIPTIONS

Pumice I.D	Sample collection coordinates (UTM)	Location	Facies	Distance from source caldera (km)	Description	Minerals Present	
Peach Spring Tuff							
2H	11N 0769813 3897926	Kingman, AZ	Distal outflow base of ignimbrite	~ 40	color: streaky light to dark lilac welded	Sanidine Plagioclase Hornblende Biotite	Sphene Quartz
3B	11N 0753712 3867728	Caliche Springs, AZ	Proximal outflow base of ignimbrite	~15	color: streaky light to dark grey non-welded	Sanidine Plagioclase Hornblende Biotite	Sphene Quartz
3D	11N 0753712 3867728	Caliche Springs, AZ	Proximal outflow base of ignimbrite	~15	color: dark grey to black abundant lithic fragments welded	Sanidine Plagioclase Hornblende Biotite	Sphene Pyroxene
5D	11N 0763890 3867387	Caliche Springs, AZ	Proximal outflow top of ignimbrite	~15	color: streaky orange and white non-welded	Sanidine Plagioclase Hornblende Biotite	Sphene Pyroxene
Cook Canyon Tuff							
7A	11N 0766368 3896529	Golden Valley, AZ	unknown* (likely distal)	N/A*	color: dark grey/brown non-welded	Plagioclase Hornblende Biotite	
7B	11N 0766368 3896529	Golden Valley, AZ	unknown* (likely distal)	N/A*	color: streaky grey to dark grey non-welded	Plagioclase Hornblende Pyroxene Biotite	Sanidine Sphene Quartz

*Source caldera for Cook Canyon Tuff is inknown

Zircon extraction and processing

Zircons were separated from individual pumice clasts through conventional mineral separation techniques (e.g., crushing, heavy liquid separation, and magnetic susceptibility separation) at the USGS sample crushing and mineral separation facilities in Menlo Park, CA. Each pumice clast was cleaned with compressed air and in deionized water using an ultrasonic bath for 5 minutes and then air-dried. Dry pumice was further crushed using a hammer and steel plate until the entire sample was approximately sand-sized. Methylene Iodide was used to isolate the heavy mineral fraction. After heavy liquid separation, the heavy mineral fraction was rinsed with acetone and deionized water, bathed in an ultrasonic bath for 5 minutes, then air-dried.

The heavy mineral separates were further separated on the basis of magnetic susceptibility using a Frantz Isodynamic separator. Zircon is generally non-magnetic, meaning that regardless of the amount of current delivered to the magnet, it will always pass through the magnet and end up on the non-magnetic side. Most published magnetic separation techniques instruct to select zircon from the least magnetic fractions, and though this fraction usually contains the majority of zircon in a given sample, it could lead to sample bias. Zircons from these pumices were observed in all magnetic fractions. To avoid sample bias, to best represent the range in size and morphology present in these samples, and to determine if there was any relationship between age and magnetic susceptibility, zircons were handpicked from all magnetic fractions with a binocular microscope.

TIMS sample preparation and analysis

For the TIMS analysis employed in this study, the thermal annealing and chemical abrasion protocols follow Mundil et al. (2004) and Mattinson (2005). Following SIMS analysis, a subset of both sectioned zircon and zircon mounted in Indium were extracted for thermal annealing and chemical abrasion treatment, which was performed at the Berkeley Geochronology Center. Whole, previously undated zircons were also included for thermal annealing and chemical abrasion treatment. All zircon were thermally annealed in an oven (1atm) for 36 hours at 850°C (Mattinson, 2005) and chemically abraded for 16 hours at 220°C in concentrated HF in pressurized dissolution capsules to remove any domains that experienced Pb loss (Mundil et al., 2004; Mattinson, 2005).

Following the thermal annealing and chemical abrasion treatment, a few sectioned zircons that previously yielded spurious SHRIMP ages (younger than the $^{40}Ar/^{39}Ar$ age of Ferguson) were taken back to Stanford USGS Micro Analysis Center and re-imaged to observe the effects of the chemical abrasion treatment on SHRIMP analysis pits and other portions of the crystal. Analysis pits that were etched by the chemical abrasion process would indicate that the anomalous ages are due to Pb loss. Zircons that were analyzed for rim ages were also returned to Stanford, re-mounted in indium, and re-analyzed via SIMS for pre- vs. post-chemical abrasion comparison. Following imaging and analysis of chemically abraded zircons, the zircons were returned to the Berkeley Geochronology Center and prepared for TIMS analysis.

Zircon U-Pb age determinations were performed at the Berkeley Geochronology Center on chemically abraded and thermally annealed sectioned zircons, whole zircons with SIMS rim ages, and whole-previously undated zircons. The majority of the analyses were performed on single zircons, as opposed to combining multiple crystals into one sample. To mitigate problems with low U rims and mass balance issues, low U tips of zircons as determined by prior SHRIMP analysis were broken off and combined for a single analysis. Care was taken to keep track of individual zircon sample numbers so that SIMS ages could be directly compared with TIMS ages. Zircons were rinsed several times in concentrated HNO_3, cleaned in ultrasonically agitated aqua regia, and rinsed again with HNO_3. Zircons were then transferred to perforated miniature PTFE capsules and spiked with ^{205}Pb-^{233}U-^{235}U-tracer solution. The capsules were placed in a 125 ml digestion vessel containing a mixture of HF and HNO_3. The digestion vessel was kept at 220°C for 6 days. After dissolution, the dried sample was loaded together with silica gel and H_3PO_4 on out-gassed Re filaments. Isotope ratios were determined on a Micromass Sector 54 mass spectrometer using a Daly-type ion counter positioned behind a WARP filter. Pb (as Pb^+) and U (as UO_2^+) were run sequentially on the same filament.

SIMS sample preparation and analysis

Selected Peach Spring Tuff and Cook Canyon Tuff zircon were either mounted along with standards in standard epoxy mounts then ground and polished to expose interiors, or mounted in indium for rim analysis at Stanford USGS Micro Analysis Center. Rim as referred to here and in the Results and Discussion below refers to the un-polished outer surface of a zircon crystal.

CL images of sectioned zircon were taken with the JEOL JSM 5600 Scanning Electron Microscope and attached Hamamatsu Cathodoluminescence Detector. The CL images of the interior of the zircons were used to identify and classify distinct types of zircon chemical zoning and as guides when selecting spots for age and trace element analysis. For spots on zircons where both age and trace element analysis were obtained, age analysis preceded trace element analysis. Zircon was also mounted in indium for analysis of crystal rims that represent the last increment of growth. Chemically abraded and thermally annealed zircons as well as untreated zircons were analyzed by SIMS to permit comparison of TIMS and SIMS results, and to allow assessment of the possible role of Pb-loss on SIMS analysis.

Zircon U-Pb ages of >300 zircon spots were determined using the SHRIMP-RG at the SUMAC at Stanford University. Individual analyses were performed using a nominally 6 nA primary beam of O_2^- with an accelerating voltage of 10 kV. Spot sizes were approximately 20 µm wide and 4-6 µm deep. Zircon standard R33 (420 Ma; Black et al., 2004; Mattinson, 2010) was used for U-Pb age determinations. All Proterozoic ages are corrected for common Pb using a $^{207}Pb/^{206}Pb$ value of 0.962, based on Stacey and Kramers (1975) Pb evolution model. All Miocene zircon ages are corrected for common Pb using a $^{207}Pb/^{206}Pb$ value of 0.855, based on whole rock values of Tertiary lavas in the region (Miller et al., 2000). $^{206}Pb/^{238}U$ ages were also adjusted for initial ^{230}Th deficit in the ^{238}U decay chain using the method of Schärer (1984), which uses the measured Th/U in zircon and assumes a constant Th/U in the melt to correct for the disequilibrium. Melt Th/U ratios were assigned to individual pumice clasts based on the ICPMS analyses of analogous samples reported by McCracken (pers. Comm., 2011). In addition to U-Pb determinations, concentrations of select trace- and rare-earth elements were collected following the analytical protocol described by Claiborne et al. (2010) with concentrations calibrated to the "MAD" zircon standard reported by Barth and Wooden (2010), with Ti concentrations calibrated to SL-13 (6.14 ppm; Hiess et al., 2008). Data were reduced using Squid II version 2.5 0 (Ludwig 2009) and Isoplot version 3.6 (Ludwig, 2008).

RESULTS

Zircon zoning and trace element variation

Trace element results (Figs. 8-12) indicate that each individual pumice clast contains zircons with edges that reflect growth from contrasting parent melt compositions and thus magmatic environments. Multiple trace element signatures exist between zircon interiors and edges despite U-Pb dates indicating coeval growth and final eruption at the same time. Cores of all Peach Spring Tuff and Cook Canyon Tuff zircon overlap in composition and define a general trend that is as expected for growth from melt undergoing fractional crystallization (e.g., Claiborne et al., 2006; 2010). The "types" of zircon are determined by edge chemistry since the range in the compositions of the cores is so large. These types are illustrated in Figure 13, and the trace element concentrations of their edges in Figure 14.

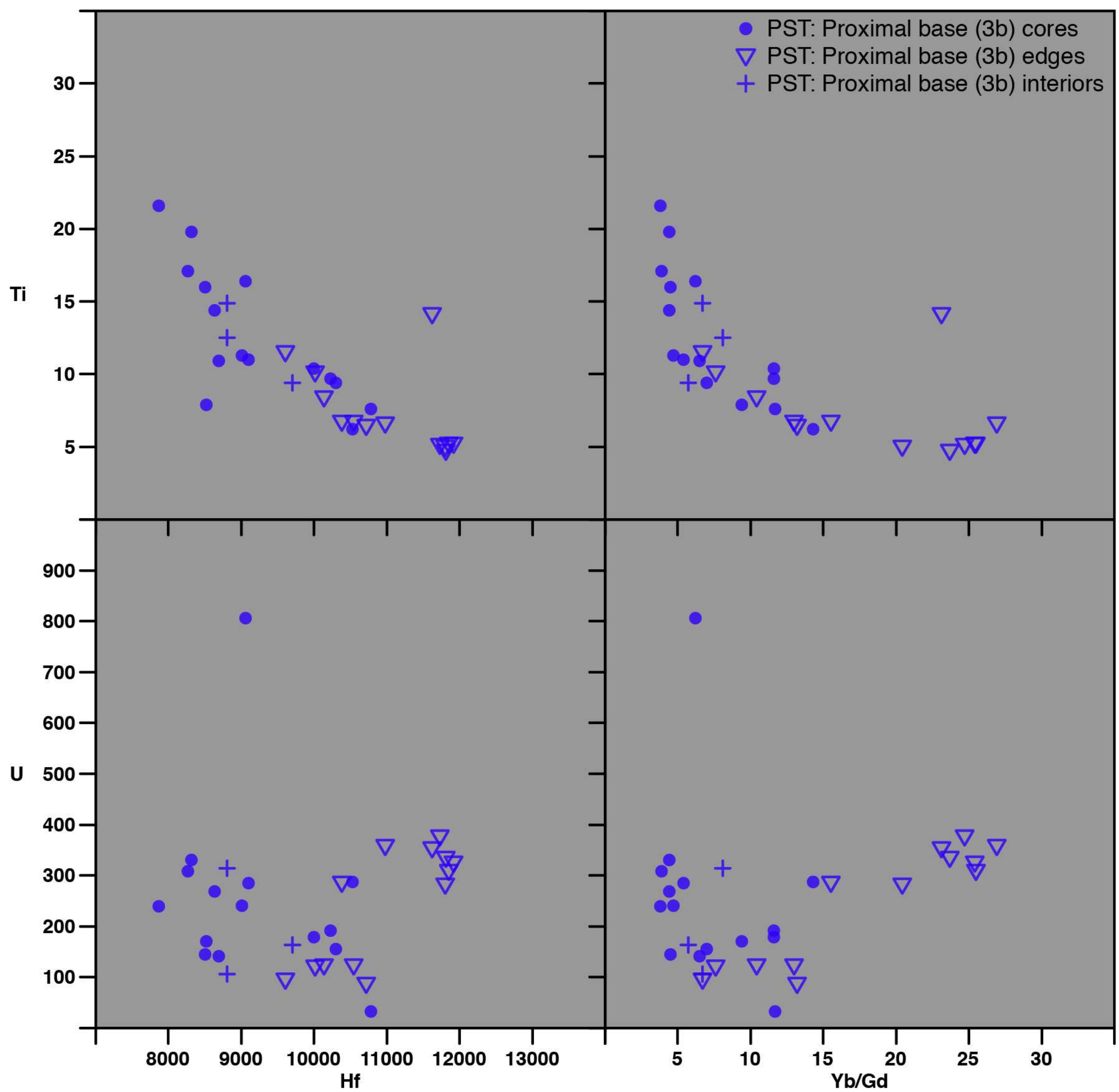

Figure 8. Trace element geochemistry from zircon in pumice collected proximal to the caldera at the base of the ignimbrite (sample 3b).

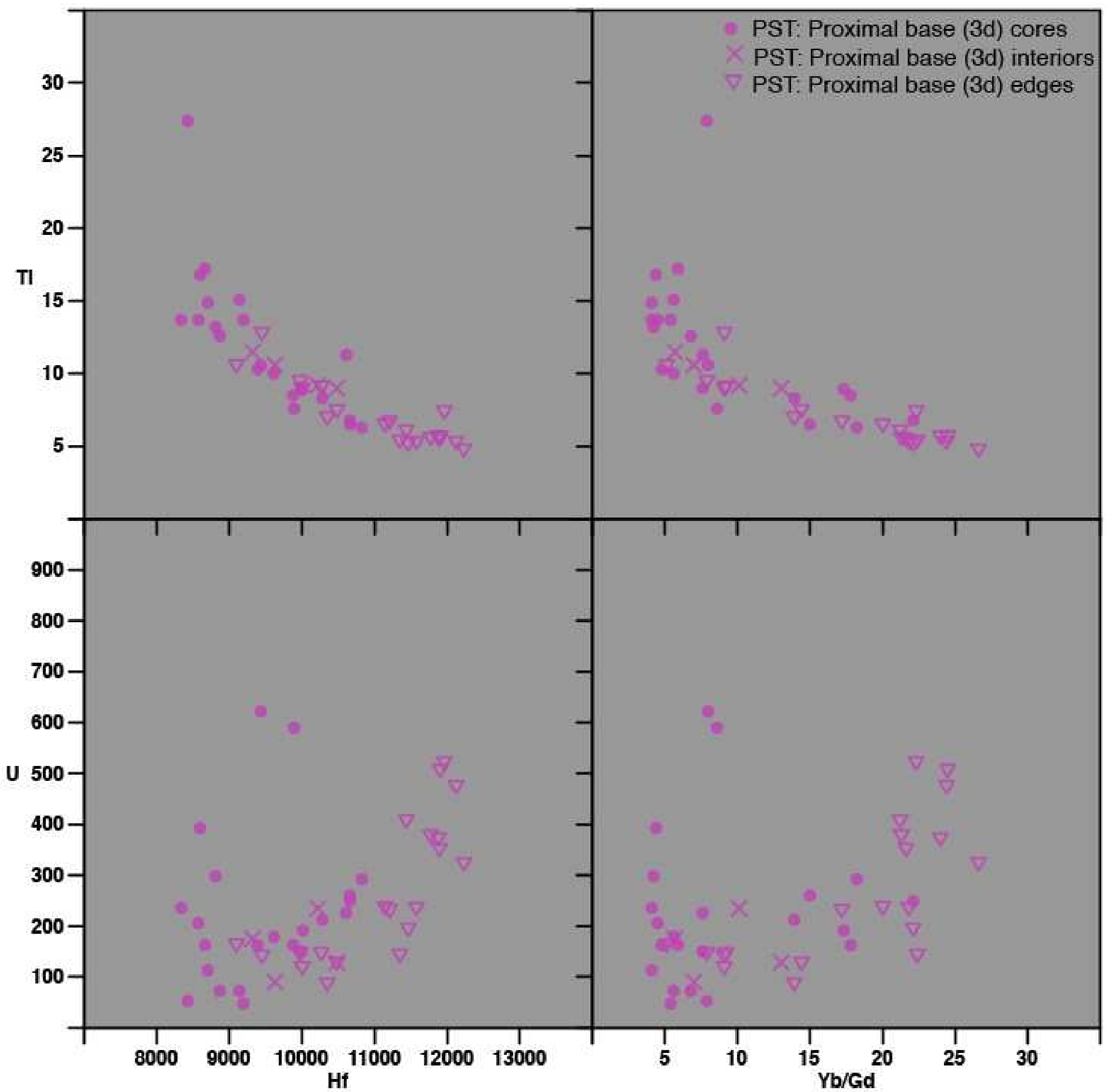

Figure 9. Trace element geochemistry for zircon in pumice collected proximal to the caldera at the base of the ignimbrite (sample 3d).

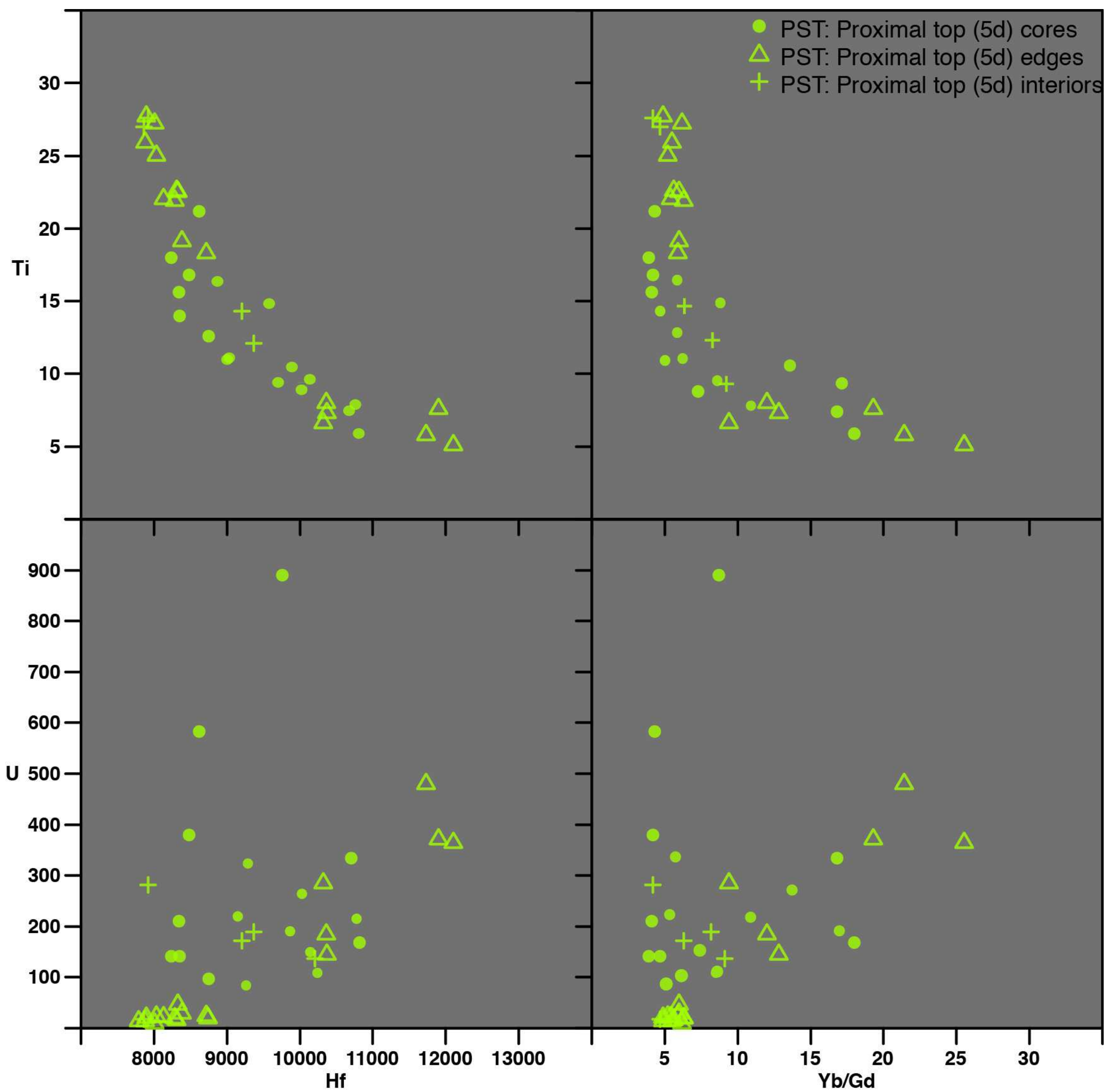

Figure 10. Trace element geochemistry from zircon in pumice collected proximal to the caldera and the top of the ignimbrite (sample 5d).

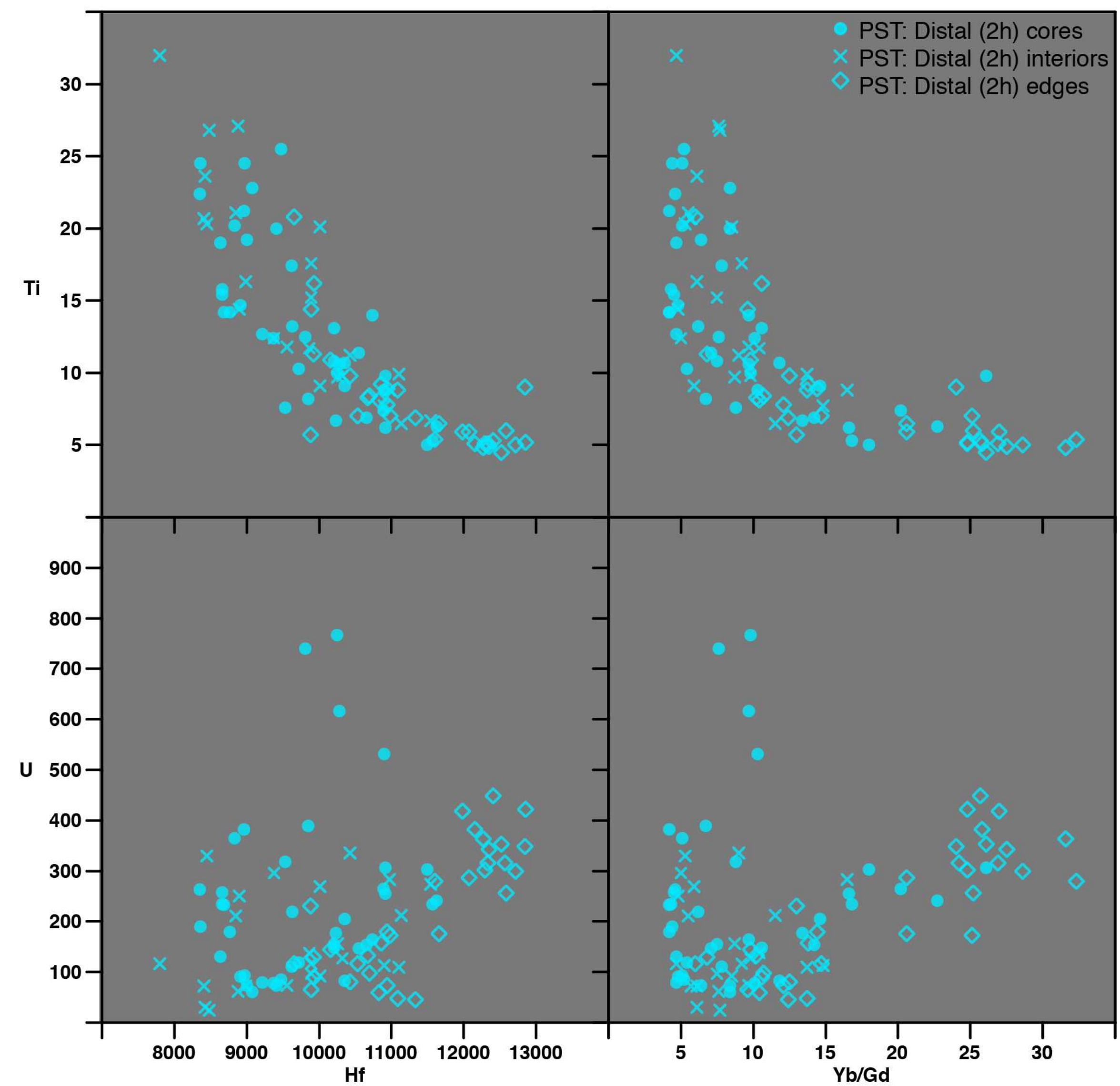

Figure 11. Trace element geochemistry of zircon in pumice collected from distal outflow near Kingman, Arizona (sample 2h).

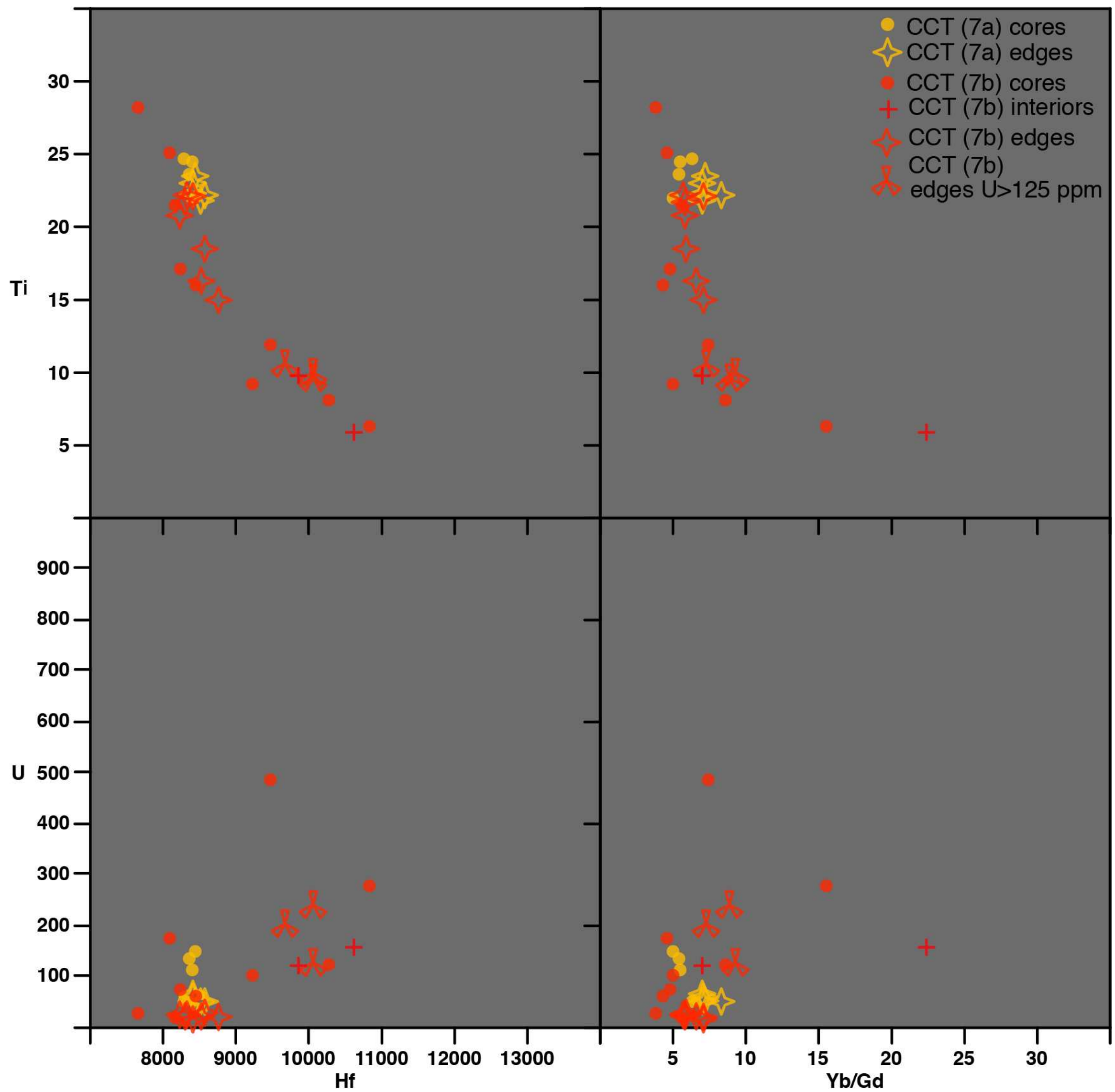

Figure 12. Trace element geochemistry of zircon from Cook Canyon Tuff pumice collected near Kingman, Arizona (samples 7a and 7b).

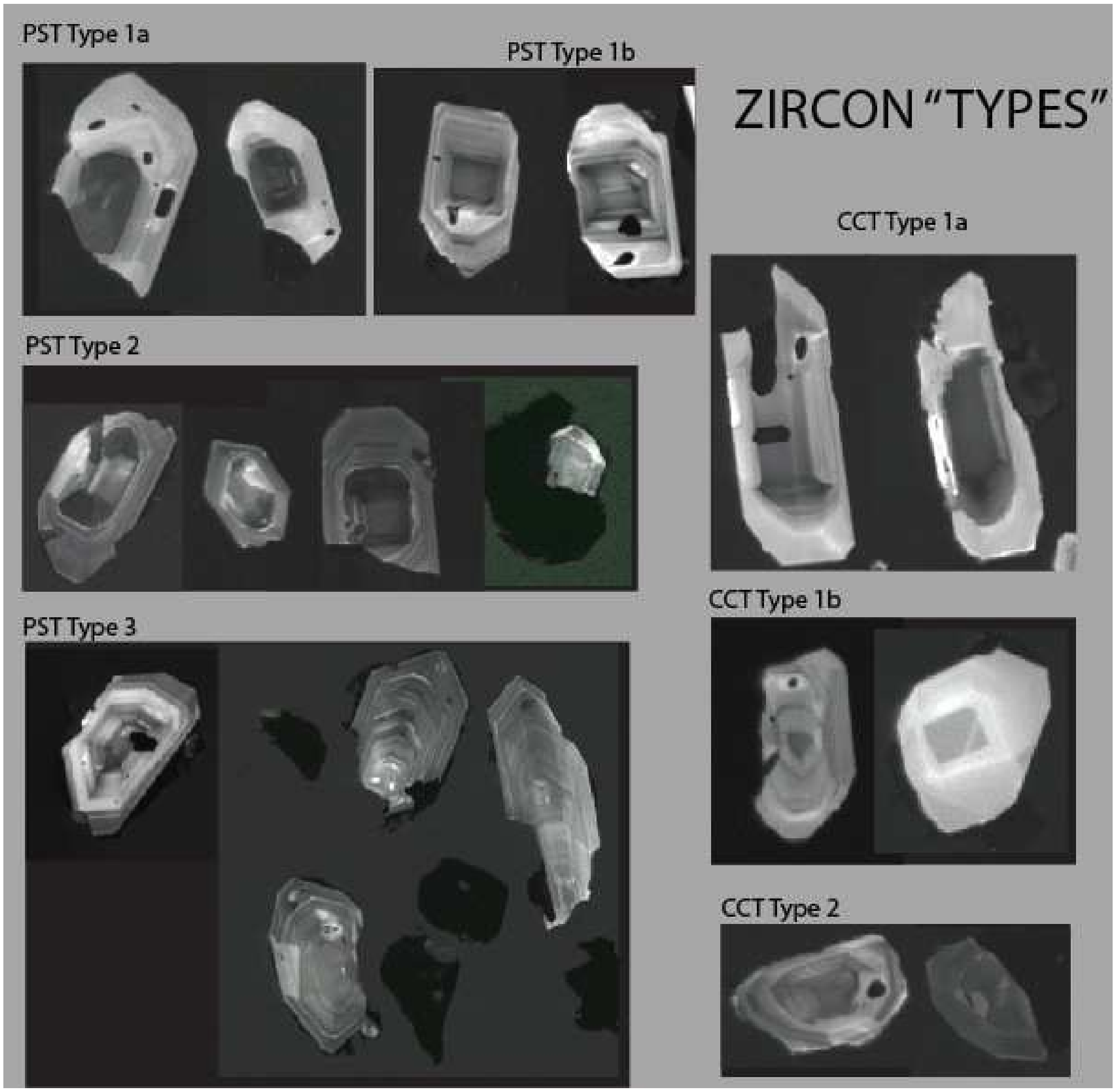

Figure 13. Peach Spring Tuff (PST) and Cook Canyon Tuff (CCT) zircon "Types" based on petrography and trace element concentrations of their edges.

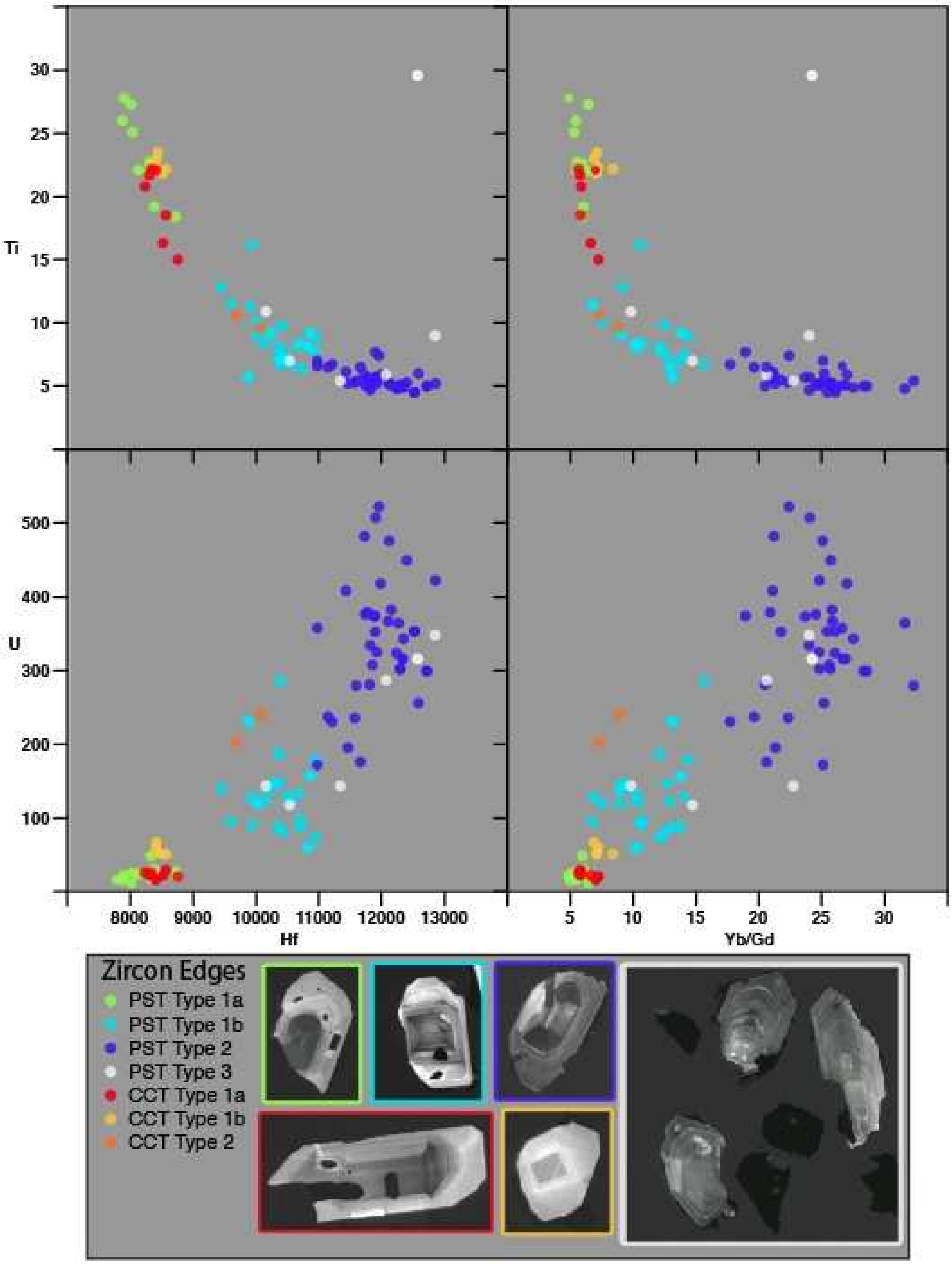

Figure 14. Trace element edge concentrations for zircon "Types" in the Peach Spring Tuff (PST) and Cook Canyon Tuff (CCT).

Peach Spring Tuff

The Peach Spring Tuff contains four types of zircon based on CL brightness and trace element content (Figs. 13 and 14).

Type 1. Zircons designated as Type 1 are found in every pumice sample analyzed in this study; however, they are more abundant in pumice collected from distal outflow (2h) and pumice collected proximal to the caldera and from the top of the ignimbrite. Type 1 zircons are euhedral to subhedral and have cores with variable zoning patterns mantled by CL-bright edges. Some have diffuse zoning with rare dark cores and some are CL-bright throughout the entire crystal. In some cases, it is difficult to observe whether zoning is continuous from core to rim due to irregular sectioning of the zircon crystals. Importantly, this type has CL-bright edges regardless of their internal textures (Fig. 13). CL-bright edges are generally associated with low U and high Ti concentrations, indicating late stage crystallization from less evolved and relatively high temperature melt that in some cases is interpreted to reflect near-eruption magma mixing and reheating events (e.g., Reid et al., 2011; Chamberlain et al., 2013).

Type 1 zircons may be subdivided into two groups also based on the trace element composition of their edges, from hereafter are referred to as Type 1a and Type 1b. As mentioned above, all Type 1 zircons have CL-bright edges, but their trace element compositions may differ (Fig 14).

Type 1a zircons have edges with low Yb/Gd ratios (≈5-10), low U (< 100 ppm), low Hf (< 9000 ppm), and high Ti (> 15 ppm) (Fig. 14). Type 1a zircons with their low-

U/high-Ti edges comprise ~50% of the zircon from pumice collected proximal to the caldera and from the top of top of the ignimbrite (sample 5d) that presumably represents late-erupted material from the base of the magma chamber (Pamukcu et al., 2013). The edges on Type 1a zircon are interpreted by Pamukcu et al. (2013) to indicate a late-stage reheating event followed by reprecipitation of zircon on variably resorbed cores. Type 1a zircons are rare in other pumice collected from the Peach Spring Tuff. However, it is worth noting that many interiors of zircons collected from all other Peach Spring Tuff pumice have identical trace element concentrations as Type 1a zircon edges (Figs. 8-12 and 14). Zircons similar to Type 1a are observed in post-Peach Spring Tuff "porphyry" intrusions and yield U-Pb dates similar to those for the Peach Spring Tuff zircon (McDowell et al., 2014), perhaps suggesting recycling of Peach Spring Tuff zircons by the post-Peach Spring Tuff granitic magmas.

Type 1b zircons have edges with relatively low Yb/Gd ratios (≈5-15), relatively low U (< 250 ppm) and Hf (≈9000-11000 ppm) concentrations, and moderate Ti (≈5-20 ppm) concentrations (Fig. 14). Type 1b zircons comprise approximately 50% of the zircon from 2h (distal pumice) and 3b (proximal base), and approximately 25% of zircon from 5d (proximal top) and 3d (proximal base). The primary differences between Type 1a and 1b zircon are that Type 1b zircon have edges with: 1) higher Hf concentrations, 2) higher Yb/Gd ratios, and 3) lower Ti concentrations than Type 1a zircon. There are almost no zircon edges with Yb/Gd ratios between 15 and 20. The only pumice sample containing zircons with this (Yb/Gd ratios between 15 and 20) is 3d, which consequently, is the most lithic-rich pumice clast sampled in this study. The lower Hf and higher Ti edge compositions of type 1a zircons indicate that their CL-bright edges grew from a hotter melt than the CL-bright edges on type 1b zircons. Since both Hf concentration and Yb/Gd ratios are taken as indicators of melt evolution/fractionation (i.e. low Hf and low Yb/Gd = less evolved)(Barth and Wooden, 2010; Claiborne et al., 2010) it is worth noting that although there is considerable overlap in their Yb/Gd ratios, a compositional gap in Hf concentration between Type 1a and 1b is evident (Fig. 14) (almost no zircon near-rims with Hf 9000-10000 ppm).

Type 2. Zircons designated Type 2 (here termed "garden variety") are abundant in the zircon separates. Type 2 zircons, are typically euhedral and have cores with variable zoning patterns. Cores have thin CL-bright mantles surrounded by oscillatory-zoned overgrowths (Figure 13). Type 2 zircons have edges with relatively high Yb/Gd ratios (≈20-30), > 100 ppm U (mostly 300-400 ppm), relatively high Hf (> 11,000 ppm) and the lowest observed Ti concentrations (≈5 ppm) (Fig. 14). The main feature separating Type 2 from Type 1 zircons is a gap normal to the overall trend of all edge analyses in Ti vs. Hf, Ti vs. U, and U vs. Yb/Gd plots. The thin CL-bright mantle suggests a punctuated chemical and/or thermal change in melt composition following the resorption of the cores of the Type 2 zircons.

Type 3. Zircons designated as Type 3 have continuous, uninterrupted zoning from core to rim (Fig. 13). Type 3 zircons are abundant in distal pumice in unidentified aggregates that appear to be glomerocrysts of various mineral phases, but less common in pumice collected proximal to the caldera. Type 3 zircons have the greatest range in trace element concentrations from core to rim. The majority of Type 3 zircons have compositional similarity to Type 2 garden-variety zircon, and rarely to Type 1b compositions (Fig. 14). The primary reason for separating Type 2 from Type 3 zircons is based on their textural appearance. Unlike Type 2 zircons, Type 3 show zoning that reflects continuous growth from core to rim.

Cook Canyon Tuff

The Cook Canyon Tuff contains three types of zircon based on CL brightness and trace element content.

Type 1. Type 1 zircons comprise more than 90% of zircon from pumice collected from the Cook Canyon Tuff. Type 1 zircons have CL-bright edges with U concentrations < 125 ppm. Cook Canyon Tuff type 1 zircons have chemically similar edges, however when considering the entire crystal, they differ in textural appearance. Cook Canyon Tuff type 1 zircons are further divided into type 1a and 1b based mainly on textural appearance, but also compositional range. Zircon crystals with edges that have U concentrations > 125 ppm are rare in the Cook Canyon Tuff. These zircons resemble Peach Spring Tuff Type 2 garden variety zircons and are hereafter referred to as Cook Canyon Tuff Type 2 zircon.

Type 1a zircons have CL-dark cores with variable trace element compositions, mantled by thick CL-bright edges. They closely resemble the Peach Spring Tuff Type 1a zircons in appearance and chemistry (Figs. 13 and 14), thus here are referred to as Cook Canyon Tuff Type 1a zircons. Type 1a zircons have edges with low Yb/Gd (5-7) ratios, relatively high Ti (15-22 ppm) concentrations, and low U (≈15-30 ppm) and Hf (≈8200-8700 ppm) concentrations (Fig. 14).

Type 1b zircons typically have subtle zoning and are relatively CL-bright from core to edge, though rare dark cores are observed (Fig.14). Type 1b zircon edges have a very limited range in composition and form a tight cluster on trace element plots (Fig. 14). Type 1b zircons have edges with Yb/Gd ratios that either overlap with Type 1a zircons or are slightly higher. Hf concentrations overlap with Type 1a zircon, but show a narrower range (average: ≈8500 ppm). The primary differences between 1a and 1b zircon edges are U and Ti concentrations. Type 1b zircons have edges with consistently higher U concentrations (≈50-70 ppm) and a narrower range in Ti concentration (≈22-24 ppm) when compared to Type 1a zircons.

It is interesting to note that Cook Canyon Tuff Type 1a and Peach Spring Tuff Type 1a zircons are similar in appearance and share nearly identical trace element chemical characteristics. On the other hand, Type 1b zircons from each tuff have edges with contrasting trace element compositions (Fig. 14).

Type 2. Type 2 zircons are rare in Cook Canyon Tuff. They lack CL-bright rims and are texturally similar to Type 2 garden-variety zircons in Peach Spring Tuff. Type 2 zircon rims have nearly identical Yb/Gd, and similar Hf, Ti and U concentrations as Peach Spring Tuff Type 1b and 2.

It is noteworthy that the cores of all Peach Spring Tuff and Cook Canyon Tuff zircon overlap in composition and worth reiterating that the zircon types are distinguished by rim/edge chemistry.

SIMS U-Pb zircon geochronology

SIMS Results for all pumices from Cook Canyon and the Peach Spring Tuff for both chemically abraded and non-chemically abraded data are presented below in Figures 15-24. Ages for the Peach Spring Tuff were also compared for individual pumices and on the basis of geographical proximity to the caldera, but there are no statistically distinguishable differences between the samples. A complete data set is included in Appendix B for the interested reader. Zircon petrography and geochemistry (i.e. zircon Types) bear on the interpretation of these Results as presented in the Discussion.

Cook Canyon Tuff Zircon: No chemical abrasion

Sectioned zircons. ^{207}Pb-corrected $^{206}Pb/^{238}U$ ages from SIMS analyses of *all* sectioned zircons from all pumice collected from the Cook Canyon Tuff range from 17.49 ± 1.40 Ma to 19.84 ± 1.38 Ma, with a weighted mean age of 18.82 ± 0.22 Ma, MSWD = 1.5 (n = 23; 95% confidence interval). The disequilibrium-corrected weighted mean age is 18.90 ± 0.22 Ma (Fig. 15).

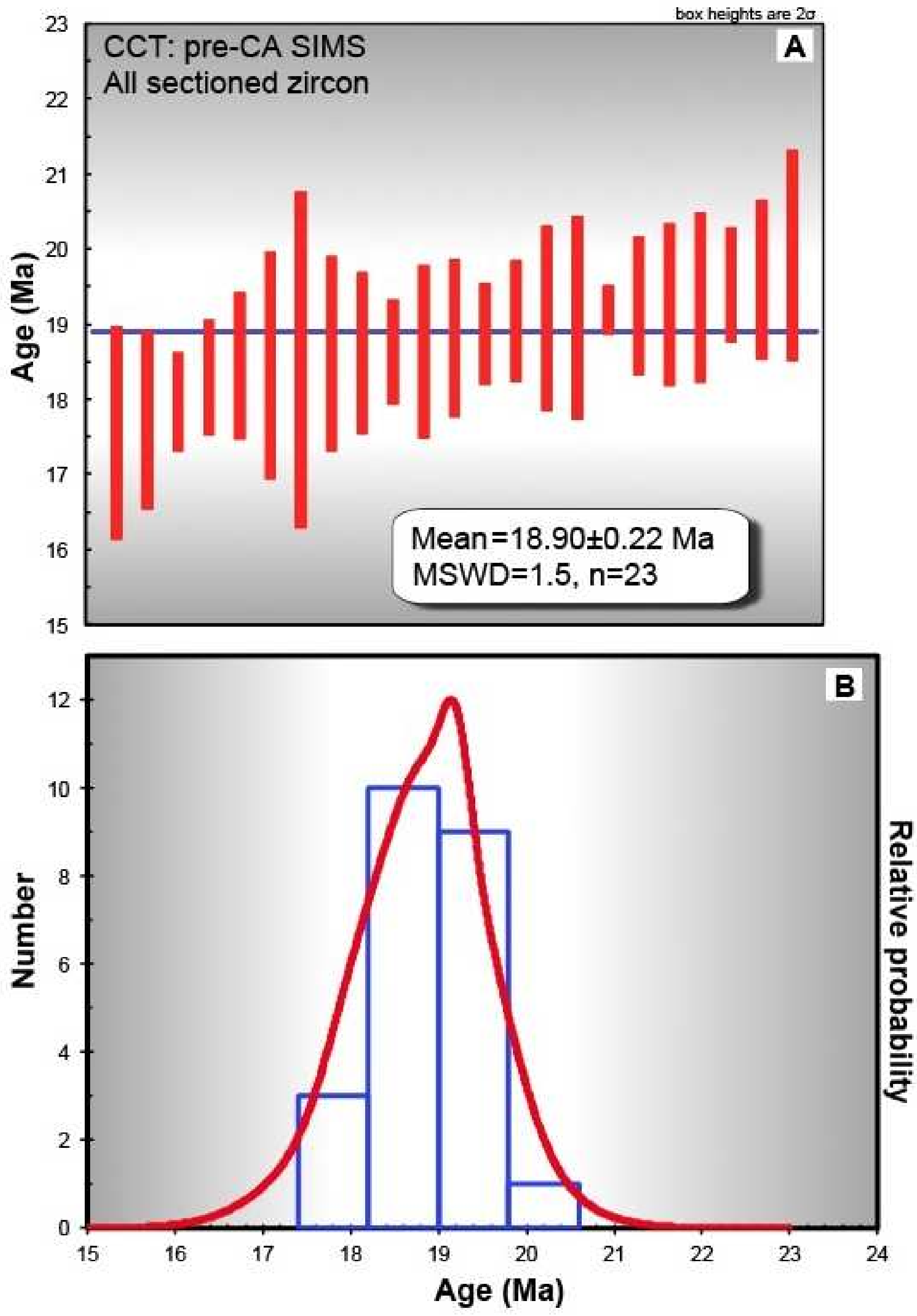

Figure 15. Pre-CA SIMS results for sectioned Cook Canyon Tuff zircon. (A) Plot of U-Pb ages showing individual data points (red bars) and the weighted mean. (B) Histograms with cumulative probability overlay. All ages are corrected for disequilibrium.

^{207}Pb-corrected ^{206}Pb/^{238}U ages from SIMS analyses of zircon *cores* from *all* pumice range from 17.92 ± 0.64 Ma to 19.45 ± 0.76 Ma with a weighted mean age of 18.84 ± 0.26 Ma, MSWD = 1.5 (n = 14; 95% confidence interval). The disequilibrium-corrected weighted mean age is 18.93 ± 0.26 Ma (Fig.16A).

^{207}Pb-corrected ^{206}Pb/^{238}U ages from SIMS analyses of zircon *interiors* from *all* pumice range from 18.39 ± 0.96 Ma to 19.84 ± 1.38 Ma with a weighted mean age of 18.88 ± 0.40 Ma, MSWD = 0.79 (n = 6; 95% confidence interval). The disequilibrium-corrected weighted mean age is 18.95 ± 0.40 Ma (Fig. 16B).

^{207}Pb-corrected ^{206}Pb/^{238}U ages from SIMS analyses of zircon *edges* from *all* pumice range from 17.47 ± 1.40 Ma to 19.51 ± 1.04 Ma and yield weighted mean age of 18.40 ± 2.9 Ma, MSWD = 3.9 (n = 3; 95% confidence interval). The disequilibrium-corrected weighted mean age is 18.50 ± 2.9 Ma (Fig.16 C).

Zircon rims. ^{207}Pb-corrected ^{206}Pb/^{238}U SIMS ages of zircon *rims* from *all* pumice range from 18.72 ± 2.7 Ma to 20.91 ± 1.08 Ma, with a weighted mean age of 19.77 ± 0.48 Ma, MSWD = 0.67 (n = 13; 95% confidence interval). The disequilibrium-corrected weighted mean age is 19.84 ± 0.48 Ma (Fig.16 D).

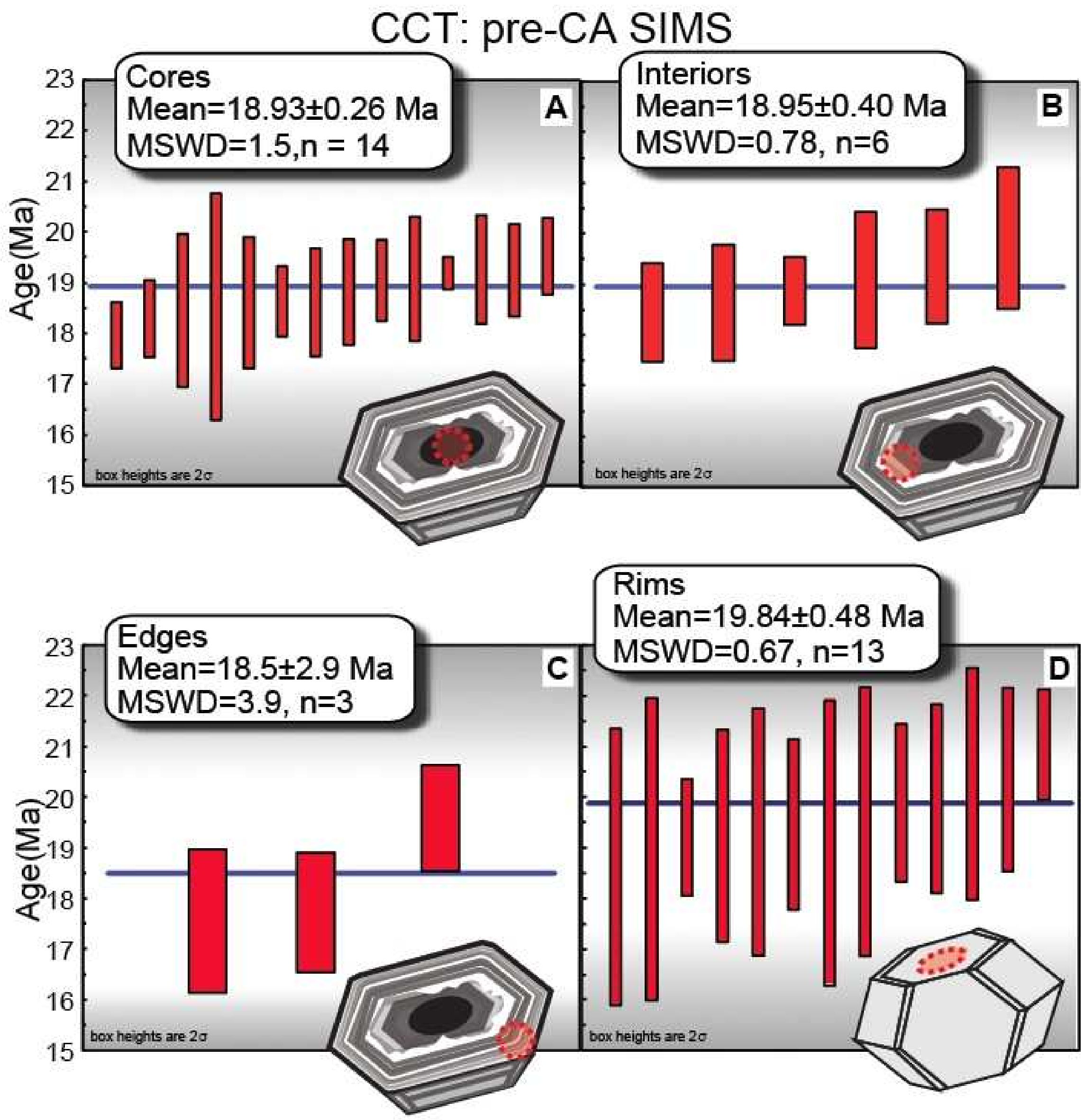

Figure 16. Pre-CA SIMS results for Cook Canyon Tuff (CCT) zircon grouped according to spot location. Plots of U-Pb ages showing individual data points (red bars) and the weighted means for (A) cores, (B) interiors, (C) edges, and (D) rims. All ages are corrected for disequilibrium

Cook Canyon Tuff Zircon: Chemically abraded zircons

Analyses of zircons that were subjected to chemical abrasion were focused on un-polished *rims* and the *edges* of sectioned crystals. Analyses of sectioned cores and interiors were not obtained.

All zircons: rims and edges. ^{207}Pb-corrected ^{206}Pb/^{238}U ages from SIMS analyses of *all* chemically abraded zircons from *all* pumice collected from the Cook Canyon Tuff range from 17.91 ± 2.94 Ma to 21.76 ± 1.02 Ma with a weighted mean age of 19.22 ± 0.35 Ma, MSWD = 2.8 (n = 33; 95% confidence interval). The disequilibrium-corrected weighted mean age is 19.29 ± 0.35 Ma (Fig. 17).

Zircon rims. ^{207}Pb-corrected ^{206}Pb/^{238}U ages from SIMS analyses of the *rims* of chemically abraded zircon range from 17.91 ± 2.94 Ma to 21.48 ± 0.96 Ma, with a weighted mean age of 19.14 ± 0.38 Ma, MSWD = 2.3 (n = 25; 95% confidence interval). The disequilibrium-corrected weighted mean age is 19.22 ± 0.38 Ma (Fig. 18A).

Zircon edges. ^{207}Pb-corrected ^{206}Pb/^{238}U ages from SIMS analyses of the *edges* of chemically abraded zircon range from 18.07 ± 1.02 Ma to 21.76 ± 1.02 Ma with a weighted mean age of 19.4 ± 1.1 Ma, MSWD = 4.8 (n = 8; 95% confidence interval). The disequilibrium-corrected weighted mean age is 19.5 ± 1.1 Ma (Fig. 18B).

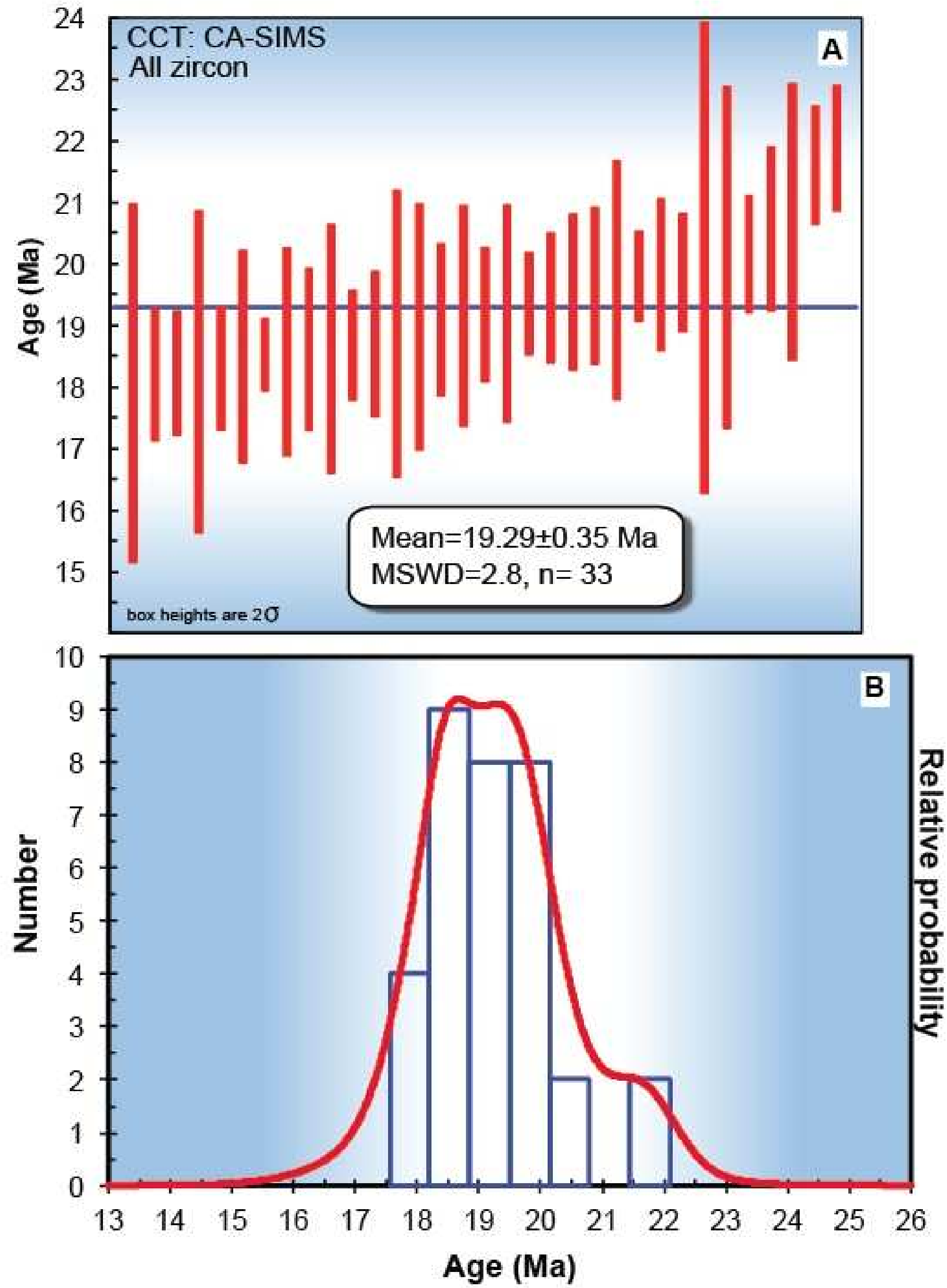

Figure 17. CA-SIMS results for all Cook Canyon Tuff (CCT) zircon. (A) Plot of U-Pb ages showing individual data points (red bars) and the weighted mean. (B) Histograms with cumulative probability overlay. All ages are corrected for disequilibrium..

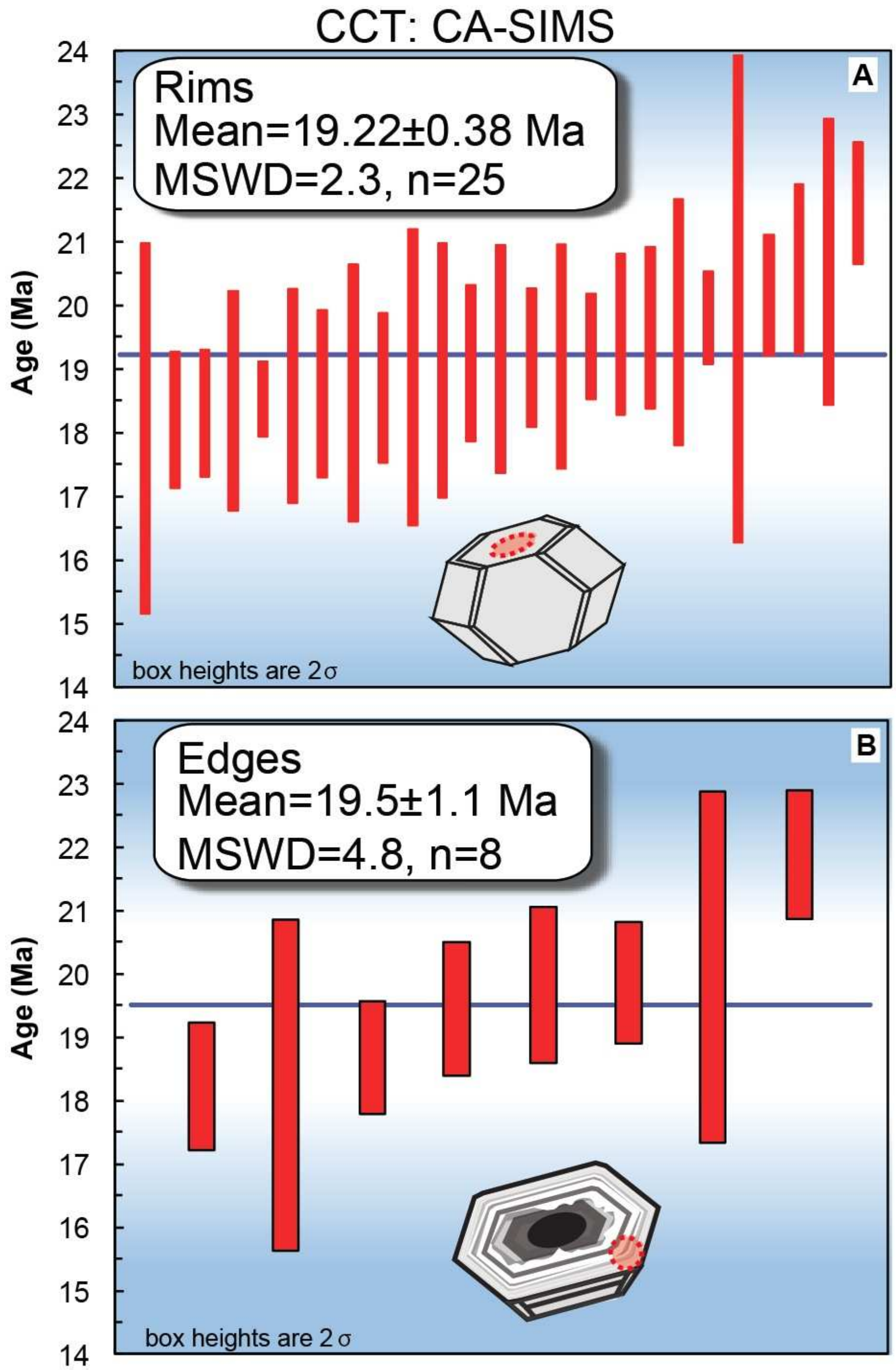

Figure 18. CA-SIMS results for Cook Canyon Tuff Zircon rims (A) and edges (B). Plots of U-Pb ages showing individual data points (red bars) and the weighted means. All ages are corrected for disequilibrium.

Peach Spring Tuff Zircon: No chemical abrasion

Sectioned zircons. ^{207}Pb-corrected ^{206}Pb/^{238}U ages from SIMS analyses of *all* sectioned zircons from *all* pumice collected from the Peach Spring Tuff range from 16.75 ± 1.18 Ma to 1751.66 ± 21.94 Ma (^{207}Pb/^{206}Pb age: 2195 ± 184 Ma). Five Proterozoic crystals yield a ^{207}Pb/^{206}Pb weighted mean age of 1485 ± 190 Ma, MSWD = 143 (n = 5; 95% confidence interval) (Fig. 19). Miocene zircon range in age from 16.75 ± 1.18 Ma to 19.69 ± 0.94 Ma, and yield a weighted mean ^{207}Pb-corrected ^{206}Pb/^{238}U age of 18.65 ± 0.10 Ma, MSWD = 2.2 (n = 119; 95% confidence interval). The disequilibrium-corrected weighted mean age is 18.72 ± 0.10 Ma (Fig. 20).

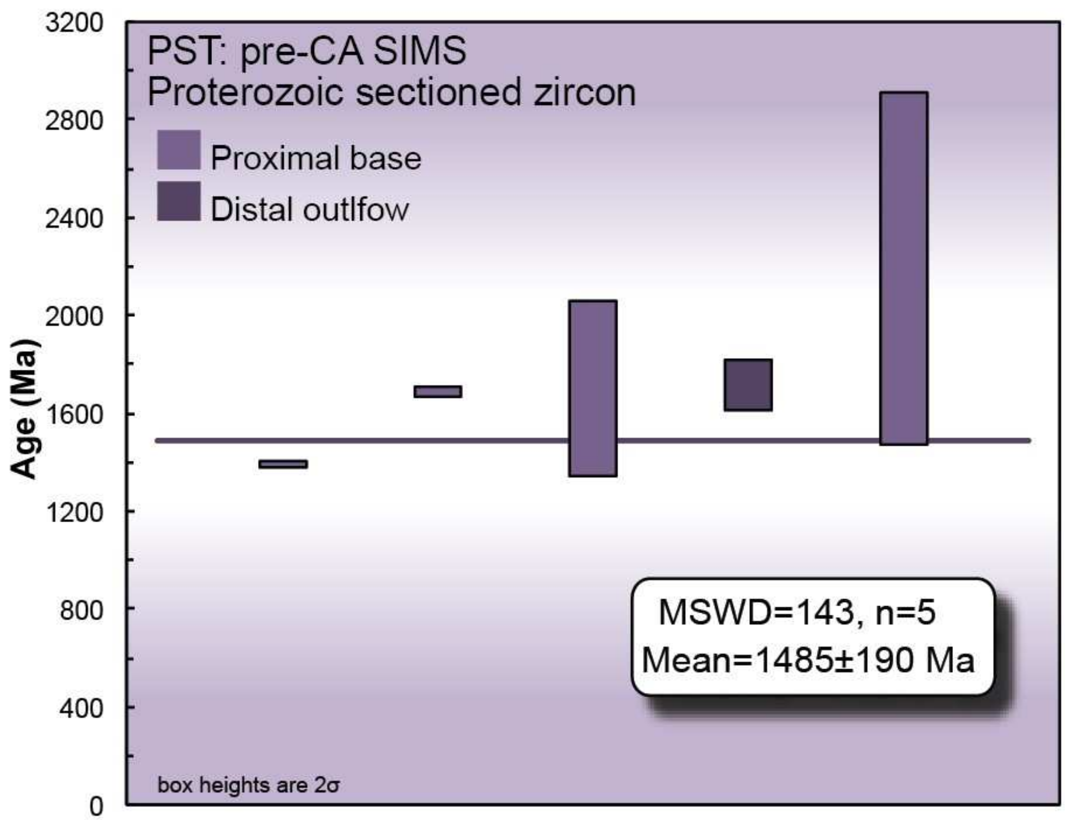

Figure 19. Peach Spring Tuff (PST) pre-CA SIMS results for Proterozoic sectioned-zircon.

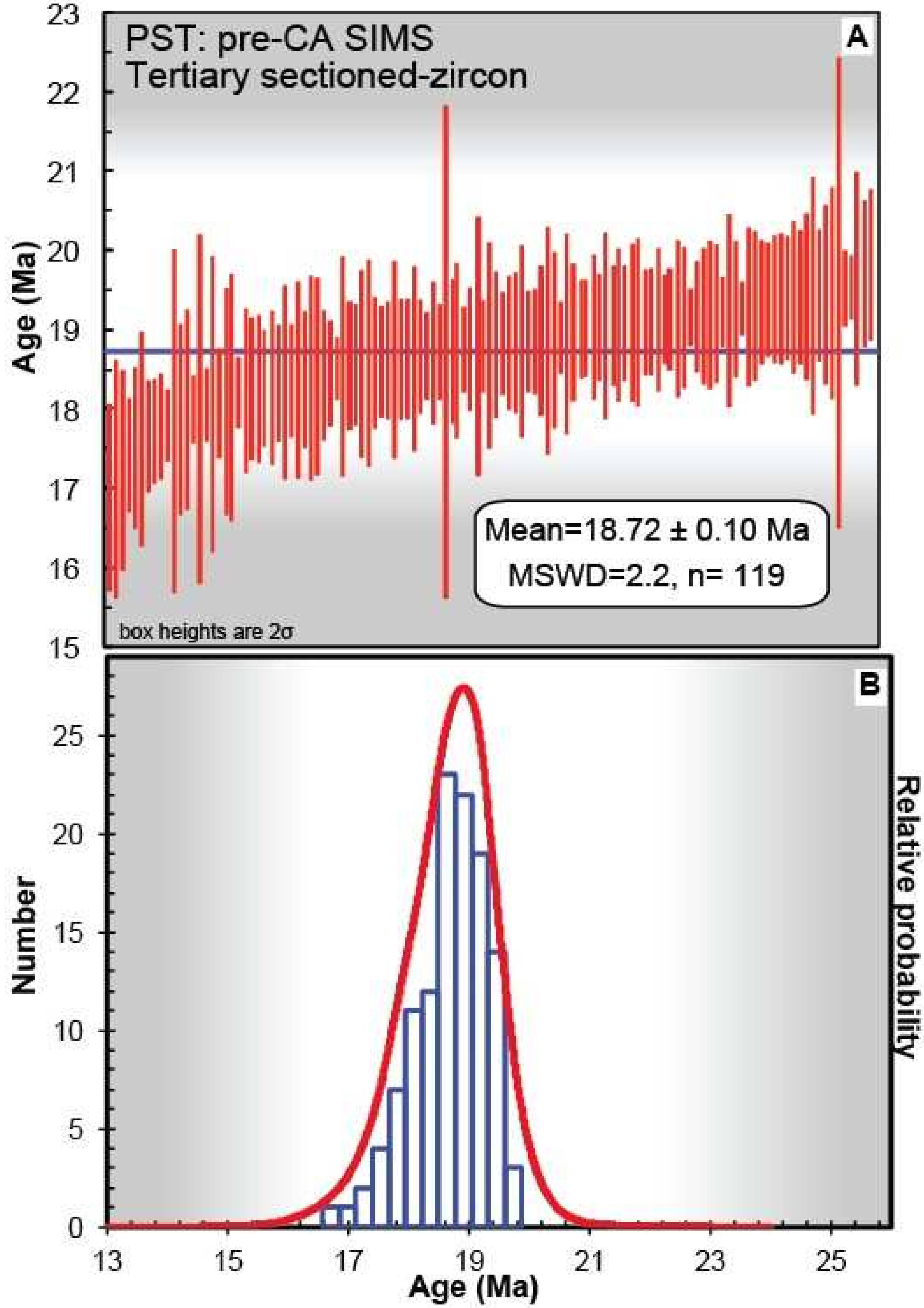

Figure 20. Peach Spring Tuff (PST) pre-CA SIMS results for Tertiary sectioned-zircon. (A) Plot of U-Pb ages showing individual data points (red bars) and the weighted mean. (B) Histograms with cumulative probability overlay All ages are corrected for disequilibrium.

^{207}Pb-corrected ^{206}Pb/^{238}U ages from SIMS analyses of individual zircon *cores* from *all* pumice range from 16.75 ± 1.18 Ma to 19.59 ± 0.92 Ma with a weighted mean age of 18.66 ± 0.14 Ma, MSWD = 2.6 (n = 72; 95% confidence interval). The disequilibrium-corrected weighted mean age is 18.73 ± 0.14 Ma (Fig. 21A).

^{207}Pb-corrected ^{206}Pb/^{238}U ages from SIMS analyses of individual zircon *interiors* from *all* pumice, range from 17.66 ± 0.44 Ma to 19.29 ± 0.82Ma with a weighted mean age of 18.67 ± 0.19 Ma, MSWD = 1.4 (n = 24; 95% confidence interval). The disequilibrium-corrected weighted mean age is 18.75 ± 0.19 Ma (Fig. 21B).

^{207}Pb-corrected ^{206}Pb/^{238}U ages from SIMS analyses of individual *edges* from *all* pumice range from 17.08 ± 1.26 Ma to 19.69 ± 0.94 Ma and yield weighted mean age of 18.56 ± 0.25 Ma, MSWD = 1.6 (n = 23; 95% confidence interval). The disequilibrium-corrected weighted mean age is 18.65 ± 0.25 Ma (Fig. 21C).

Zircon rims. ^{207}Pb-corrected ^{206}Pb/^{238}U ages from SIMS analyses of zircon *rims* from *all* Peach Spring Tuff pumice range from 13.16 ± 3.25 Ma to 1751.07 ± 88.89 Ma (^{207}Pb/^{206}Pb age = 2855 ± 184 Ma). Fifteen Proterozoic crystals yield a ^{207}Pb/^{206}Pb weighted mean age of 1680 ± 31 Ma, MSWD = 16 (n = 15; 95% confidence interval) (Fig. 22). Crystals that yield Tertiary dates range in age from 13.16 ± 3.25 Ma to 20.45 ± 6.06, and yield a ^{207}Pb-corrected ^{206}Pb/^{238}U weighted mean age of 18.64 ± 0.29 Ma, MSWD = 2.4 (n = 42; 95% confidence interval). The disequilibrium-corrected weighted mean age is 18.73 ± 0.29 Ma (Fig. 21D).

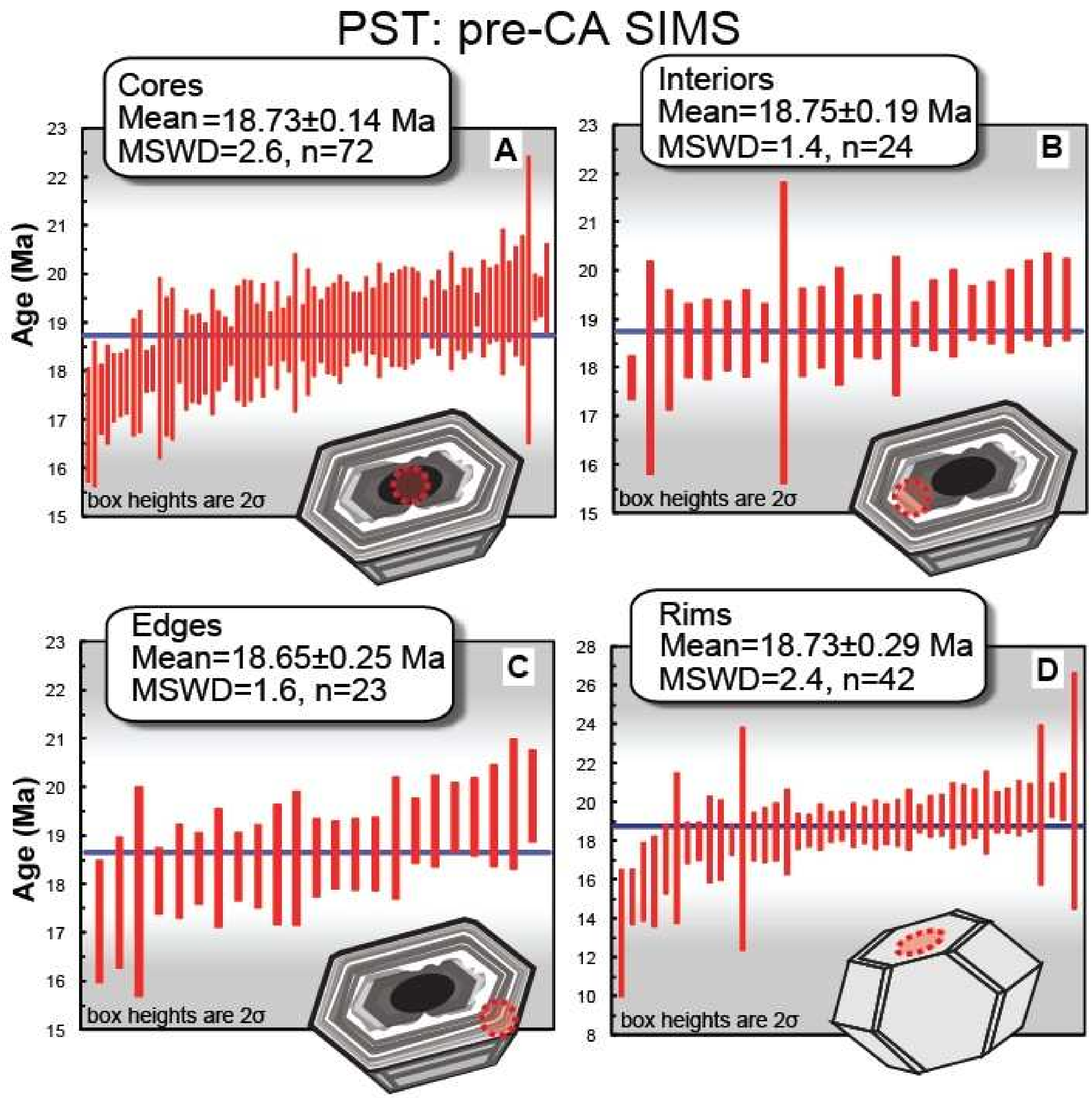

Figure 21. Pre-CA SIMS results for Peach Spring Tuff (PST) sectioned zircon grouped according to spot location. Plots of U-Pb ages showing individual data points (red bars) and the weighted means for (A) cores, (B) interiors, (C) edges, and (D) rims. All ages are corrected for disequilibrium.

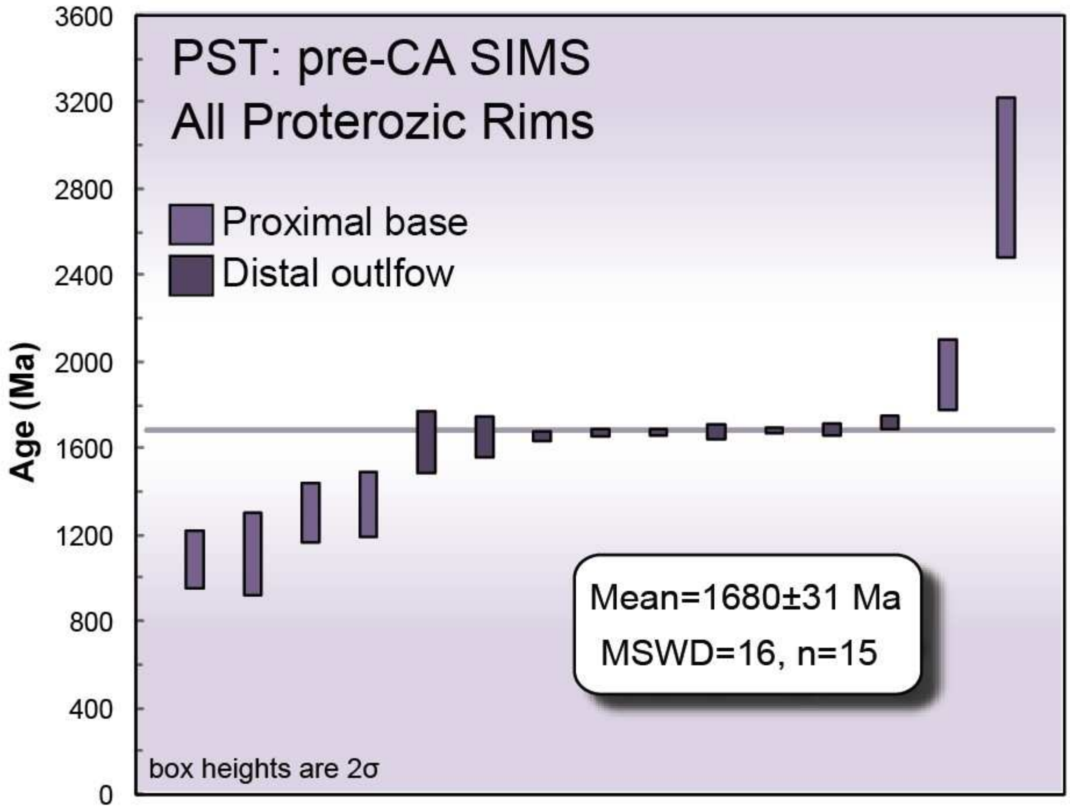

Figure 22. Pre-CA SIMS results from Proterozoic zircon rims in the Peach Spring Tuff (PST).

Peach Spring Tuff Zircon: Chemically abraded zircons

Analyses of zircons that were subjected to chemical abrasion were focused on un-polished *rims* and the *edges* of sectioned crystals. Analyses of sectioned cores and interiors were not obtained.

All zircons: rims and edges. ^{207}Pb-corrected $^{206}Pb/^{238}U$ ages from SIMS analyses of *all* chemically abraded zircon from *all* Peach Spring Tuff pumice range from 16.40 ± 2.0 Ma to 22.28 ± 4.44 Ma, with a weighted mean age of 18.74 ± 0.22 Ma, MSWD = 4.4 (n = 65; 95% confidence interval). The disequilibrium-corrected weighted mean age is 18.84 ± 0.22 (Fig. 23).

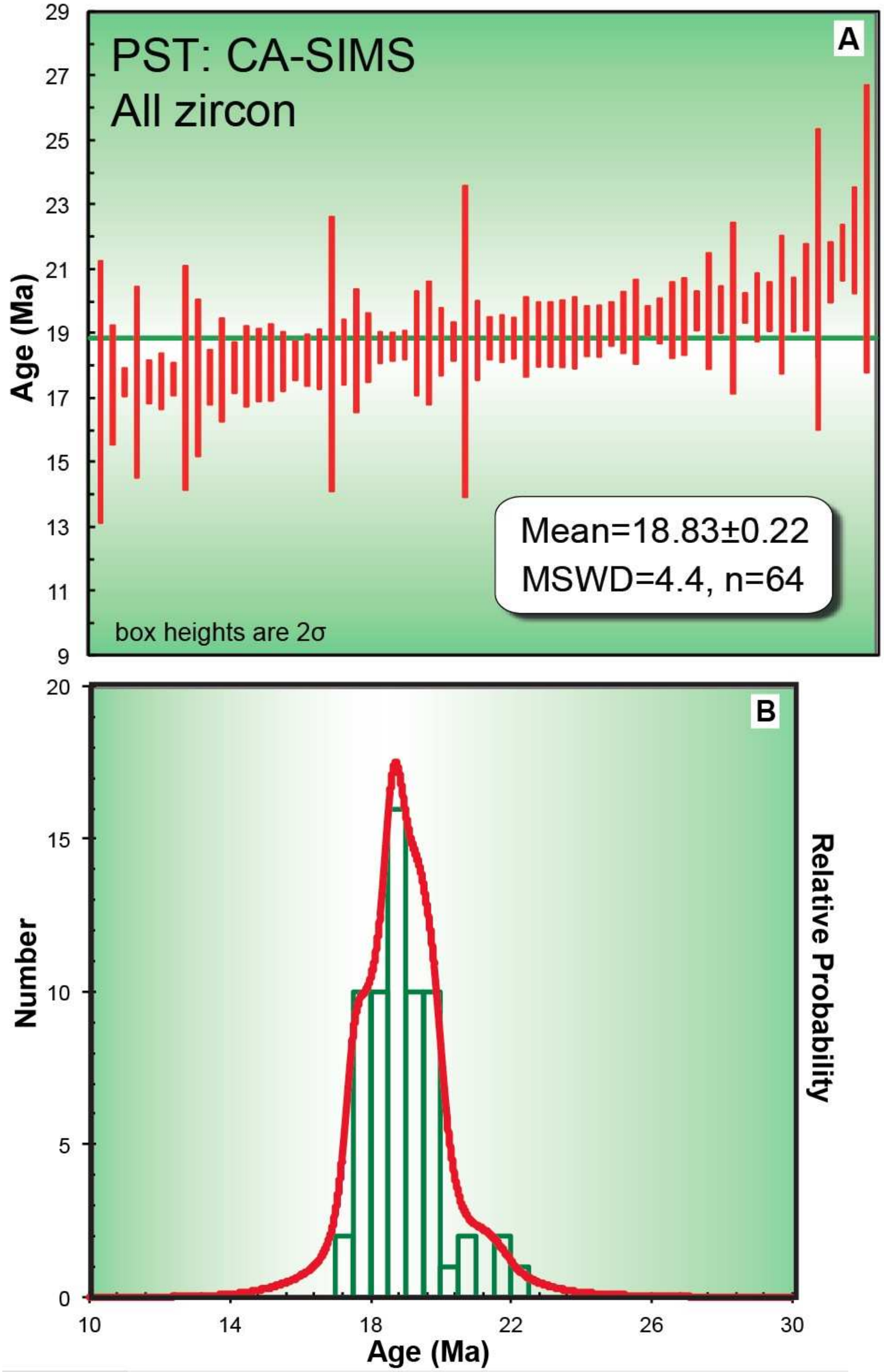

Figure 23. Peach Spring Tuff (PST) chemically abraded (CA)-SIMS results. (A) Plot of U-Pb ages showing individual data points (red bars) and the weighted mean. (B) Histograms with cumulative probability overlay. All ages are corrected for disequilibrium.

Zircon rims. ^{207}Pb-corrected ^{206}Pb/^{238}U ages from SIMS analyses of the *rims* of chemically abraded zircon from *all* Peach Spring Tuff pumice range from 17.34 ± 1.86 Ma to 21.44 ± 0.86 Ma, with a ^{207}Pb-corrected ^{206}Pb/^{238}U weighted mean age of 18.69 ± 0.26 Ma, MSWD = 4.6 (n = 43; 95% confidence interval). The disequilibrium-corrected weighted mean age is 18.78 ± 0.26 (Fig. 24A).

Zircon edges. ^{207}Pb-corrected ^{206}Pb/^{238}U ages from SIMS analyses of the *edges* of sectioned chemically abraded zircon from *all* Peach Spring Tuff pumice range from 16.40 ± 2.0 Ma to 22.18 ± 4.44 Ma, with a ^{207}Pb-corrected ^{206}Pb/^{238}U weighted mean age of 18.87 ± 0.42 Ma, MSWD = 4.6 (n = 21; 95% confidence interval). The disequilibrium-corrected weighted mean age is 18.98 ± 0.42 (Fig. 24B.)

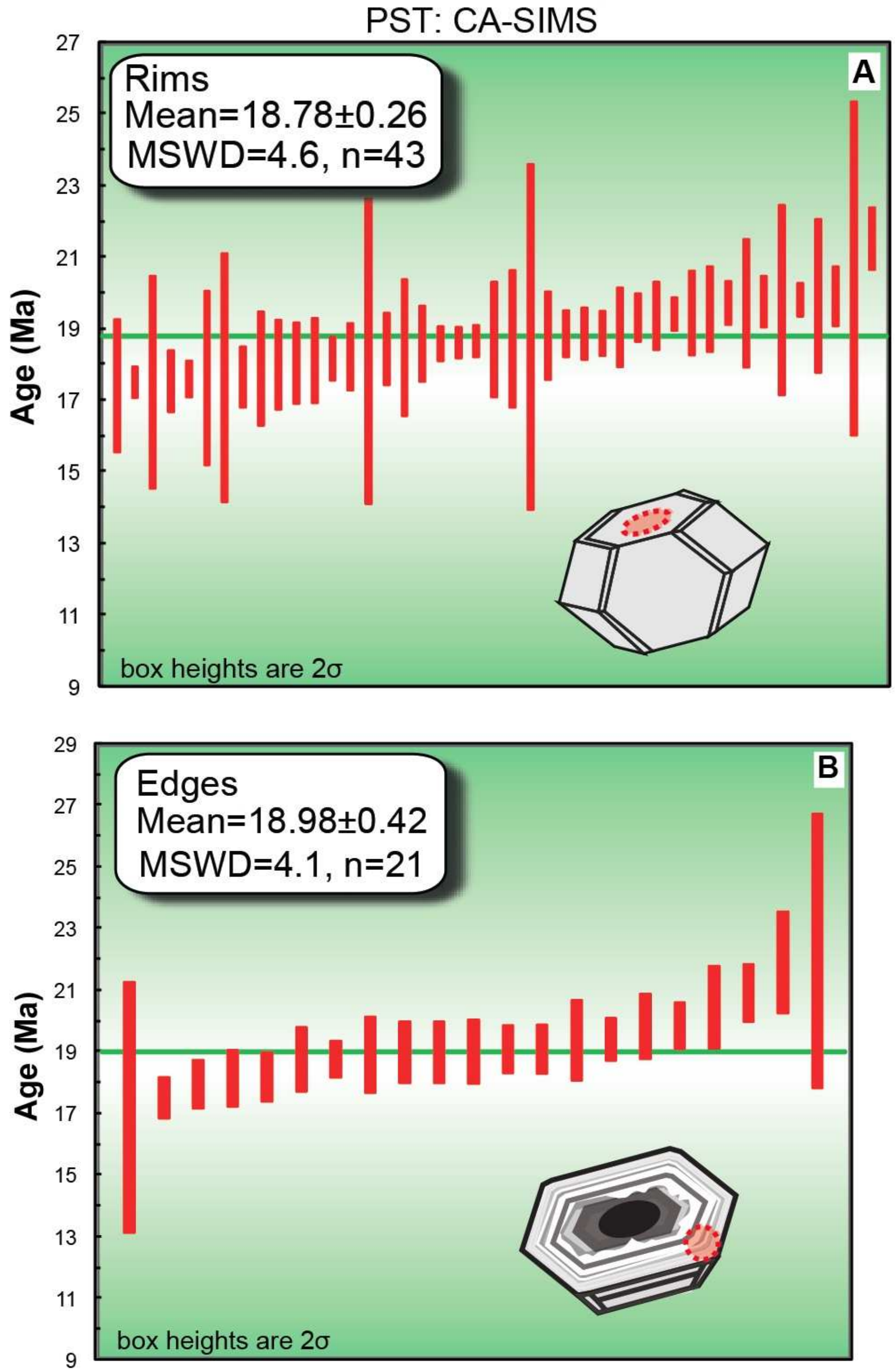

Figure 24. Peach Spring Tuff (PST) CA-SIMS results for zircon rims (A) and zircon edges (B). Plots of U-Pb ages showing individual data points (red bars) and the weighted means. All ages are corrected for disequilibrium.

TIMS U-Pb zircon geochronology

The results of total dissolution CA-TIMS are presented below and in Figures 25 and 26. As with the SIMS analysis, the ages reported represent composites from zircons from all samples for the two separate tuffs.

Cook Canyon Tuff Zircon

Disequilibrium- and blank-corrected $^{206}Pb/^{238}U$ ages from CA-TIMS analyses of zircon from pumice collected from the Cook Canyon Tuff range from 18.98 ± 0.22 Ma to 1073.73 ± 0.53 Ma. Three analyses, representing the combined tips of zircon with low-uranium rims (Type 1a), yield $^{206}Pb/^{238}U$ ages of 19.29 ± 0.39 Ma, 19.45 ± 0.26 Ma and 21.38 ± 1.22 Ma. Excluding the single Proterozoic zircon, the weighted mean $^{206}Pb/^{238}U$ age is 19.34 ± 0.31 Ma, MSWD = 5.3 (n = 11; 95% confidence interval) (Fig. 25).

Peach Spring Tuff Zircon

Disequilibrium- and blank-corrected $^{206}Pb/^{238}U$ ages from CA-TIMS analyses of zircon from all pumice collected from the Peach Spring Tuff range from 18.08 ± 0.12 Ma to 22.00 ± 0.53 Ma with a weighted mean age of 18.87 ± 0.19 Ma, MSWD = 40 (n = 21; 95% confidence interval) (Fig. 26). A single analysis represents the combined tips of Type 1a zircon with low-uranium rims and yields a $^{206}Pb/^{238}U$ age of 19.11 ± 0.38 Ma.

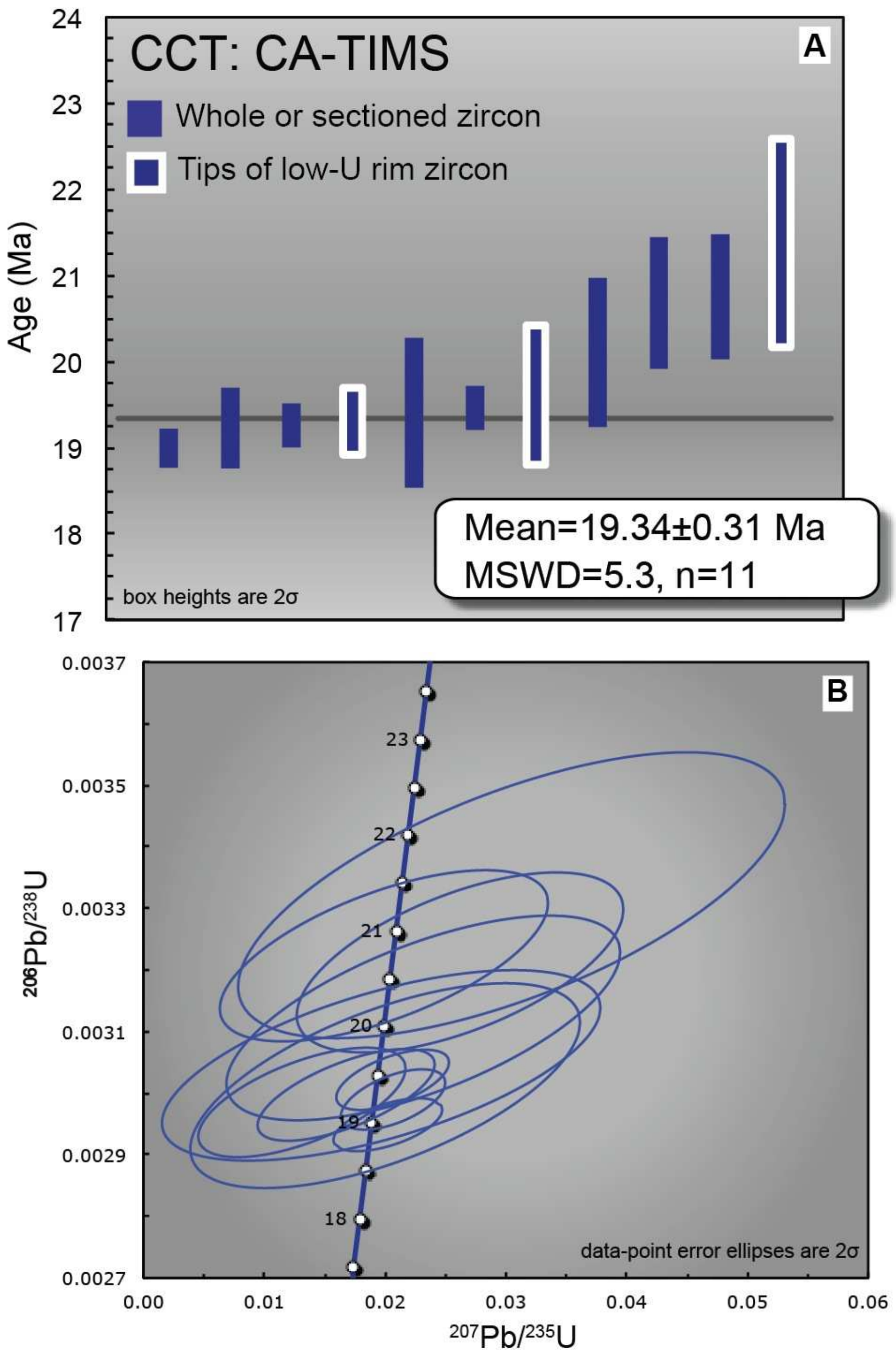

Figure 25. Cook Canyon Tuff (CCT) CA-TIMS results. (A) Plot of U-Pb ages showing individual data points (blue bars) and the weighted mean. (B) Concordia plot of individual analyses (blue ellipses). All ages are corrected for disequilibrium.

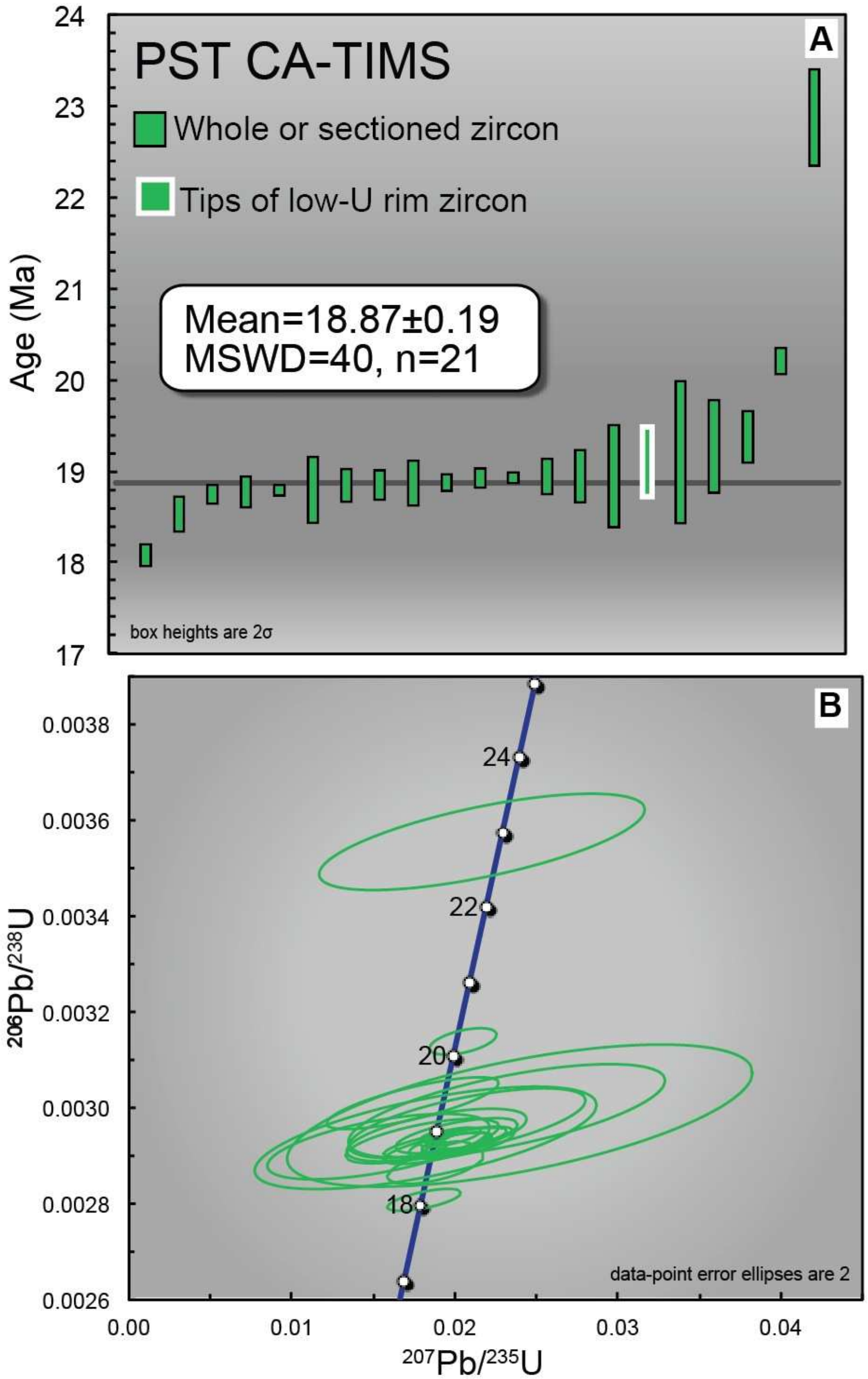

Figure 26. Peach Spring Tuff (PST) CA-TIMS results. (A) Plot of U-Pb ages showing individual data points (green bars) and the weighted mean. (B) Concordia plot of individual analyses (green ellipses). All ages are corrected for disequilibrium.

DISCUSSION

The zircon ages reported above for both the SIMS and TIMS results commonly have MSWD values indicating scatter beyond that explained by analytical uncertainty alone. Such scatter has traditionally been interpreted to reflect either Pb-loss (e.g., Mattinson, 1994; McClelland and Mattinson, 1996) or inheritance (e.g., Gulson and Krogh, 1973; Bachmann et al., 2010), often leading to discordant U-Pb zircon data.

The dramatic increase in analytical precision now achieved by conventional U-Pb ID-TIMS analysis shows clearly that single zircon crystals in a single rock sample may also yield a range of *concordant* crystallization ages that reflect the assembly and evolution of the magma system (e.g., Rivera et al., 2013, 2014; Wotzlaw et al., 2013). Additionally, SIMS dating of young zircon employing both U-Pb and U-Th analysis demonstrates that zircons may grow over several 10^5 years in a common magma system (e.g., Reid et al., 1997; Vazquez and Reid, 2002; Miller and Wooden, 2004; Charlier et al., 2005; Schmitt et al., 2010) and be recycled into later pulses or increments of magma (e.g., Bacon and Lowenstern, 2005; Claiborne et al., 2010; Charlier et al., 2010; Stelten and Cooper, 2012).

Because the TIMS U-Pb ages for the Peach Spring and Cook Canyon Tuffs are concordant within error (Fig. 27), the scatter must be due to either: 1) minor Pb-loss that does not result in discernible U-Pb age discordance; 2) protracted autocrystic crystallization of zircon within the magma chamber; or 3) recycling of earlier-formed antecrystic zircon in later pulses of magma as the magma systems that produced the ignimbrites were being constructed (e.g., Miller et al., 2007), or some combination of these. In addition, for the Peach Spring Tuff, there is marked age discordance between much of the U-Pb zircon data and the 18.78 ± 0.02 Ma $^{40}Ar/^{39}Ar$ sanidine age of Ferguson et al. (2013), including dates that scatter to values younger than 18.78 Ma. There are no high-precision sanidine $^{40}Ar/^{39}Ar$ dates for the Cook Canyon Tuff.

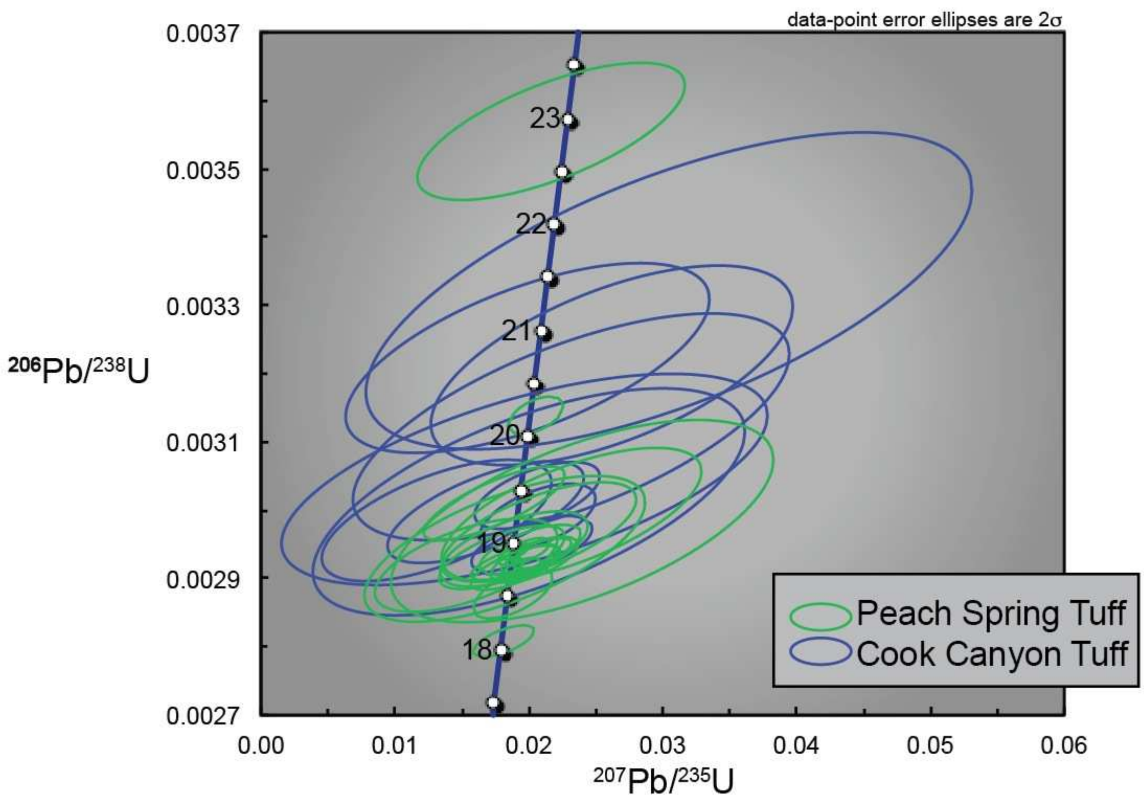

Figure 27. Peach Spring Tuff (PST) and Cook Canyon Tuff (CCT) CA-TIMS results showing concordance of the data. All ages are corrected for disequilibrium.

Interpretation of the data requires resolution of the cause(s) for the excess scatter, because one of the primary goals of this thesis is to determine a precise and accurate timescale for the assembly and residence time of the giant magma body that produced the Peach Spring supereruption, and the earlier, more modest-sized Cook Canyon eruption. Much of the remainder of the Discussion explores the different possibilities for the age scatter for both tuffs and explores possible causes for the age discordance between the $^{40}Ar/^{39}Ar$ sanidine age (Ferguson et al., 2013) and U-Pb zircon ages for the Peach Spring Tuff, starting with the problem of Pb-loss.

Because the chemical abrasion process is designed to mitigate Pb-loss, it is informative to consider the observations made on zircons subjected to chemical abrasion, as they may provide important context for the age interpretations and the possibility of Pb loss.

Pre- and post-chemical abrasion observations

Scanning electron microscopic images obtained from chemically abraded zircon reveal the majority of (>90%) of Peach Spring Tuff zircon have potentially been affected by Pb-loss (see Appendix F for a full collection of CA-zircon images). Application of the chemical abrasion treatment: 1) etched zircon rims to varying degrees; 2) preferentially dissolved entire portions of crystals with little to no etching on zircon rims; 3) etched the outermost portion of zircon, leaving a spongy texture; 4) completely removed all crystal faces and attacked the crystals so extensively that they are essentially unrecognizable as zircon, and 5) preferentially dissolved cores of sectioned zircon, without attacking rims. In contrast, application of the same chemical abrasion treatment to the Cook Canyon Tuff zircons did not produce many physical effects that could be identified visually for most crystals that were examined (Fig.29 A).

The few zircons in the Cook Canyon Tuff that appeared the most affected by the chemical abrasion treatment (Fig. 29 B), yielded ages that are older than ages obtained from the base of pre-Peach Spring Tuff caldera units (see Fig. 6) as reported in McDowell et al. (2014).

The visual confirmation that Peach Spring Tuff zircon had been etched to highly variable degrees and the extensive attack observed for some of the zircons suggests that the anomalously young ages obtained from both SIMS and TIMS analyses could be attributable to Pb-loss. In addition, most of the SIMS sputter pits that yield spurious dates, i.e. several 10^5 years younger than the 18.78 ± 0.02 Ma $^{40}Ar/^{39}Ar$ sanidine age, are associated with etching and/or preferential annealing by the combined annealing and CA technique, suggesting that the young ages relative to the $^{40}Ar/^{39}Ar$ age are due to Pb loss.

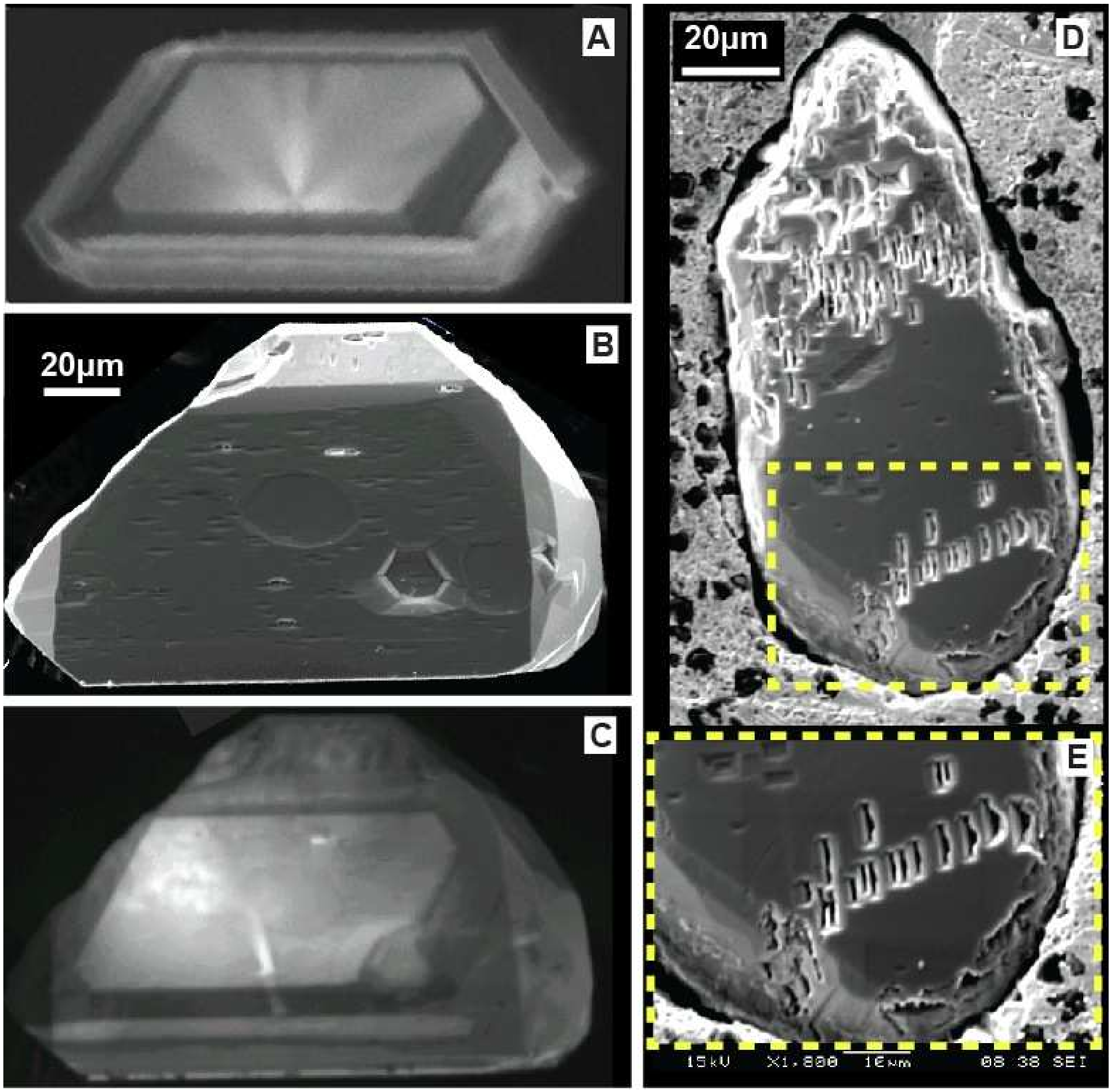

Figure 28. Cathodoluminescence (CL) image (A) of Peach Spring Tuff (PST) zircon prior to SIMS analysis. Post-chemical abrasion secondary electron image (B) and CL (C) of the same zircon as in (A). D) PST zircon showing considerable etching. E) Magnification of yellow dashed box in (D).

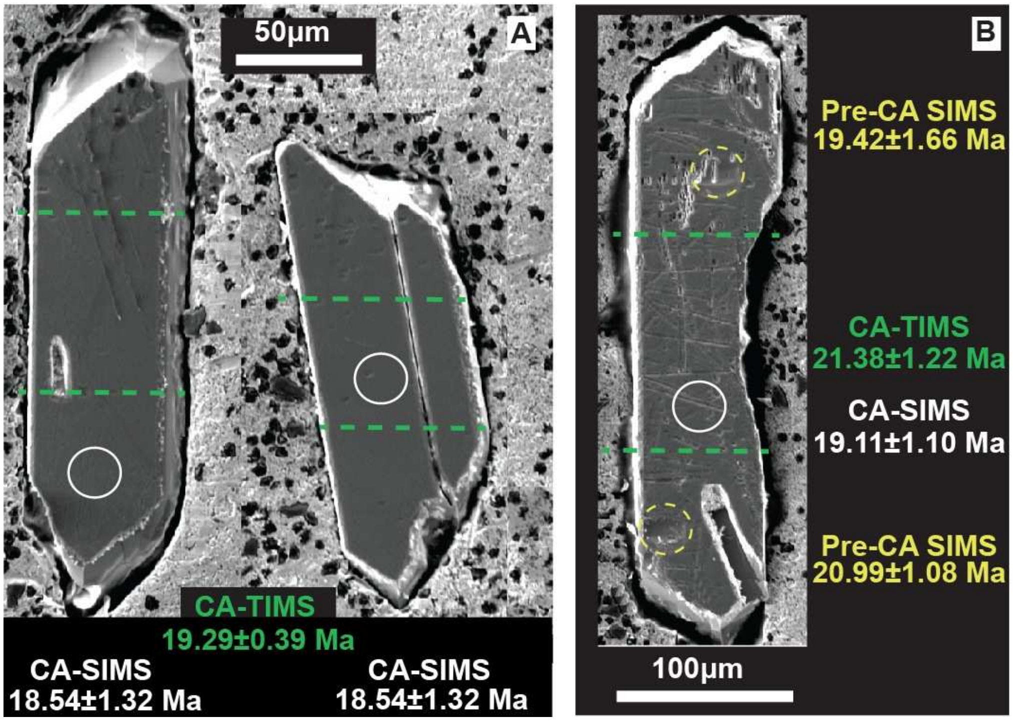

Figure 29. (A) Cook Canyon Tuff Zircons (CCT) unaffected by CA-treatment and (B) most-affected by CA-treatment. Yellow dashed circle denotes pre-CA SIMS analysis spot (note annealed analysis pit). White circles denote CA-SIMS analysis spots. Green dashed-lines indicate where tips were broken off for CA-TIMS analysis. Crystals in (A) were combined with the tips of one other crystal. Tips from zircon in (B) were combined with the tips of two other zircons.

A more detailed crystal-to-crystal comparison was also undertaken for rims from specific zircon crystals. Pre- and post-chemical abrasion ages were obtained from the same crystals. For Peach Spring zircon, the pre-chemical abrasion ages were obtained during two separate sessions to account for any possible systematic age bias between sessions. Because the zircons had to be extracted from the mount for chemical abrasion, and because the Peach Spring Tuff zircons reacted strongly to the chemical abrasion treatment, it was not possible to visually correlate every chemically abraded-zircon to its untreated counterpart. After chemical abrasion, 13 Peach Spring Tuff and five Cook Canyon Tuff zircons could be recognized and thus compared with their pre-chemical abrasion counterparts. Some, but not all, anomalously young Peach Spring Tuff zircon rim ages (< ca. 18 Ma) obtained prior to CA-treatment, shifted to older (> ca. 20 Ma) ages. Greater differences are observed in pre- versus post-CA ages of the Peach Spring Tuff zircon, whereas the Cook Canyon Tuff zircon ages hardly changed.

Prior to chemical abrasion treatment, disequilibrium corrected ages from SIMS analyses of individual zircon rims (6 spots on 5 zircons) from the Cook Canyon Tuff ranged from 18.80 ± 2.7 Ma to 20.99 ± 1.08 Ma, with a ^{207}Pb-corrected ^{206}Pb/^{238}U weighted mean age of 19.83 ± 0.99 Ma, MSWD = 1.5 (n = 6; 95% confidence interval) (Fig. 30 A). SIMS analyses of the same zircon rims after chemical abrasion range from 18.80 ± 2.34 Ma to 20.51 ± 1.34 Ma, with a ^{207}Pb-corrected ^{206}Pb/^{238}U weighted mean age of 19.66 ± 0.51 Ma, MSWD = 0.80 (n = 5; 95% confidence interval) (Fig. 30 B).

Prior to chemical abrasion treatment, disequilibrium corrected ages from SIMS analyses of individual zircon rims (19 spots on the 13 identifiable zircons) from the Peach Spring Tuff ranged from 13.24 ± 4.42 Ma to 20.53 ± 6.06 Ma, with a ^{207}Pb-corrected ^{206}Pb/^{238}U weighted mean age of 18.52 ± 0.48 Ma, MSWD = 1.8 (n = 19; 95% confidence interval)(Fig. 31A). SIMS analyses (14 spots on 13 crystals) of the same zircon rims after chemical abrasion range from 17.51 ± 0.44 Ma to 21.53 ± 0.86 Ma, with a ^{207}Pb-corrected ^{206}Pb/^{238}U weighted mean age of 18.74 ± 0.60 Ma, MSWD = 8.1 (n = 14; 95% confidence interval) (Fig. 31 B).

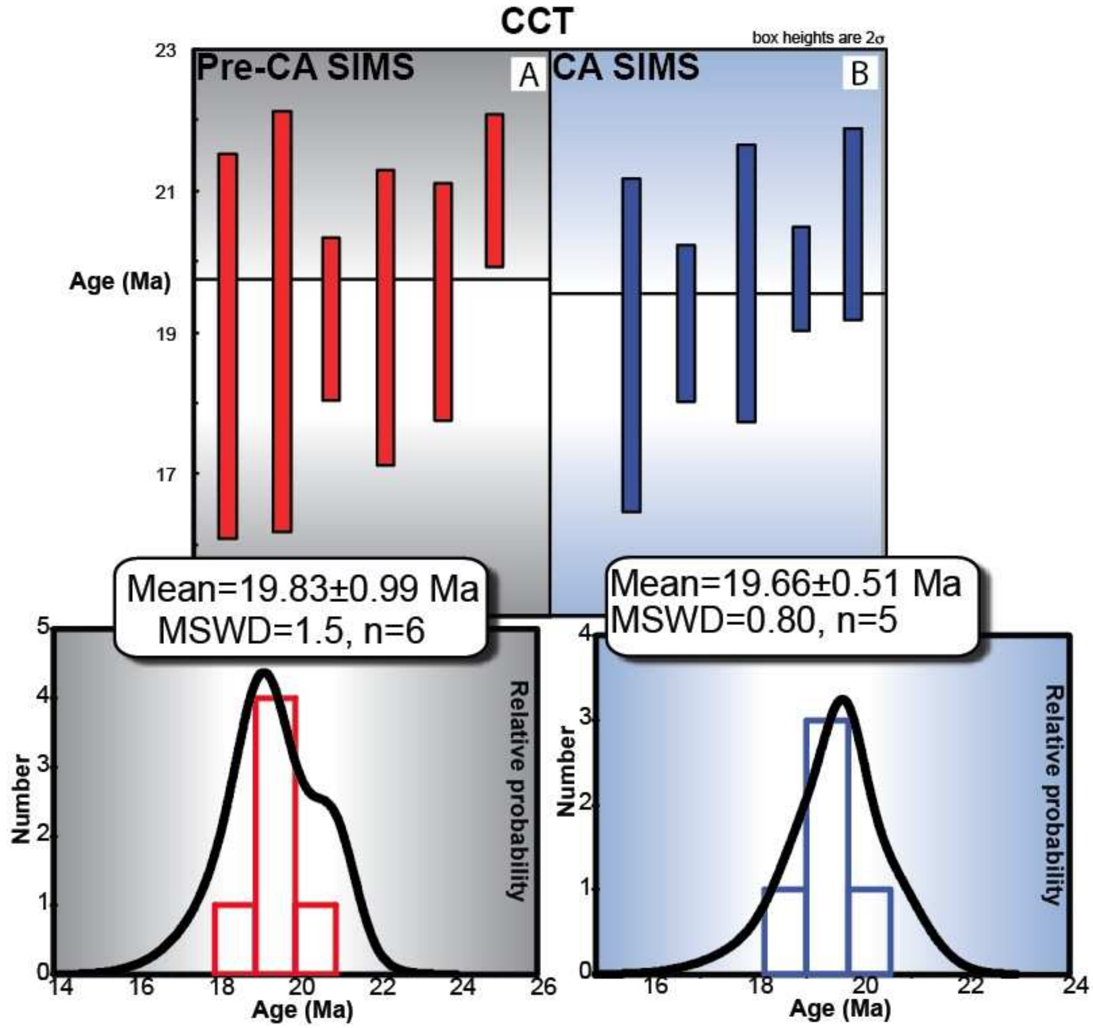

Figure 30. Cook Canyon Tuff (CCT) comparison of pre-CA SIMS (A) to CA-SIMS analyses (B) of the same zircon crystals. Plots of U-Pb ages (top) showing individual data points (red bars for pre-CA and Blue bars for CA-SIMS) and the weighted mean for each and histograms with cumulative probability overlays (bottom) All ages are corrected for disequilibrium.

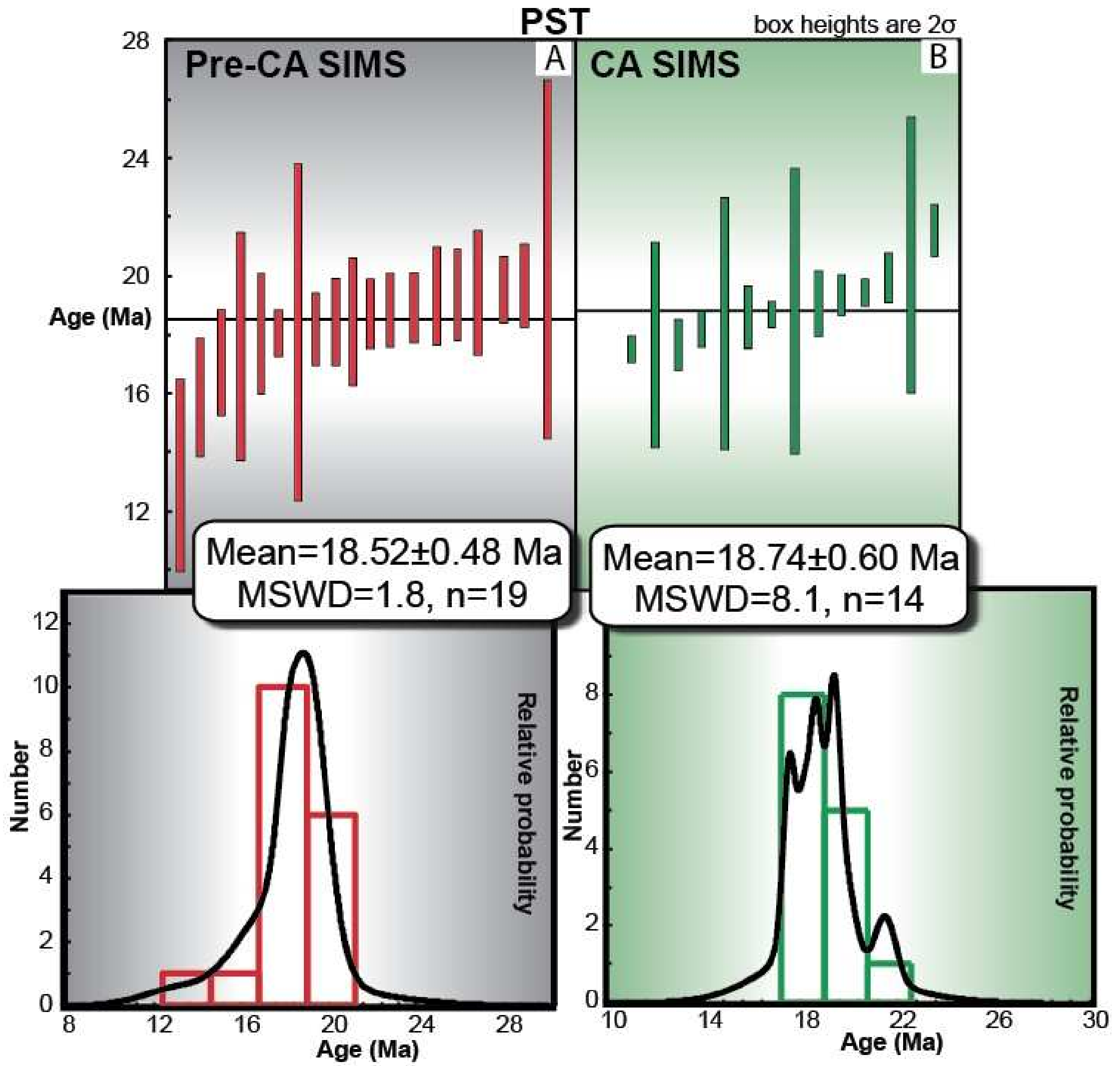

Figure 31. Peach Spring Tuff (PST) comparison of pre-CA SIMS (A) to CA-SIMS analyses (B) of the same zircon crystals. Plots of U-Pb ages (top) showing individual data points (red bars for pre-CA and Blue bars for CA-SIMS) and the weighted mean for each and histograms with cumulative probability overlays (bottom). All ages are corrected for disequilibrium.

For Peach Spring Tuff analyses, the age range post-chemical abrasion shows a shift to an older range suggesting that lead loss has affected the rims. However, the weighted means for pre- and post-chemical abrasion for the zircons overlap within error, and for most individual zircon spot analyses, the CA-SIMS ages are within error of the age obtained during at least one of the pre-CA SIMS analytical sessions. The most significant result is that precision is significantly increased after chemical abrasion treatment for most zircons, except the Type 1 zircons with very low-U rims.

The pre- and post-CA comparison of specific zircons as well as comparisons of the weighted mean age from pre- and post-CA demonstrates that the chemical abrasion process likely helps to mitigate the effects of lead loss, and that zircons from the Peach Spring Tuff were affected by Pb loss, but perhaps the least ambiguous example of Pb-loss comes from the two youngest and precise CA-TIMS ages for Peach Spring Tuff zircon. The dates for these two zircons are 18.08 ± 0.12 Ma and 18.53 ± 0.19 Ma, and thus post-date the 18.78 ± 0.02 Ma $^{40}Ar/^{39}Ar$ sanidine age reported by Ferguson et al. (2013) by 700 ± 61 k.y. and 250 ± 100 k.y., respectively. Given the precision of these ages, it is likely that they have been affected by Pb-loss that was not completely removed by the chemical abrasion process. Several ID-TIMS studies note that a minority of zircon may retain domains with Pb-loss despite application of the chemical abrasion technique (e.g., Davydov et al., 2010; Schoene et al., 2010; Meyers et al., 2012). Kryza et al. (2012) observed a similar phenomenon, where SIMS analyses of chemically abraded zircon shifted the dominant population to older ages but did not completely remove the effects of Pb-loss from all crystals.

Complications with the interpretation of U-Pb and $^{40}Ar/^{39}Ar$ age discordance

As noted above, zircon ages that postdate a sanidine $^{40}Ar/^{39}Ar$ age are perhaps most simply explained by incomplete removal of Pb loss by the chemical abrasion technique. However, the $^{40}Ar/^{39}Ar$ method is not without problems and complications that may also bear on interpretation of anomalously young U-Pb ages. In particular, the accuracy of an $^{40}Ar/^{39}Ar$ date is dependent on: 1) the assumed age of the fluence monitor used to produce ^{39}Ar (MacDougall and Harrison, 1999); and 2) proper correction for any excess or inherited Ar.

The Ferguson et al. (2013) Peach Spring Tuff $^{40}Ar/^{39}Ar$ age of 18.78 Ma is calibrated to the 28.20 Ma age reported by Kuiper et al. (2008) for the Fish Canyon Tuff irradiation fluence monitor based on the astronomical ages of Pliocene sediments and tephras in Moroccan marine deposits. However, astronomical dating of Pleistocene deep-sea sediments and the Bruhnes-Matuyama geomagnetic boundary using the same "tuning" approach performed by Kuiper et al. (2008) indicates a Fish Canyon sanidine age of 27.93 Ma age (Channell et al., 2010; Westerhold et al., 2012). If the Peach Spring Tuff $^{40}Ar/^{39}Ar$ sanidine age is instead referenced to 27.93 Ma for the Fish Canyon Tuff, then the eruption age would be 18.60 Ma. Eruption dates reported by workers using a Fish Canyon sanidine age of 27.84 Ma (e.g. Nielson et al., 1990; and Miller et al., 1998; Hillhouse, 2010) range from 18.42 ± 0.07 to 18.71 ± 0.03 Ma.

Incompletely degassed sanidine xenocrysts are recognized in many studies, including Quaternary rhyolite lavas and tuffs at Yellowstone, Wyoming (Gansecki et al., 1996, 1998), Miocene tuff from McCullough Pass caldera, Nevada (Spell, 2011), Miocene rhyolite from Tanzania (Renne et al., 2012), and tephras derived from Mono Craters (Zimmerman et al., 2006; Cassata et al., 2010). They were also reported in the Peach Spring Tuff by Neilson et al. (1990) and Miller et al. (1998). In this context it is interesting to note that reported individual sanidine ages in Ferguson et al. (2013) range from 18.6 to 19.0 Ma (i.e. as much as 0.4 Ma variation), probability density distributions for several individual samples from the Ferguson et al. (2013) data set show significant shoulders both above and below the grand mean, and 7 of 8 samples have MSWD's indicating age complexity in the sanidine population.

Ferguson et al. (2013) reported single crystal sanidine ages that range from 18.63 ± 0.14 Ma to 19.02 ± 0.13 Ma (relative to Fish Canyon Tuff sanidine with an age of 28.2 Ma) with a difference of 39 ± 19 k.y. Hillhouse et al. (2010) report single crystal sanidine ages that range from 18.190 ± 0.500 Ma to 19.810 ± 1.173 Ma (relative to Fish Canyon Tuff sanidine with an age of 27.84 Ma), and the difference between oldest and youngest ages is 1.62 ± 1.28 Ma. Note that though the error on this difference is large, it still requires spread in the single crystal dates. Regardless of which age is used for the Fish Canyon Tuff fluence monitor, spread well outside of analytical error is observed across multiple data sets.

Allowing for the eruption age to be as young as 18.60 Ma (plausible given the issues noted) reduces significantly the number of anomalously young SIMS rim ages, and coincides with the dominant CA-SIMS age for all chemically abraded zircon. Only one of the high precision TIMS ages (at 18.08 ± 0.1 Ma) would still be younger than an 18.6 Ma eruption age. Resolution of this problem is beyond the scope of the present study but clearly highlights the need for more work to resolve the ongoing issues with U-Pb and $^{40}Ar/^{39}Ar$ age discordance. Further investigation could include ultra-high precision $^{40}Ar/^{39}Ar$ dating (e.g., Phillips and Matchan, 2013) to evaluate the extent to which near-eruption recycling of antecrystic or xenocrystic sanidine also affects the Peach Spring Tuff sanidine population.

Timescale of zircon crystallization in the Peach Spring Tuff and Cook Canyon magma reservoirs

The total duration of zircon growth, and the timescale over which any magma related to either the Peach Spring Tuff or Cook Canyon Tuff may have resided in the crust, clearly depends on the determination of accurate eruption ages. From the preceding analysis, an age of 18.6 Ma is taken as a likely minimum for eruption but given the uncertainties, the eruption age could range anywhere from 18.6 to 18.8 Ma.

Regardless of the complications associated with the eruption age, the large dispersion of the age data for both tuffs both the Peach Spring Tuff (MSWD=40 for TIMS) and Cook Canyon Tuff cannot be explained purely by Pb-loss. It thus seems evident that recycling of earlier formed antecrystic and/or xenocrystic zircon has taken place during the assembly of both the Peach Spring and Cook Canyon magma bodies given. Identifying “coherent” age populations, if they exist, is important for distinguishing autocrystic (i.e. near-eruption magmatic) crystallization from discrete earlier periods of zircon growth (antecrysts) and to evaluate crystallization intervals and potential residence time of the Peach Spring Tuff and Cook Canyon Tuff magmas.

In order to try to understand the age spectra for crystallization of zircon in the Peach Spring Tuff and Cook Canyon Tuff magmas, two methods were employed: 1) progressive binning of the youngest apparent high-precision TIMS U-Pb ages as outlined by Gansecki et al. (1996, 1998), Dallegge (2008), and Sageman (2014) for $^{40}Ar/^{39}Ar$ ages; and 2) deconvolution of age components using the Sambridge and Compston (1994) "Unmix" algorithm (as implemented in Isoplot v. 3.6 of Ludwig, 2008) for both the high-precision TIMS data and the SIMS data. Note that for the SIMS data, method 2 using the Unmix algorithm is applied to all chemically abraded zircon, which includes analyses of unpolished rims and the outer increments of growth of sectioned edges, as identified by CL images, in an attempt to obviate the limitations of whole crystal TIMS analysis, which cannot truly capture the last increment of growth.

For method (1), following Sageman et al. (2014), the youngest precise date in each U-Pb data set is identified, then progressively older U-Pb dates are combined until the calculated MSWD value for that combined subset of dates exceeds the 95% confidence interval for a single coherent population given the analytical uncertainties and accumulated number of dates (see Mahon, 1996). The individual U-Pb date that causes the MSWD to exceed the critical value for a single population is not included with the younger dates, and is used a starting point for calculating the next older age population. Method 2, using the Sambridge and Compston (1994) "Unmix" algorithm in Isoplot, yields nearly identical age groupings or "modes" for the high-precision TIMS data as those obtained from method 1.

Peach Spring Tuff

Ignoring the youngest outlier at 18.08 Ma that likely shows the effects of Pb-loss after chemical abrasion, the youngest precise zircon age of 18.53 ± 0.19 Ma is within error of the sanidine eruption age relative to Fish Canyon Tuff sanidine with an age of 27.93 Ma ($FCT_{27.93}$), however post-dates the sanidine eruption age relative to Fish Canyon Tuff sanidine with an age of 28.2 Ma ($FCT_{28.2}$) (Fig. 32). The youngest coherent group of zircon is 18.809 ± 0.056 Ma (MSWD=2; n=10). This is within error of the both the sanidine $^{40}Ar/^{39}Ar$ age of Ferguson et al. (2013) referenced to FCT= 28.2 Ma and FCT=27.93 Ma (Figure 32). This age (18.53 ± 0.19 Ma) is therefore considered to represent autocrystic growth in the main magma body either 30 ± 60 k.y. ($FCT_{28.2}$) or 210 ± 60 k.y. ($FCT_{27.93}$) prior to eruption.

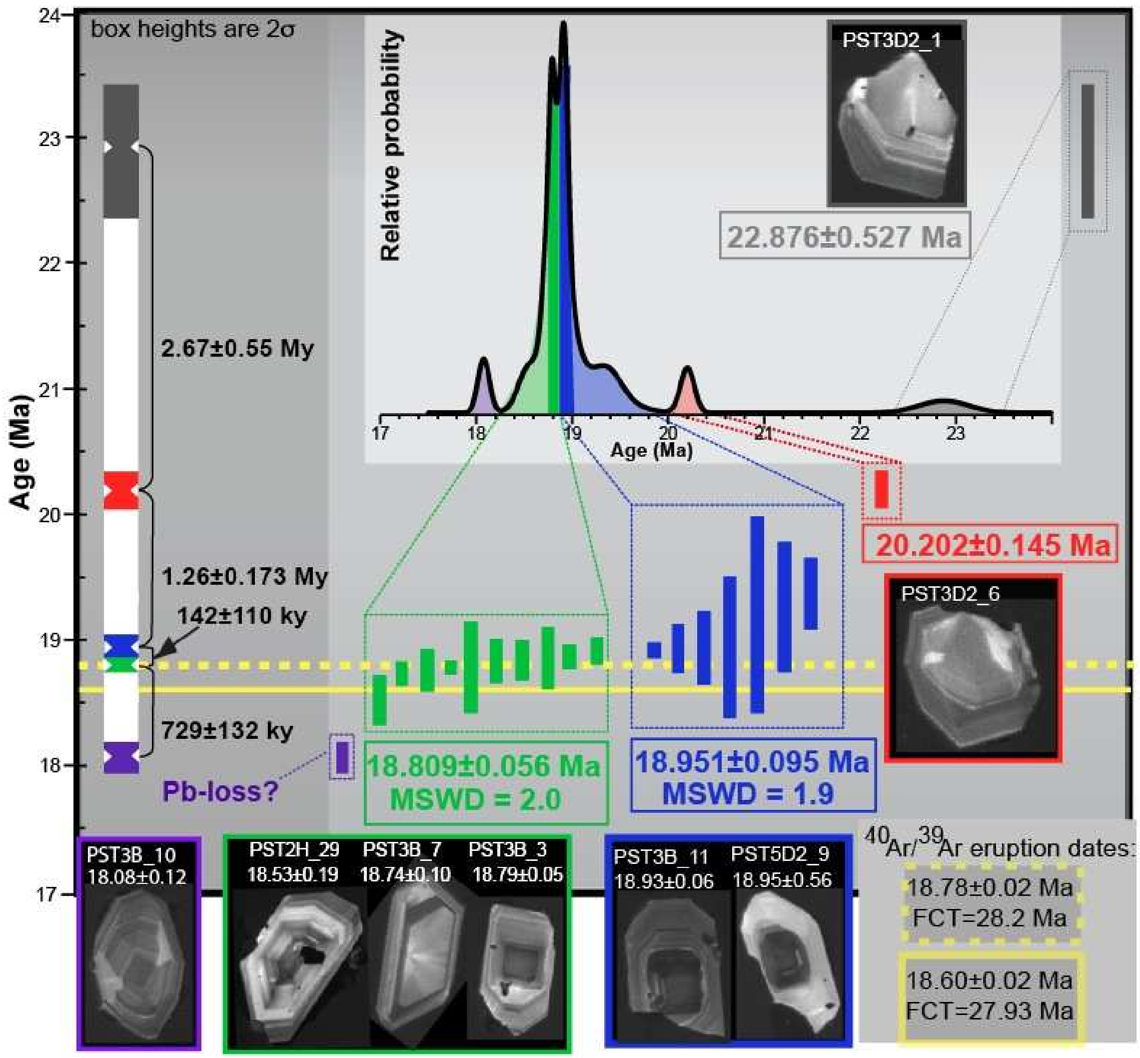

Figure 32. Peach Spring Tuff zircon populations grouped by methods described in the text. Weighted means for each population are presented in text of same color and plotted on the left side of the figure (darkest grey box). Note that the probability plot (lightest grey box) corroborates grouping the zircons in this way. Difference in age between each group is printed in black. The figure shows the eruption date from Ferguson et al. (2013) recalculated at different Fish Canyon Tuff (FCT) sanidine dates. All ages are corrected for disequilibrium

An apparent population at 18.951 ± 0.095 Ma (MSWD=1.9; n=7) pre-dates the youngest group by 142 ± 110 k.y., and represents a hiatus of at least 32 k.y. (Fig. 32). This population is dominated by type 1a zircon. As discussed in more detail below, there is evidence that these zircons may be related to the Cook Canyon magma system. The two oldest single TIMS zircon dates are outliers at 20.202 ± 0.145 Ma and 22.876 ± 0.527 Ma. McDowell et al. (2014) reports similar single, whole-zircon CA-TIMS dates in pre-Peach Spring Tuff units, and post-Peach Spring intrusives and lavas. Minor basanite lavas that extend to ca. 21 Ma are found in the earliest Miocene stratigraphy of the Colorado River Extensional Corridor (Bradshaw, 1993), but there is otherwise no reported intermediate to silicic magmatism of this age. All data are concordant; therefore these outlier dates do not represent “mixed” zircon of different ages comprising small volume inherited Precambrian cores with Miocene overgrowths (Fig. 26). Instead, these are likely indirect evidence of the earliest intrusive Miocene magmatism in the Silver Creek magma system.

Cook Canyon Tuff

Apparent crystallization dates from individual zircons in the Cook Canyon Tuff span 18.98 ± 0.22 Ma to 1073.73 ± 18.75 Ma. The single Proterozoic date is the first direct evidence for assimilation of Proterozoic crustal material by the Cook Canyon Tuff magma. The youngest precise CA-TIMS crystallization date of 18.98 ± 0.22 is within error of the mean age given by the youngest coherent group of Peach Spring Tuff zircons and nearly identical to the mean age of the second and slightly older population (Fig. 33). The youngest precise Cook Canyon Tuff date is within 20 ± 22 k.y. of the Peach Spring Tuff sanidine age at $FCT_{28.2}$ and 38 ± 22 k.y. of the Peach Spring Tuff sanidine age at $FCT_{27.93}$ and is interpreted to represent the maximum possible age of the Cook Canyon Tuff eruption. Combining all analyses (excluding the single Proterozoic zircon) yields a crystallization age with scatter beyond what may be attributed to analytical uncertainties. Combining the youngest six analyses yields a crystallization age of 19.17 ± 0.26 Ma with an MSWD of 1.80, and is also within error of the sanidine age for the Peach Spring Tuff. The oldest two zircons yield identical dates within error with a mean age of 20.71 ± 0.52 Ma (MSWD=0.017), and similar to the oldest zircon dates from the Peach Spring Tuff.

Antecrystic zircon growth

The zircons that are not obviously inherited or xenocrystic and that predate the eruption ages (outside of error) of the Peach Spring Tuff and Cook Canyon Tuff by more than several 10^5 years clearly suggest recycling of zircon antecrysts. A greater than 200 k.y. difference between the U-Pb and $^{40}Ar/^{39}Ar$ ages appears to be the case for an appreciable number of zircons in the Peach Spring Tuff and Cook Canyon Tuff and these are interpreted as recycled antecrysts. The antecrysts are related to the magma system(s) giving rise to the eruptions, and the ages are reasonable given the volumes and plausible conductive cooling times of shallow silicic magma bodies (e.g., Costa, 2008). The apparent zircon antecrysts in the two tuffs yield similar age groupings, and suggest that both the Peach Spring Tuff and Cook Canyon Tuff magmas recycled a common population of antecrysts.

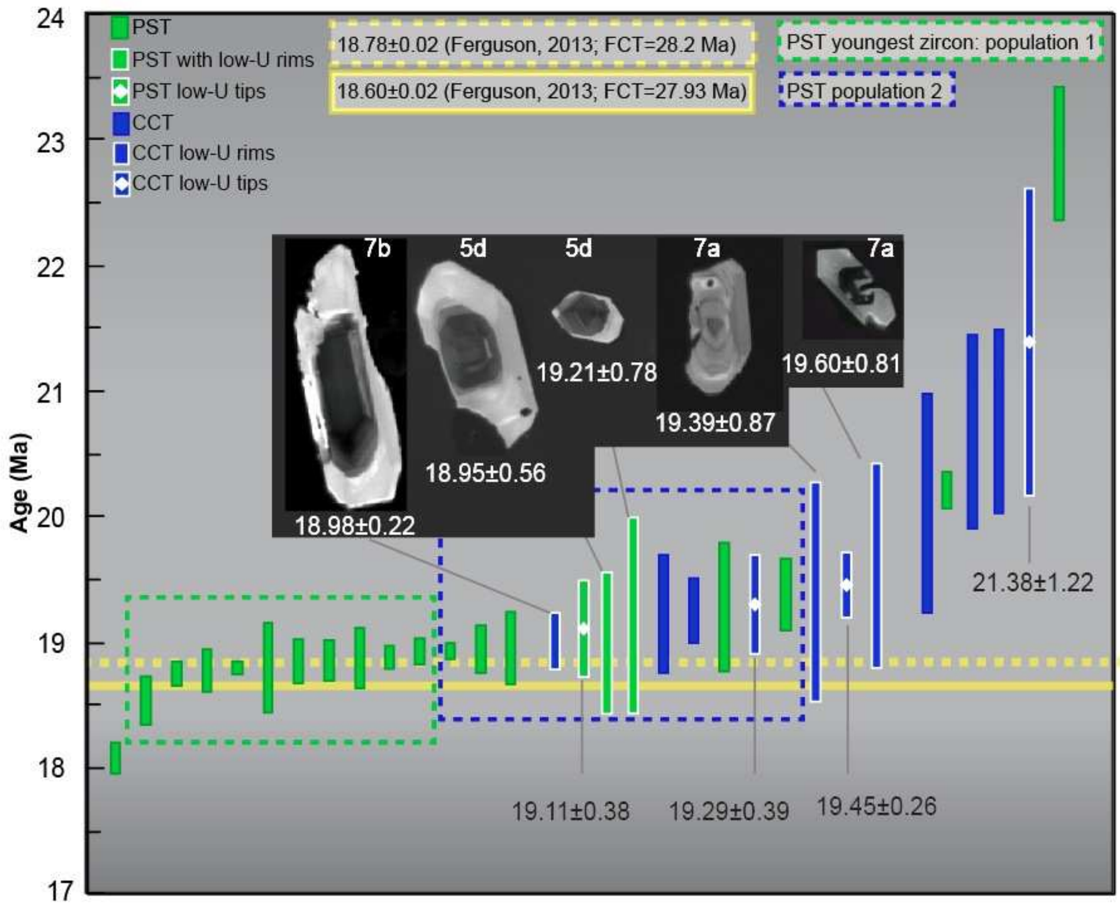

Figure 33. Rank order plot of CA-TIMS Peach Spring Tuff (PST) and Cook Canyon Tuff (CCT) zircon results showing the overlap between Cook Canyon Tuff ages with all but the youngest coherent group (enclosed by green dashed box) of Peach Spring Tuff zircon ages. Cook Canyon Tuff zircon show the greatest overlap with the next older group of Peach Spring Tuff Zircon (PST population 2; enclosed by blue dashed box). Pumice sample numbers are listed above each zircon image. All ages are corrected for disequilibrium

Probability density plots of CA-SIMS analyses of Peach Spring Tuff and Cook Canyon Tuff also indicate multi-modal distribution of ages that are similar. Deconvolution of apparent Gaussian age populations using the "Unmix" function in Isoplot (version 3.6; Ludwig, 2008) suggest four modes for Peach Spring Tuff (17.76 ± 0.38 Ma [16%], 18.68 ± 0.22 Ma [50%], 19.56 ± 0.25 Ma [31%], 21.06 ± 0.95 Ma [3%]) (Fig. 34A) and three for Cook Canyon Tuff (18.61 ± 0.44 Ma [45%], 19.54 ± 0.44 Ma [48%], and 21.63 ± 0.77 Ma [7%]) (Fig. 34B).

The three deconvolved modes yielded by Isoplot for the Cook Canyon Tuff are identical within error to the oldest three apparent modes for the Peach Spring Tuff, and both the Peach Spring Tuff and Cook Canyon Tuff are dominated by age modes at ca. 18.7 and 19.5 Ma (>81% for Peach Spring Tuff and >89% for Cook Canyon Tuff). Thus, the SIMS data corroborate the CA-TIMS data that suggest antecryst kinship.

The "unmixed" age mode at ca. 18.0 Ma in the Peach Spring Tuff clearly postdates even the youngest plausible estimate of the eruption age, and is thus again most likely attributed to lead loss. One could perhaps question whether lead loss should lead to a discrete "mode" at 18.0 Ma, but given the large errors in the individual modes, and the *a priori* assumption of discrete age components by the Sambridge and Compston (1994) algorithm, it may be pushing the limitations of interpretation to attach significance to this low age "shoulder" (Fig. 34 A).

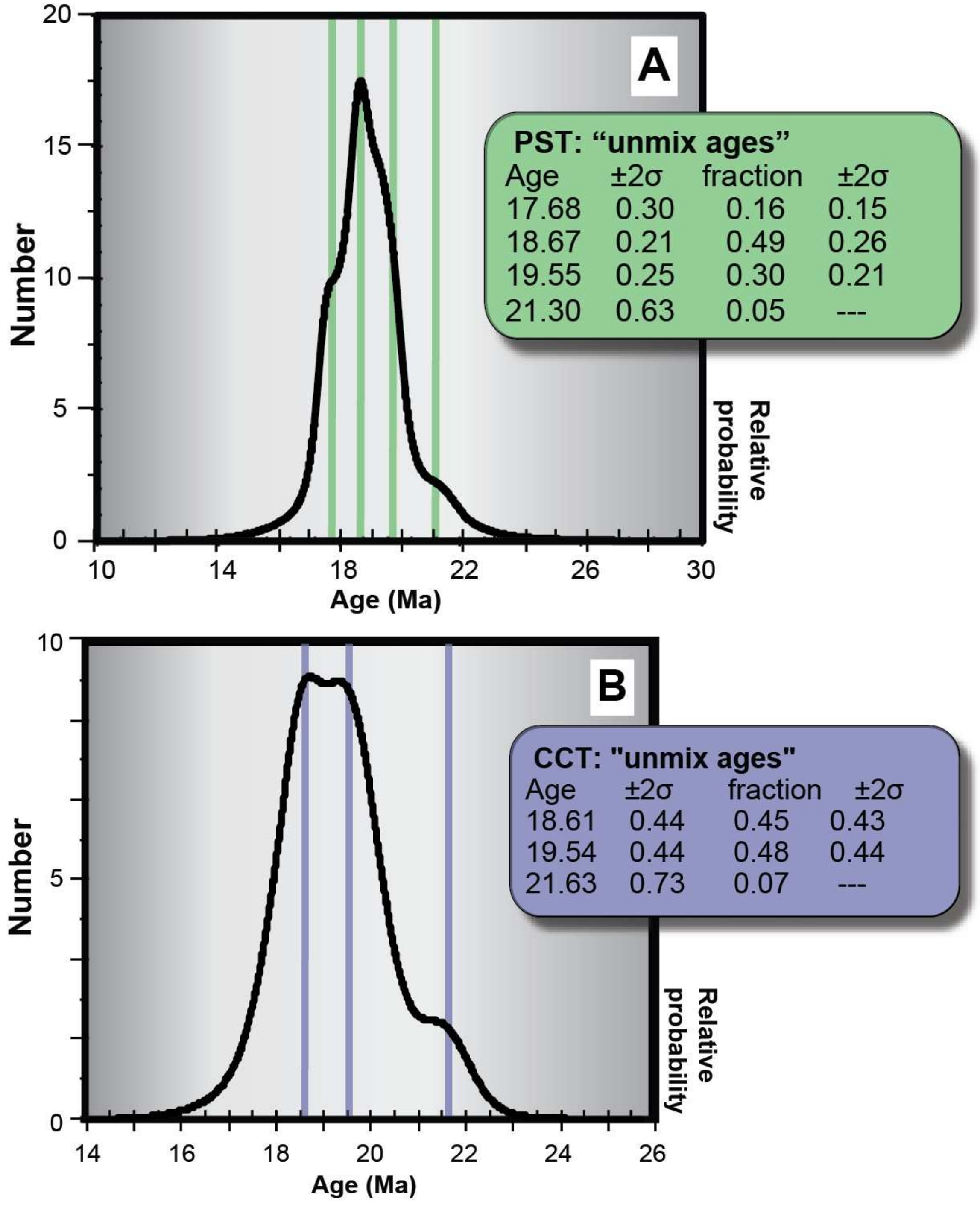

Figure 34. “Unmix” age modes for chemically abraded rims and ages of (A) Peach Spring Tuff (PST) zircon, and (B) Cook Canyon Tuff (CCT) zircon. All ages are corrected for disequilibrium.

When data for only zircon with low-U edges or rims are considered for the Peach Spring Tuff, the anomalously young “shoulder” does, however, become more pronounced (Fig. 35), and comprises 68% of the data. The two suggested age modes (in the low-U/high-Ti data set), 17.79 ± 0.33 Ma (68%) and 19.63 ± 0.80 Ma (32%), are identical to two of the four age modes suggested by the entire data set (Figs. 34 A and 35). The fact that a Peach Spring Tuff- “like” eruption date is not present among Type 1a zircon demands an alternative to the current model that posits eruption triggering by a mafic recharge event (Pamukcu et al., 2013). Given that the rim-glass or rim-crystal interface (if zircon is included in another mineral) has the largest diffusion gradient it is perhaps not surprising that the relative amount of Pb loss, as shown by the number of anomalously young ages on rims, would be higher than in the post-CA data set as a whole. That the anomalous 18.0 Ma age becomes even more defined for the Type 1 Peach Spring zircons suggests the relative proportion of Pb loss for the rims is similar and compositionally controlled in part.

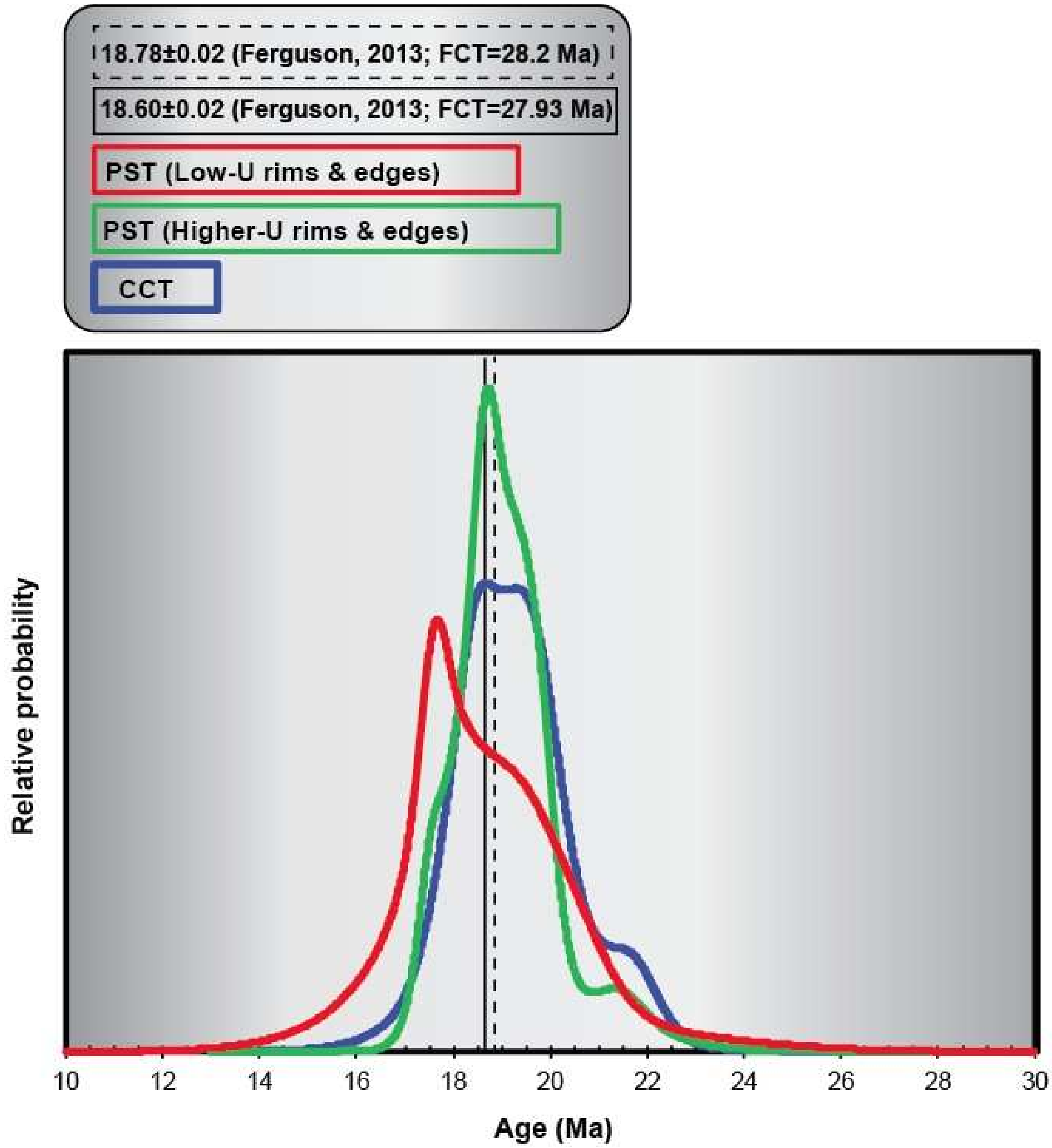

Figure 35. Plot with overlay of probability density curves for Peach Spring Tuff (PST) zircons with low-U edges or rims (red), Peach Spring Tuff zircons with higher-U edges or rims (green), and Cook Canyon Tuff (CCT) zircons. Note: almost all Cook Canyon Tuff zircons lave low-U edges or rims. Black dashed line denotes 40Ar/39Ar sanidine age from Ferguson et al. (2013) relative to the Fish Canyon Tuff (FCT) 40Ar/39Ar sanidine age of 28.2 Ma, and the solid black line denotes the same age relative to the Fish Canyon Tuff 40Ar/39Ar sanidine age of 27.93 Ma. All ages used to construct this plot are corrected for disequilibrium.

Trace element constraints on antecryst zircon growth

The geochronological results of this study indicate that a significant proportion of the crystal cargo erupted in the Peach Spring Tuff magma represents recycled material from an evolving magma "reservoir" or subvolcanic region that also provided antecrysts of identical age (within error) to Cook Canyon Tuff magma. The trace element and textural characteristics noted earlier provide additional information that bears on the relationship of antecrystic zircon to the evolving subvolcanic reservoir that produced both tuffs.

There is considerable similarity in texture as well as compositional overlap of zircon in Peach Spring Tuff and Cook Canyon Tuff. The only case where there is not textural similarity and compositional overlap is in Type 2 zircons of the Peach Spring Tuff. Edges of type 2 zircons in Peach Spring Tuff have trace element compositions that indicate they grew in magmatic environments that were cooler, more-evolved, and more fractionated when compared to the other zircon types. Importantly however, these zircons have ages that are either >19.5 Ma or <18.9 Ma

Cores from the Peach Spring and Cook Canyon Tuff, pre-Peach Spring lava flows, and post-Peach Spring lava flows and intrusives are variable in trace element compositions but together define a trend that is consistent with fractionation. The principal exception are cores from Cook Canyon Tuff sample 7a, which cluster at the less evolved regions of the trace element trend at low Hf (cf. Claiborne et al., 2006). The same clustering is also observed for zircon rims from sample 7a (see Fig. 12), and suggests that these zircons came from a silicic magma more primitive than that in which zircons from the other units grew.

CA-TIMS analyses of zircon from sample 7a yield U-Pb dates of approximately 19.5 Ma (Fig. 33), and the ages were obtained from zircons dominated by CL-bright rims over higher-U/higher Ti cores. Despite having cores with variable zoning patterns and CL-luminosity, the trend from core to edge still indicates cooling rather than heating. These dates likely constrain the crystallization age of this chemically distinct low Hf group because CA-TIMS ages are weighted by the higher-U cores (vs. the low-U rims). And since geochemistry indicates uninterrupted similar chemistry from core to rim in these zircons, they likely reflect growth from a cooling magma following a mafic recharge event.

Zircon yielding CA-TIMS ages older than approximately 19.6 Ma occur in both Peach Spring Tuff and Cook Canyon Tuff samples, indicating recycling of antecrystic cores, probably sourced in older Miocene intrusions beneath the Peach Spring Tuff-Cook Canyon Tuff volcanic system. Zircons of similar old age also occur in post-Peach Spring Tuff intrusions (McDowell et al., 2014). The distinct trace element compositions for Peach Spring Tuff and Cook Canyon Tuff zircons yielding the same U-Pb ages indicates coeval crystallization from distinct melts, perhaps reflecting heterogeneity of the subvolcanic magma reservoir which was at various states of crystallization and with variably fractionated melt (e.g., Vazquez and Reid, 2004).

Peach Springs Tuff Zircon

The two dominant age modes in the Peach Spring Tuff zircon data could indicate punctuated growth or recycling of antecrysts and xenocrysts from pre-Peach Spring Tuff magmas. Punctuated growth can occur upon input of initially undersaturated magma that then reaches saturation, which results in a pulse of zircon crystallization (Harrison et al., 2007), or alternatively if the magma becomes rapidly undersaturated at some point, thereby dissolving zircon and erasing geochronological evidence of its growth in the magma system. Such changes would reflect heating and/or chemical changes resulting in undersaturation following magma mixing or mafic underplating,

The punctuated 142 ± 110 k.y. crystallization interval

Considering the time it takes for solidification of various sized magma bodies, Costa (2008) evaluated the residence times vs. volume relations reported for silicic volcanic deposits associated with caldera-related systems. If the estimated erupted volume of Peach Spring Tuff magma (>600 km^3: Young and Brennan, 1974; Glazner et al. 1986; >640 km^3; Ferguson et al., 2013; >700 km^3: McDowell et al., 2014) represents the volume of magma stored prior to eruption, i.e., most if not all was emptied out by the eruption, then it could not reside for more than approximately 200 k.y. before it cooled conductively below its solidus (Costa, 2008). Thus, it is not unreasonable to postulate that the 142 k.y. interval is indicative of the residence time of eruptible Peach Spring Tuff magma. Note that if the eruption age is closer to 18.6 Ma then this would indicate magma residence time of ca. 300 k.y. Alternatively, the magma chamber could have been nearly dead from a thermal perspective, and the interval instead represents the time of thermal dormancy. It was then rejuvenated by heat from intrusion of new hot magma resulting in relatively rapid buildup of eruptible magma.

Possible evidence for heating by addition of new hot magma into the Peach Spring Tuff magma chamber may come from the resorbed cores (type 1 and type 2) and high Ti rims in Peach Spring Tuff Type 1a and 1b zircon, which are presumably from the last erupted portion of Peach Spring Tuff and the bottom of the magma chamber (Figs. 13, 14, 32 and 33). CL imaging of sanidine from Peach Spring Tuff (Fig. 36) also shows CL bright rims, which in other studies are correlated with high temperature growth, and consistent with addition of hot magma into the Peach Spring Tuff chamber. This is the explanation favored by Pamukcu et al. (2013) for rejuvenation and unlocking of a semi-solid crystal mush that ultimately led to the eruption of the Peach Spring Tuff magma body. It is interesting to note that sanidine from single pumice clasts show evidence for growth in distinct chemical and thermal environments; just as the zircon show. CL imaging of sanidine from a single pumice clast (Fig. 37) shows both CL-bright resorbed cores mantled by CL dark rims, and CL-dark resorbed cores mantled by CL-bright rims.

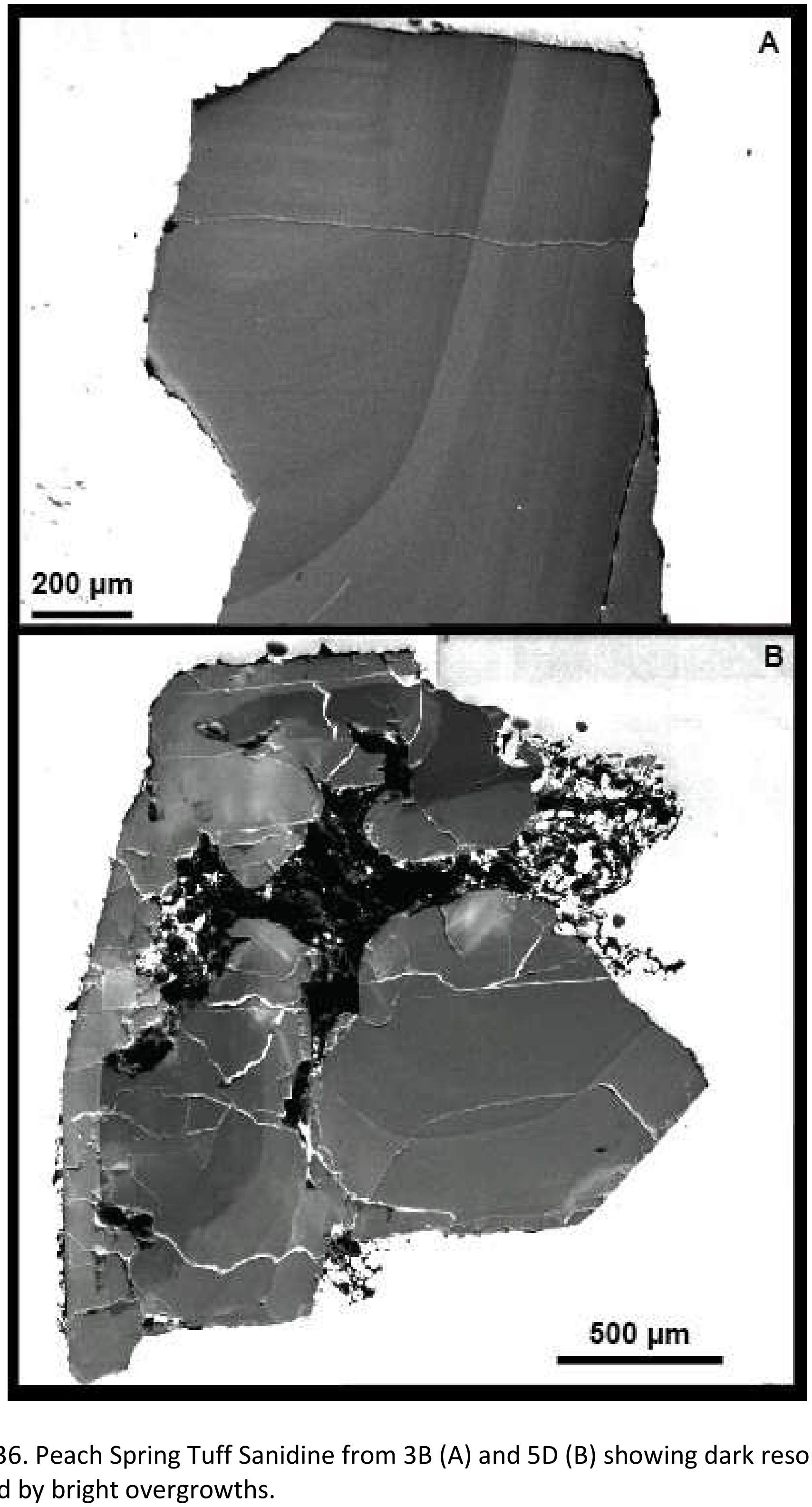

Figure 36. Peach Spring Tuff Sanidine from 3B (A) and 5D (B) showing dark resorbed cores mantled by bright overgrowths.

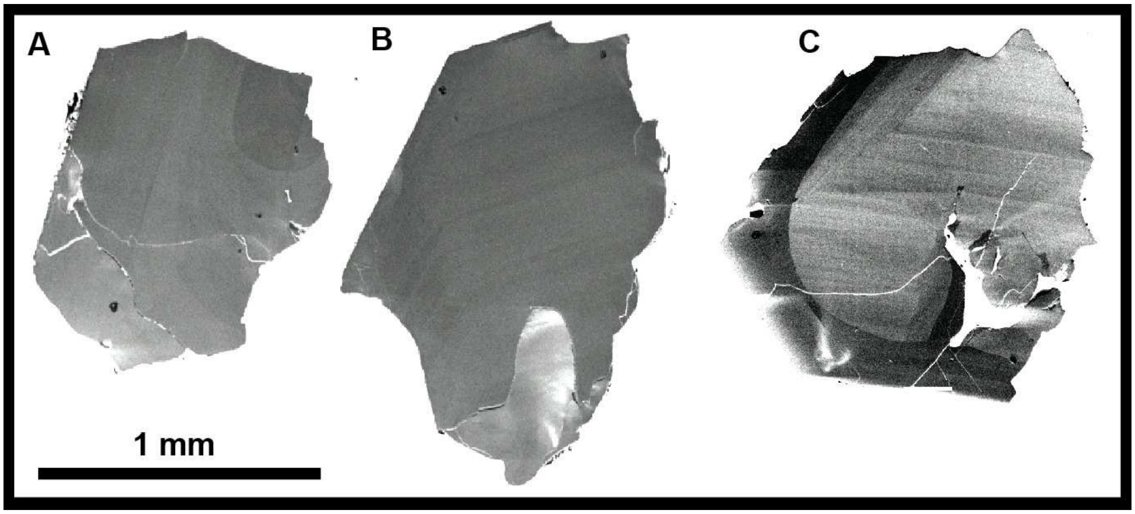

Figure 37. (A) Dark resorbed core mantled by CL-bright rim, (B) continuous CL-dark zoning from core to rim (bright CL area is an artifact-fracture), and (C) bright resorbed core mantled by dark rim.

The Pamukcu et al. (2013) study did not have the benefit of the high precision geochronology. The critical question unaddressed in Pamukcu et al is the age or timing of the mafic recharge event relative to the eruption age as determined by this study, and what the youngest zircons actually record. The youngest coherent group of zircons from the Peach Spring Tuff (that yield the 18.809 ± 0.056 Ma age) is comprised of type 1b and Type 2 zircons (Fig. 32). These zircons do not have Low-U/high-Ti rims thought to be indicative of a mafic recharge event close to the time of eruption. Many zircons show petrographic evidence for a resorption event, but the trace element data recorded for edges of these zircons indicates that the edges grew from two distinct melts (e.g., the edges of Type 1b and Type 2 zircon; Fig 14), neither of which indicate mafic recharge. The CL-bright rims in the youngest group correlate to Type 1b zircons, and though low in U content, have only slightly elevated Ti concentrations (Ti: 5-10ppm) relative to the Type 2 zircons (Ti ≈ 5ppm) (Figs. 14 and 32). Other trace element data indicates that Type 1b edge compositions are intermediate between Types 1a and 2 (Fig. 14). Thus the trace element composition of CL bright *young* rims (i.e. those in the 18.8 Ma age group) is always between the most mafic (type 1a) and the most felsic (type 2) zircons. The youngest zircons, although showing some resorption in their cores, do not record growth from a less fractionated and hotter magma. Instead, the zircons all record growth from a cooler (e.g., lower Ti) magma (Fig. 14).

Zircon with CL bright edges and trace element data that supports growth from a less evolved magma is observed in the older (18.951±0.095 Ma) zircon population. Furthermore, tips broken off low-U/high-Ti-rimmed Peach Spring Tuff zircon and analyzed via CA-TIMS yield an age of 19.11±0.38 Ma (Fig. 38). Although the error is large, and makes this age just within error of the Peach Spring Tuff eruption age, it is more likely related to pre-Peach Spring Tuff magmatism. Tips broken off low-U/high-Ti-rimmed Cook Canyon Tuff zircons yield ages of 19.29 ± 0.39 Ma, 19.45 ± 0.26 Ma and 21.38 ± 1.22 Ma. Combining the zircon tips results from both tuffs yields a weighted mean age of 19.38±0.62 Ma, MSWD= 4.4 (n=4; 95% confidence interval). Ignoring the ca. 21 Ma result, the mean becomes 19.33±0.18 Ma, MSWD = 1.18 (n = 3/4; 95% confidence interval)(Fig. 38).

It is also important to recall that CA-SIMS analyses of the low-U/high-Ti rims yield ages that are either anomalously young (≈18.0 Ma) or anomalously old (≈19.5 Ma) to be near eruption age zircon (Fig. 35), and since the former is attributed to residual Pb-loss, the low-U/High-T Type 1a zircons apparently pre-date the Peach Spring Tuff eruption on the order of 200 to 400 k.y. depending on the actual eruption age of the Peach Spring Tuff. Thus, rather than recording a mafic recharge event that might have triggered the eruption of the Peach Spring Tuff (e.g., Pamukcu et al., 2013), the low-U/High-T, Type 1A zircons may instead represent recycled xenocrysts picked up from a nearby residual Cook Canyon Tuff magma body.

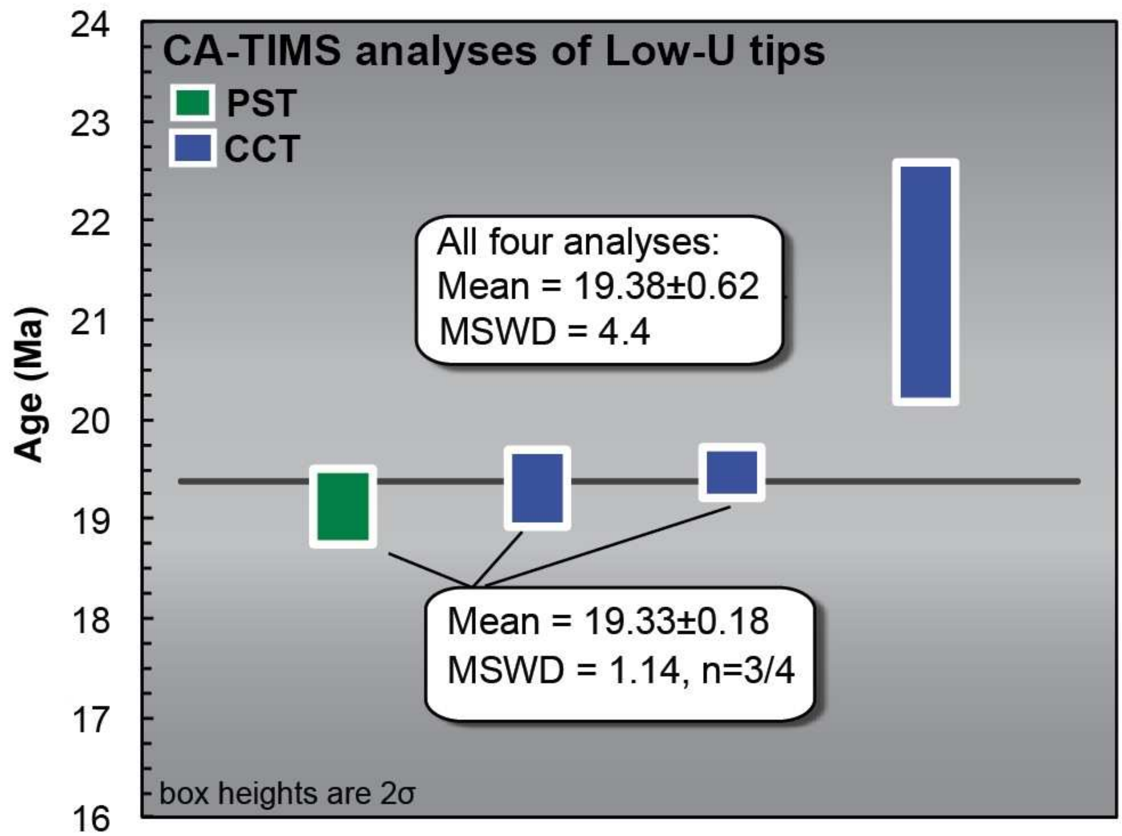

Figure 38. CA-TIMS analyses of the combined tips broken off of low-U zircons from the Peach Spring Tuff (PST) and Cook Canyon Tuff (CCT).

An alternative explanation is that these zircons are derived from a distinct body of magma that was sourced from the same source that produced the Alcyone trachyte. Whole rock Sr, Nd, and Hf isotope data as well as zircon Hf and O isotope data for the Peach Spring Tuff and Alcyone trachyte (Frazier, 2013; Overton et al., 2013; McDowell et al., 2014) are identical within error, whereas the Cook Canyon Tuff has somewhat more primitive (mantle-like) isotopic composition. This would suggest that the CL-bright zircons are derived from the subvolcanic reservoir associated with eruption of the Alcyone trachyte, although the Cook Canyon Tuff remains insufficiently studied to rule out a Cook Canyon magma or mush body as the source of the low-U/High-T zircons. Given the current uncertainties in the age of Alcyone trachyte from McDowell et al. (2014), it is permissible that the Alcyone trachyte and Peach Spring Tuff essentially represent a compositional and temporal continuum. In other words, the Alcyone trachyte was the volcanic counterpart of a growing and compositionally evolving crystal mush-magma body that ultimately culminated in the Peach Spring Tuff supereruption.

Interestingly, McDowell et al. (2014) also report similar CL-bright zircons in the post-caldera intrusions (Moss and Times Porphyry), which overlap the whole rock and zircon isotopic values for Cook Canyon Tuff (Overton et al., 2013; McDowell, 2014). This might suggest that the Silver Creek post-caldera intrusions are unrelated to the Peach Spring Tuff and are instead linked to the Cook Canyon Tuff, which would further imply that the Silver Creek caldera was the source of the Cook Canyon Tuff. Testing this connection requires considerably more detailed zircon geochronology by both CA-SIMS and CA-TIMS on the Moss and Times porphyries as well as on Cook Canyon Tuff.

All of the data combined, (whole rock and zircon isotopes and zircon geochemistry and geochronology) strongly suggest that the Cook Canyon Tuff magma body and Peach Spring Tuff magma body were discrete magma systems that were closely related in time and possibly overlapping in space.

CONCLUSIONS

The data presented in this thesis lead to the following conclusions:

1. The application of chemical abrasion and thermal annealing techniques are critical to producing robust and accurate zircon dates for the Peach Spring and Cook Canyon Tuffs, obtained by either TIMS or SIMS.
2. U-Pb zircon dates from the Peach Spring Tuff show a prominent pulse of zircon growth at 18.809 ± 0.056 Ma, and thus close to the age of eruption if the eruption age is taken as 18.78 ± 0.02 Ma (Ferguson et al. 2013). This would imply appreciable magma build up in a relatively short time interval (on the order of 50-100 k.y.). Supereruptions can thus form on geologically short time scales.
3. Conclusion (2) must be qualified by the recognition that the sanidine dates in Ferguson et al. (2013) could have uncertainties that, together with the U-Pb data presented here, call into question the accuracy of the inferred eruption age based on sanidine. Possible significant systematic uncertainty is

associated with the age of the Fish Canyon Tuff sanidine fluence monitor, and random geologic uncertainty is associated with possible excess Ar from incompletely degassed sanidine xenocrysts. These uncertainties allow a plausible eruption age of 18.6 Ma for the Peach Spring Tuff, which is in remarkable agreement with the dominant SIMS age given by rims of Type 1b and Type 2 chemically abraded zircons inferred to be cognate autocrysts in the Peach Spring Tuff.

4. The distinct age peak at 18.951 ± 0.095 is likely defined by antecrysts that represent a major pulse of zircon growth in the Peach Spring Tuff magma chamber. The zircons extending to ages older than this are either antecrysts or possibly xenocrysts from residual Cook Canyon Tuff magma or crystal mush that were entrained in the main Peach Spring reservoir that erupted. Support for recycling of Cook Canyon xenocrysts comes from the U-Pb dates from the CL-bright Type 1a zircons that are distinctly older ca. 19.3-19.5 Ma than the zircons that define the major crystallization peaks in the Peach Spring Tuff. Alternatively, the Type 1a zircons are antecrysts/xenocrysts recycled from earlier intrusions related to the Alcyone trachyte eruption.
5. U-Pb zircon dates from the Cook Canyon Tuff show a minimum age of 18.98 ± 0.22 Ma, which must correspond to the maximum eruption age of the Cook Canyon Tuff. Like the Peach Spring Tuff, the Cook Canyon Tuff has recycled older antecrystic and xenocrystic zircon (several hundred thousand years).

6. The closeness of the Peach Spring Tuff eruption age and the maximum eruption age of the Cook Canyon Tuff, as well as the observation that zircons from Cook Canyon Tuff were entrained in the Peach Spring Tuff supereruption suggests that the two tuffs erupted from the same caldera, possibly from two distinct but spatially and temporally overlapping magma systems.

REFERENCES CITED

Bachmann, O., and Bergantz, G.W., 2003, Rejuvenation of the Fish Canyon magma body: A window into the evolution of large-volume silicic magma systems: Geology, v. 31, no. 9, p.789-792.

Bachmann, O., and Bergantz, G.W., 2004, On the origin of crystal-poor rhyolites: extracted from batholithic crystal mushes: Journal of Petrology, v. 45, p. 1565-1582.

Bachmann, O., and Bergantz, G., 2008, The magma reservoirs that feed supereruptions: Elements, v. 4, p. 17-21.

Bachmann, O., Schoene, B., Schnyder, C., and Spikings, R., 2010, The $^{40}Ar/^{39}Ar$ and U-Pb dating of young rhyolites in the Kos-Nisyros volcanic complex, Eastern Aegean Arc, Greece: age discordance due to excess 40Ar in biotite: Geochemistry, Geophysics, Geosystems, v. 11, 14 p.

Bacon, C.R., and Lowenstern, J.B., 2005, Late Pleistocene granodiorite source for recycled zircon and phenocrysts in rhyodacite lava at Crater Lake, Oregon: Earth and Planetary Science Letters, v. 233, p. 277-293.

Barth, A.P., and Wooden, J.L., 2010, Coupled elemental and isotopic analyses of polygenetic zircons from granitic rocks by ion microprobe, with implications for melt evolution and the sources of granitic magmas: Chemical Geology, v. 277, p. 149-159.

Barboni, M., and Schoene, B., 2014, Short eruption window revealed by absolute crystal growth rates in a granitic magma: Nature Geoscience, v. 7, p. 524-528, doi: 10.1038/ngeo2185.

Bindeman, I.N., Schmitt, A.K., and Valley, J.W., 2006, U–Pb zircon geochronology of silicic tuffs from the Timber Mountain/Oasis Valley caldera complex, Nevada: rapid generation of large volume magmas by shallow-level re-melting: Contributions to Mineralogy and Petrology: v. 152, p. 649-665.

Black, L., Kamo, S., Allen, C., Davis, D.W., Aleinikoff, J., Valley, J.W., Mundil, R., Campbell, I.H., Korsuch, R.J., Williams, I.S., and Foudoulis, C., 2004, Improved $^{206}Pb/^{238}U$ microprobe geochronology by the monitoring of a trace-element-related matrix effect; SHRIMP, ID–TIMS, ELA–ICP–MS and oxygen isotope documentation for a series of zircon standards: Chemical Geology, v. 205, p. 115-140.

Bolhar, R., Ring, U., and Allen, C.M., 2010, An integrated zircon geochronological and geochemical investigation into the Miocene plutonic evolution of the Cyclades, Aegean Sea, Greece: Part 1: Geochronology: Contributions to Mineralogy and Petrology, v. 160, p.719-742.

Buesch, D.C., and Valentine, G.A., 1986, Peach Springs Tuff and volcanic stratigraphy of the southern Cerbat Mountains, Kingman, Arizona, *in* Nielson, J.E., and Glazner, A.F., eds., Cenozoic Stratigraphy, Structure and Mineralization in the Mojave Desert: Geological Society of America, Cordilleran Section, 82d, Los Angeles, California, March 1986, Guidebook and Volume, Field Trips 5 and 6, p. 7-14.

Burgisser, A., and Bergantz, G.W., 2011, A rapid mechanism to remobilize and homogenize highly crystalline magma bodies: Nature, v. 471, p. 212-215.

Cassata, W.S., Singer, B.S., Liddicoat, J.C., and Coe, R.S., 2010, Reconciling discrepant chronologies for the geomagnetic excursion in the Mono Basin, California: Insights from new $^{40}Ar/^{39}Ar$ dating experiments and a revised relative paleointensity correlation: Quaternary Geochronology, v. 5, p. 533-543.

Chamberlain, K.J., Wilson, C. J.N., Wooden, J.L., Charlier, B.L.A., and Ireland, T.R., 2013, New perspectives on the Bishop Tuff from zircon textures, ages and trace elements: Journal of Petrology, v. 55, p. 395-426.

Channell, J.E.T., Hodell, D.A., Singer, B.S., and Xuan, C., 2010, Reconciling astrochronological and $^{40}Ar/^{39}Ar$ ages for the Matuyama-Brunhes boundary and late Matuyama Chron: Geochemistry, Geophysics, Geosystems, v. 11, no. 12, QOAA12, doi:10.1029/2010GC003203.

Charlier, B.L.A., Wilson, C.J.N., Lowenstern, J.B., Blake, S., Van Calsteren, P.W., and Davidson, J.P., 2005, Magma generation at a large, hyperactive silicic volcano (Taupo, New Zealand) revealed by U-Th and U-Pb systematics in zircons: Journal of Petrology, v. 46, p. 3-32.

Charlier, B.L.A., and Wilson, C.J.N., 2010, Chronology and evolution of caldera-forming and post-caldera magma systems at Okataina Volcano, New Zealand from zircon U–Th model-age spectra: Journal of Petrology v. 51, p. 1121-1141.

Cherniak, D.J., Hanchar, J.M., and Watson, E.B., 1997, Diffusion of tetravalent cations in zircon: Contributions to Mineralogy and Petrology, v. 127, no. 4, p. 383-390.

Cherniak, D.J., and Watson, E.B., 2001, Pb diffusion in zircon: Chemical Geology, v. 172, p. 5-24.

Claiborne, L.L., Miller, C. F., Walker, B.A., Wooden, J.L., Mazdab, F.K., and Bea, F., 2006, Tracking magmatic processes through Zr/Hf ratios in rocks and Hf and Ti zoning in zircons: an example from the Spirit Mountain batholith, Nevada: Mineralogical Magazine, v. 70, p. 517-543.

Claiborne, L.L., Miller, C.F., Flanagan, D.M., Clynne, M.A., and Wooden, J.L., 2010, Zircon reveals protracted magma storage and recycling beneath Mount St. Helens: Geology, v. 38, p. 1011-1014.

Cooper, K.M., and Kent, A.J., 2014, Rapid remobilization of magmatic crystals kept in cold storage: Nature, v. 506, p. 480-483.

Costa, F., 2008, Residence times of silicic magmas associated with calderas: Developments in Volcanology, v. 10, p. 1-55.

Dallegge, T.A., 2008, $^{40}Ar/^{39}Ar$ Geochronology of lavas from the Central Plateau Member of Plateau Rhyolite with implications for magma residence times and eruptive reoccurrence intervals, Yellowstone National Park: Mountain Geologist, v. 45, p. 77-98.

Davis, D.W., Krogh, T.E., and Williams, I.S., 2003, Historical development of zircon geochronology: Reviews in mineralogy and geochemistry, v. 53, p. 145-181.

Davydov, V.I., Crowley, J.L., Schmitz, M.D., and Poletaev, V.I., 2010, High-precision U-Pb zircon age calibration of the global Carboniferous time scale and Milankovitch band cyclicity in the Donets basin, eastern Ukraine: Geochemistry, Geophysics, Geosystems, v. 11, no. 2, Q0AA04, 10.1029/2009GC002736.

Deering, C.D., Bachmann, O., and Vogel, T.A., 2011, The Ammonia Tanks Tuff: Erupting a melt-rich rhyolite cap and its remobilized crystal cumulate: Earth and Planetary Science Letters, v. 310, p. 518-525.

Deino, A., and Potts, R., 1992, Age-probability spectra for examination of single-crystal $^{40}Ar/^{39}Ar$ dating results: Examples from Olorgesailie, Southern Kenya Rift: Quaternary International, v. 13, p. 47-53.

de Silva, S.L., and Gosnold, W.D., 2007, Episodic construction of batholiths: insights from the spatiotemporal development of an ignimbrite flare-up: Journal of Volcanology and Geothermal Research, v. 167, p. 320-335.

Ferguson, C.A., 2008, Silver Creek caldera, probable source of the Miocene Peach Spring Tuff, Oatman Mining District, Arizona: Geological Society of America Abstracts with Programs, v. 40, no. 1, p. 33.

Ferguson, C.A., McIntosh, W.C., and Miller, C.F., 2013, Silver Creek caldera-The tectonically dismembered source of the Peach Spring Tuff: Geology, v. 41, p. 3-6.

Gansecki, C.A., Mahood, G.A., and McWilliams, M.O., 1996, $^{40}Ar/^{39}Ar$ geochronology of rhyolites erupted following collapse of the Yellowstone caldera, Yellowstone Plateau volcanic field: implications for crustal contamination: Earth and Planetary Science Letters, v. 142, p. 91-107.

Gansecki, C.A., Mahood, G.A., and McWilliams, M.O., 1998, New ages for the climactic eruptions at Yellowstone: single-crystal $^{40}Ar/^{39}Ar$ dating identifies contamination: Geology, v. 26, p. 343-346.

Gaudio, S., 2003, Discrimination and correlation of the Peach Springs Tuff and Peach Springs age-equivalent ignimbrites by geochronology, petrography, and incompatible element geochemistry from the Northern Colorado River Extensional Corridor, Central Basin and Range Province, USA [B.S. Thesis]: Wooster, College of Wooster, 67 p.

Glazner, A.F., Nielson, J.E., Howard, K.A., and Miller, D.M., 1986, Correlation of the Peach Springs Tuff, a large-volume ignimbrite sheet in California and Arizona: Geology, v. 14, p. 840-843.

Glazner, A.F., Bartley, J.M., Coleman, D.S., Gray, W., and Taylor, R.Z., 2004, Are plutons assembled over millions of years by amalgamation from small magma chambers?: GSA today, v. 14, p. 4-12.

Gulson, B.L., and Krogh, T.E., 1973, Old lead components in the young Bergell Massif, southeast Swiss Alps: Contributions to Mineralogy and Petrology, v. 40, p. 239-252.

Gusa, S., Nielson, J.E., and Howard, K.A., 1987, Heavy-mineral suites confirm the wide extent of the Peach Springs Tuff in California and Arizona, USA: Journal of Volcanology and Geothermal Research, v. 33, p. 343-347.

Halliday, A.N., Mahood, G.A., Holden, P., Metz, J.M., Dempster, T.J., and Davidson, J.P., 1989, Evidence for long residence times of rhyolitic magma in the Long Valley magmatic system: The isotopic record in precaldera lavas of Glass Mountain: Earth and Planetary Science Letters, v. 94, p. 274-290.

Heumann, A., Davies, G.R. and Elliott, T., 2002, Crystallization history of rhyolites at Long Valley, California, inferred from combined U-series and Rb-Sr isotope systematics: Geochimica et Cosmochimica Acta, v. 66, p. 1821-1837.

Hiess, J., Nutman, A.P., Bennett, V.C., and Holden, P., 2008, Ti-in-zircon thermometry applied to contrasting Archean metamorphic and igneous systems: Chemical Geology, v. 247, p. 323-338.

Hildreth, W., 2004, Volcanological perspectives on Long Valley, Mammoth Mountain, and Mono Craters: several contiguous but discrete systems: Journal of Volcanology and Geothermal Research, v. 136, p. 169-198.

Hillhouse, J.W., Turrin, B., and Miller, D.M., 2010, Correlation of the Miocene Peach Spring Tuff with the geomagnetic polarity time scale and new constraints on tectonic rotations in the Mojave Desert, California, *in* Reynolds, R. E., and Miller, D. M., eds., Overboard in the Mojave: Desert Studies Consortium, California State University, Fullerton, p. 105-121.

Huber, C., Bachmann, O., and Dufek, J., 2011, Thermo-mechanical reactivation of locked crystal mushes: Melting-induced internal fracturing and assimilation processes in magmas: Earth and Planetary Science Letters, v. 304, p. 443-454.

Ireland, T.R., and Williams, I.S., 2003, Considerations in zircon geochronology by SIMS, *in* Hanchar, J.M., Hoskin, P.W.O., eds., Zircon: Reviews in Mineralogy and Geochemistry, v. 53 p. 215–241.

Kennedy, B., and Stix, J., 2007, Magmatic processes associated with caldera collapse at Ossipee ring dyke, New Hampshire: Geological Society of America Bulletin, v. 119, p. 3-17.

Krogh, T.E., 1982a Improved accuracy of U-Pb zircon dating by selection of more concordant fractions using a high gradient magnetic separation technique: Geochimica et Cosmochimica Acta, v. 46, p. 631-635.

Krogh, T.E., 1982b, Improved accuracy of U-Pb ages by the creation of more concordant systems using an air abrasion technique: Geochimica et Cosmochimica Acta, v. 46, p. 637-649.

Kryza, R., Crowley, Q.G., Larionov, A., Pin, C., Oberc-Dziedzic, T., and Mochnacka, K., 2012, Chemical abrasion applied to SHRIMP zircon geochronology: An example from the Variscan Karkonosze Granite (Sudetes, SW Poland): Gondwana Research, v. 21, p. 757-767.

Kuiper, K.F., Deino, A., Hilgen, F.J., Krijgsman, W., Renne, P.R., and Wijbrans, J.R., 2008, Synchronizing rock clocks of Earth history: Science, v. 320, p. 500-504.

Ludwig, K., 2008, User's manual for Isoplot 3.6: A geochronological toolkit for Microsoft excel: Berkeley Geochronology Center Special Publication, v. 4, 57 p.

Ludwig, K., 2009, Squid 2 (rev. 2.5): A user's manual: Berkeley Geochronology Center Special Publication, v. 5, 104 p.

MacDougall, I., and Harrison, T.M., 1999, Geochronology and Thermochronology by the $^{40}Ar/^{39}Ar$ Method: Oxford University Press, 269 pp.

Mahon, K.I., 1996, The New "York" regression: Application of an improved statistical method to geochemistry: International Geology Review, v. 38, p. 293-303.

Mahood, G.A., 1990, Evidence for long residence times of rhyolitic magma in the Long Valley magmatic system: The isotopic record in precaldera lavas of Glass Mountain: Reply: Earth and Planetary Science Letters, v. 99, p. 395-399.

Mark, D. F., Petraglia, M., Smith, V. C., Morgan, L. E., Barfod, D. N., Ellis, B. S., Pearce, N.J., Pal, J.N., and Korisettar, R., 2013, A high-precision $^{40}Ar/^{39}Ar$ age for the Young Toba Tuff and dating of ultra-distal tephra: Forcing of Quaternary climate and implications for hominin occupation of India: Quaternary Geochronology, v. 10, doi: 10.1016/j.quageo.2012.12.004..

Mattinson, J.M., 1994, A study of complex discordance in zircons using step-wise dissolution techniques: Contributions to Mineralogy and Petrology: v. 116, p. 117-129.

Mattinson, J.M., 2010, Analysis of the relative decay constants of235 U and 238U by multi-step CA-TIMS measurements of closed-system natural zircon samples: Chemical Geology, v. 275, p. 186-198.

McClelland, W.C., and Mattinson, J.M., 1996, Resolving high precision U-Pb ages from Tertiary plutons with complex zircon systematics: Geochimica et Cosmochimica Acta, v. 60, no. 20, p. 3955-3965.

McDowell, S.M., Miller, C.F., Mundil, R., Ferguson, C.A., and Wooden, J.L., 2014, Zircon evidence for a ~200 k.y. supereruption-related thermal flare-up in the Miocene southern Black Mountains, western Arizona, USA: Contributions to Mineralogy and Petrology, v. 168, p. 1-21.

Memeti, V., Paterson, S.R., Matzel, J., Mundil, R., and Okaya, D., 2010, Magmatic lobes as "snapshots" of magma chamber growth and evolution in large, composite batholiths: an example from the Tuolumne Intrusion, Sierra Nevada, CA: Geological Society of America Bulletin, v. 24, p. 1912-1931.

Miller, D.M., Leslie, S.R., Hillhouse, J.W., Wooden, J.L., Vazquez, J.A., and Reynolds, R.E., 2010, Reconnaissance geochronology of tuffs in the Miocene Barstow Formation: implications for basin evolution and tectonics in the central Mojave Desert, California, *in* Reynolds, R. E., and Miller, D. M., eds., Overboard in the Mojave: Desert Studies Consortium, California State University, Fullerton, p.70-84.

Miller, J.S., Heizler, M.T., and Miller, C.F., 1998, Timing of magmatism, basin formation, and tilting at the west edge of the Colorado River extensional corridor: Results from single-crystal $^{40}Ar/^{39}Ar$ geochronology of Tertiary rocks in the Old Woman Mountains area, southeastern California: The Journal of Geology, v. 106, p. 195-210.

Miller, J.S., Glazner, A.F., Farmer, G.L., Suayah, I.B., and Keith, L.A., 2000, A Sr, Nd, and Pb isotopic study of mantle domains and crustal structure from Miocene volcanic rocks in the Mojave Desert, California: Geological Society of America Bulletin, v. 112, p. 1264-1279.

Miller, J., and Wooden, J., 2004, Residence, resorption, and recycling of zircons in the Devils Kitchen rhyolite, Coso volcanic field, California: Journal of Petrology, v. 45, p. 2155-2170.

Miller, J.S., Matzel, J.E., Miller, C.F., Burgess, S.D., and Miller, R.B., 2007, Zircon growth and recycling during the assembly of large, composite arc plutons: Journal of Volcanology and Geothermal Research, v. 167, p. 282-299.

Meyers, S.R., Siewert, S.E., Singer, B.S., Sageman, B.B., Condon, D.J., Obradovich, J. D., and Sawyer, D. A., 2012, Intercalibration of radioisotopic and astrochronologic time scales for the Cenomanian-Turonian boundary interval, Western Interior Basin, USA: Geology, v. 40, p. 7-10.

Mundil, R., Ludwig, K.R., Metcalfe, I., and Renne, P.R., 2004, Age and timing of the Permian mass extinctions: U-Pb dating of closed-system zircons: Science, v. 305, p. 1760-1763.

Murphy, R.T., Faulds, J.E., and Hillemeyer, F.L., 2004, Preliminary geologic map of the north half of the Union Pass Quadrangle, Mojave County, Arizona: Nevada Bureau of Mines and Geology, 1:24,000 scale.

Nielson, J.E., Lux, D.R., Dalrymple, G.B., and Glazner, A.F., 1990, Age of the Peach Springs Tuff, southeastern California and western Arizona: Journal of Geophysical Research, v. 95, p. 571-580.

Nielson, J.E., and Beratan, K.K., 1995, Stratigraphic and structural synthesis of a Miocene extensional terrane, southeast California and west-central Arizona: Geological Society of America Bulletin, v. 107, p. 241-252.

Pallister, J.S., Hoblitt, R.P., and Reyes, A.G., 1992, A basalt trigger for the 1991 eruptions of Pinatubo Volcano?: Nature, v. 356, p. 426-428.

Pamukcu, A.S., Carley, T.L., Gualda, G.A.R., Miller, C.F., and Ferguson, C.A., 2013, The evolution of the Peach Spring giant magma body: Evidence from accessory mineral textures and compositions, bulk pumice and glass geochemistry, and rhyolite-MELTS modeling: Journal of Petrology, v. 54, p. 1109-1148.

Parrish, R.R., and Noble, S.R., 2003, Zircon U-Th-Pb geochronology by isotope dilution—thermal ionization mass spectrometry (ID-TIMS): Reviews in Mineralogy and Geochemistry, v. 53, p. 183-213.

Pearthree, P.A., Ferguson, C.A., Johnson, B.J., and Guynn, J., 2009, Geologic map and report for the proposed State Route 95 realignment corridor, Mohave County, Arizona: Arizona Geological Survey DGM-65, v. 1, 5 sheets, 1:24,000 scale, 44 p.

Pupin, J., and Turco, G., 1972, Application of morphological data of accessory zirconium in endogenous petrology: Comptes Renddus Hebdomadaires Des Seances De L Academie Des Sciences Serie D, v. 275, p. 799.

Phillips, D., and Matchan, E.L., 2013, Ultra-high precision $^{40}Ar/^{39}Ar$ ages for Fish Canyon Tuff and Alder Creek Rhyolite sanidine: New dating standards required?: Geochimica et Cosmochimica Acta, v. 121, p. 229-239.

Rampino, M.R., Self, S., and Stothers, R.B., 1988, Volcanic winters: Annual Review of Earth and Planetary Science, v. 16, p. 73-99.

Rampino, M.R., and Self, S., 1992, Volcanic winter and accelerated glaciation following the Toba super-eruption: Nature, v. 359, p. 50-52.

Ransome, F.L. (1923). Geology of the Oatman Gold District, Arizona: A Preliminary Report. US Government Printing Office.

Reid, M.R., Coath, C.D., Harrison, T.M., and McKeegan, K.D., 1997, Prolonged residence times for the youngest rhyolites associated with Long Valley Caldera: 230Th-238U microprobe dating of young zircons: Earth and Planetary Science Letters, v. 150, p. 27-39.

Reid, M.R., 2003, Timescales of magma transfer and storage in the crust, in Rudnick, R.L., ed., Treatise on geochemistry: Amsterdam, Elsevier, p. 263-292

Reid, M.R., 2008, How long does it take to supersize an eruption?: Elements, v. 4, p. 23-28.

Reid, M.R., Vazquez, J.A., and Schmitt, A.K., 2011, Zircon-scale insights into the history of a supervolcano, Bishop Tuff, Long Valley, California, with implications for the Ti-in-zircon geothermometer: Contributions to Mineralogy and Petrology, v. 161, no. 2, p. 293-311.

Renne P.R., Mundil, R., Balco G., Min, K.W., and Ludwig K.R., 2010, Joint determination of ^{40}K decay constants and $^{40}Ar^*/^{40}K$ for the Fish Canyon sanidine standard, and improved accuracy for $^{40}Ar/^{39}Ar$ geochronology: Geochimica et Cosmochimica Acta, v. 74, p. 5349-5367.

Renne, P.R., Mulcahy, S.R., Cassata, W.S., Morgan, L. E., Kelley, S. P., Hlusko, L. J., and Njau, J. K., 2012, Retention of inherited Ar by alkali feldspar xenocrysts in a magma: Kinetic constraints from Ba zoning profiles: Geochimica et Cosmochimica Acta, v. 93, p. 129-142.

Rivera, T.A., Storey, M., Schmitz, M. D., and Crowley, J. L., 2013, Age intercalibration $^{40}Ar/^{39}Ar$ sanidine and chemically distinct U-Pb zircon populations from the Alder Creek Rhyolite Quaternary geochronology standard: Chemical Geology, v. 345, p. 87-98.

Rivera, T.A., Schmitz, M.D., Crowley, J.L., and Storey, M., 2014, Rapid magma evolution constrained by zircon petrochronology and $^{40}Ar/^{39}Ar$ sanidine ages for the Huckleberry Ridge Tuff, Yellowstone, USA: Geology, v. 42, p. 643-646.

Sageman, B.B., Singer, B.S., Meyers, S.R., Siewert, S.E., Walaszczyk, I., Condon, D.J., Jicha, B.R., Obradovich, J.D., and Sawyer, D.A., 2014, Integrating $^{40}Ar/^{39}Ar$, U-Pb, and astronomical clocks in the Cretaceous Niobrara Formation, Western Interior Basin, USA: Geological Society of America Bulletin, v. 126, no. 7-8, p. 956.

Sambridge, M.S., and Compston, W., 1994, Mixture modeling of multi-component data sets with application to ion-probe zircon ages: Earth and Planetary Science Letters, v. 128, p. 373-390.

Samson, S.D., and Alexander Jr, E.C., 1987, Calibration of the interlaboratoty $^{40}Ar/^{39}Ar$ dating standard, MMhb-1: Chemical Geology, v. 66, p. 27-34.

Schärer, U., 1984, The effect of initial ^{230}Th disequilibrium on young U-Pb ages: the Makalu case, Himalaya: Earth and Planetary Science Letters, v. 67, p. 191-204.

Schoene, B., Guex, J., Bartolini, A., Schaltegger, U., and Blackburn, T.J., 2010, Correlating the end-Triassic mass extinction and flood basalt volcanism at the 100 ka level: Geology, v. 38, no. 5, p. 387-390.

Schmitt, A.K., Lindsay, J.M., de Silva, S., and Trumbull, R.B., 2003, U-Pb zircon chronostratigraphy of early-Pliocene ignimbrites from La Pacana, North Chile; implications for the formation of stratified magma chambers: Journal of Volcanology and Geothermal Research, v. 120, p. 43-53.

Schmitt, A.K., Stockli, D.F., Lindsay, J.M., Robertson, R., Lovera, O.M., and Kislitsyn, R., 2010, Episodic growth and homogenization of plutonic roots in arc volcanoes from combined U–Th and (U–Th)/He zircon dating: Earth and Planetary Science Letters, v. 295, p. 91-103.

Schmitz, M.D., Bowring, S.A., and Ireland, T.R., 2003, Evaluation of Duluth Complex anorthositic series (AS3) zircon as a U-Pb geochronological standard: New high-precision isotope dilution thermal ionization mass spectrometry results: Geochimica et Cosmochimica Acta, v. 67, p. 3665-3672.

Schmitt, A.K., Stockli, D.F., Lindsay, J.M., Robertson, R., Lovera, O.M., and Kislitsyn, R., 2010, Episodic growth and homogenization of plutonic roots in arc volcanoes from combined U–Th and (U–Th)/He zircon dating: Earth and Planetary Science Letters, v. 295, p. 91–103, doi: 10.1016/j.epsl.2010.03.028.

Self, S., Goff, G., Gardner, J.N., Wright, J.V., and Kite, W.M., 1986, Explosive rhyolitic volcanism in the Jemez Mountains: Vent locations, caldera development and relation to regional structure: Journal of Geophysical Research, v. 91, p. 1779-1798.

Self, S., 2006, The effects and consequences of very large explosive volcanic eruptions: Royal Society of London Philosophical Transaction, ser. A, v. 364, p. 2073-2097.

Silver, L.T., and Deutsch, S., 1963, Uranium-lead isotopic variations in zircons: a case study: The Journal of Geology, v. 71, p. 721-758.

Simon, J.I., and Reid, M.R., 2005, The pace of rhyolite differentiation and storage in an 'archetypal' silicic magma system, Long Valley, California: Earth and Planetary Science Letters, v. 235, p. 123-140.

Simon, J.I., Renne, P.R., and Mundil, R., 2008, Implications of pre-eruptive magmatic histories of zircons for U–Pb geochronology of silicic extrusions: Earth and Planetary Science Letters, v. 266, p. 82-194.

Sparks, S.R., and Sigurdsson, H., 1977, Magma mixing: a mechanism for triggering acid explosive eruptions: Nature, v. 267, p. 315-318.

Sparks, R.S.J., Huppert, H.E., and Wilson, C.J.N., 1990, Evidence for long residence times of rhyolitic magma in the Long Valley magmatic system: The isotopic record in precaldera lavas of Glass Mountain: Comment: Earth and Planetary Science Letters, v. 99, p. 387-389.

Sparks, S., Self, S., Grattan, J., Oppenheimer, C., Pyle, D., and Rymer, H., 2005, Super eruptions: Global effects and future threats: London, Geological Society, Report of a Geological Society of London Working Group, p. 1-24.

Spell, T.L., Smith, E. I., Sanford, A., and Zanetti, K.A., 2001, Systematics of xenocrystic contamination: preservation of discrete feldspar populations at McCullough Pass Caldera revealed by $^{40}Ar/^{39}Ar$ dating: Earth and Planetary Science Letters, v. 190, p. 153-165.

Stacey, J.S., and Kramers, J.D., 1975, Approximation of terrestrial Pb isotope evolution by two-stage model: Earth and Planetary Science Letters, v. 26, p. 207-221.

Stelten, M.E., and Cooper, K.M., 2012, Constraints on the nature of the subvolcanic reservoir at South Sister volcano, Oregon from U-series dating combined with sub-crystal trace-element analysis of plagioclase and zircon: Earth and Planetary Science Letters, v. 313, p. 1-11.

Storm, S., Shane, P., Schmitt, A., and Lindsay, J.M., 2011, Decoupled crystallization and eruption histories of the rhyolite magmatic system at Tarawera volcano revealed by zircon ages and growth rates: Contributions to Mineralogy and Petrology, v. 163, p. 505-519.

Storm, S., Shane, P., Schmitt, A., and Lindsay, J.M., 2010, Contrasting punctuated zircon growth in two syn-erupted Rhyolite magmas from Tarawera volcano: insights to crystal diversity in magmatic systems, Earth and Planetary Science Letters, v. 310, p. 511-520.

Tappa, M.J., Coleman, D.S., Mills, R.D., and Samperton, K.M., 2011, The plutonic record of a silicic ignimbrite from the Latir volcanic field, New Mexico: Geochemistry, Geophysics, Geosystems, v. 12, no. 10, Q10011, doi: 10.1029/20011GC003700.

Tilton, G.R., 1960, Volume diffusion as a mechanism for discordant lead ages: Journal of Geophysical Research, v. 65, p. 2933-2945.

Vazquez, J.A., Reid, M.R., 2002, Time scales of magma storage and differentiation of voluminous high-silica rhyolites at Yellowstone Caldera, Wyoming: Contributions to Mineralogy and Petrology, v. 144, p. 274-285.

Vazquez, J.A., and Reid, M.R., 2004, Probing the accumulation history of the voluminous Toba magma: Science, v. 305, p. 991-994.

Walker Jr, B.A., Miller, C.F., Lowery-Claiborne, L., Wooden, J.L., and Miller, J.S., 2007, Geology and geochronology of the Spirit Mountain batholith, southern Nevada: implications for timescales and physical processes of batholith construction: Journal of Volcanology and Geothermal Research, v. 167, p. 239-262.

Wark, D.A., Hildreth, W., Spear, F.S., Cherniak, D.J., and Watson, E.B., 2007, Pre-eruption recharge of the Bishop magma system: Geology, v. 35, p. 235-238.

Watson, E.B., and Harrison, T.M., 1983, Zircon saturation revisited: temperature and composition effects in a variety of crustal magma types: Earth and Planetary Science Letters, v. 64, p. 295-304.

Wells, R.E., and Hillhouse, J.W., 1989, Paleomagnetism and tectonic rotation of the lower Miocene Peach Spring Tuff: Colorado Plateau, Arizona, to Barstow, California: Geological Society of America Bulletin, v. 101, p. 846-863.

Westerhold, T., Röhl, U., and Laskar, J., 2012, Time scale controversy: Accurate orbital calibration of the early Paleogene: Geochemistry, Geophysics, Geosystems, v. 13, no. 6, Q06015, doi: 10.1029/2012GC004096.

Wetherill, G.W., 1956, Discordant uranium-lead ages, 1: American Geophysical Union Transactions, v. 37, p. 320-26.

Wetherill, G.W., 1963, Discordant uranium-lead ages, 2, Discordant ages resulting from diffusion of lead and uranium: Journal of Geophysical Research, v. 68, p. 2156-2202.

Wilds, N., 1997 $^{40}Ar/^{39}Ar$ dating of the extensional anticlines in the southern part of the Black Mountain accommodation zone [Senior Independent Study Thesis]: Wooster, College of Wooster, 47 p.

Wotzlaw, J.F., Schaltegger, U., Frick, D.A., Dungan, M.A., Gerdes, A., and Günther, D., 2013, Tracking the evolution of large-volume silicic magma reservoirs from assembly to supereruption: Geology, v. 41, p. 867-870.

Young, R.A., and Brennan, W.J., 1974, The Peach Springs Tuff: Its bearing on structural evolution of the Colorado Plateau and development of Cenozoic drainage in Mohave County, Arizona: Geological Society of America Bulletin, v. 85, p. 83-90.

Zimmerman, S.H., Hemming, S.R., Kent, D.V., and Searle, S.Y., 2006, Revised chronology for late Pleistocene Mono Lake sediments based on paleointensity correlation to the global reference curve: Earth and Planetary Science Letters, v. 252, p. 94-106.

APPENDIX A: SIMS ZIRCON TRACE ELEMENT ABUNDANCES

TABLE A1: PEACH SPRING TUFF ZIRCON SIMS TRACE ELEMENT ABUNDANCES

Spot Name	Li (ppm)	Be (ppm)	B (ppm)	F (ppm)	P (ppm)	Sc (ppm)	Ti from 49 (ppm)	Y (ppm)	Nb (ppm)	La (ppm)	Ce (ppm)	Nd (ppm)
2H-1.1C	0.0	1.0	0.0	21	671	87	21.0	2755	26	0.358	321	6.7
2H-35.2T	0.0	0.5	0.1	20	303	38	8.3	1130	11	0.119	100	1.8
2H-35.3E	0.0	0.1	0.1	962	645	37	9.8	773	7	5.531	60	3.6
2H-36.1e	0.0	14.1	0.1	18	366	49	15.2	1066	5	0.087	70	3.5
2H-36.2E	0.0	2.0	0.0	15	195	43	8.9	767	7	0.075	74	1.0
2H-37.1E	0.0	0.0	0.0	9	572	39	8.4	1017	8	0.099	54	0.7
2H-37.1I	0.0	37.9	0.1	43	721	36	12.4	5105	24	0.184	225	10.6
2H-38.1E	0.0	12.5	0.4	200	454	56	20.8	1326	7	3.736	129	4.6
2H-39.1E	0.0	0.0	0.1	9	400	47	16.2	622	4	0.078	51	1.2
2H-39.2C	0.0	0.0	0.1	24	248	39	25.5	996	2	0.141	54	5.3
2H-39.3I	0.0	0.0	0.0	15	244	37	17.6	622	4	0.104	74	1.9
2H-40.1C	0.0	0.0	0.1	11	562	43	6.9	997	9	0.052	61	0.7
2H-40.2E	0.0	0.2	0.0	20	229	50	5.1	1215	22	0.100	127	1.1
2H-41.1C	0.0	0.0	0.0	9	321	40	10.7	663	6	0.106	51	0.9
2H-41.2E	0.0	0.2	0.1	16	198	54	4.9	1200	24	0.070	113	0.9
2H-42.1C	0.0	2.9	0.1	41	464	67	14.2	3395	8	5.927	193	16.6
2H-42.2E	0.0	4.3	0.0	11	188	28	7.8	731	6	0.074	57	0.7
2H-43.1C	0.0	21.4	0.1	64	546	59	10.0	3002	48	0.268	283	3.0
2H-43.2E	0.0	2.6	0.1	17	245	50	5.3	1225	24	0.080	127	1.1
2H-44.1I	0.0	0.1	0.0	12	401	45	7.7	725	7	0.104	53	0.9
2H-45.1T	0.0	0.1	0.0	17	215	45	5.2	1032	16	0.079	104	0.9
2H-45.2C	0.0	1.1	0.1	24	718	62	12.5	3915	57	0.122	342	4.5
2H-46.1C	0.0	10.0	0.1	30	254	44	24.5	1306	2	1.023	63	7.4
2H-46.2C	0.0	0.5	0.1	14	273	44	22.8	604	3	0.089	48	1.6
2H-46.3C	0.0	0.4	0.1	17	265	38	20.1	624	4	0.115	73	1.6

TABLE A1 (continued): PEACH SPRING TUFF ZIRCON SIMS TRACE ELEMENT ABUNDANCES

Spot Name	Sm (ppm)	Eu (ppm)	Gd (ppm)	Ho (ppm)	Tb (ppm)	Dy (ppm)	Er (ppm)	Tm (ppm)	Yb (ppm)	Lu (ppm)	Th (ppm)	U (ppm)
2H-1.1C	15.31	4.187	126	120	36.4	353	458	85	586	97	1635	451
2H-35.2T	3.96	0.898	31	46	10.2	116	192	40	313	56	181	133
2H-35.3E	1.54	0.606	19	32	6.6	71	134	29	232	41	77	81
2H-36.1e	5.93	1.675	35	41	10.1	104	169	34	266	48	148	97
2H-36.2E	2.13	0.732	18	29	6.1	65	139	30	258	48	208	179
2H-37.1E	2.42	0.670	26	41	9.7	105	177	35	276	48	97	98
2H-37.1I	24.18	5.030	200	233	66.3	668	863	146	1006	153	661	296
2H-38.1E	8.15	2.559	56	56	15.8	156	229	43	331	57	241	117
2H-39.1E	2.63	0.905	19	26	6.4	67	115	24	203	36	114	90
2H-39.2C	8.53	2.801	48	41	12.4	117	159	33	248	43	174	85
2H-39.3I	3.44	1.038	21	26	6.5	70	110	23	195	35	177	117
2H-40.1C	2.16	0.535	21	38	7.7	89	173	36	299	55	143	154
2H-40.2E	2.04	0.393	17	42	7.0	90	215	50	445	88	508	382
2H-41.1C	2.07	0.740	17	27	5.8	65	119	24	200	37	82	83
2H-41.2E	1.86	0.421	17	40	6.7	86	219	51	469	90	381	343
2H-42.1C	27.76	6.367	173	147	47.1	443	552	100	723	121	432	179
2H-42.2E	2.19	0.582	18	29	6.8	74	132	27	215	39	83	73
2H-43.1C	8.06	1.597	78	121	27.5	304	511	100	761	125	1626	767
2H-43.2E	2.15	0.420	17	43	7.3	93	220	51	448	88	645	449
2H-44.1I	1.80	0.576	16	29	5.6	68	130	29	242	45	104	113
2H-45.1T	1.87	0.385	16	36	5.9	78	181	43	396	75	561	422
2H-45.2C	12.33	2.398	116	161	39.0	422	657	124	883	141	1654	740
2H-46.1C	10.79	3.623	61	53	16.1	152	217	41	312	54	202	93
2H-46.2C	3.00	1.070	21	24	6.3	63	105	20	174	33	91	61
2H-46.3C	3.31	0.991	21	25	6.7	68	111	23	183	33	134	92

TABLE A1 (continued): PEACH SPRING TUFF ZIRCON SIMS TRACE ELEMENT ABUNDANCES

Spot Name	Li (ppm)	Be (ppm)	B (ppm)	F (ppm)	P (ppm)	Sc (ppm)	Ti from 49 (ppm)	Y (ppm)	Nb (ppm)	La (ppm)	Ce (ppm)	Nd (ppm)
2H-46.4E	0.0	2.4	0.1	23	165	60	7.0	768	10	0.095	63	0.7
2H-57.1C	0.0	165.6	0.1	75	1010	94	18.7	6900	22	0.532	294	18.8
2H-60.1C	0.0	0.1	0.1	22	294	55	17.4	804	5	0.088	87	2.5
2H-67.1I	0.0	2.5	0.1	21	236	46	6.7	991	14	0.103	102	1.1
2H-70.1C	0.0	26.3	0.1	37	292	34	9.1	2956	12	0.449	129	7.0
2H-47.1C	0.0	0.2	0.1	21	258	55	20.0	650	3	0.169	54	1.7
2H-47.2E	0.0	0.6	0.1	23	168	48	6.0	1019	17	0.189	88	0.8
2H-48.1C	0.0	0.2	0.0	21	378	68	6.3	1048	10	0.112	67	1.3
2H-49.1C	0.0	0.3	0.0	30	375	41	7.6	3321	16	0.246	142	6.0
2H-49.2T	0.0	0.1	0.0	17	236	62	5.9	1279	24	0.135	119	1.0
2H-50.1C	0.0	0.0	0.0	11	691	43	6.7	1340	10	0.315	67	0.9
2H-51.1C	0.0	0.1	0.0	15	438	46	8.8	2325	33	0.131	208	2.3
2H-51.2E	0.0	0.0	0.0	11	172	66	5.4	1064	23	0.130	81	0.6
2H-52.1C	0.0	0.2	0.0	18	131	49	5.3	1522	6	0.172	80	1.9
2H-53.1C	0.0	21.6	0.1	34	742	82	21.2	6203	25	1.218	408	21.5
2H-53.2C	0.0	9.3	0.0	7	636	86	20.2	2762	26	0.250	293	6.6
2H-53.3T	0.0	0.0	0.0	4	133	18	6.9	350	4	0.211	38	0.3
2H-54.1I	0.0	1.3	0.0	8	410	46	9.8	1066	6	0.088	58	1.9
2H-54.2I	0.0	0.7	0.0	9	269	45	11.7	961	8	0.292	78	1.7
2H-55.1C	0.0	0.1	0.0	15	460	53	19.0	2228	7	0.303	147	8.9
2H-55.2C	0.0	0.0	0.0	9	555	46	21.1	1814	11	0.114	153	4.8
2H-55.3C	0.0	0.0	0.0	181	990	48	11.2	1607	21	36.939	190	15.9
2H-55.4E	0.0	0.0	0.1	13	197	37	9.0	944	18	0.600	89	0.8
2H-56.1C	0.0	0.0	0.0	36	389	38	14.0	995	8	4.070	77	2.8
2H-56.2I	0.0	0.1	0.0	10	223	53	8.8	874	9	0.641	100	1.7

TABLE A1 (continued): PEACH SPRING TUFF ZIRCON SIMS TRACE ELEMENT ABUNDANCES

Spot Name	Sm (ppm)	Eu (ppm)	Gd (ppm)	Ho (ppm)	Tb (ppm)	Dy (ppm)	Er (ppm)	Tm (ppm)	Yb (ppm)	Lu (ppm)	Th (ppm)	U (ppm)
2H-46.4E	1.48	0.491	12	28	4.8	61	139	32	298	61	160	172
2H-57.1C	40.96	9.379	256	213	72.6	653	823	229	1436	186	688	228
2H-60.1C	4.42	1.671	29	33	8.7	85	140	29	227	41	169	111
2H-67.1I	2.39	0.575	0	37	7.2	90	182	39	320	60	374	274
2H-70.1C	11.73	2.846	0	114	29.3	316	471	88	722	119	510	269
2H-47.1C	3.41	1.222	23	26	6.9	73	117	23	195	34	108	73
2H-47.2E	1.84	0.315	15	35	6.1	76	179	40	385	72	345	256
2H-48.1C	2.54	0.579	17	36	6.4	93	197	43	392	77	252	241
2H-49.1C	11.49	2.359	83	121	26.8	292	495	99	737	130	560	318
2H-49.2T	2.13	0.369	18	43	7.1	89	230	54	491	97	513	418
2H-50.1C	2.83	0.632	27	51	10.0	116	221	46	366	64	188	177
2H-51.1C	6.17	1.189	57	92	21.1	239	401	78	585	97	1053	531
2H-51.2E	1.45	0.324	14	36	5.3	74	190	46	440	90	224	280
2H-52.1C	3.72	0.924	29	53	10.6	120	246	56	484	91	355	234
2H-53.1C	44.82	10.427	295	270	84.7	795	991	174	1232	195	1094	382
2H-53.2C	14.86	3.973	117	123	35.9	349	457	83	598	98	1129	365
2H-53.3T	0.83	0.253	9	14	2.8	35	64	14	114	21	40	46
2H-54.1I	4.01	1.317	31	42	10.1	108	188	39	302	55	145	127
2H-54.2I	3.63	1.259	27	39	8.8	97	167	35	281	50	168	137
2H-55.1C	14.85	4.872	107	98	29.3	278	371	70	499	84	317	130
2H-55.2C	9.54	2.883	73	80	22.0	227	300	55	401	63	546	211
2H-55.3C	7.80	1.552	46	67	16.1	170	276	54	418	71	647	336
2H-55.4E	1.64	0.296	15	33	5.3	70	170	39	349	67	419	348
2H-56.1C	3.94	0.911	28	39	8.8	98	164	34	272	50	221	164
2H-56.2I	2.65	0.735	18	32	6.5	76	152	35	297	57	409	283

TABLE A1 (continued): PEACH SPRING TUFF ZIRCON SIMS TRACE ELEMENT ABUNDANCES

Spot Name	Li (ppm)	Be (ppm)	B (ppm)	F (ppm)	P (ppm)	Sc (ppm)	Ti from 49 (ppm)	Y (ppm)	Nb (ppm)	La (ppm)	Ce (ppm)	Nd (ppm)
2H-56.3T	0.0	0.1	0.0	6	195	40	5.9	852	13	0.091	88	0.8
2H-57.2E	0.0	0.5	0.0	4	224	46	7.0	949	10	0.137	71	1.0
2H-58.1C	0.0	0.0	0.0	10	295	63	19.2	1131	3	0.171	53	5.4
2H-58.2E	0.0	0.0	0.0	4	203	41	14.4	547	4	0.053	62	1.2
2H-59.1I	0.0	0.0	0.0	9	233	47	11.8	752	5	0.027	55	1.2
2H-59.2I	0.0	0.4	0.0	11	185	46	6.5	1702	5	0.054	80	3.1
2H-60.2C	0.0	0.0	0.0	7	269	52	12.4	780	5	0.045	59	1.6
2H-61.1I	0.0	0.1	0.0	6	163	46	23.6	543	1	0.075	29	2.2
2H-61.2I	0.0	0.1	0.0	18	386	70	32.0	2299	4	0.350	77	10.8
2H-61.3I	0.0	0.0	0.0	9	159	43	26.8	393	1	0.052	22	1.6
2H-61.4	0.0	0.0	0.0	10	229	41	10.9	804	6	0.051	75	1.5
2H-62.2C	0.0	0.2	0.0	7	576	110	24.5	2694	9	0.401	280	15.6
2H-62.3I	0.0	0.0	0.0	6	367	67	20.7	1011	5	0.119	117	3.9
2H-62.4I	0.0	0.0	0.0	20	370	51	16.3	804	4	4.976	98	3.9
2H-62.5E	0.1	0.0	0.6	31	192	41	29.6	941	17	3.185	95	1.2
2H-63.1	0.0	0.2	0.0	13	167	17	8.8	450	4	0.341	41	0.5
2H-63.2C	0.0	1.5	0.1	22	307	47	12.7	1803	5	0.067	101	5.9
2H64.1E	0.0	1.3	0.0	12	196	37	9.2	684	8	0.028	71	0.8
2H64.2I	0.0	0.0	0.0	9	417	34	9.9	722	7	0.060	47	0.8
2H-64.3C	0.0	1.0	0.0	10	307	37	13.1	897	7	0.065	65	1.7
2H-65.1C	0.0	0.4	0.1	32	181	54	5.0	1752	8	0.105	86	3.2
2H-65.2E	0.0	0.1	0.0	11	211	51	4.8	1051	21	0.057	96	0.7
2H-66.1C	0.0	0.1	0.0	16	724	74	22.4	2746	18	0.139	255	6.8
2H-66.2E	0.0	0.0	0.0	17	376	35	11.3	1381	11	0.094	110	2.2
2H-67.2C	0.0	5.5	0.0	15	256	67	9.1	1209	15	0.078	85	1.6

TABLE A1 (continued): PEACH SPRING TUFF ZIRCON SIMS TRACE ELEMENT ABUNDANCES

Spot Name	Sm (ppm)	Eu (ppm)	Gd (ppm)	Ho (ppm)	Tb (ppm)	Dy (ppm)	Er (ppm)	Tm (ppm)	Yb (ppm)	Lu (ppm)	Th (ppm)	U (ppm)
2H-56.3T	1.81	0.422	15	31	5.7	71	161	37	315	60	360	287
2H-57.2E	2.46	0.588	22	36	7.3	87	172	37	320	60	118	117
2H-58.1C	7.37	3.059	46	49	13.2	132	192	39	294	52	135	74
2H-58.2E	2.42	0.913	17	22	5.3	58	95	20	158	29	83	65
2H-59.1I	2.97	1.090	22	30	7.3	77	125	28	215	40	88	74
2H-59.2I	5.88	1.574	44	65	14.6	157	289	62	509	93	340	212
2H-60.2C	3.09	1.209	23	32	8.0	82	138	29	227	43	93	78
2H-61.1I	3.92	2.259	27	25	7.2	74	107	21	162	30	52	30
2H-61.2I	17.77	9.842	115	100	30.0	280	384	71	537	92	282	116
2H-61.3I	2.60	1.557	18	18	5.3	55	82	17	140	24	38	24
2H-61.4	3.03	0.986	24	32	7.3	79	146	30	238	43	169	144
2H-62.2C	25.79	9.801	156	124	41.8	383	480	90	690	115	692	190
2H-62.3I	6.63	2.545	43	43	11.9	118	164	32	248	45	158	72
2H-62.4I	5.27	1.890	34	33	9.2	92	137	27	211	38	126	72
2H-62.5E	1.71	0.339	15	33	5.4	67	171	40	363	70	361	316
2H-63.1	1.14	0.298	10	19	4.3	49	82	18	135	24	42	48
2H-63.2C	11.87	2.778	75	70	20.6	190	259	48	354	60	141	79
2H64.1E	2.24	0.611	17	27	5.9	67	126	28	236	42	185	157
2H64.2I	1.81	0.529	16	28	6.1	69	126	28	217	40	100	110
2H-64.3C	3.70	0.755	25	37	8.6	92	161	34	269	49	167	148
2H-65.1C	4.32	1.087	34	62	11.6	139	310	70	608	112	470	303
2H-65.2E	1.57	0.329	14	37	5.9	77	194	48	436	87	405	364
2H-66.1C	15.43	3.955	122	123	37.0	363	450	79	565	89	800	263
2H-66.2E	5.76	1.356	48	60	15.8	166	242	44	326	54	188	129
2H-67.2C	3.64	1.020	30	50	10.4	121	237	52	434	82	217	205

TABLE A1 (continued): PEACH SPRING TUFF ZIRCON SIMS TRACE ELEMENT ABUNDANCES

Spot Name	Li (ppm)	Be (ppm)	B (ppm)	F (ppm)	P (ppm)	Sc (ppm)	Ti from 49 (ppm)	Y (ppm)	Nb (ppm)	La (ppm)	Ce (ppm)	Nd (ppm)
2H-68.1C	0.0	21.7	0.0	24	273	58	6.2	1474	9	0.111	80	2.8
2H-69.1E	0.0	0.6	0.0	9	147	39	6.5	559	7	0.045	63	0.5
2H-69.2C	0.0	0.3	0.0	9	310	54	27.1	588	3	0.078	50	1.7
2H-71.1C	0.0	0.1	0.1	22	240	89	9.8	1052	18	0.798	99	1.4
2H-72.1C	0.0	9.2	0.1	31	251	39	11.4	1538	5	0.088	76	4.6
2H-73.1E	0.0	0.1	0.0	17	211	47	5.1	1082	18	0.122	106	0.8
2H-73.2C	0.0	0.5	0.0	23	258	39	10.8	1539	5	0.141	75	4.3
2H-74.1E	0.0	0.3	0.1	8	786	39	5.7	1554	11	0.050	72	1.0
2H-74.2C	0.0	42.4	0.0	16	594	60	10.6	3158	47	0.126	269	3.1
2H-75.1E	0.0	0.0	0.0	7	181	22	8.1	558	5	0.035	51	0.5
2H-75.2C	0.0	1.1	0.1	21	602	73	15.8	4425	13	0.382	260	17.4
2H-76.1C	0.0	4.0	0.0	12	504	43	13.2	1789	15	0.060	147	3.2
2H-76.2C	0.0	49.8	0.1	36	641	51	14.2	4643	12	0.277	229	15.0
2H-77.1C	0.0	2.4	0.0	29	610	51	15.4	4648	13	0.337	245	15.3
2H-77.2I	0.0	4.7	0.0	16	678	83	20.3	2675	21	0.257	284	6.7
2H-77.3E	0.0	2.6	0.0	16	187	39	5.0	871	14	0.097	86	0.8
2H-78.1C	0.0	2.1	0.1	73	731	39	8.2	5103	28	0.602	254	9.4
2H-79.1C	0.0	0.5	0.0	20	201	79	7.4	1299	16	0.077	91	1.6
2H-79.2E	0.0	0.2	0.0	17	205	43	5.1	903	14	0.067	90	0.8
2H-80.1C	0.0	0.4	0.1	23	321	37	10.3	2221	6	0.098	94	5.6
2H-80.2I	0.0	0.6	0.1	23	543	53	14.4	4187	13	0.259	213	13.6
2H-80.3E	0.3	0.3	2.8	65	467	54	78.1	1764	21	8.942	189	4.7
2H-81.1E	0.0	0.5	0.1	12	209	42	4.5	910	17	0.040	90	0.7
2H-81.2I	0.0	0.6	0.0	9	373	40	9.7	1382	12	0.058	115	1.8
2H-81.3C	0.0	0.7	0.1	11	307	55	14.7	2035	4	0.196	105	9.6

TABLE A1 (continued): PEACH SPRING TUFF ZIRCON SIMS TRACE ELEMENT ABUNDANCES

Spot Name	Sm (ppm)	Eu (ppm)	Gd (ppm)	Ho (ppm)	Tb (ppm)	Dy (ppm)	Er (ppm)	Tm (ppm)	Yb (ppm)	Lu (ppm)	Th (ppm)	U (ppm)
2H-68.1C	4.22	1.090	29	52	10.0	111	247	55	480	91	342	255
2H-69.1E	1.06	0.376	10	20	3.6	43	103	24	215	43	187	176
2H-69.2C	3.28	1.419	22	24	6.9	66	107	21	170	31	96	62
2H-71.1C	2.12	0.632	17	37	6.3	77	195	48	440	91	332	306
2H-72.1C	8.45	2.275	54	60	15.8	158	253	49	383	67	239	147
2H-73.1E	1.87	0.380	15	37	5.9	80	190	45	400	78	375	316
2H-73.2C	8.59	2.653	54	64	16.8	169	268	54	402	69	254	155
2H-74.1E	3.50	0.707	34	63	12.6	151	282	57	449	75	283	231
2H-74.2C	8.88	1.668	82	125	28.8	321	533	106	800	130	1080	617
2H-75.1E	1.64	0.410	16	23	5.4	63	101	20	162	28	62	60
2H-75.2C	35.09	8.732	227	197	62.3	578	736	133	964	157	622	234
2H-76.1C	7.77	1.770	64	81	21.9	228	303	56	398	63	455	219
2H-76.2C	30.52	7.288	223	207	65.1	616	768	137	946	153	604	233
2H-77.1C	31.54	7.667	221	204	64.3	614	774	138	1003	162	682	258
2H-77.2I	14.44	3.558	111	117	33.9	335	444	82	592	95	1070	330
2H-77.3E	1.59	0.242	12	31	4.9	64	158	37	340	66	355	299
2H-78.1C	18.93	3.509	156	210	50.5	532	792	148	1038	164	776	389
2H-79.1C	3.07	0.864	24	47	8.6	103	233	56	487	95	297	265
2H-79.2E	1.45	0.320	13	31	5.2	67	163	37	334	62	370	302
2H-80.1C	12.68	3.126	90	95	27.0	266	365	65	484	79	229	119
2H-80.2I	26.73	7.147	203	190	58.3	565	729	134	966	157	614	251
2H-80.3E	8.54	2.105	62	73	20.0	201	287	54	400	67	448	201
2H-81.1E	1.45	0.312	14	31	4.8	66	167	39	356	67	440	353
2H-81.2I	5.02	1.134	42	58	13.5	149	238	47	364	61	245	156
2H-81.3C	15.35	5.635	99	87	27.5	252	336	63	479	82	210	91

TABLE A1 (continued): PEACH SPRING TUFF ZIRCON SIMS TRACE ELEMENT ABUNDANCES

Spot Name	Li (ppm)	Be (ppm)	B (ppm)	F (ppm)	P (ppm)	Sc (ppm)	Ti from 49 (ppm)	Y (ppm)	Nb (ppm)	La (ppm)	Ce (ppm)	Nd (ppm)
3B_1.1C	0.0	6.8	0.0	22	381	54	16.0	2885	7	0.096	152	11.5
3B_1.2E	0.0	5.8	0.1	20	244	82	6.6	1411	33	0.025	124	1.1
3B_10.1C	0.0	0.0	0.0	32	191	52	6.2	1892	8	0.026	90	4.1
3B_10.2E	0.0	0.1	0.1	17	215	46	4.7	1031	19	0.013	107	0.9
3B_11.1C	0.0	0.2	0.1	50	1004	75	16.4	5658	81	0.053	478	7.3
3B_11.2E	0.0	0.0	0.1	15	223	51	5.2	1163	21	0.018	113	1.0
3B_12.2E	0.3	0.3	0.1	1331	1082	65	6.1	1312	28	28.917	200	17.9
3B_13.1C	0.0	7.0	0.1	80	651	34	11.3	4622	17	0.173	196	10.9
3B_14.1C	0.0	2.0	0.1	24	749	59	19.8	3173	27	0.056	269	6.0
3B_14.2E	0.0	0.0	0.1	14	332	32	11.5	1134	9	0.015	90	1.7
3B_15.1C	0.1	0.2	0.6	204	593	66	14.4	4484	15	0.529	280	17.5
3B_15.2I	0.0	26.1	0.1	24	424	44	9.4	2348	9	0.066	128	6.4
3B_15.3E	6.7	0.2	0.7	118	344	56	14.1	1221	24	5.113	146	4.4
3B_2.1C	0.0	2.8	0.0	22	772	37	10.9	2064	9	0.046	90	3.2
3B_2.2C	0.0	15.7	0.0	57	580	34	11.0	4621	19	0.061	199	10.3
3B_2.3I	0.0	2.6	0.1	24	296	32	14.9	1146	9	0.223	106	2.2
3B_2.4E	0.0	0.0	0.0	19	248	26	8.4	996	11	0.063	84	1.1
3B_3.1C	0.1	1.7	0.1	42	835	77	17.1	6059	20	0.228	382	21.6
3B_3.2E	0.3	0.0	0.1	15	240	36	6.7	890	10	0.008	82	0.9
3B_4.1C	0.0	1.3	0.1	18	262	48	10.4	982	11	0.013	96	1.6
3B_4.2E	0.0	5.9	0.1	25	182	45	5.0	1353	13	0.044	86	1.4
3B_5.1C	0.0	18.4	0.2	41	783	116	21.6	4497	19	0.304	375	21.1
3B_5.2E	0.0	1.6	0.1	20	309	32	10.1	1125	10	0.047	90	1.5
3B_6.1C	0.0	0.0	0.1	13	514	43	9.7	1111	10	0.041	66	1.4
3B_6.2E	0.0	0.0	0.0	16	211	49	5.1	1041	20	0.015	104	0.8

TABLE A1 (continued): PEACH SPRING TUFF ZIRCON SIMS TRACE ELEMENT ABUNDANCES

Spot Name	Sm (ppm)	Eu (ppm)	Gd (ppm)	Ho (ppm)	Tb (ppm)	Dy (ppm)	Er (ppm)	Tm (ppm)	Yb (ppm)	Lu (ppm)	Th (ppm)	U (ppm)
3B_1.1C	20.97	6.994	141	124	38.3	360	469	86	638	108	369	145
3B_1.2E	2.28	0.528	20	49	7.9	103	244	59	532	103	355	358
3B_10.1C	6.41	1.681	42	68	13.8	159	323	69	596	111	482	287
3B_10.2E	1.71	0.371	15	34	5.7	75	174	41	360	69	440	334
3B_11.1C	19.95	4.052	187	236	62.5	649	906	164	1155	178	1875	806
3B_11.2E	1.83	0.344	17	38	6.3	82	195	47	421	78	400	325
3B_12.2E	4.94	0.592	21	44	7.5	94	227	54	499	97	557	437
3B_13.1C	23.32	4.997	186	198	59.0	575	727	126	869	132	556	241
3B_14.1C	16.37	3.934	138	141	42.6	420	513	88	609	93	993	331
3B_14.2E	4.53	1.083	39	49	12.9	134	193	36	265	43	134	95
3B_15.1C	33.95	9.283	222	194	62.3	564	726	131	966	158	740	269
3B_15.2I	13.69	3.461	94	97	27.1	269	376	70	532	90	332	163
3B_15.3E	2.59	0.437	19	40	7.0	90	205	48	428	82	457	353
3B_2.1C	8.31	2.156	67	87	22.2	233	334	61	438	69	233	141
3B_2.2C	20.51	5.352	166	189	52.0	526	718	127	905	140	631	285
3B_2.3I	5.03	1.492	40	49	12.8	133	194	36	268	44	171	106
3B_2.4E	3.11	0.754	26	41	9.1	105	174	35	269	45	166	123
3B_3.1C	45.47	11.404	300	256	81.9	757	934	166	1186	189	960	308
3B_3.2E	2.34	0.542	21	34	7.2	84	152	32	270	47	149	123
3B_4.1C	3.30	0.992	24	37	8.4	92	165	34	278	50	244	179
3B_4.2E	2.79	0.614	23	46	8.3	105	231	53	471	91	352	281
3B_5.1C	39.49	11.384	247	195	63.1	571	708	127	940	155	813	239
3B_5.2E	3.79	0.949	36	46	11.9	127	186	36	271	44	169	120
3B_6.1C	3.33	0.979	28	44	9.7	111	194	42	328	57	214	192
3B_6.2E	1.65	0.377	15	35	5.7	73	175	42	368	71	511	376

TABLE A1 (continued): PEACH SPRING TUFF ZIRCON SIMS TRACE ELEMENT ABUNDANCES

Spot Name	Li (ppm)	Be (ppm)	B (ppm)	F (ppm)	P (ppm)	Sc (ppm)	Ti from 49 (ppm)	Y (ppm)	Nb (ppm)	La (ppm)	Ce (ppm)	Nd (ppm)
3B_7.1C	0.0	0.0	0.1	9	885	41	7.9	1637	11	0.021	79	1.6
3B_7.2I	0.0	0.3	0.1	23	729	58	12.5	2687	31	0.025	208	3.2
3B_7.3E	0.0	0.0	0.0	9	156	18	6.4	507	9	0.018	52	0.4
3B_8.1C	0.0	0.0	0.1	10	149	15	7.6	314	4	0.011	33	0.2
3B_8.2E	0.0	0.1	0.1	12	297	58	6.7	1661	24	0.016	153	1.5
3B_9.1C	0.0	0.0	0.0	25	247	32	9.4	1555	5	0.025	74	3.4
3B_9.2E	0.0	0.0	0.1	15	205	42	5.2	872	16	0.014	90	0.7
3D-1.1	0.2	1.2	0.1	60	830	34	13.2	5875	21	0.094	253	13.2
3D-1.2E	2.1	0.1	0.2	21	250	53	7.4	1217	22	0.019	128	1.0
3D-1_2.1C	0.0	0.2	0.0	15	231	66	8.5	914	12	0.009	65	1.1
3D-1_3.1C	0.0	3.8	0.1	25	223	75	8.9	1103	15	0.024	84	1.4
3D-1_4.1E	0.0	0.9	0.0	9	339	39	7.0	814	8	0.013	57	0.7
3D-1_4.2I	0.0	24.9	0.1	22	446	41	11.5	2489	14	0.035	149	5.8
3D-1_6.1I	0.0	0.0	0.1	13	337	45	9.2	1351	16	0.019	123	1.7
3D-2_1.1C	0.0	0.7	0.1	15	219	50	13.7	1057	3	0.010	76	3.4
3D-2_1.2E	0.0	0.8	0.1	17	228	48	5.5	1037	16	0.009	106	0.9
3D-2_2.1C	0.1	1.7	0.1	104	551	44	7.6	5487	33	0.254	311	10.0
3D-2_2.2E	0.0	0.0	0.1	14	235	50	5.7	1095	19	0.014	113	1.0
3D-2_3.1C	0.0	6.0	0.1	17	238	60	15.1	1156	5	0.031	65	6.0
3D-2_3.2I	0.0	2.0	0.1	13	201	34	9.0	638	7	0.013	64	0.8
3D-2_3.3E	0.0	2.5	0.1	15	193	41	5.3	831	14	0.019	87	0.7
3D-2_4.1C	0.0	33.3	0.1	67	856	70	10.6	4621	51	0.068	327	6.1
3D-2_4.2E	0.0	3.8	0.1	17	175	41	5.2	793	12	0.014	77	0.7
3D-2_5.1C	0.0	8.0	0.1	175	460	68	8.3	1383	13	13.835	120	11.6

TABLE A1 (continued): PEACH SPRING TUFF ZIRCON SIMS TRACE ELEMENT ABUNDANCES

Spot Name	Sm (ppm)	Eu (ppm)	Gd (ppm)	Ho (ppm)	Tb (ppm)	Dy (ppm)	Er (ppm)	Tm (ppm)	Yb (ppm)	Lu (ppm)	Th (ppm)	U (ppm)
3B_7.1C	5.09	1.223	44	67	16.0	173	276	55	410	67	225	171
3B_7.2I	8.82	1.969	77	109	26.2	285	443	84	625	100	502	314
3B_7.3E	1.20	0.269	11	20	4.0	46	86	18	143	25	84	87
3B_8.1C	0.79	0.238	8	13	2.9	33	55	11	92	16	28	33
3B_8.2E	3.64	0.698	32	61	12.3	146	287	61	501	91	377	285
3B_9.1C	8.02	2.233	55	64	16.8	168	256	50	385	64	249	155
3B_9.2E	1.52	0.344	12	29	5.0	61	146	34	307	57	396	308
3D-1.1	30.25	6.605	254	260	78.4	773	939	159	1066	163	743	298
3D-1.2E	2.19	0.460	19	42	7.4	89	210	48	426	80	844	522
3D-1_2.1C	2.42	0.689	18	33	6.6	78	162	37	324	65	147	162
3D-1_3.1C	2.70	0.972	22	40	7.7	94	197	44	385	77	205	192
3D-1_4.1E	1.80	0.499	18	32	6.5	73	140	29	248	44	90	88
3D-1_4.2I	12.44	2.937	94	108	29.6	299	408	73	541	87	344	175
3D-1_6.1I	4.29	1.012	35	52	12.1	135	226	45	354	60	367	235
3D-2_1.1C	7.60	2.359	47	43	13.1	127	176	33	254	45	91	48
3D-2_1.2E	2.04	0.438	17	35	6.3	80	179	42	370	69	489	352
3D-2_2.1C	20.54	3.801	163	240	59.0	640	1003	192	1406	220	1367	590
3D-2_2.2E	2.02	0.420	16	36	6.4	80	184	43	379	72	521	373
3D-2_3.1C	9.24	3.406	50	47	13.8	131	187	36	277	49	136	73
3D-2_3.2I	1.84	0.566	15	25	5.1	60	110	24	198	36	145	128
3D-2_3.3E	1.72	0.365	13	29	5.1	64	144	33	290	55	287	236
3D-2_4.1C	15.75	2.933	136	188	46.6	510	768	146	1083	172	1128	622
3D-2_4.2E	1.43	0.319	13	28	4.9	63	136	32	277	52	210	195
3D-2_5.1C	5.55	1.335	30	47	9.3	107	219	49	423	80	257	213

TABLE A1 (continued): PEACH SPRING TUFF ZIRCON SIMS TRACE ELEMENT ABUNDANCES

Spot Name	Li (ppm)	Be (ppm)	B (ppm)	F (ppm)	P (ppm)	Sc (ppm)	Ti from 49 (ppm)	Y (ppm)	Nb (ppm)	La (ppm)	Ce (ppm)	Nd (ppm)
3D-2_5.2E	0.0	4.2	0.1	20	242	51	6.1	1132	19	0.017	118	1.1
3D-2_6.1C	0.0	0.6	0.1	26	181	53	6.5	1725	7	0.041	85	3.5
3D-2_6.2E	0.0	0.1	0.0	19	205	49	4.8	1117	20	0.015	109	0.9
3D-2_7.1C	0.0	0.1	0.1	16	461	66	17.2	1637	13	0.046	162	4.1
3D-2_7.2E	0.0	0.0	0.1	13	244	48	7.5	972	12	0.009	87	1.2
3D-2_8.1C	0.0	0.3	0.2	22	227	80	6.8	1179	22	0.012	94	1.0
3D-2_8.2E	0.0	1.1	0.0	21	250	54	5.7	1229	23	0.020	131	1.1
3D-2_9.1C	0.0	0.3	0.1	21	452	42	14.9	2779	7	0.045	124	8.6
3D-2_9.2E	0.1	0.1	0.2	20	232	47	5.6	1013	17	0.013	103	0.9
3D-3_1.1C	0.0	1.2	0.0	14	547	61	13.7	4367	14	0.108	254	15.6
3D-3_1.2I	0.0	0.4	0.1	12	306	30	10.6	1040	8	0.013	85	1.6
3D-3_1.3E	0.0	0.6	0.1	14	281	34	9.0	1013	10	0.013	85	1.3
3D-3_3.1C	0.0	2.4	0.1	66	834	103	16.8	5629	27	0.129	393	17.0
3D-3_3.2E	0.0	0.0	0.1	16	310	38	9.5	1383	13	0.028	112	2.0
3D-3_4.1C	0.1	0.1	0.1	30	271	28	11.3	1573	6	0.031	79	3.5
3D-3_7.1C	0.2	3.0	0.1	18	722	46	12.6	1254	6	0.079	63	1.7
3D-3_7.2E	0.0	12.7	0.1	44	420	24	10.6	2709	8	0.044	101	6.9
3D-4_1.1C	0.0	26.9	0.2	37	387	29	10.0	2956	11	0.047	124	6.3
3D-4_1.2E	0.0	1.3	0.1	18	206	48	6.7	851	12	0.021	88	1.0
3D-4_2.1C	0.0	7.0	0.1	31	433	33	10.3	3176	10	0.052	126	7.8
3D-4_2.2E	0.0	1.7	0.1	17	236	58	6.5	1048	18	0.022	93	1.0
3D-4_6.1C	0.0	0.0	0.1	11	296	56	27.4	535	3	0.037	42	1.7
3D-4_6.2E	0.0	0.9	0.1	15	153	43	5.4	659	11	0.022	57	0.4
3D-4_7.1C	0.0	12.8	0.3	48	246	37	9.0	1645	6	0.164	80	3.7
3D-4_7.2E	0.0	2.0	0.2	29	287	48	12.8	890	9	0.097	82	1.7

TABLE A1 (continued): PEACH SPRING TUFF ZIRCON SIMS TRACE ELEMENT ABUNDANCES

Spot Name	Sm (ppm)	Eu (ppm)	Gd (ppm)	Ho (ppm)	Tb (ppm)	Dy (ppm)	Er (ppm)	Tm (ppm)	Yb (ppm)	Lu (ppm)	Th (ppm)	U (ppm)
3D-2_5.2E	2.37	0.435	18	38	7.1	86	188	43	380	70	624	408
3D-2_6.1C	5.43	1.490	36	60	11.8	139	280	62	540	101	425	261
3D-2_6.2E	1.72	0.335	16	37	6.1	80	193	46	417	78	384	324
3D-2_7.1C	8.83	2.365	65	70	19.7	196	271	50	381	64	369	162
3D-2_7.2E	2.81	0.598	22	37	7.6	89	169	37	309	56	158	129
3D-2_8.1C	2.25	0.596	20	41	7.3	91	207	49	431	85	242	249
3D-2_8.2E	1.95	0.386	18	41	6.9	89	209	48	433	82	806	507
3D-2_9.1C	20.00	5.069	130	118	38.2	367	442	77	529	82	257	113
3D-2_9.2E	1.87	0.420	17	34	6.4	78	178	40	355	65	530	379
3D-3_1.1C	32.80	7.835	221	198	61.9	590	730	128	914	146	627	236
3D-3_1.2I	4.36	1.054	34	43	11.6	122	174	33	239	39	124	90
3D-3_1.3E	3.46	0.826	29	40	9.7	106	168	34	260	44	165	119
3D-3_3.1C	37.72	8.774	259	235	74.6	706	882	157	1132	182	1077	393
3D-3_3.2E	5.36	1.224	42	57	13.7	148	227	44	335	57	232	147
3D-3_4.1C	7.63	1.598	54	64	16.2	171	267	52	414	69	371	225
3D-3_7.1C	4.70	1.336	41	53	13.6	146	207	38	279	46	95	73
3D-3_7.2E	15.78	3.561	112	124	35.2	348	471	82	568	87	322	164
3D-4_1.1C	14.66	3.611	108	121	33.1	343	469	84	603	95	357	179
3D-4_1.2E	1.76	0.418	16	30	5.6	71	150	32	283	53	294	231
3D-4_2.1C	16.53	3.648	128	136	39.5	387	499	88	618	97	337	162
3D-4_2.2E	2.07	0.449	18	36	6.8	84	181	41	353	67	291	237
3D-4_6.1C	3.13	1.314	19	22	5.6	58	91	18	153	27	79	52
3D-4_6.2E	1.06	0.269	11	23	4.1	51	119	27	250	48	127	144
3D-4_7.1C	7.67	2.367	54	67	16.6	170	271	52	410	71	257	150
3D-4_7.2E	3.50	1.284	27	35	8.5	91	151	31	247	45	192	141

TABLE A1 (continued): PEACH SPRING TUFF ZIRCON SIMS TRACE ELEMENT ABUNDANCES

Spot Name	Li (ppm)	Be (ppm)	B (ppm)	F (ppm)	P (ppm)	Sc (ppm)	Ti from 49 (ppm)	Y (ppm)	Nb (ppm)	La (ppm)	Ce (ppm)	Nd (ppm)
3D-4_8.1C	0.0	0.2	0.1	362	255	53	6.3	1586	7	1.921	87	4.0
3D-4_8.2E	0.0	0.1	0.1	54	281	50	5.3	1122	20	0.260	116	1.3
3D-4_9.1C	0.0	27.2	0.1	98	519	54	13.7	3661	11	0.229	192	12.5
3D-4_9.2E	0.0	0.2	0.1	11	321	34	9.1	1170	12	0.025	97	1.6
5D-1_1.1C	0.0	22.3	0.1	26	258	41	7.8	1868	8	0.254	81	3.3
5D-1_1.2I	0.0	9.2	0.2	28	529	45	12.1	2202	26	2.314	148	4.1
5D-1_1.3E	0.0	1.2	0.1	15	207	45	5.2	978	18	0.020	100	0.8
5D-1_2.1C	0.0	0.7	0.2	16	275	32	9.5	907	9	0.095	80	1.4
5D-1_2.2	0.0	2.0	0.2	11	304	36	9.3	1134	11	0.014	100	1.5
5D-1_3.1C	0.1	0.1	0.1	25	318	47	10.8	1902	6	0.035	99	5.3
5D-1_3.2I	0.0	0.0	0.1	8	439	47	14.3	1479	12	0.009	126	2.7
5D-1_3.3E	0.0	0.0	0.1	16	277	44	8.1	1030	11	0.018	97	1.2
5D-1_4.1C	0.0	8.1	0.1	65	557	41	10.9	4325	19	0.317	204	9.5
5D-1_4.2E	0.0	2.1	0.2	18	273	47	7.7	1092	22	0.892	348	3.0
5D-1_5.1C	0.0	1.3	0.1	19	304	75	10.3	1387	20	0.171	115	1.8
5D-1_5.2E	0.0	2.1	0.1	14	269	63	5.9	1567	31	0.018	163	1.4
5D-1_6.1C	0.1	0.3	0.1	32	532	54	16.0	2115	19	1.223	178	4.5
5D-1_6.2E	0.0	0.9	0.1	29	379	54	6.7	3329	16	0.044	164	5.8
5D-1_7.1C	0.0	4.2	0.2	17	301	69	9.3	1029	13	0.013	71	1.3
5D-1_7.2E	0.0	2.5	0.1	17	222	41	7.4	851	11	0.004	77	1.0
5D-2_1.1C	0.0	0.1	0.1	26	475	45	14.0	3239	8	0.081	153	11.3
5D-2_1.2E	0.0	0.0	0.0	3	326	77	27.8	529	3	0.053	91	3.9
5D-2_10.1C	0.0	4.7	0.1	34	764	142	27.6	3113	20	0.119	417	13.8
5D-2_10.2E	0.0	0.1	0.0	9	269	45	18.4	558	3	0.022	78	1.6

TABLE A1 (continued): PEACH SPRING TUFF ZIRCON SIMS TRACE ELEMENT ABUNDANCES

Spot Name	Sm (ppm)	Eu (ppm)	Gd (ppm)	Ho (ppm)	Tb (ppm)	Dy (ppm)	Er (ppm)	Tm (ppm)	Yb (ppm)	Lu (ppm)	Th (ppm)	U (ppm)
3D-4_8.1C	4.83	1.283	31	56	10.5	123	276	62	563	105	490	292
3D-4_8.2E	1.92	0.386	16	38	6.4	82	190	45	401	75	702	476
3D-4_9.1C	26.26	6.112	178	160	50.3	480	606	109	793	128	528	206
3D-4_9.2E	4.20	1.005	33	47	11.4	124	201	39	300	50	212	147
5D-1_1.1C	6.47	1.455	43	64	14.3	157	281	58	473	84	311	215
5D-1_1.2I	7.39	1.531	62	91	22.1	245	367	70	508	79	274	189
5D-1_1.3E	1.71	0.306	14	32	5.6	72	169	40	362	68	486	367
5D-1_2.1C	3.52	0.914	29	38	9.5	103	162	33	246	42	147	109
5D-1_2.2	4.09	0.918	33	46	10.8	118	192	38	296	51	210	137
5D-1_3.1C	11.17	2.698	76	74	22.5	215	284	52	385	63	157	84
5D-1_3.2I	6.64	1.611	54	61	17.3	173	244	44	339	54	353	172
5D-1_3.3E	3.05	0.747	24	38	8.4	95	170	37	290	51	291	187
5D-1_4.1C	18.60	4.488	146	175	47.0	477	686	127	908	147	712	324
5D-1_4.2E	2.90	0.538	20	37	6.9	85	188	43	379	70	529	374
5D-1_5.1C	3.74	1.001	31	51	10.8	123	236	51	423	79	361	264
5D-1_5.2E	2.61	0.558	25	53	9.5	120	265	61	529	100	734	482
5D-1_6.1C	10.00	2.289	80	90	25.3	259	349	63	464	74	536	220
5D-1_6.2E	12.33	2.322	91	128	31.3	333	549	109	857	143	545	287
5D-1_7.1C	2.74	0.889	22	38	7.6	90	184	41	360	70	188	190
5D-1_7.2E	2.53	0.645	20	32	6.8	78	144	30	254	47	175	147
5D-2_1.1C	20.77	4.764	148	140	42.9	411	532	96	701	116	347	141
5D-2_1.2E	5.96	2.452	29	23	7.3	65	88	17	141	26	58	23
5D-2_10.1C	23.71	8.360	157	130	41.1	385	488	89	665	108	1307	282
5D-2_10.2E	3.44	1.301	25	24	6.8	70	96	19	147	26	52	27

TABLE A1 (continued): PEACH SPRING TUFF ZIRCON SIMS TRACE ELEMENT ABUNDANCES

Spot Name	Li (ppm)	Be (ppm)	B (ppm)	F (ppm)	P (ppm)	Sc (ppm)	Ti from 49 (ppm)	Y (ppm)	Nb (ppm)	La (ppm)	Ce (ppm)	Nd (ppm)
5D-2_11.1C	0.1	1.1	0.3	60	1045	61	14.5	5361	110	0.036	400	4.5
5D-2_11.2E	0.0	0.0	0.1	10	271	61	22.7	465	2	0.030	68	2.2
5D-2_12.1C	0.0	1.1	0.1	60	641	87	15.6	4653	12	0.221	301	19.7
5D-2_12.2E	0.0	0.0	0.0	11	357	64	22.6	823	5	0.030	103	3.5
5D-2_2.1C	0.0	0.5	0.1	19	556	72	18.0	3559	10	0.136	231	16.6
5D-2_2.2E	0.0	0.4	0.1	7	317	50	19.2	647	3	0.030	77	2.3
5D-2_3.1C	0.0	3.9	0.1	13	286	54	5.9	876	8	0.014	57	1.1
5D-2_3.2E	0.0	0.1	0.1	8	292	67	36.0	388	2	12.299	75	7.1
5D-2_4.1C	0.0	0.0	0.0	8	277	78	27.0	574	2	0.030	63	4.3
5D-2_4.2E	0.0	0.0	0.1	12	268	63	26.0	407	2	0.020	62	2.3
5D-2_5.1C	0.0	0.0	0.1	12	245	57	7.4	984	13	0.021	110	1.4
5D-2_5.2E	0.0	0.7	0.1	12	320	71	25.1	534	2	0.026	88	3.2
5D-2_6.1C	0.0	0.9	0.0	27	342	35	8.8	2081	10	0.021	102	3.7
5D-2_6.2E	0.0	0.9	0.1	11	260	57	22.0	487	2	0.017	76	1.9
5D-2_7.1C	0.0	0.1	0.0	16	611	53	12.6	1741	6	0.036	96	4.8
5D-2_7.2E	0.0	0.0	0.1	14	234	51	27.3	274	1	0.020	39	1.3
5D-2_8.1C	0.0	37.4	0.1	36	921	56	21.2	3972	44	0.027	344	6.5
5D-2_8.2E	0.3	0.0	0.5	44	243	47	43.9	449	3	1.156	74	2.0
5D-2_9.1C	0.0	0.2	0.1	70	963	61	16.8	6650	33	0.133	415	16.8
5D-2_9.2E	0.0	0.0	0.1	18	289	59	22.1	516	3	0.031	82	2.6

Spot names ending in "C" represent core analyses, "I" represent interior analyses and "E" represent edge analyses.

TABLE A1 (continued): PEACH SPRING TUFF ZIRCON SIMS TRACE ELEMENT ABUNDANCES

Spot Name	Sm (ppm)	Eu (ppm)	Gd (ppm)	Ho (ppm)	Tb (ppm)	Dy (ppm)	Er (ppm)	Tm (ppm)	Yb (ppm)	Lu (ppm)	Th (ppm)	U (ppm)
5D-2_11.1C	14.00	1.650	137	210	50.5	562	868	165	1194	179	1757	890
5D-2_11.2E	3.96	1.787	23	20	6.1	58	81	16	127	23	40	19
5D-2_12.1C	38.31	11.922	242	194	63.8	585	738	135	998	164	653	210
5D-2_12.2E	5.93	1.857	36	34	9.9	97	137	26	215	39	101	49
5D-2_2.1C	31.23	7.265	188	155	50.2	455	563	101	734	123	417	141
5D-2_2.2E	3.97	1.471	27	27	7.7	76	107	21	163	29	60	31
5D-2_3.1C	2.23	0.544	17	30	5.6	69	147	34	299	58	187	168
5D-2_3.2E	4.34	2.189	21	16	5.0	46	64	13	104	19	36	16
5D-2_4.1C	6.21	3.111	32	24	7.7	72	96	18	152	27	42	17
5D-2_4.2E	3.68	1.894	20	17	5.0	49	68	14	109	21	36	16
5D-2_5.1C	2.62	0.727	20	36	6.9	83	166	37	327	61	503	334
5D-2_5.2E	5.03	2.185	27	22	7.1	67	91	18	143	26	65	26
5D-2_6.1C	9.11	1.987	69	87	21.8	234	350	67	500	82	260	149
5D-2_6.2E	3.25	1.564	21	20	5.8	58	81	17	133	24	43	22
5D-2_7.1C	9.81	2.646	73	74	21.7	207	290	55	420	71	196	97
5D-2_7.2E	1.95	1.340	12	11	3.4	32	47	10	77	15	22	12
5D-2_8.1C	18.68	4.308	167	174	52.6	515	634	108	725	106	1939	583
5D-2_8.2E	2.91	1.288	20	19	5.4	54	78	15	123	22	42	22
5D-2_9.1C	39.84	8.658	302	289	88.7	845	1049	182	1274	196	1023	380
5D-2_9.2E	4.18	1.848	25	22	6.6	62	86	17	137	25	52	24

Spot names ending in "C" represent core analyses, "I" represent interior analyses and "E" represent edge analyses.

TABLE A2: COOK CANYON TUFF ZIRCON SIMS TRACE ELEMENT ABUNDANCES

Spot Name	Li (ppm)	Be (ppm)	B (ppm)	F (ppm)	P (ppm)	Sc (ppm)	Ti from 49 (ppm)	Y (ppm)	Nb (ppm)	La (ppm)	Ce (ppm)	Nd (ppm)	Sm (ppm)
7A_1.1C	0.0	0.2	0.1	40	391	68	19.2	2902	64	0.050	347	6.8	15.62
7A_1.2E	0.0	0.0	0.3	22	196	33	23.5	403	3	0.083	47	1.1	2.24
7A_2.1C	0.0	0.1	0.1	29	241	48	23.6	1405	4	0.129	85	7.5	11.02
7A_2.1E	0.0	0.0	0.1	12	187	33	21.8	394	2	0.029	44	1.2	2.27
7A_3.1C	0.0	0.0	0.1	15	201	41	24.7	562	3	0.137	45	2.2	3.59
7A_3.2E	0.0	0.0	0.1	14	211	38	23.0	475	3	0.017	54	1.5	2.75
7A_4.1C	0.0	0.0	0.1	25	227	45	22.0	1302	4	0.082	98	7.6	12.55
7A_4.2E	0.0	0.0	0.1	9	218	35	22.3	435	3	0.043	47	1.4	2.53
7A_5.1C	0.0	1.7	0.1	26	225	44	24.5	1253	3	0.086	71	7.1	9.44
7A_5.2E	0.0	0.1	0.1	12	195	40	22.2	468	2	0.020	45	1.4	2.50
7B_1.1C	0.0	0.1	0.1	10	269	66	21.5	597	2	0.025	67	3.2	4.86
7B_1.2E	0.0	0.0	0.0	8	262	57	21.7	484	2	0.024	76	2.2	3.55
7B_10.1C	0.0	0.3	0.2	45	197	58	6.3	1787	9	0.076	90	3.0	5.12
7B_11.1C	0.0	0.1	0.2	35	412	67	17.1	1968	5	0.068	116	8.7	15.35
7B_11.2E	0.0	0.0	0.1	9	222	46	22.1	347	2	0.013	62	1.3	2.10
7B_2.1C	0.0	3.7	0.1	24	364	27	9.2	2178	7	0.018	97	4.0	11.47
7B_2.2I	0.0	0.7	0.1	12	364	24	9.8	1203	11	0.021	93	1.5	4.50
7B_2.3E	0.0	0.4	0.1	8	269	44	18.5	583	3	0.013	75	1.6	3.33
7B_3.1C	0.0	1.5	0.1	43	1513	67	17.4	8139	185	0.041	621	8.1	27.02
7B_3.2E	0.0	0.0	0.1	14	529	28	10.6	1863	21	0.015	127	1.9	6.11
7B_4.1C	0.0	1.4	0.1	37	642	46	11.9	2800	39	0.018	236	3.3	8.86
7B_4.2E	0.0	0.5	0.1	8	281	56	20.8	528	2	0.017	82	2.4	4.12
7B_5.1C	0.0	5.1	0.1	18	288	86	28.2	1154	1	0.139	92	14.0	15.18
7B_5.2E	0.0	0.4	0.1	8	263	48	16.3	630	3	0.063	66	1.6	3.40

TABLE A2: COOK CANYON TUFF ZIRCON SIMS TRACE ELEMENT ABUNDANCES

Spot Name	Eu (ppm)	Gd (ppm)	Ho (ppm)	Tb (ppm)	Dy (ppm)	Er (ppm)	Tm (ppm)	Yb (ppm)	Lu (ppm)	Th (ppm)	U (ppm)
7A_1.1C	4.192	106	109	31.5	313	414	78	549	84	3790	1231
7A_1.2E	1.038	15	16	4.2	42	66	13	107	19	75	53
7A_2.1C	4.046	61	56	16.4	154	220	41	330	58	288	136
7A_2.1E	1.072	15	16	3.9	42	66	13	106	19	71	51
7A_3.1C	1.520	23	22	5.9	59	90	19	145	27	87	51
7A_3.2E	1.243	18	18	5.0	50	77	16	124	23	100	67
7A_4.1C	4.292	67	57	17.4	158	222	43	338	58	324	150
7A_4.2E	1.200	17	17	4.5	47	72	14	122	22	93	61
7A_5.1C	3.663	54	50	14.5	140	198	38	295	51	236	113
7A_5.2E	1.190	16	19	5.1	49	78	16	134	24	71	51
7B_1.1C	2.206	29	26	7.7	74	103	20	162	30	44	20
7B_1.2E	1.688	22	20	6.0	57	81	16	127	23	45	22
7B_10.1C	1.299	37	62	12.8	147	297	65	565	106	449	278
7B_11.1C	4.165	92	81	24.3	231	308	57	437	74	183	75
7B_11.2E	1.177	14	15	4.1	40	59	12	98	18	30	16
7B_2.1C	2.348	89	93	27.4	270	351	62	442	69	182	103
7B_2.2I	1.010	40	52	13.2	140	204	38	283	46	182	122
7B_2.3E	1.218	25	25	7.0	70	98	19	145	26	52	29
7B_3.1C	2.763	248	338	88.3	926	1311	236	1635	237	3332	1266
7B_3.2E	0.872	56	78	19.7	217	310	56	408	62	337	203
7B_4.1C	1.832	82	113	28.8	306	447	84	602	93	1179	487
7B_4.2E	1.738	24	22	6.8	64	88	18	140	24	53	26
7B_5.1C	6.877	70	49	16.7	144	182	34	265	47	92	28
7B_5.2E	1.250	25	27	7.4	76	108	21	166	28	42	22

TABLE A2 (continued): COOK CANYON TUFF ZIRCON SIMS TRACE ELEMENT ABUNDANCES

Spot Name	Li (ppm)	Be (ppm)	B (ppm)	F (ppm)	P (ppm)	Sc (ppm)	Ti from 49 (ppm)	Y (ppm)	Nb (ppm)	La (ppm)	Ce (ppm)	Nd (ppm)	Sm (ppm)
7B_6.1C	0.0	0.1	0.1	20	620	105	25.1	2147	11	0.093	236	9.4	16.70
7B_6.2E	0.0	0.1	0.1	16	383	46	9.6	1449	15	0.015	130	2.0	4.74
7B_7.1C	0.0	0.2	0.1	19	278	58	16.0	1636	3	0.056	93	9.4	14.56
7B_7.2E	0.0	0.3	0.1	15	309	38	10.0	1111	10	0.020	90	1.4	3.99
7B_8.1C	0.0	0.7	0.1	18	188	60	5.9	781	12	0.018	60	0.7	1.33
7B_8.2E	0.0	0.0	0.2	11	243	43	15.0	577	3	0.022	60	1.3	2.94
7B_9.1C	0.0	0.2	0.1	16	215	35	8.1	1514	5	0.019	75	3.0	6.76
7B_9.2E	0.0	0.0	0.1	6	295	58	22.2	530	3	0.018	81	2.3	4.23

TABLE A2 (continued): COOK CANYON TUFF ZIRCON SIMS TRACE ELEMENT ABUNDANCES

Spot Name	Eu (ppm)	Gd (ppm)	Ho (ppm)	Tb (ppm)	Dy (ppm)	Er (ppm)	Tm (ppm)	Yb (ppm)	Lu (ppm)	Th (ppm)	U (ppm)
7B_6.1C	5.816	106	90	28.1	267	350	64	491	83	584	175
7B_6.2E	1.169	40	57	13.2	149	239	47	354	61	448	241
7B_7.1C	5.448	86	70	22.2	204	264	48	370	64	152	62
7B_7.2E	1.069	33	46	11.4	121	195	39	304	53	181	128
7B_8.1C	0.356	13	27	4.6	58	134	31	285	57	138	158
7B_8.2E	0.987	21	25	6.4	67	101	20	152	27	36	21
7B_9.1C	1.660	50	66	16.2	173	279	55	433	75	210	124
7B_9.2E	1.770	25	22	6.7	63	90	18	141	26	55	26

TABLE A3: PROTEROZIC ZIRCON FROM PEACH SPRING TUFF AND COOK CANYON TUFF SIMS TRACE ELEMENT ABUNDANCES

Spot Name	Li (ppm)	Be (ppm)	B (ppm)	F (ppm)	P (ppm)	Sc (ppm)	Ti from 49 (ppm)	Y (ppm)	Nb (ppm)	La (ppm)	Ce (ppm)	Nd (ppm)
3B_12.1C	12.5	0.0	0.1	49	408	59	21.6	735	5	0.885	23	1.6
3D-1_5.1I	137.1	0.7	0.1	19	160	15	5.2	322	5	0.011	11	0.2
3D-3_8.1C	195.2	0.2	0.1	12	775	105	10.6	1310	2	0.193	11	1.5
3D-3_8.2E	306.6	0.2	0.2	104	514	110	3.5	654	4	0.040	4	0.2
3D-3_2.1C	171.3	0.3	5.6	44	479	61	10.3	1496	8	1.648	42	4.3
3D-3_2.2E	165.1	0.2	0.2	8	211	21	7.0	552	6	0.023	22	0.4
3D-3_5.1C	33.5	0.1	0.4	10	332	56	23.1	607	4	0.018	20	0.9
3D-3_6.1C	84.3	0.1	0.1	9	237	39	9.9	457	4	0.027	16	0.5
3D-3_6.2E	277.2	0.0	0.1	12	223	28	7.3	555	7	0.027	22	0.6
3D-4_3.1C	272.4	0.0	0.1	19	1117	136	10.8	2251	6	0.403	17	2.6
3D-4_4.1C	264.0	0.2	0.4	21	218	25	5.8	568	6	0.053	23	0.4
3D-4_4.2E	462.8	0.4	0.3	9	224	27	6.6	598	8	0.011	24	0.4
3D-4_5.1C	160.7	1.2	0.3	10	134	11	4.9	238	4	0.037	14	0.2
3D-4_5.2E	103.8	0.1	0.2	11	202	30	9.7	429	6	0.021	18	0.3
3D-5_1.1C	30	0.0	0.1	8	256	40	7.2	424	4	0.041	16	0.6
3D-5_1.2E	140	0.3	0.5	16	287	37	5.2	705	4	0.044	21	1.0
3D-5_10.1C	133	0.1	0.3	5	264	42	9.1	619	6	0.010	25	0.6
3D-5_10.2E	295	1.9	1.7	147	476	89	35.5	1203	12	1.038	160	2.9
3D-5_2.1C	148	0.2	0.2	9	361	47	5.4	803	6	0.033	32	1.6
3D-5_2.2E	266	0.8	0.2	60	450	78	5.7	806	9	0.010	18	0.5
3D-5_3.1C	162	0.2	0.3	205	2770	215	14.2	4384	10	0.035	8	2.2
3D-5_3.2E	306	0.1	0.2	11	257	38	7.4	603	7	0.011	20	0.4
3D-5_4.1C	270	81.8	27.1	2095	1588	212	52.9	5224	29	12.847	135	60.5
3D-5_4.2E	326	1.3	0.2	13	254	53	4.5	409	8	0.035	11	0.3
3D-5_5.1C	329	2.1	2.1	666	2029	461	45.8	4439	11	21.759	90	76.9

TABLE A3 (continued): PROTEROZIC ZIRCON FROM PEACH SPRING TUFF AND COOK CANYON TUFF SIMS TRACE ELEMENT ABUNDANCES

Spot Name	Sm (ppm)	Eu (ppm)	Gd (ppm)	Ho (ppm)	Tb (ppm)	Dy (ppm)	Er (ppm)	Tm (ppm)	Yb (ppm)	Lu (ppm)	Th (ppm)	U (ppm)
3B_12.1C	2.36	0.480	18	29	6.2	70	132	29	237	43	98	78
3D-1_5.1I	0.52	0.091	4	11	1.8	25	61	15	138	26	51	290
3D-3_8.1C	3.74	0.732	36	60	13.3	157	274	57	469	82	88	165
3D-3_8.2E	0.78	0.088	8	25	4.1	55	123	26	218	42	32	393
3D-3_2.1C	5.78	1.279	42	62	14.1	155	270	56	449	80	265	281
3D-3_2.2E	1.30	0.154	11	22	4.1	49	101	24	208	40	153	397
3D-3_5.1C	1.99	0.455	16	25	5.6	64	107	22	183	32	60	62
3D-3_6.1C	1.20	0.255	11	18	3.9	44	81	17	143	27	51	77
3D-3_6.2E	1.31	0.201	12	21	4.3	52	104	23	207	38	153	355
3D-4_3.1C	4.25	0.629	40	94	17.1	216	453	103	903	164	174	974
3D-4_4.1C	1.12	0.146	10	22	3.8	48	104	24	208	40	130	247
3D-4_4.2E	1.15	0.163	11	22	4.3	54	118	27	245	47	199	507
3D-4_5.1C	0.32	0.083	3	9	1.4	18	46	12	117	24	76	338
3D-4_5.2E	0.90	0.138	8	17	3.3	41	80	18	154	28	81	194
3D-5_1.1C	1.15	0.361	10	17	3.5	41	76	17	138	26	41	68
3D-5_1.2E	1.75	0.380	16	28	5.6	66	127	27	235	43	89	175
3D-5_10.1C	1.54	0.229	13	24	4.9	58	111	24	199	35	103	179
3D-5_10.2E	0.38	0.412	24	45	8.7	107	230	55	513	99	306	809
3D-5_2.1C	2.64	0.547	21	32	7.2	80	142	31	260	46	133	215
3D-5_2.2E	1.54	0.131	16	33	6.4	79	147	31	269	51	104	574
3D-5_3.1C	7.01	0.227	72	160	30.4	382	751	161	1302	223	212	722
3D-5_3.2E	1.14	0.135	11	23	4.4	54	115	26	229	43	130	402
3D-5_4.1C	48.08	17.175	209	182	55.7	536	744	151	1190	203	1477	3270
3D-5_4.2E	0.62	0.089	6	16	2.4	34	82	20	183	36	86	654
3D-5_5.1C	53.39	28.664	236	142	50.8	424	494	95	715	117	311	467

TABLE A3 (continued): PROTEROZIC ZIRCON FROM PEACH SPRING TUFF AND COOK CANYON TUFF SIMS TRACE ELEMENT ABUNDANCES

Spot Name	Li (ppm)	Be (ppm)	B (ppm)	F (ppm)	P (ppm)	Sc (ppm)	Ti from 49 (ppm)	Y (ppm)	Nb (ppm)	La (ppm)	Ce (ppm)	Nd (ppm)
3D-5_7.2E	345	0.2	0.4	165	1067	150	6.9	1557	7	0.035	5	0.6
3D-5_8.1C	250	0.5	0.6	12	254	32	6.7	425	5	0.030	12	0.3
3D-5_8.2E	206	0.4	1.3	11	168	19	7.3	393	4	0.088	15	0.4
3D-5_9.1C	93	0.0	0.2	15	226	34	14.7	437	4	0.025	16	0.5
3D-5_9.2E	257	0.2	0.3	6	432	87	6.1	901	10	0.012	25	0.8
7A_6.1I	13.1	0.0	0.0	10	2135	175	30.4	3867	2	0.090	9	5.4
7A_6.2E	15.9	0.0	0.2	11	2027	186	19.9	3253	3	0.092	6	2.6

TABLE A3 (continued): PROTEROZIC ZIRCON FROM PEACH SPRING TUFF AND COOK CANYON TUFF SIMS TRACE ELEMENT ABUNDANCES

Spot Name	Sm (ppm)	Eu (ppm)	Gd (ppm)	Ho (ppm)	Tb (ppm)	Dy (ppm)	Er (ppm)	Tm (ppm)	Yb (ppm)	Lu (ppm)	Th (ppm)	U (ppm)
3D-5_7.2E	2.01	0.183	21	60	9.9	133	306	74	669	125	88	754
3D-5_8.1C	0.70	0.064	7	16	2.8	37	78	18	150	28	73	292
3D-5_8.2E	0.75	0.183	6	14	2.7	33	74	17	159	30	81	311
3D-5_9.1C	0.93	0.209	10	18	3.4	43	78	17	142	26	53	91
3D-5_9.2E	2.12	0.217	19	34	6.9	80	170	40	363	71	303	830
7A_6.1I	10.05	1.652	87	156	31.8	391	677	135	1063	181	110	100
7A_6.2E	6.70	1.067	66	128	26.4	326	549	110	883	147	62	111

APPENDIX B: SIMS U-PB ZIRCON DATA

TABLE B1: PEACH SPRING TUFF PRE-CA SIMS SECTIONED ZIRCON RESULTS

Spot Name	ppm U	ppm Th	232Th /238U	207corr 206Pb /238U Age (Ma)	1s err	Total 238 /206	% err	Total 207 /206	% err
3B_10.1C	232	362	1.61	**18.07**	**0.22**	357	1.2	0.0447	7.0
3B_11.1C	707	1679	2.45	**18.13**	**0.46**	355	2.5	0.0476	8.2
3B_14.1C	317	905	2.95	**17.30**	**0.35**	372	2.0	0.0470	5.9
3B_15.1C	318	971	3.16	**18.56**	**0.27**	348	1.4	0.0427	6.2
3B_16.1C	260	398	1.58	**19.32**	**0.57**	334	2.9	0.0442	6.5
3B_17.1C	517	1334	2.66	**18.68**	**0.29**	343	1.5	0.0498	4.4
3B_18.1C	810	1665	2.12	**19.02**	**0.49**	340	2.6	0.0436	3.5
3B_2.2C	275	566	2.12	**18.74**	**0.56**	310	2.9	0.1258	3.7
3B_3.1C	272	805	3.06	**18.65**	**0.38**	344	2.0	0.0500	5.8
3B_1.2E	252	250	1.02	**18.39**	**0.69**	352	3.8	0.0420	6.9
3B_11.2E	291	344	1.22	**18.19**	**0.61**	354	3.3	0.0466	6.1
3B_12.2E	380	488	1.33	**17.08**	**0.63**	365	3.7	0.0725	4.7
3B_2.4E	112	141	1.30	**18.81**	**0.63**	347	3.3	0.0344	13.0
3B_4.2E	244	245	1.04	**18.22**	**0.43**	353	2.2	0.0470	12.7
3B_6.2E	325	422	1.34	**17.48**	**0.68**	367	3.9	0.0492	6.0
3B_8.2E	245	310	1.30	**19.26**	**0.40**	335	1.9	0.0440	13.1
3B_9.2E	300	447	1.54	**8.93**	**11.14**	172	18.2	0.6629	35.8
3B_7.2I	283	441	1.61	**18.23**	**0.62**	351	3.4	0.0518	6.3

TABLE B1 (continued): PEACH SPRING TUFF PRE-CA SIMS SECTIONED ZIRCON RESULTS

Scharer method using constant melt Th/U

Spot Name	Melt (glass) 232Th/238U	Th/U zircon/melt	Disequilibrium corrected Age (Ma)	1 sigma error	Delta age
3B_10.1C	6.33	0.26	**18.15**	**0.22**	0.081
3B_11.1C	6.33	0.39	**18.20**	**0.46**	0.067
3B_14.1C	6.33	0.47	**17.36**	**0.35**	0.058
3B_15.1C	6.33	0.50	**18.62**	**0.27**	0.055
3B_16.1C	6.33	0.25	**19.40**	**0.57**	0.082
3B_17.1C	6.33	0.42	**18.74**	**0.29**	0.063
3B_18.1C	6.33	0.34	**19.09**	**0.49**	0.073
3B_2.2C	6.33	0.34	**18.81**	**0.56**	0.073
3B_3.1C	6.33	0.48	**18.71**	**0.38**	0.056
3B_1.2E	6.33	0.16	**18.48**	**0.69**	0.092
3B_11.2E	6.33	0.19	**18.28**	**0.61**	0.088
3B_12.2E	6.33	0.21	**17.17**	**0.63**	0.086
3B_2.4E	6.33	0.21	**18.90**	**0.63**	0.087
3B_4.2E	6.33	0.16	**18.32**	**0.43**	0.091
3B_6.2E	6.33	0.21	**17.56**	**0.68**	0.086
3B_8.2E	6.33	0.21	**19.34**	**0.40**	0.087
3B_9.2E	6.33	0.24	**9.01**	**11.14**	0.083
3B_7.2I	6.33	0.25	**18.31**	**0.62**	0.081

TABLE B1 (continued): PEACH SPRING TUFF PRE-CA SIMS SECTIONED ZIRCON RESULTS

Spot Name	ppm U	ppm Th	232Th /238U	207corr 206Pb /238U Age (Ma)	1s err	Total 238 /206	% err	Total 207 /206	% err
3D-1_2.1c	140	122	0.90	**16.16**	**0.58**	374	2.9	0.0957	16.8
3D-4_8.1C	229	372	1.68	**16.75**	**0.59**	384	3.5	0.0466	7.3
3D-2_2.1C	542	1235	2.35	**17.38**	**0.51**	369	2.9	0.0503	8.1
3D-1_4.CI	164	311	1.95	**17.52**	**0.35**	371	1.9	0.0380	10.1
3D-1_3.1c	182	174	0.99	**17.63**	**0.33**	362	1.8	0.0538	7.4
3D-1_1.1C	204	445	2.25	**17.74**	**0.60**	363	3.4	0.0468	6.8
3D-4_10.1C	134	394	3.03	**17.95**	**0.93**	356	5.1	0.0529	14.4
3D-2_10.1C	206	379	1.91	**18.02**	**0.78**	331	3.6	0.1049	17.3
3D-2_5.1C	201	240	1.23	**18.09**	**0.52**	355	2.8	0.0477	7.7
3D-5_11.1C	1085	3433	3.27	**18.15**	**0.44**	353	2.4	0.0497	3.1
3D-3_1.1C	208	546	2.71	**18.27**	**0.64**	350	3.4	0.0515	14.4
3D-2_11.1C	717	1516	2.18	**18.71**	**0.32**	342	1.7	0.0508	3.9
3D-2_4.1C	701	1409	2.08	**18.88**	**0.31**	341	1.6	0.0460	8.5
3D-3_3.1C	439	1323	3.11	**18.95**	**0.38**	335	2.0	0.0569	4.5
3D-3_9.1C	170	334	2.03	**19.59**	**0.46**	329	2.3	0.0455	8.2
3D-3_11.1C	158	401	2.61	**19.35**	**1.49**	277	7.3	0.1805	8.8
3D-3_10.1E	84	113	1.39	**17.71**	**1.08**	365	6.1	0.0435	13.7
3D-2_1.2E	293	380	1.34	**18.13**	**0.48**	356	2.6	0.0436	6.6
3D-2_10.2E	268	216	0.83	**18.40**	**0.40**	349	2.2	0.0480	6.8
3D-2_2.2E	313	420	1.39	**18.46**	**0.35**	349	1.9	0.0459	5.8
3D-4_8.2E	441	642	1.50	**18.49**	**0.38**	348	2.0	0.0475	8.6

TABLE B1 (continued): PEACH SPRING TUFF PRE-CA SIMS SECTIONED ZIRCON RESULTS

Scharer method using constant melt Th/U

Spot Name	Melt (glass) 232Th/238U	Th/U zircon/melt	Disequilibrium corrected Age (Ma)	1 sigma error	Delta age
3D-1_2.1c	6.33	0.14	**16.25**	**0.58**	0.094
3D-4_8.1C	6.33	0.27	**16.83**	**0.59**	0.080
3D-2_2.1C	6.33	0.37	**17.45**	**0.51**	0.069
3D-1_4.CI	6.33	0.31	**17.60**	**0.35**	0.076
3D-1_3.1c	6.33	0.16	**17.73**	**0.33**	0.092
3D-1_1.1C	6.33	0.36	**17.81**	**0.60**	0.070
3D-4_10.1C	6.33	0.48	**18.01**	**0.93**	0.057
3D-2_10.1C	6.33	0.30	**18.09**	**0.78**	0.076
3D-2_5.1C	6.33	0.19	**18.18**	**0.52**	0.088
3D-5_11.1C	6.33	0.52	**18.20**	**0.44**	0.053
3D-3_1.1C	6.33	0.43	**18.34**	**0.64**	0.062
3D-2_11.1C	6.33	0.34	**18.78**	**0.32**	0.072
3D-2_4.1C	6.33	0.33	**18.96**	**0.31**	0.073
3D-3_3.1C	6.33	0.49	**19.01**	**0.38**	0.056
3D-3_9.1C	6.33	0.32	**19.66**	**0.46**	0.074
3D-3_11.1C	6.33	0.41	**19.42**	**1.49**	0.064
3D-3_10.1E	6.33	0.22	**17.79**	**1.08**	0.085
3D-2_1.2E	6.33	0.21	**18.22**	**0.48**	0.086
3D-2_10.2E	6.33	0.13	**18.50**	**0.40**	0.095
3D-2_2.2E	6.33	0.22	**18.55**	**0.35**	0.085
3D-4_8.2E	6.33	0.24	**18.58**	**0.38**	0.083

TABLE B1 (continued): PEACH SPRING TUFF PRE-CA SIMS SECTIONED ZIRCON RESULTS

Spot Name	ppm U	ppm Th	232Th /238U	207corr 206Pb /238U Age (Ma)	1s err	Total 238 /206	% err	Total 207 /206	% err
3D-5_12.1I	136	188	1.43	**17.86**	**1.10**	361	6.2	0.0450	10.6
3D-4_1.3I	242	465	1.99	**18.43**	**0.38**	349	2.0	0.0471	6.7
3D-5_15.1I	716	1713	2.47	**18.60**	**0.30**	344	1.6	0.0509	3.4
3D-5_16.1I	991	1551	1.62	**19.04**	**0.43**	339	2.2	0.0437	3.3
5D-1_6.1C	142	284	2.06	**16.97**	**0.75**	367	4.4	0.0737	6.4
5D-1_5.1C	289	453	1.62	**17.57**	**0.33**	365	1.8	0.0488	6.2
5D-1_7.1C	176	168	0.99	**17.83**	**0.63**	361	3.5	0.0466	8.1
5D-2_19.1C	67	158	2.44	**17.91**	**0.23**	359	1.0	0.0473	13.2
5D-1_1.1C	183	236	1.33	**17.95**	**0.71**	355	4.0	0.0541	6.5
5D-2_12.1C	173	508	3.04	**18.13**	**0.37**	353	2.0	0.0514	8.1
5D-2_8.1C	448	1358	3.13	**18.30**	**0.41**	352	2.2	0.0469	4.9
5D-2_22.1C	256	329	1.33	**18.30**	**0.33**	351	1.7	0.0490	6.9
5D-2_20.1C	133	252	1.95	**18.43**	**0.59**	352	3.2	0.0408	10.3
5D-2_5.1C	284	406	1.48	**18.44**	**0.65**	348	3.5	0.0488	5.7
5D-2_17.1C	697	1959	2.90	**18.51**	**0.58**	347	3.1	0.0485	3.8
5D-2_10.1C	197	825	4.32	**18.51**	**0.62**	347	3.2	0.0477	15.5
5D-2_9.1C	387	1126	3.01	**18.61**	**0.55**	344	2.9	0.0506	8.8
5D-2_3.1C	150	165	1.13	**18.65**	**0.82**	348	4.4	0.0403	9.1
5D-1_10.1C	207	309	1.54	**18.66**	**0.65**	347	3.5	0.0422	7.5
5D-1_11.1C	311	499	1.66	**18.70**	**0.44**	345	2.3	0.0454	9.7

TABLE B1 (continued): PEACH SPRING TUFF PRE-CA SIMS SECTIONED ZIRCON RESULTS

Scharer method using constant melt Th/U

Spot Name	Melt (glass) 232Th/238U	Th/U zircon/melt	Disequilibrium corrected Age (Ma)	1 sigma error	Delta age
3D-5_12.1I	6.33	0.23	**17.94**	**1.10**	0.085
3D-4_1.3I	6.33	0.31	**18.51**	**0.38**	0.075
3D-5_15.1I	6.33	0.39	**18.67**	**0.30**	0.067
3D-5_16.1I	6.33	0.26	**19.12**	**0.43**	0.081
5D-1_6.1C	9.45	0.22	**17.05**	**0.75**	0.085
5D-1_5.1C	9.45	0.17	**17.66**	**0.33**	0.090
5D-1_7.1C	9.45	0.10	**17.93**	**0.63**	0.098
5D-2_19.1C	9.45	0.26	**17.99**	**0.23**	0.081
5D-1_1.1C	9.45	0.14	**18.04**	**0.71**	0.094
5D-2_12.1C	9.45	0.32	**18.21**	**0.37**	0.074
5D-2_8.1C	9.45	0.33	**18.37**	**0.41**	0.073
5D-2_22.1C	9.45	0.14	**18.40**	**0.33**	0.094
5D-2_20.1C	9.45	0.21	**18.52**	**0.59**	0.087
5D-2_5.1C	9.45	0.16	**18.53**	**0.65**	0.092
5D-2_17.1C	9.45	0.31	**18.58**	**0.58**	0.076
5D-2_10.1C	9.45	0.46	**18.57**	**0.62**	0.059
5D-2_9.1C	9.45	0.32	**18.68**	**0.55**	0.075
5D-2_3.1C	9.45	0.12	**18.74**	**0.82**	0.096
5D-1_10.1C	9.45	0.16	**18.75**	**0.65**	0.091
5D-1_11.1C	9.45	0.18	**18.79**	**0.44**	0.090

TABLE B1 (continued): PEACH SPRING TUFF PRE-CA SIMS SECTIONED ZIRCON RESULTS

Spot Name	ppm U	ppm Th	232Th /238U	207corr 206Pb /238U Age (Ma)	1s err	Total 238 /206	% err	Total 207 /206	% err
5D-1_9.1I	209	293	1.45	**18.71**	**0.32**	341	1.6	0.0529	6.8
5D-2_14.1C	462	932	2.08	**18.92**	**0.48**	340	2.5	0.0460	4.9
5D-2_16.1C	404	1525	3.90	**18.94**	**0.59**	338	3.1	0.0520	4.8
5D-2_21.1I	233	477	2.12	**18.96**	**0.53**	339	2.7	0.0486	12.0
5D-2_15.1C	260	636	2.53	**18.96**	**0.50**	338	2.6	0.0492	6.3
5D-2_23.1C	460	1590	3.57	**19.01**	**0.45**	339	2.3	0.0463	4.9
5D-2_13.1C	163	292	1.86	**19.02**	**0.44**	339	2.3	0.0457	8.0
5D-2_6.1C	133	229	1.78	**19.02**	**0.18**	335	0.8	0.0546	7.9
5D-1_8.1C	232	355	1.58	**19.03**	**0.35**	341	1.7	0.0391	13.8
5D-2_11.1C	817	1485	1.88	**19.06**	**0.43**	340	2.3	0.0415	3.9
5D-2_2.1C	189	603	3.30	**19.12**	**0.61**	334	3.1	0.0521	7.2
5D-2_24.1C	743	1191	1.66	**19.21**	**0.39**	336	2.0	0.0444	4.0
5D-2_25.1C	587	1415	2.49	**19.28**	**0.39**	333	2.0	0.0494	4.2
5D-2_1.1C	111	264	2.46	**19.30**	**0.75**	338	3.8	0.0367	22.5
5D-2_25.2I	307	446	1.50	**15.73**	**0.56**	405	3.6	0.0552	6.4
5D-1_4.1E	385	569	1.53	**17.92**	**0.34**	357	1.9	0.0508	5.6
5D-1_13.1I	245	412	1.74	**18.57**	**0.45**	339	2.2	0.0651	10.7
5D-2_18.1C	320	681	2.20	**19.13**	**0.43**	333	2.2	0.0545	5.5
5D-1_12.1C	254	323	1.31	**19.29**	**0.41**	332	2.1	0.0496	6.1

TABLE B1 (continued): PEACH SPRING TUFF PRE-CA SIMS SECTIONED ZIRCON RESULTS

Scharer method using constant melt Th/U

Spot Name	Melt (glass) 232Th/238U	Th/U zircon/melt	Disequilibrium corrected Age (Ma)	1 sigma error	Delta age
5D-1_9.1I	9.45	0.15	**18.80**	**0.32**	0.092
5D-2_14.1C	9.45	0.22	**19.01**	**0.48**	0.085
5D-2_16.1C	9.45	0.41	**19.00**	**0.59**	0.064
5D-2_21.1I	9.45	0.22	**19.04**	**0.53**	0.085
5D-2_15.1C	9.45	0.27	**19.04**	**0.50**	0.080
5D-2_23.1C	9.45	0.38	**19.08**	**0.45**	0.068
5D-2_13.1C	9.45	0.20	**19.10**	**0.44**	0.088
5D-2_6.1C	9.45	0.19	**19.11**	**0.18**	0.089
5D-1_8.1C	9.45	0.17	**19.12**	**0.35**	0.091
5D-2_11.1C	9.45	0.20	**19.15**	**0.43**	0.087
5D-2_2.1C	9.45	0.35	**19.19**	**0.61**	0.071
5D-2_24.1C	9.45	0.18	**19.30**	**0.39**	0.090
5D-2_25.1C	9.45	0.26	**19.36**	**0.39**	0.080
5D-2_1.1C	9.45	0.26	**19.38**	**0.75**	0.081
5D-2_25.2I	9.45	0.16	**15.82**	**0.56**	0.092
5D-1_4.1E	9.45	0.16	**18.01**	**0.34**	0.091
5D-1_13.1I	9.45	0.18	**18.66**	**0.45**	0.089
5D-2_18.1C	9.45	0.23	**19.21**	**0.43**	0.084
5D-1_12.1C	9.45	0.14	**19.39**	**0.41**	0.094

TABLE B1 (continued): PEACH SPRING TUFF PRE-CA SIMS SECTIONED ZIRCON RESULTS

Spot Name	ppm U	ppm Th	232Th /238U	207corr 206Pb /238U Age (Ma)	1s err	Total 238 /206	% err	Total 207 /206	% err
2H-24.1C	241	523	2.25	**17.9**	**0.2**	355	1.1	0.0574	7.2
2H-32.1C	140	173	1.28	**18.4**	**0.2**	345	0.8	0.0582	9.1
2H-20.1C	263	321	1.26	**18.5**	**0.4**	347	2.0	0.0491	6.9
2H-11.1C	363	752	2.14	**18.6**	**2**	245	6.0	0.2823	12.0
2H-10.1C	682	3501	5.30	**18.7**	**0.3**	343	1.4	0.0484	4.5
2H-18.1C	202	696	3.55	**18.7**	**0.5**	341	2.3	0.0522	12.9
2H-4.2C	331	680	2.12	**18.7**	**0.5**	341	2.5	0.0532	6.0
2H-19.1C	245	347	1.46	**18.8**	**0.2**	343	1.1	0.0455	7.4
2H-30.1C	297	513	1.78	**18.8**	**0.4**	340	2.3	0.0499	6.4
2H-9.1C	505	1289	2.64	**18.9**	**0.3**	339	1.6	0.0493	5.1
2H-27.1C	253	662	2.71	**18.9**	**0.3**	337	1.7	0.0531	6.5
2H-21.1C	461	864	1.94	**19.1**	**0.5**	336	2.4	0.0468	5.4
2H-25.1C	629	1354	2.22	**19.1**	**0.4**	333	2.1	0.0554	3.8
2H-29.2C	218	868	4.12	**19.2**	**0.5**	338	2.6	0.0398	8.7
2H-5.1C	233	550	2.44	**19.4**	**0.7**	332	3.4	0.0478	8.1
2H-23.1C	493	1011	2.12	**19.4**	**0.2**	331	0.9	0.0470	8.5
2H-12.1C	910	2362	2.68	**19.4**	**0.2**	332	1.2	0.0460	3.9
2H-7C	358	732	2.11	**19.1**	**0.2**	336	1.1	0.0486	5.9
2H-24.2E	264	287	1.12	**18.5**	**0.4**	348	1.9	0.0470	7.8
2H-28.2E	204	232	1.17	**18.7**	**0.6**	342	3.2	0.0503	7.9
2H-28.1E	204	332	1.68	**18.7**	**0.7**	345	3.8	0.0421	8.2

TABLE B1 (continued): PEACH SPRING TUFF PRE-CA SIMS SECTIONED ZIRCON RESULTS

Scharer method using constant melt Th/U

Spot Name	Melt (glass) 232Th/238U	Th/U zircon/melt	Disequilibrium corrected Age (Ma)	1 sigma error	Delta age
2H-24.1C	5.34	0.42	**17.94**	**0.21**	0.063
2H-32.1C	5.34	0.24	**18.46**	**0.19**	0.083
2H-20.1C	5.34	0.24	**18.58**	**0.38**	0.083
2H-11.1C	5.34	0.40	**18.67**	**1.56**	0.065
2H-10.1C	5.34	0.99	**18.70**	**0.27**	0.001
2H-18.1C	5.34	0.66	**18.76**	**0.46**	0.037
2H-4.2C	5.34	0.40	**18.81**	**0.47**	0.066
2H-19.1C	5.34	0.27	**18.85**	**0.22**	0.079
2H-30.1C	5.34	0.33	**18.92**	**0.43**	0.073
2H-9.1C	5.34	0.49	**18.97**	**0.30**	0.055
2H-27.1C	5.34	0.51	**18.99**	**0.33**	0.054
2H-21.1C	5.34	0.36	**19.21**	**0.46**	0.070
2H-25.1C	5.34	0.42	**19.20**	**0.41**	0.064
2H-29.2C	5.34	0.77	**19.24**	**0.50**	0.025
2H-5.1C	5.34	0.46	**19.42**	**0.67**	0.059
2H-23.1C	5.34	0.40	**19.49**	**0.20**	0.066
2H-12.1C	5.34	0.50	**19.48**	**0.24**	0.054
2H-7C	5.34	0.40	**19.17**	**0.22**	0.066
2H-24.2E	5.34	0.21	**18.56**	**0.37**	0.086
2H-28.2E	5.34	0.22	**18.80**	**0.60**	0.085
2H-28.1E	5.34	0.32	**18.81**	**0.72**	0.075

TABLE B1 (continued): PEACH SPRING TUFF PRE-CA SIMS SECTIONED ZIRCON RESULTS

Spot Name	ppm U	ppm Th	232Th /238U	207corr 206Pb /238U Age (Ma)	1s err	Total 238 /206	% err	Total 207 /206	% err
2H-34.1E	390	544	1.44	**19.3**	**0.4**	332	1.8	0.0509	5.5
2H-31.1E	284	763	2.77	**18.2**	**0.4**	353	2.0	0.0470	7.5
2H-29.1E	193	201	1.08	**19.7**	**0.5**	327	2.4	0.0454	9.0
2H-4.1E	378	497	1.36	**18.3**	**0.6**	348	3.4	0.0560	5.9
2H-9.2E	269	308	1.18	**19.0**	**0.4**	340	1.9	0.0453	7.2
2H-25.2E	474	692	1.51	**19.0**	**0.3**	319	1.7	0.0948	3.6
2H-32.2E	213	258	1.25	**19.5**	**0.5**	331	2.6	0.0453	14.5
2H-26.1I	216	359	1.72	**17.7**	**0.2**	361	1.2	0.0531	7.6
2H-13.1I	365	475	1.34	**18.5**	**0.4**	325	1.9	0.1011	8.3
2H-22.1I	347	427	1.27	**18.6**	**0.5**	347	2.4	0.0440	6.4
2H-33.1I	411	829	2.08	**18.7**	**0.4**	342	2.2	0.0511	5.3
2H-3.1I	277	362	1.35	**18.7**	**0.3**	342	1.7	0.0503	6.9
2H-15.1I	962	3028	3.25	**18.9**	**0.5**	340	2.4	0.0465	3.5
2H-16.1I	349	662	1.96	**19.0**	**0.3**	337	1.6	0.0506	6.0
2H-14.1I	428	923	2.23	**19.0**	**0.3**	337	1.4	0.0485	5.4
2H-2.1I	261	893	3.54	**19.2**	**0.2**	335	0.7	0.0465	7.7
2H-17.1I	389	570	1.51	**19.3**	**0.4**	332	2.1	0.0518	5.6
2H-8I	245	314	1.33	**19.3**	**0.5**	335	2.4	0.0439	13.0
2H-34.2I	409	649	1.64	**19.3**	**0.4**	333	2.2	0.0490	5.7
2h-36I	257	413	1.66	**18.2**	**0.4**	350	1.9	0.0533	7.1
2h-35I	214	331	1.60	**18.5**	**0.4**	343	1.9	0.0571	7.4

TABLE B1 (continued): PEACH SPRING TUFF PRE-CA SIMS SECTIONED ZIRCON RESULTS

Scharer method using constant melt Th/U

Spot Name	Melt (glass) 232Th/238U	Th/U zircon/melt	Disequilibrium corrected Age (Ma)	1 sigma error	Delta age
2H-34.1E	5.34	0.27	**19.33**	**0.36**	0.080
2H-31.1E	5.34	0.52	**18.27**	**0.37**	0.052
2H-29.1E	5.34	0.20	**19.78**	**0.47**	0.087
2H-4.1E	5.34	0.25	**18.35**	**0.62**	0.081
2H-9.2E	5.34	0.22	**19.04**	**0.36**	0.085
2H-25.2E	5.34	0.28	**19.05**	**0.33**	0.078
2H-32.2E	5.34	0.23	**19.57**	**0.52**	0.084
2H-26.1I	5.34	0.32	**17.74**	**0.22**	0.074
2H-13.1I	5.34	0.25	**18.53**	**0.41**	0.082
2H-22.1I	5.34	0.24	**18.68**	**0.45**	0.083
2H-33.1I	5.34	0.39	**18.78**	**0.42**	0.067
2H-3.1I	5.34	0.25	**18.80**	**0.33**	0.082
2H-15.1I	5.34	0.61	**18.99**	**0.45**	0.043
2H-16.1I	5.34	0.37	**19.09**	**0.32**	0.069
2H-14.1I	5.34	0.42	**19.09**	**0.28**	0.064
2H-2.1I	5.34	0.66	**19.22**	**0.16**	0.037
2H-17.1I	5.34	0.28	**19.35**	**0.41**	0.078
2H-8I	5.34	0.25	**19.36**	**0.48**	0.082
2H-34.2I	5.34	0.31	**19.37**	**0.42**	0.076
2h-36I	5.34	0.31	**18.31**	**0.35**	0.075
2h-35I	5.34	0.30	**18.61**	**0.36**	0.077

TABLE B2: COOK CANYON TUFF PRE-CA SIMS SECTIONED ZIRCON RESULTS

Spot Name	ppm U	ppm Th	232Th /238U	207corr 206Pb /238U Age (Ma)	1s err	Total 238 /206	% err	Total 207 /206	% err
7A_1.1C	1704	5206	3.16	**17.92**	**0.32**	358	1.8	0.0485	2.9
7A_2.1C	114	217	1.97	**18.23**	**0.38**	352	2.0	0.0501	9.3
7A_5.1C	105	228	2.24	**18.47**	**1.11**	352	6.0	0.0385	12.1
7B_2.1C	110	198	1.87	**18.54**	**0.64**	346	3.4	0.0485	10.3
7B_4.1C	333	755	2.34	**18.55**	**0.53**	348	2.8	0.0448	5.2
7B_6.1C	182	650	3.68	**18.78**	**0.52**	341	2.7	0.0509	7.5
7B_4.3C	376	760	2.09	**18.98**	**0.40**	338	2.0	0.0502	9.5
7A_4.1C	152	304	2.07	**19.02**	**0.61**	342	3.2	0.0382	9.5
7B_8.1C	174	143	0.85	**19.10**	**0.16**	339	0.7	0.0419	8.5
7B_12.1C	111	145	1.36	**19.18**	**0.53**	335	2.7	0.0478	9.6
7A_7.1C	441	1492	3.50	**19.20**	**0.45**	335	2.3	0.0469	4.0
7B_9.1C	110	158	1.49	**19.45**	**0.38**	335	1.9	0.0361	10.7
7B_10.2E	294	317	1.11	**16.97**	**0.44**	378	2.6	0.0494	6.0
7B_7.2E	102	143	1.45	**17.49**	**0.70**	332	3.4	0.1250	12.6
7B_6.2E	159	270	1.75	**17.66**	**0.59**	363	3.3	0.0493	8.0
7B_3.2E	146	244	1.73	**19.51**	**0.52**	310	2.1	0.0951	13.7
7B_2.2I	201	384	1.97	**18.38**	**0.48**	346	2.6	0.0555	6.5
7B_14.1I	136	267	2.03	**18.39**	**0.75**	353	4.0	0.0397	9.3

TABLE B2 (continued): COOK CANYON TUFF PRE-CA SIMS SECTIONED ZIRCON RESULTS

Scharer method using constant melt Th/U

Spot Name	Melt (glass) 232Th/238U	Th/U zircon/melt	Disequilibrium corrected Age (Ma)	1 sigma error	Delta age
7A_1.1C	6.63	0.48	17.98	**0.32**	**0.06**
7A_2.1C	6.63	0.30	18.30	**0.38**	**0.08**
7A_5.1C	6.63	0.34	18.54	**1.11**	**0.07**
7B_2.1C	6.63	0.28	18.62	**0.64**	**0.08**
7B_4.1C	6.63	0.35	18.63	**0.53**	**0.07**
7B_6.1C	6.63	0.56	18.83	**0.52**	**0.05**
7B_4.3C	6.63	0.31	19.06	**0.40**	**0.07**
7A_4.1C	6.63	0.31	19.09	**0.61**	**0.08**
7B_8.1C	6.63	0.13	19.20	**0.16**	**0.10**
7B_12.1C	6.63	0.20	19.27	**0.53**	**0.09**
7A_7.1C	6.63	0.53	19.25	**0.45**	**0.05**
7B_9.1C	6.63	0.22	19.53	**0.38**	**0.08**
7B_10.2E	6.63	0.17	17.06	**0.44**	**0.09**
7B_7.2E	6.63	0.22	17.57	**0.70**	**0.09**
7B_6.2E	6.63	0.26	17.74	**0.59**	**0.08**
7B_3.2E	6.63	0.26	19.59	**0.52**	**0.08**
7B_2.2I	6.63	0.30	18.46	**0.48**	**0.08**
7B_14.1I	6.63	0.31	18.46	**0.75**	**0.08**

TABLE B2 (continued): COOK CANYON TUFF PRE-CA SIMS SECTIONED ZIRCON RESULTS

Spot Name	ppm U	ppm Th	232Th /238U	207corr 206Pb /238U Age (Ma)	1s err	Total 238 /206	% err	Total 207 /206	% err
7B_8.3I	141	128	0.94	**18.55**	**0.57**	345	3.0	0.0514	8.3
7B_3.3I	925	2205	2.46	**18.81**	**0.33**	341	1.8	0.0495	3.1
7B_7.3I	79	202	2.65	**19.03**	**0.67**	340	3.4	0.0423	13.8
7B_13.1I	152	435	2.95	**19.30**	**0.56**	331	2.9	0.0516	8.0
7B_8.4I	172	270	1.63	**19.84**	**0.69**	284	3.0	0.1463	8.9

TABLE B2 (continued): COOK CANYON TUFF PRE-CA SIMS SECTIONED ZIRCON RESULTS

Scharer method using constant melt Th/U

Spot Name	Melt (glass) 232Th/238U	Th/U zircon/melt	Disequilibrium corrected Age (Ma)	1 sigma error	Delta age
7B_8.3I	6.63	0.14	18.65	**0.57**	**0.09**
7B_3.3I	6.63	0.37	18.88	**0.33**	**0.07**
7B_7.3I	6.63	0.40	19.09	**0.67**	**0.07**
7B_13.1I	6.63	0.44	19.36	**0.56**	**0.06**
7B_8.4I	6.63	0.25	19.92	**0.69**	**0.08**

TABLE B3: PRE-CA SIMS SECTIONED CRYSTAL RESULTS FOR PROTEROZOIC ZIRCON

Spot Name	ppm U	ppm Th	232Th /238U	207corr 206Pb /238U Age (Ma)	1s err	204corr 207Pb /206Pb Age (Ma)	1s err	Total 238 /206	% err	Total 207 /206	% err
3D-2_12.1C	668	408	0.63	1321.63	29.84	1397	7	4	2.3	0.0889	0.3
3D-5_13.3E	81	50	0.63	1454.43	23.21	1706	178	4	1.6	0.1047	0.8
3D-5_13.1C	146	107	0.76	1664.86	41.09	1692	11	3	2.5	0.1036	0.6
3D-5_13.2I	124	53	0.44	1716.03	61.11	2195	358	2	1.5	0.3854	4.0
2H-1.1C	598	344	0.59	1752	11	1719	51	3	0.6	0.1053	0.4

TABLE B3 (continued): PRE-CA SIMS SECTIONED CRYSTAL RESULTS FOR PROTEROZOIC ZIRCON

	Scharer method using constant melt Th/U				
Spot Name	**Melt (glass) 232Th/238U**	**Th/U zircon/melt**	**Disequilibrium corrected Age (Ma)**	**1s err**	**Delta age**
3D-2_12.1C	6.33	0.10	1321.73	29.84	0.100
3D-5_13.3E	6.33	0.10	1454.52	23.21	0.098
3D-5_13.1C	6.33	0.12	1664.95	41.08	0.091
3D-5_13.2I	6.33	0.07	1716.13	61.10	0.101
2H-1.1C	5.34	0.11	1751.75	10.97	0.093

APPENDIX C: CA-TIMS U-PB ZIRCON GEOCHRONOLOGY DATA

TABLE C1: ALL CA-TIMS U-PB DATA

Sample Name	diseq.corr. $^{206}Pb^*/^{238}U$		$^{207}Pb^*/^{235}U$		cm.Pb (pg)	Th/U	$^{207}Pb/^{235}U$	2σ %er	diseq.corr. $^{206}Pb/^{238}U$	2s %er	ρ
Peach Spring Tuff											
MLPT4Z3b10	**18.08**	**0.12**	**18.2**	**1.85**	**1.3**	1.34	0.0181	10.15	0.002808	0.67	.65
PST2H_29	**18.53**	**0.19**	**18.9**	**2.41**	**2.4**	2.03	0.0188	12.75	0.002879	1.05	.59
PST3B_7	**18.74**	**0.10**	**19.5**	**1.27**	**1.5**	1.31	0.0194	6.53	0.002912	0.52	.58
MLPT3bZ02	**18.77**	**0.17**	**19.1**	**2.74**	**1.2**	1.42	0.0190	14.36	0.002916	0.91	.71
PST3B_3	**18.79**	**0.05**	**18.9**	**0.68**	**1.0**	1.72	0.0188	3.62	0.002919	0.29	.56
MLPT3bZ03	**18.79**	**0.36**	**15.4**	**5.62**	**1.5**	2.30	0.0153	36.41	0.002920	1.91	.59
MLPT3bZ01	**18.85**	**0.18**	**20.5**	**2.67**	**1.1**	1.35	0.0204	13.00	0.002928	0.93	.66
PST3D2_8	**18.85**	**0.16**	**19.5**	**3.09**	**1.1**	1.46	0.0194	15.83	0.002928	0.85	.77
MLPT3bZ04	**18.87**	**0.24**	**18.1**	**3.86**	**1.0**	1.33	0.0180	21.31	0.002931	1.29	.66
MLPT4Z5d1.1	**18.88**	**0.09**	**20.6**	**1.44**	**1.8**	1.52	0.0205	7.00	0.002932	0.49	.53
PST3D5_12	**18.92**	**0.10**	**19.8**	**1.56**	**1.2**	1.33	0.0197	7.90	0.002939	0.55	.65
MLPT4Z3b11	**18.93**	**0.06**	**19.0**	**0.86**	**1.2**	1.72	0.0189	4.54	0.002940	0.33	.58
MLPT3bZ06	**18.94**	**0.19**	**20.2**	**3.09**	**1.3**	1.34	0.0201	15.27	0.002942	1.02	.65
PST2H_32	**18.95**	**0.29**	**19.0**	**4.54**	**1.2**	1.33	0.0189	23.88	0.002943	1.53	.61
MLPT4Z5d29	**18.95**	**0.56**	**18.3**	**8.62**	**1.4**	2.37	0.0182	47.07	0.002944	2.96	.64
5DZ1,11*	**19.11**	**0.38**	**20.9**	**5.97**	**1.1**	2.56	0.0208	28.61	0.002968	2.00	.65
MLPT4Z5d28	**19.21**	**0.78**	**24.1**	**11.71**	**2.4**	2.53	0.0240	48.64	0.002984	4.06	.61
MLPT3bZ05	**19.27**	**0.51**	**23.3**	**7.97**	**1.8**	1.40	0.0232	34.24	0.002994	2.67	.65
PST3D1_3	**19.37**	**0.28**	**17.5**	**4.33**	**1.1**	1.38	0.0174	24.71	0.003010	1.47	.78
PST3D2_6	**20.20**	**0.14**	**20.6**	**1.69**	**1.6**	1.76	0.0205	8.20	0.003139	0.72	.52
PST3D2_1	**22.88**	**0.53**	**21.8**	**8.20**	**4.0**	2.51	0.0217	37.68	0.003555	2.31	.67

TABLE C1 (continued): ALL CA-TIMS U-PB DATA

Sample Name	diseq.corr. $\frac{^{206}Pb}{^{204}Pb}$	corr. $\frac{^{206}Pb}{^{204}Pb}$	corr. $\frac{^{207}Pb}{^{204}Pb}$	corr. $\frac{^{208}Pb}{^{204}Pb}$	diseq.corr. $\frac{^{238}U}{^{206}Pb}$	2σ %er	diseq.corr. $\frac{^{207}Pb}{^{206}Pb}$	2σ %er	tot.diseq.corr. $\frac{^{238}U}{^{206}Pb}$	2σ %er
Peach Spring Tuff										
MLPT4Z3b10	96	96	19.2	71.0	356.07	0.67	0.04676	9.73	287.71	0.19
PST2H_29	93	93	19.2	86.2	347.37	1.05	0.04735	12.16	278.86	0.91
PST3B_7	135	134	21.2	86.6	343.42	0.52	0.04828	6.25	296.55	0.37
MLPT3bZ02	83	82	18.6	66.9	342.97	0.91	0.04716	13.72	266.39	0.28
PST3B_3	232	231	25.5	154.4	342.57	0.29	0.04660	3.47	315.31	0.23
MLPT3bZ03	43	43	16.5	56.1	342.52	1.91	0.03796	35.31	196.89	0.23
MLPT3bZ01	79	78	18.6	63.7	341.56	0.93	0.05051	12.41	261.51	0.41
PST3D2_8	126	125	20.8	87.5	341.49	0.85	0.04805	15.18	291.39	0.24
MLPT3bZ04	60	60	17.5	55.6	341.17	1.29	0.04444	20.48	236.57	0.39
MLPT4Z5d1.1	127	126	21.1	90.3	341.02	0.49	0.05070	6.76	291.50	0.25
PST3D5_12	127	127	20.9	84.0	340.20	0.55	0.04852	7.55	290.95	0.30
MLPT4Z3b11	177	176	23.0	124.3	340.10	0.33	0.04651	4.36	304.61	0.18
MLPT3bZ06	71	71	18.2	60.6	339.89	1.02	0.04948	14.63	252.19	0.32
PST2H_32	51	51	17.1	51.8	339.74	1.53	0.04642	22.99	217.74	0.41
MLPT4Z5d29	35	35	16.3	50.4	339.72	2.96	0.04469	45.22	160.73	0.21
5DZ1,11	44	44	16.9	58.5	336.90	2.00	0.05059	27.34	194.79	0.29
MLPT4Z5d28	30	30	16.3	47.3	335.10	4.06	0.05801	46.29	129.43	0.19
MLPT3bZ05	37	37	16.7	46.3	334.04	2.67	0.05593	32.56	168.48	0.28
PST3D1_3	84	84	18.4	66.7	332.22	1.47	0.04192	23.59	259.43	0.94
PST3D2_6	108	107	19.8	87.9	318.59	0.72	0.04734	7.86	264.09	0.61
PST3D2_1	41	41	16.6	56.3	281.29	2.31	0.04410	36.17	156.35	0.62

Sample Name	2σ %er	diseq.corr. $\frac{^{204}Pb}{^{206}Pb}$	2σ %er	tot.diseq.corr. $\frac{^{238}U}{^{206}Pb}$	2σ %er
MLPT4Z3b10	0.41	0.01041	1.5	287.71	0.19
PST2H_29	0.66	0.01071	2.6	278.86	0.91
PST3B_7	0.43	0.00740	1.5	296.55	0.37
MLPT3bZ02	0.67	0.01211	2.3	266.39	0.28
PST3B_3	0.11	0.00432	1.4	315.31	0.23
MLPT3bZ03	0.70	0.02309	0.8	196.89	0.23
MLPT3bZ01	0.60	0.01271	1.8	261.51	0.41
PST3D2_8	2.63	0.00796	5.3	291.39	0.24
MLPT3bZ04	0.74	0.01663	1.8	236.57	0.39
MLPT4Z5d1.1	1.19	0.00788	1.1	291.50	0.25
PST3D5_12	0.68	0.00785	2.1	290.95	0.30
MLPT4Z3b11	0.05	0.00566	0.9	304.61	0.18
MLPT3bZ06	0.88	0.01400	1.8	252.19	0.32
PST2H_32	0.78	0.01948	1.2	217.74	0.41
MLPT4Z5d29	0.30	0.02861	1.2	160.73	0.21
5DZ1,11*	0.47	0.02291	1.4	194.79	0.29
MLPT4Z5d28	0.27	0.03334	0.7	129.43	0.19
MLPT3bZ05	0.42	0.02689	1.4	168.48	0.28
PST3D1_3	0.77	0.01189	4.9	259.43	0.94
PST3D2_6	0.35	0.00929	1.1	264.09	0.61
PST3D2_1	0.48	0.02413	1.7	156.35	0.62

TABLE C1 (continued): ALL CA-TIMS U-PB DATA

Sample Name	diseq.corr. $^{206}Pb^*/^{238}U$		$^{207}Pb^*/^{235}U$		cm.Pb (pg)	Th/U	$^{207}Pb/^{235}U$	2σ %er	diseq.corr. $^{206}Pb/^{238}U$	2s %er	ρ
Cook Canyon Tuff											
PST7B_4	**18.98**	**0.22**	**20.3**	**3.70**	**1.6**	2.24	0.0202	18.20	0.002949	1.19	.57
MLCCT7BZ05	**19.21**	**0.47**	**13.2**	**7.07**	**0.8**	1.92	0.0131	53.47	0.002985	2.43	.62
MLCCT7BZ01	**19.25**	**0.26**	**20.8**	**3.55**	**3.7**	1.61	0.0207	17.10	0.002990	1.34	.56
7B22,23,29*	**19.29**	**0.39**	**16.9**	**6.03**	**0.8**	1.84	0.0168	35.71	0.002997	2.03	.66
MLPT4Z7a	**19.39**	**0.87**	**20.1**	**13.26**	**1.7**	1.89	0.0200	65.91	0.003012	4.51	.62
7BZ2,5*	**19.45**	**0.26**	**20.7**	**3.83**	**1.1**	1.91	0.0206	18.49	0.003022	1.32	.58
PST7A_7	**19.60**	**0.81**	**19.8**	**14.92**	**0.8**	2.25	0.0197	75.38	0.003045	4.15	.61
MLCCT7BZ06	**20.10**	**0.87**	**23.2**	**13.37**	**1.0**	2.19	0.0232	57.51	0.003122	4.35	.64
MLCCT7BZ03	**20.67**	**0.77**	**26.3**	**11.07**	**1.5**	2.14	0.0262	42.16	0.003212	3.72	.59
MLCCT7BZ04	**20.74**	**0.73**	**20.0**	**11.16**	**0.9**	1.62	0.0199	55.79	0.003223	3.52	.62
7BZ3,6,20*	**21.38**	**1.22**	**30.5**	**18.51**	**1.6**	2.05	0.0305	60.72	0.003321	5.71	.64
MLCCT7BZ02	**1073.73**	**18.75**	**1522.1**	**26.73**	**1.4**	0.39	3.4772	1.76	0.181237	1.73	.99

*** Analysis represents combined tips broken off zircon with low-U rims**

TABLE C1 (continued): ALL CA-TIMS U-PB DATA

Sample Name	diseq.corr. $^{206}Pb/^{204}Pb$	corr. $^{206}Pb/^{204}Pb$	corr. $^{207}Pb/^{204}Pb$	corr. $^{208}Pb/^{204}Pb$	diseq.corr. $^{238}U/^{206}Pb$	2σ %er	diseq.corr. $^{207}Pb/^{206}Pb$	2σ %er	tot.diseq.corr. $^{238}U/^{206}Pb$	2σ %er
Cook Canyon Tuff										
PST7B_4	64	63	17.9	70.2	339.11	1.19	0.04967	17.54	241.10	0.52
MLCCT7BZ05	38	38	16.2	50.1	335.00	2.43	0.03174	52.00	173.93	0.39
MLCCT7BZ01	58	58	17.6	58.2	334.47	1.34	0.05000	16.40	228.42	0.78
7B22,23,29	44	44	16.6	52.9	333.62	2.03	0.04048	34.40	193.89	0.49
MLPT4Z7a	29	29	16.1	44.3	331.97	4.51	0.04785	63.22	121.54	0.49
7BZ2,5	56	56	17.5	61.0	330.94	1.32	0.04941	17.76	223.01	0.54
PST7A_7	31	31	16.2	47.3	328.38	4.15	0.04664	72.94	136.36	0.71
MLCCT7BZ06	30	30	16.2	45.8	320.29	4.35	0.05350	54.82	121.75	0.35
MLCCT7BZ03	31	31	16.4	46.8	311.30	3.72	0.05887	40.08	129.28	1.29
MLCCT7BZ04	32	32	16.2	45.0	310.26	3.52	0.04455	53.68	132.08	0.34
7BZ3,6,20	27	27	16.2	43.5	301.08	5.71	0.06605	57.23	95.49	0.38
MLCCT7BZ02	1028	1042	156.1	159.2	5.52	1.73	0.13918	0.30	5.42	2.24

*** Analysis represents combined tips broken off zircon with low-U rims**

TABLE C1 (continued): ALL CA-TIMS U-PB DATA

Sample Name	2σ %er	diseq.corr. $^{204}Pb/^{206}Pb$	2σ %er	tot.diseq.corr. $^{238}U/^{206}Pb$	2σ %er
PST7B_4	1.31	0.01569	1.5	241.10	0.52
MLCCT7BZ05	0.27	0.02610	1.0	173.93	0.39
MLCCT7BZ01	0.53	0.01720	0.8	228.42	0.78
7B22,23,29*	0.36	0.02273	1.6	193.89	0.49
MLPT4Z7a	0.33	0.03441	0.9	121.54	0.49
7BZ2,5*	0.67	0.01770	0.9	223.01	0.54
PST7A_7	1.69	0.03175	2.0	136.36	0.71
MLCCT7BZ06	0.29	0.03366	1.2	121.75	0.35
MLCCT7BZ03	0.21	0.03175	0.6	129.28	1.29
MLCCT7BZ04	0.41	0.03117	0.9	132.08	0.34
7BZ3,6,20*	0.20	0.03708	1.1	95.49	0.38
MLCCT7BZ02	0.21	0.00097	1.5	5.42	2.24

*** Analysis represents combined tips broken off zircon with low-U rims**

APPENDIX D: CATHODOLUMINESCENCE IMAGES OF SECTIONED ZIRCON AND ANALYSIS SPOT LOCATIONS

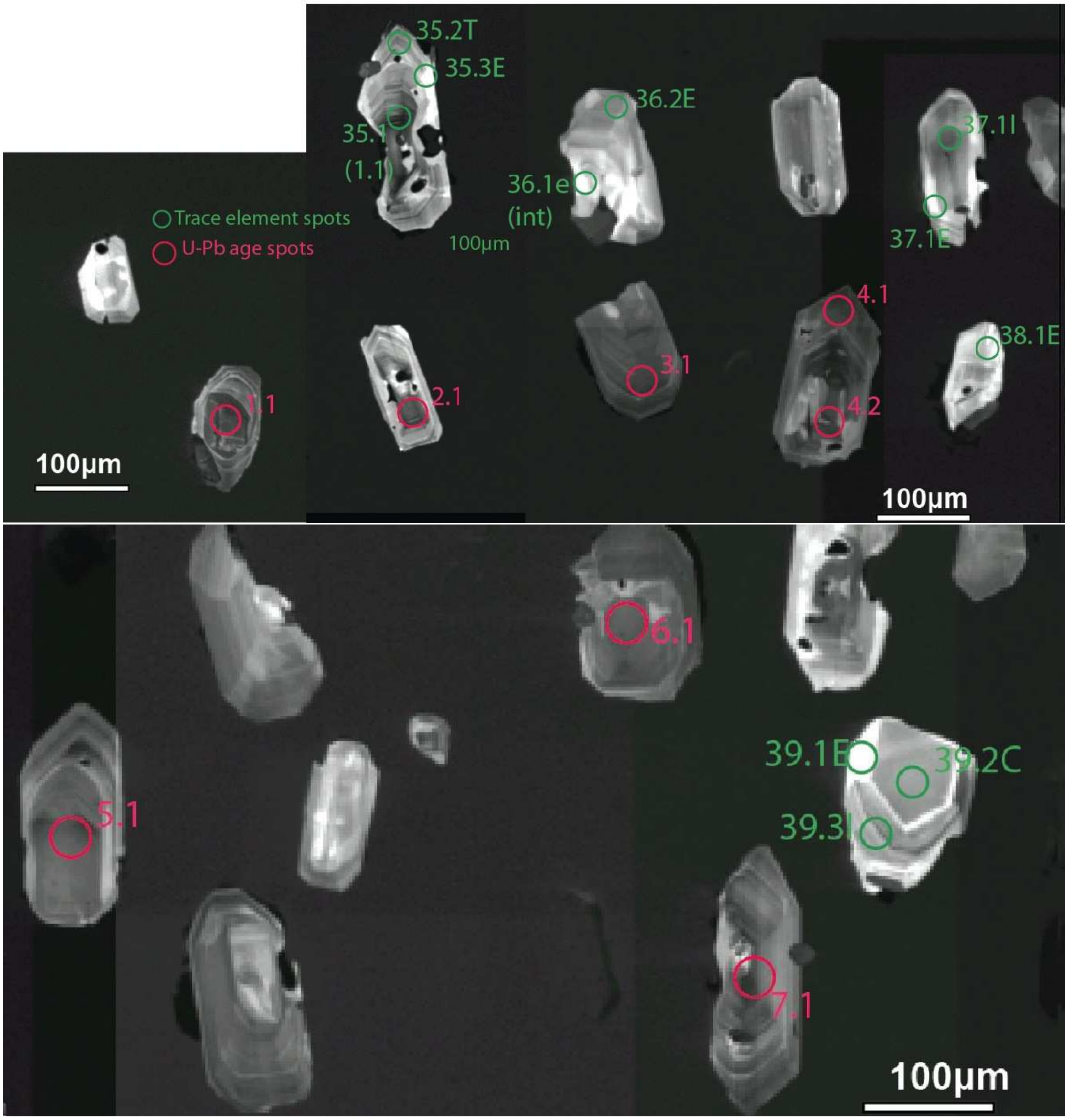

Figure D1. Cathodoluminescence mages from pumice sample 2h

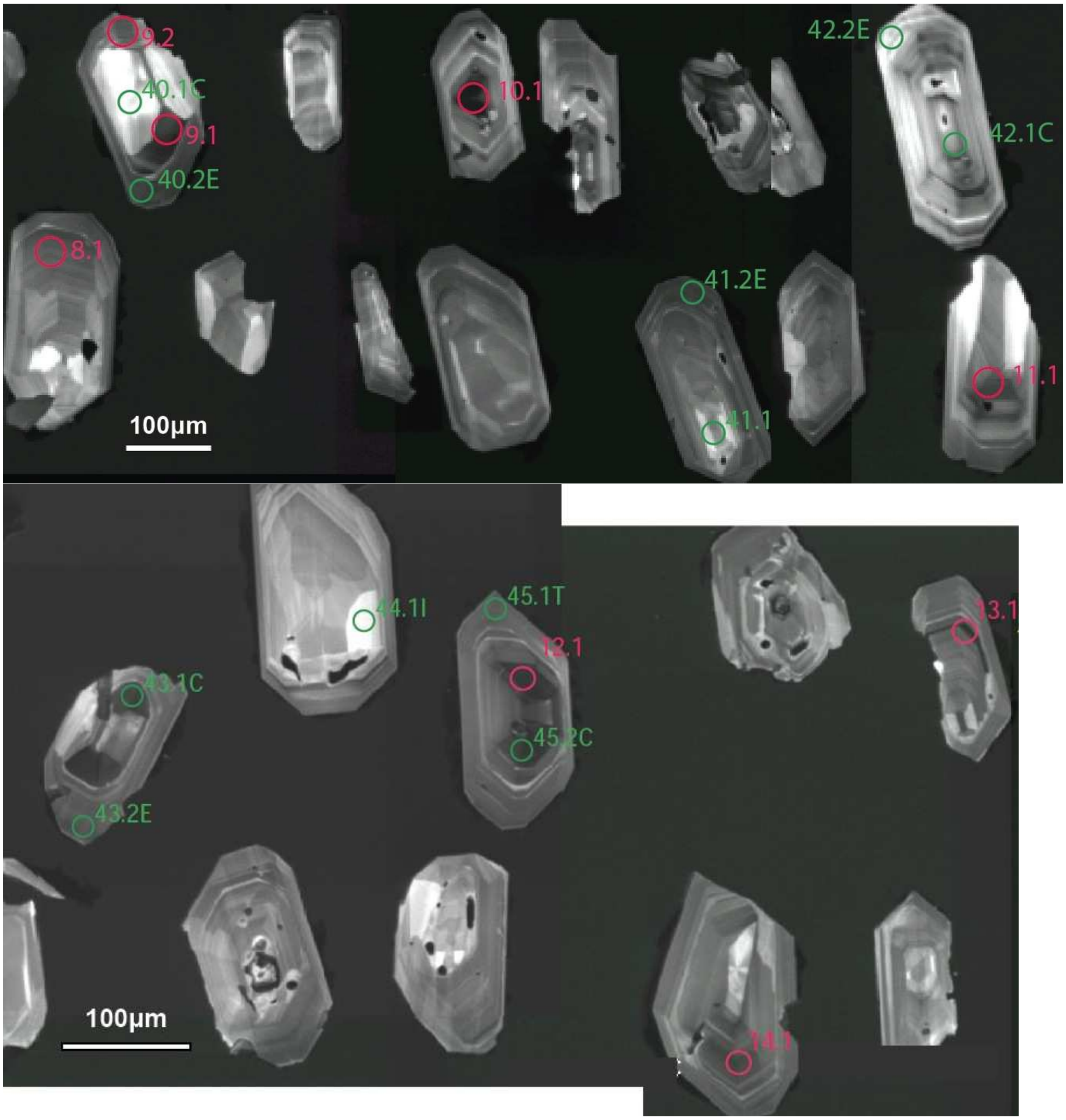

Figure D1. (continued)

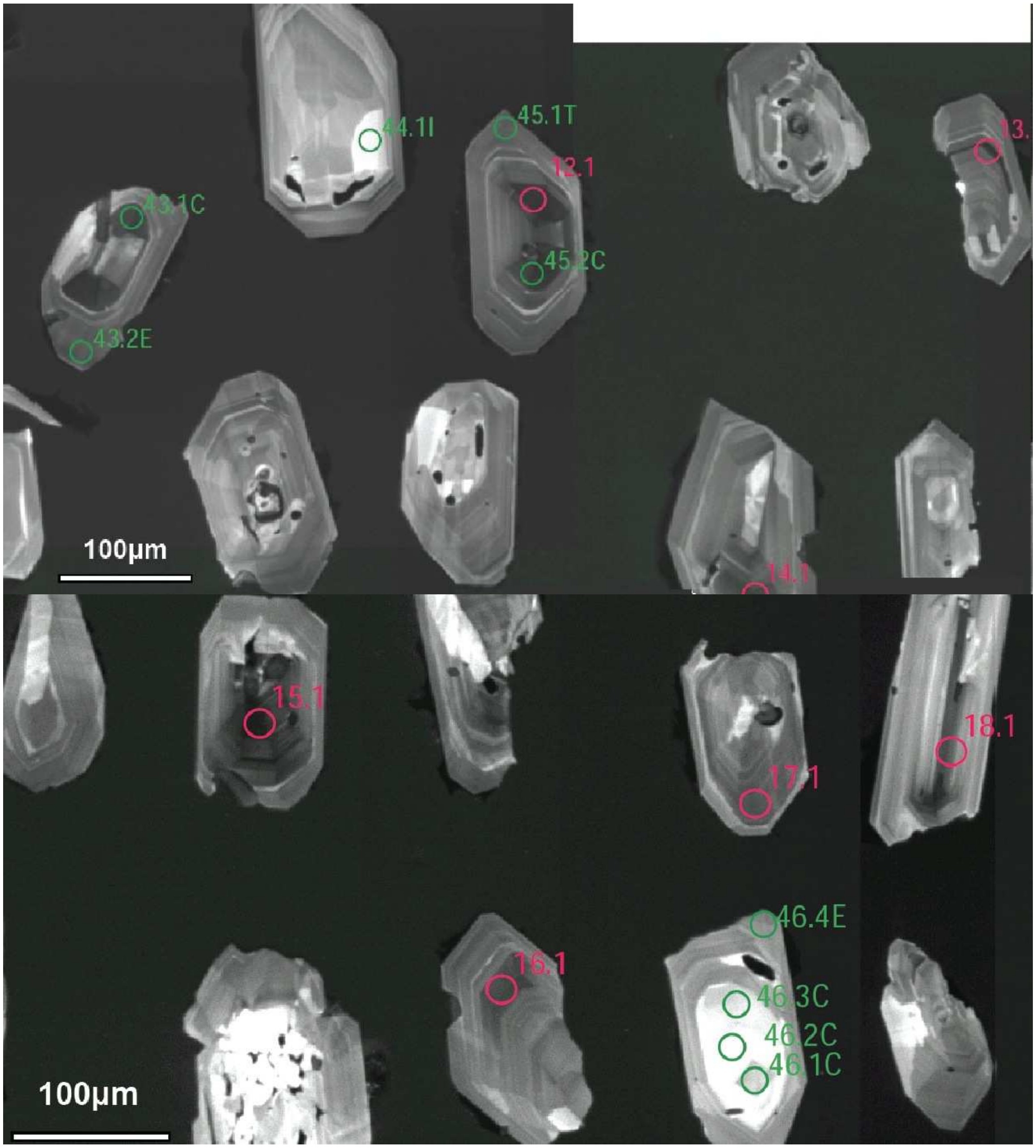

Figure D1. (continued)

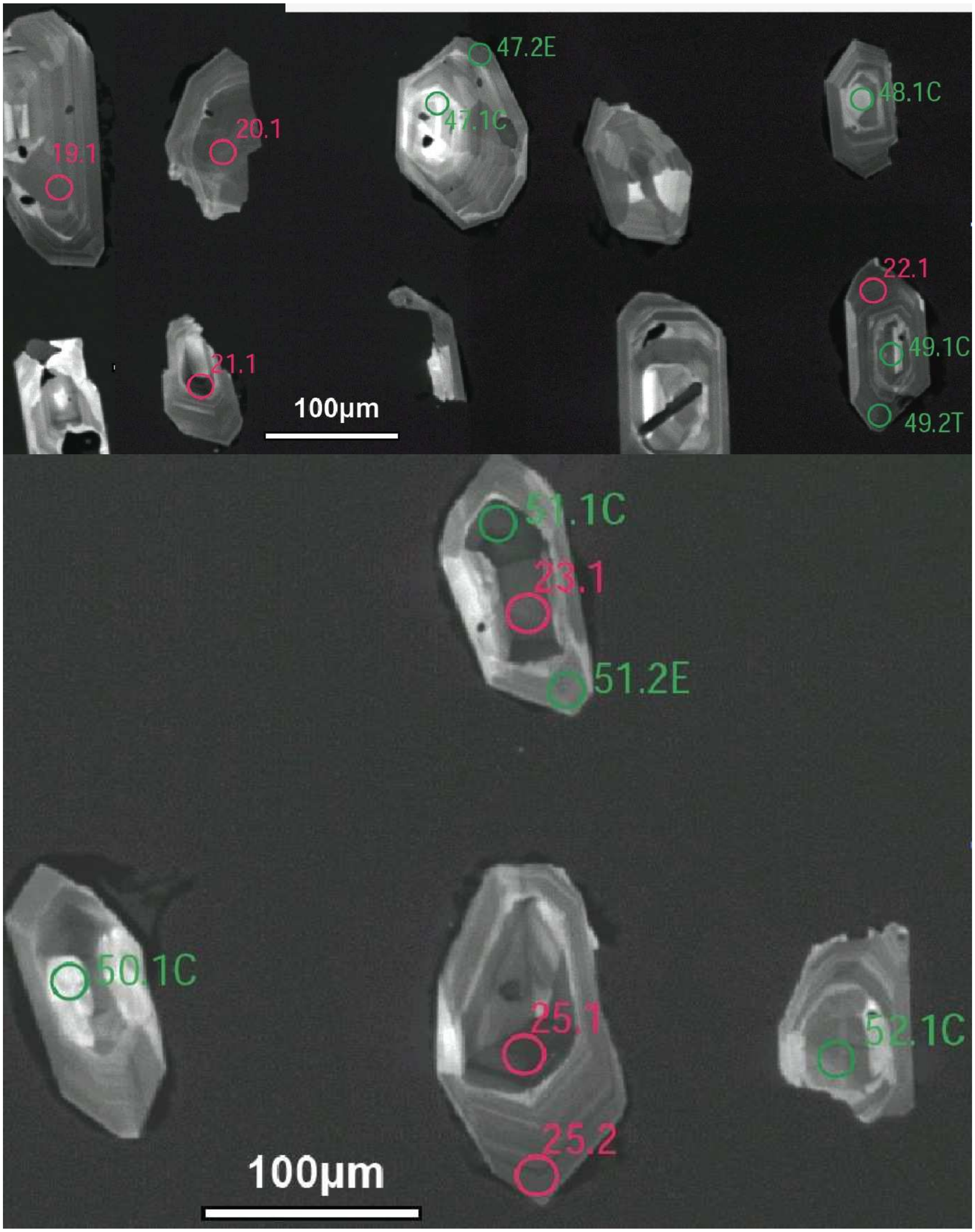

Figure D1. (continued)

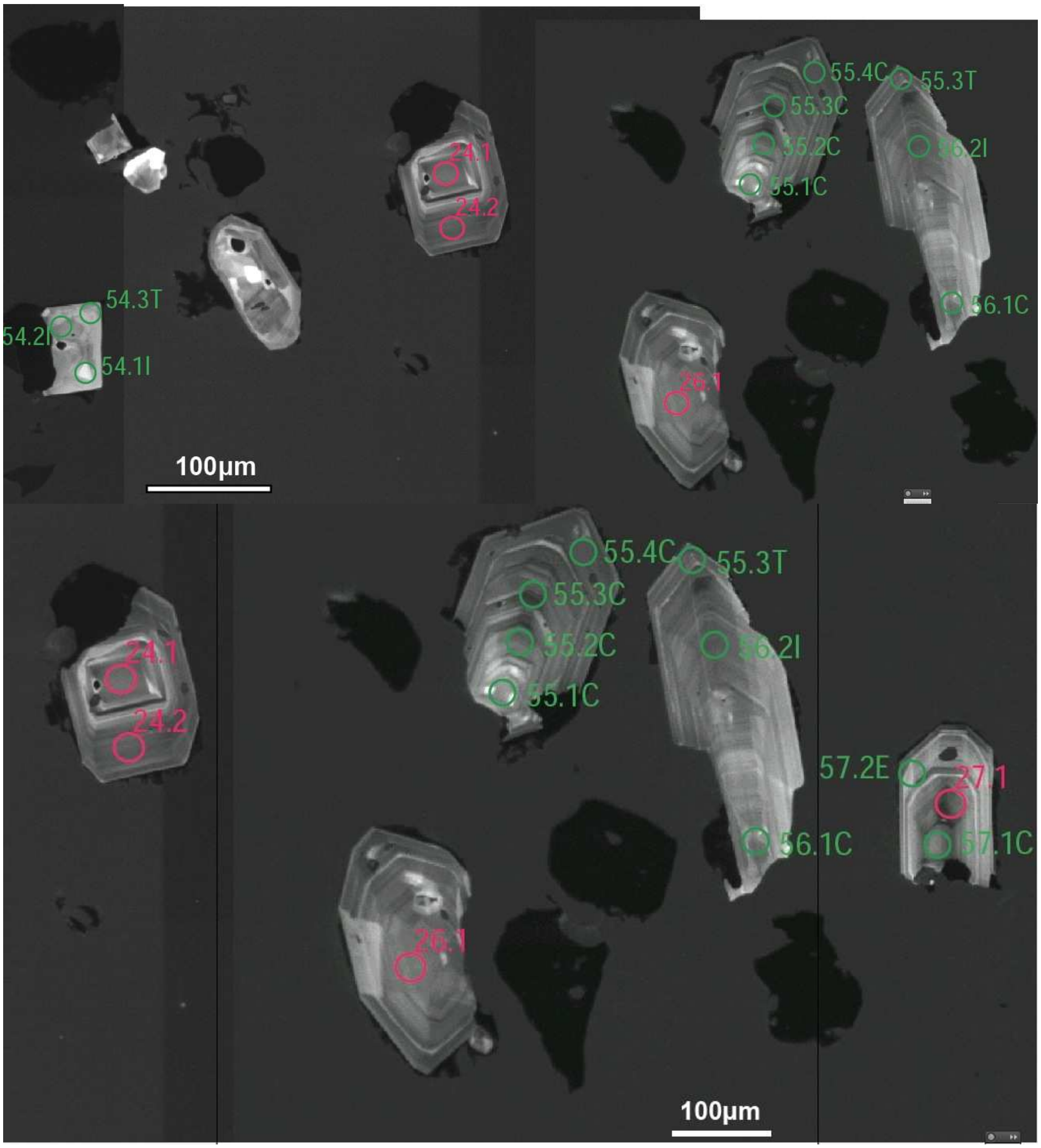

Figure D1. (continued)

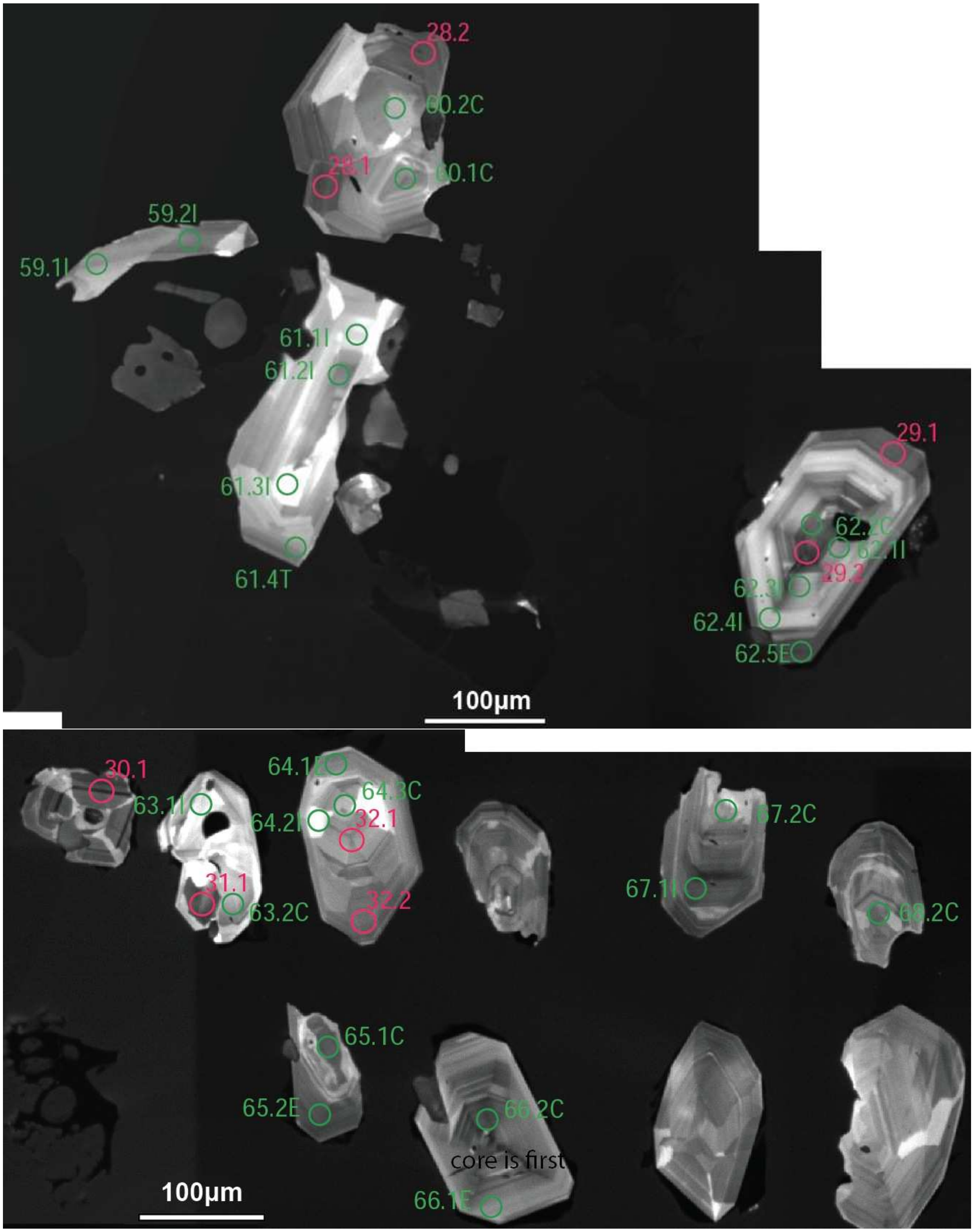

Figure D1. (continued)

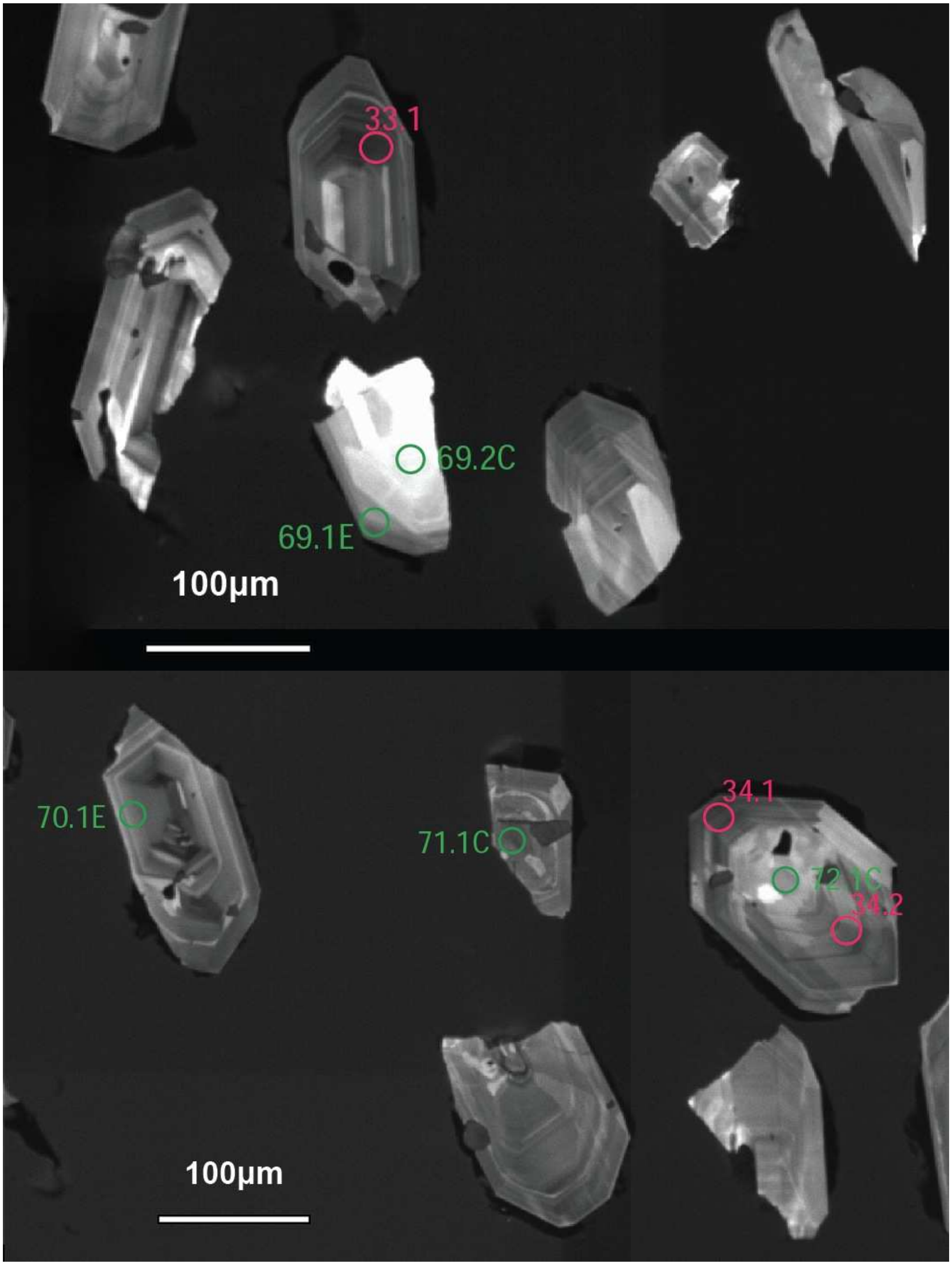

Figure D1. (continued)

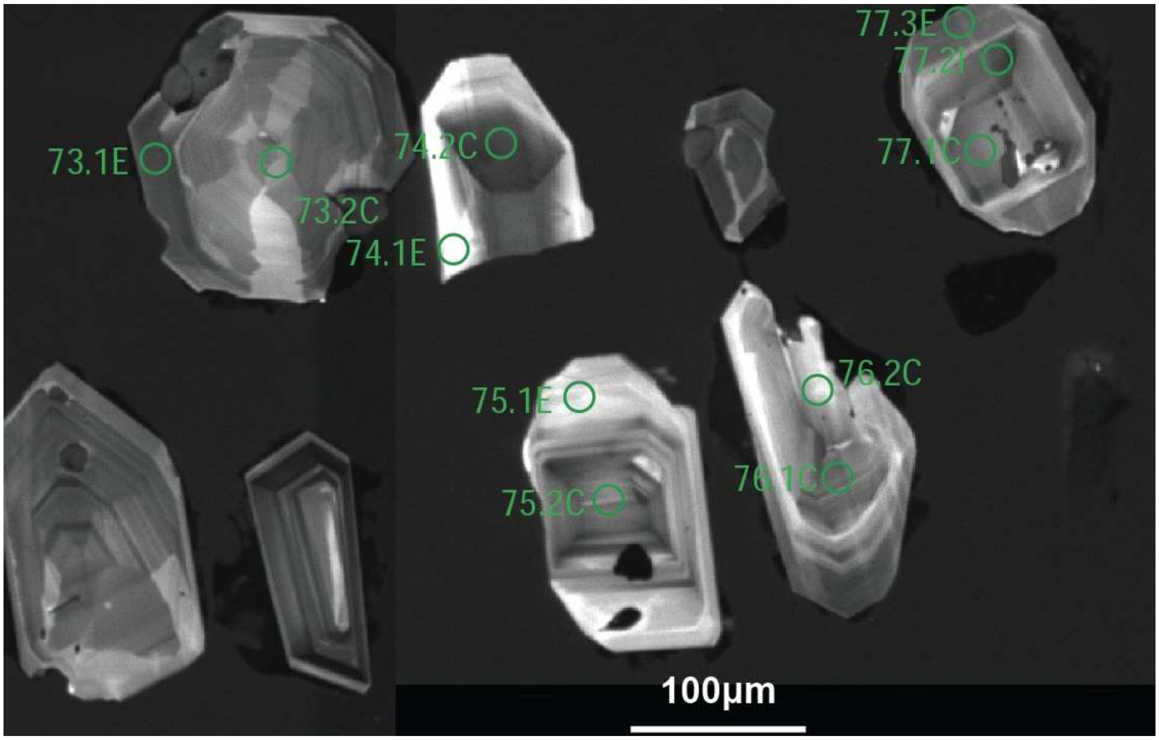

Figure D1. (continued)

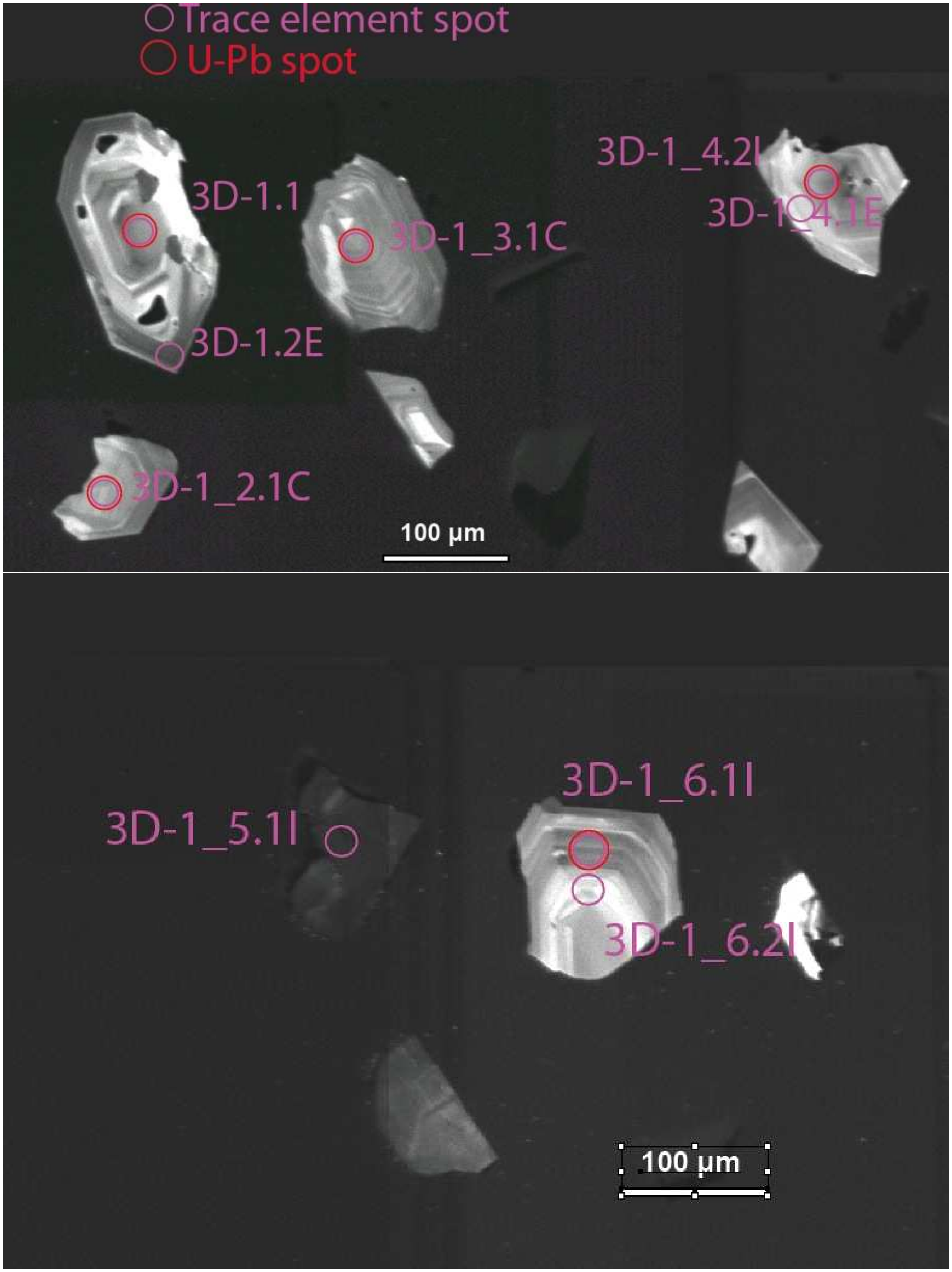

Figure D2. Cathodoluminescence mages from pumice sample 3d

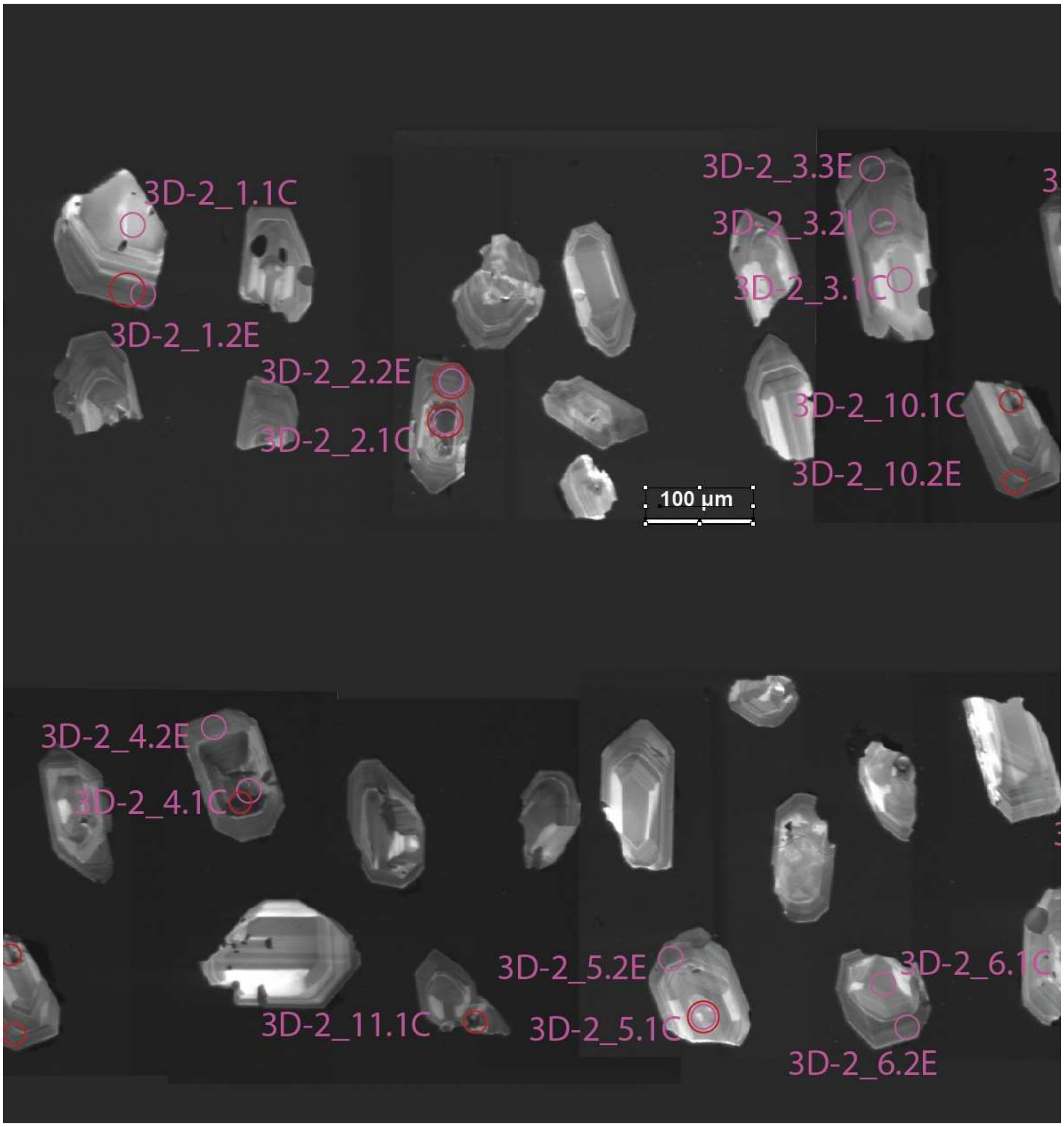

Figure D2. (continued)

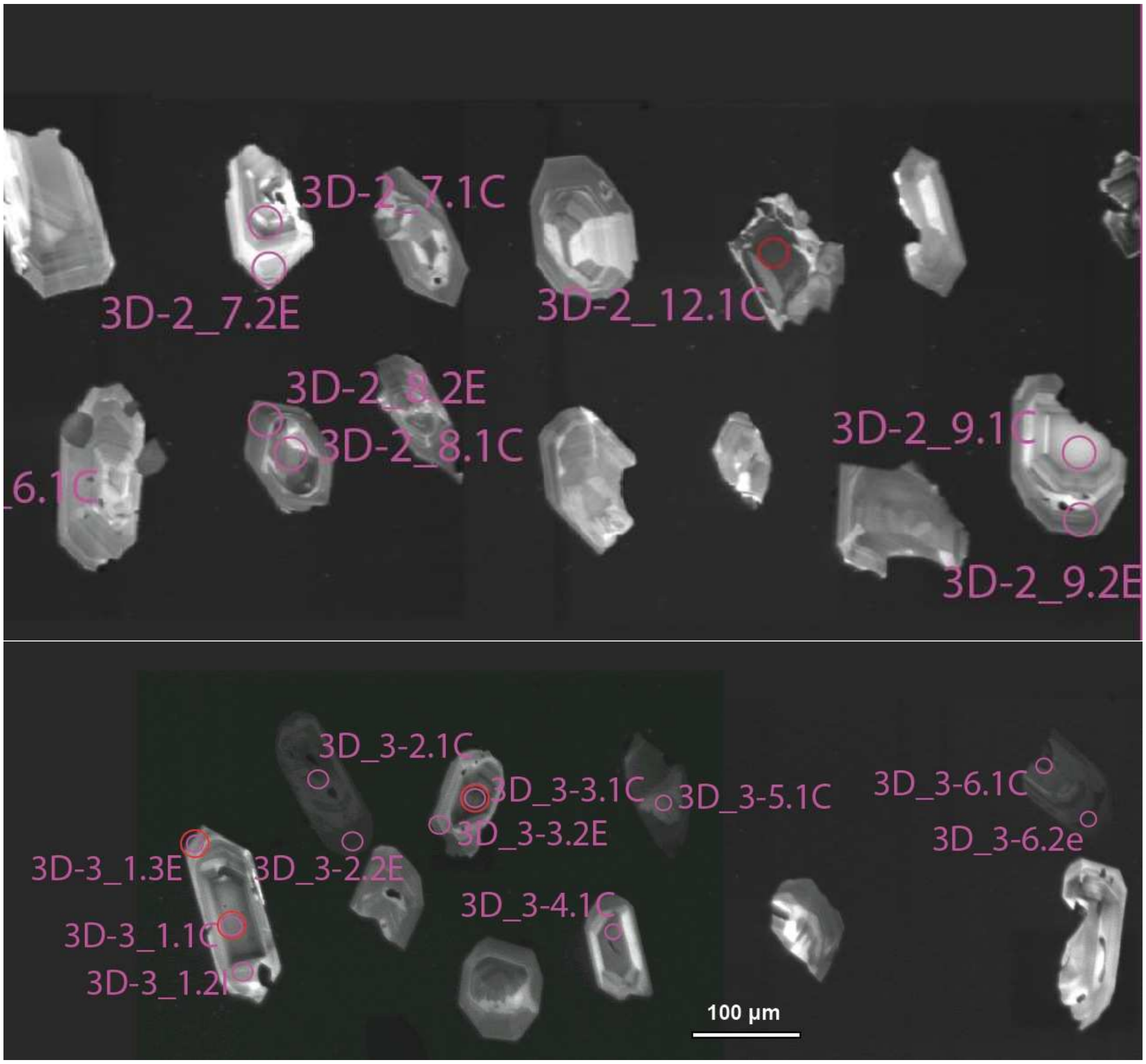

Figure D2. (continued)

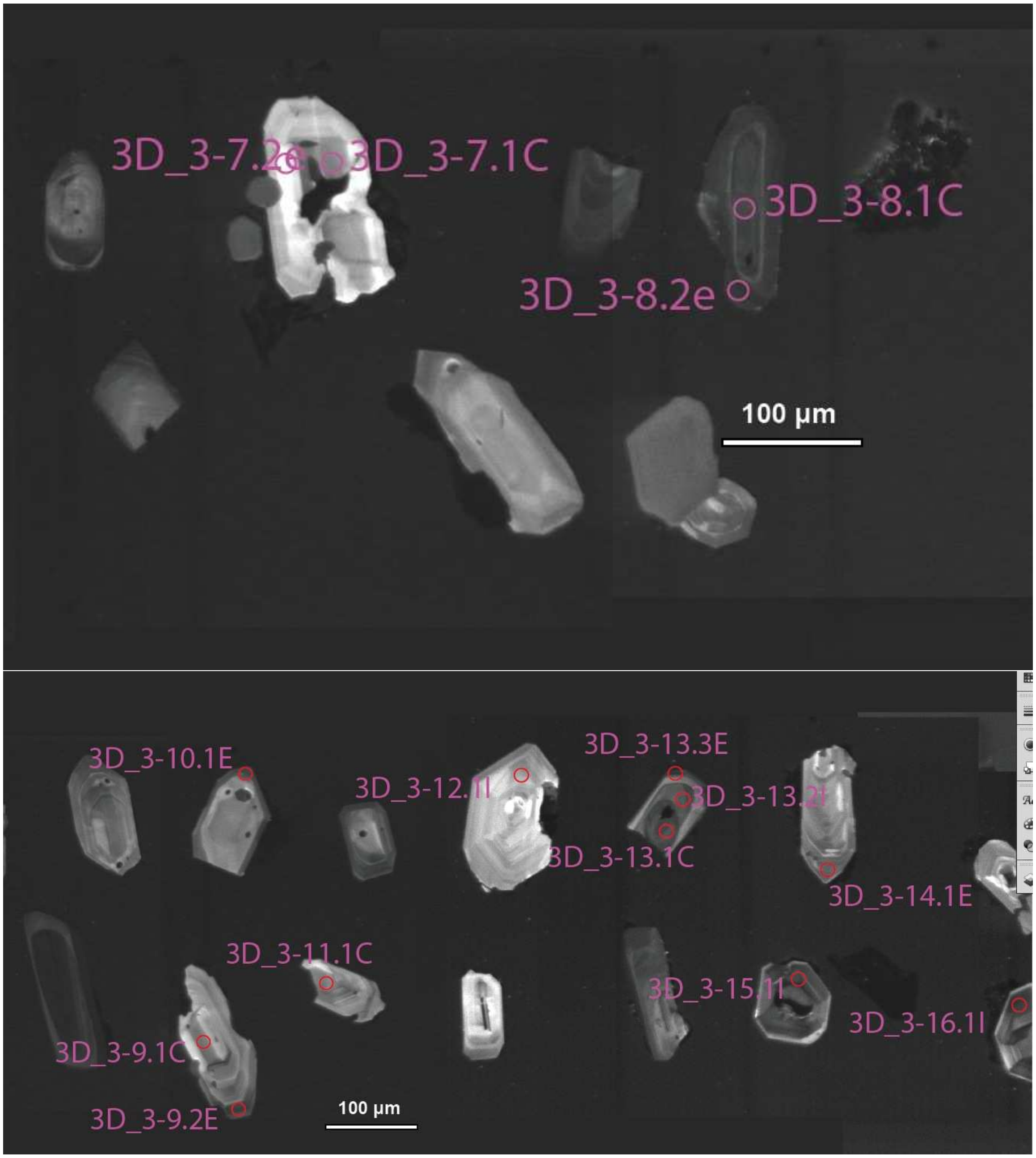

Figure D2. (continued)

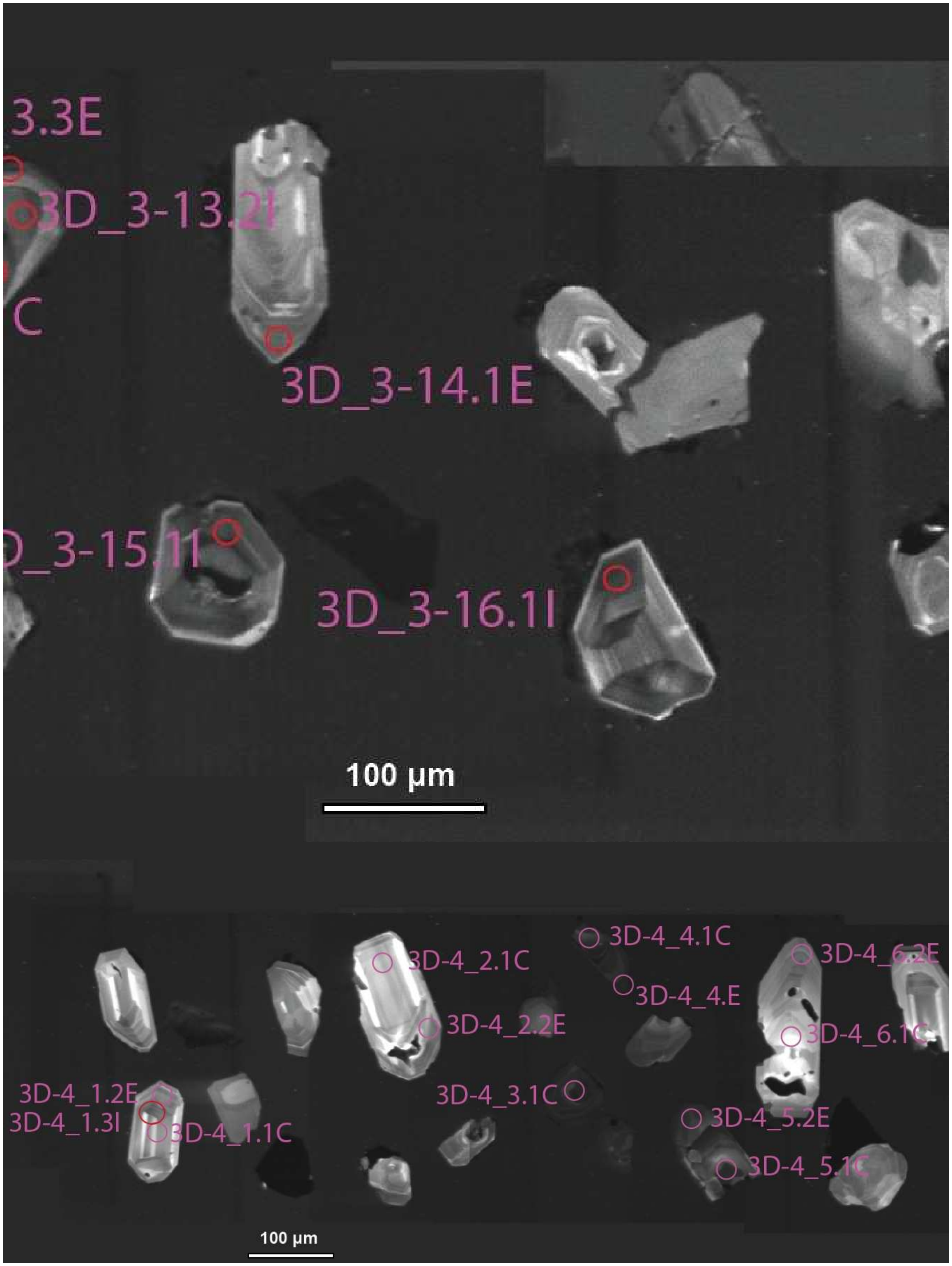

Figure D2. (continued)

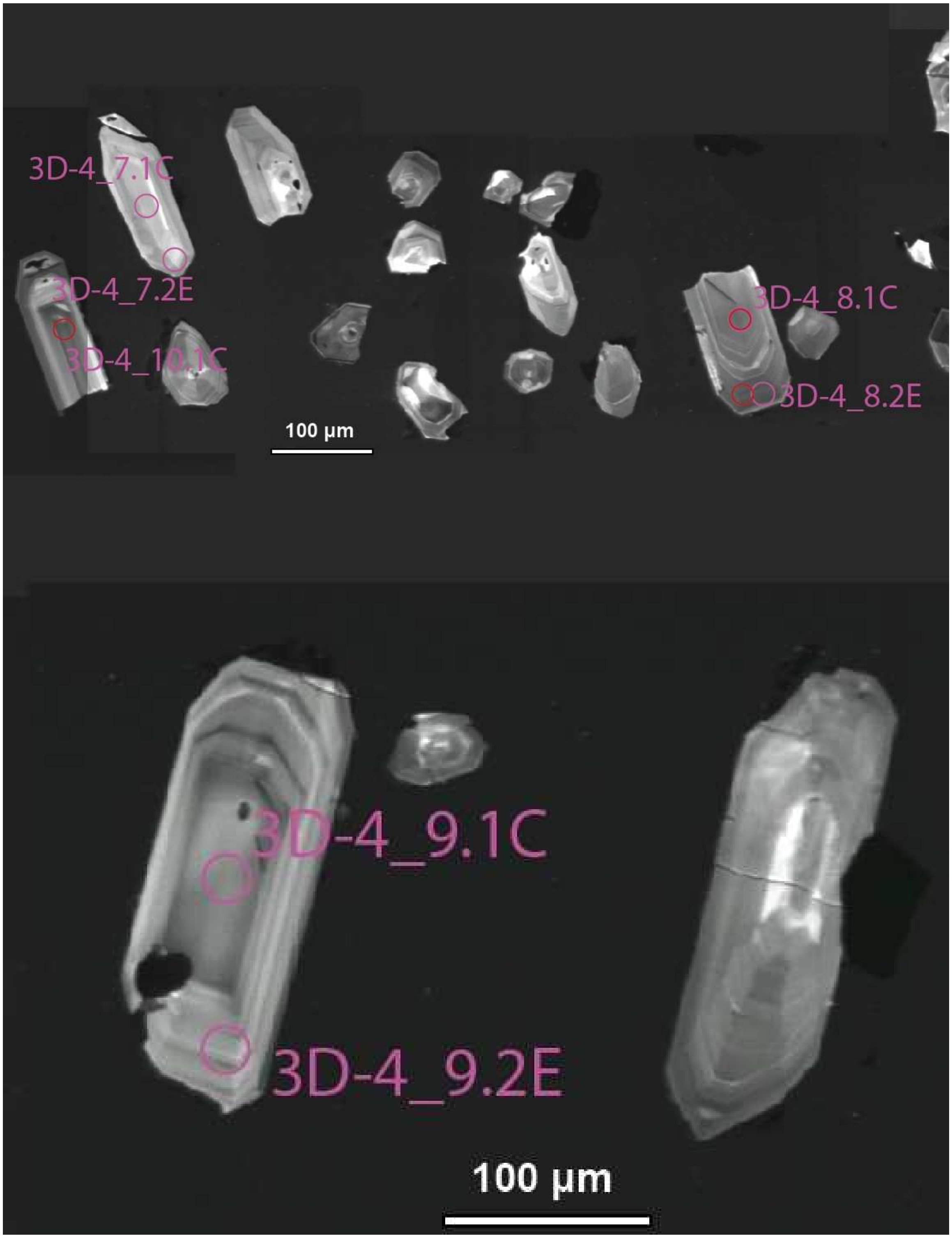

Figure D2. (continued)

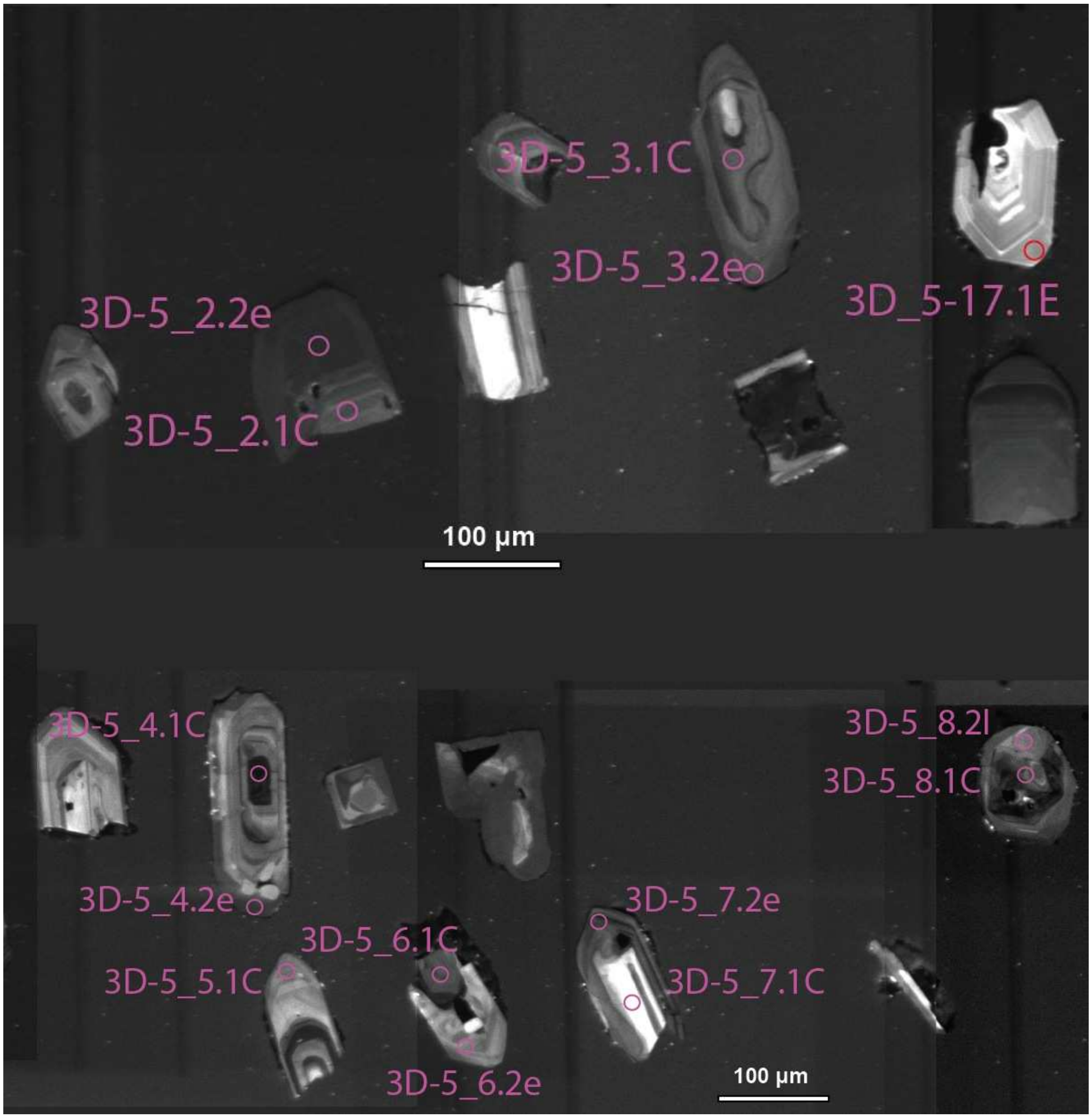

Figure D2. (continued)

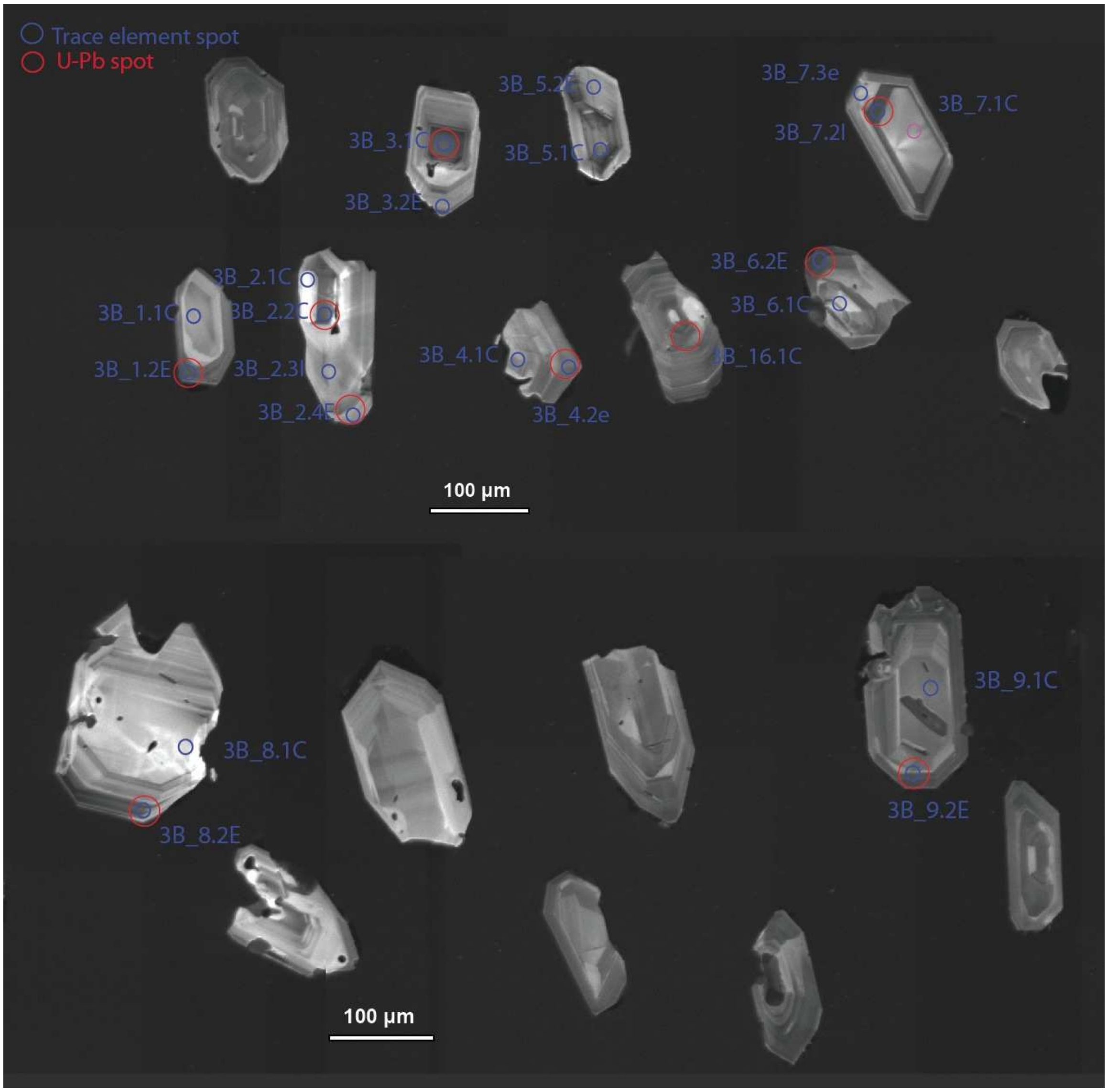

Figure D3. Cathodoluminescence mages from pumice sample 3b.

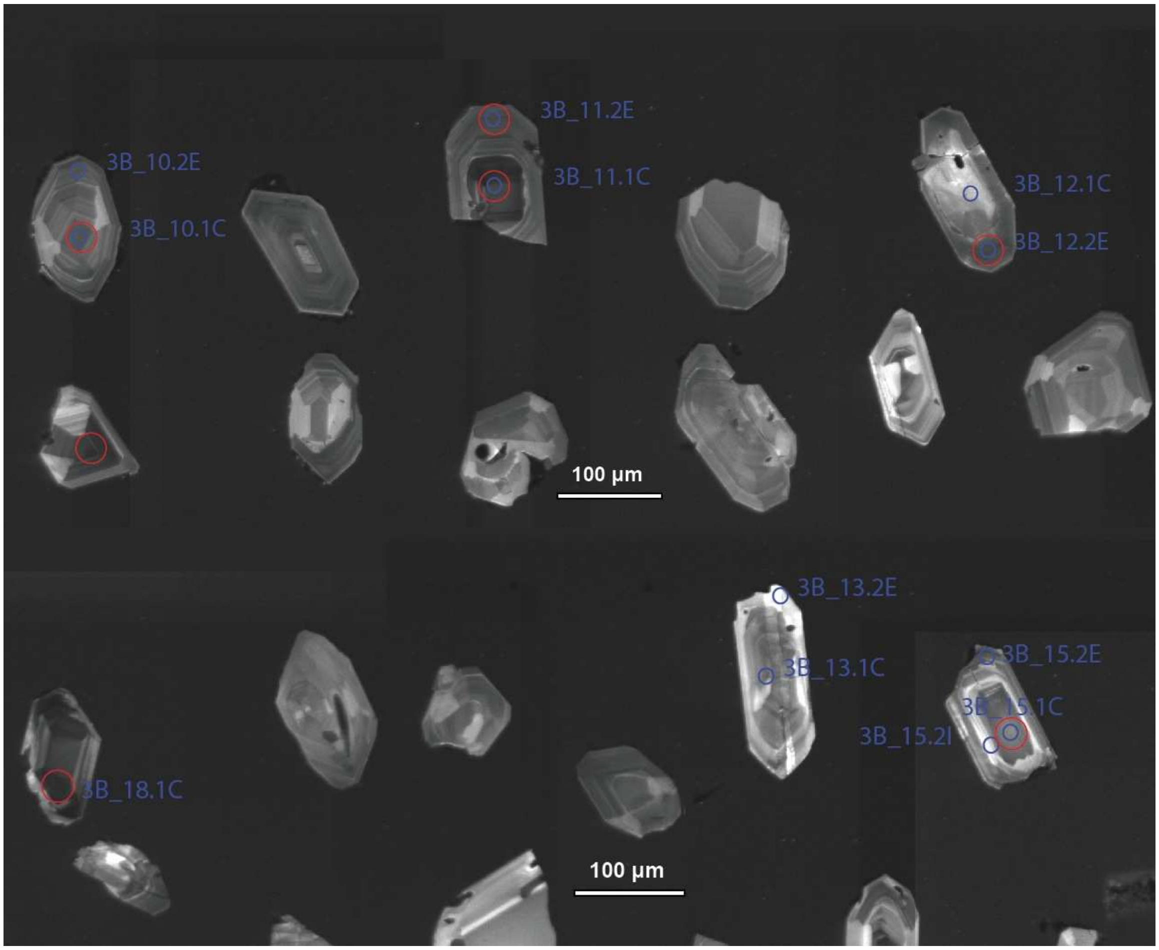

Figure D3. (continued)

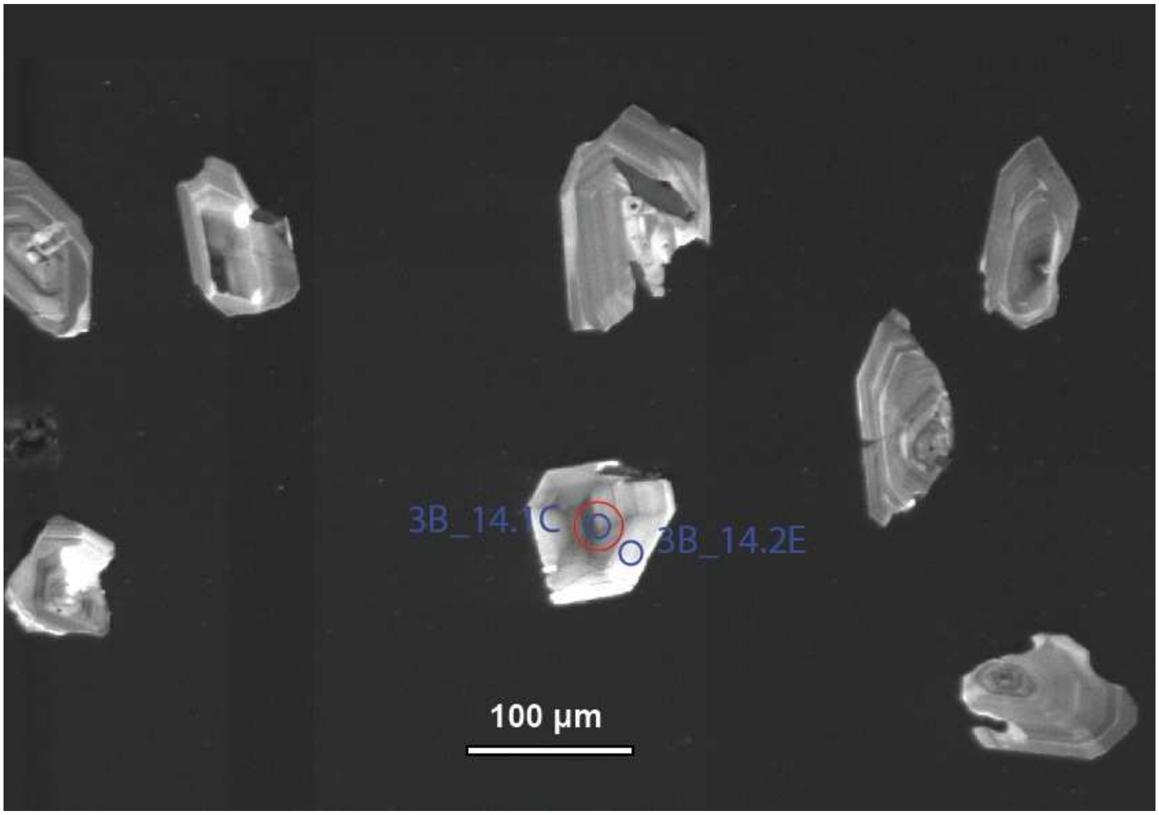

Figure D3. (continued)

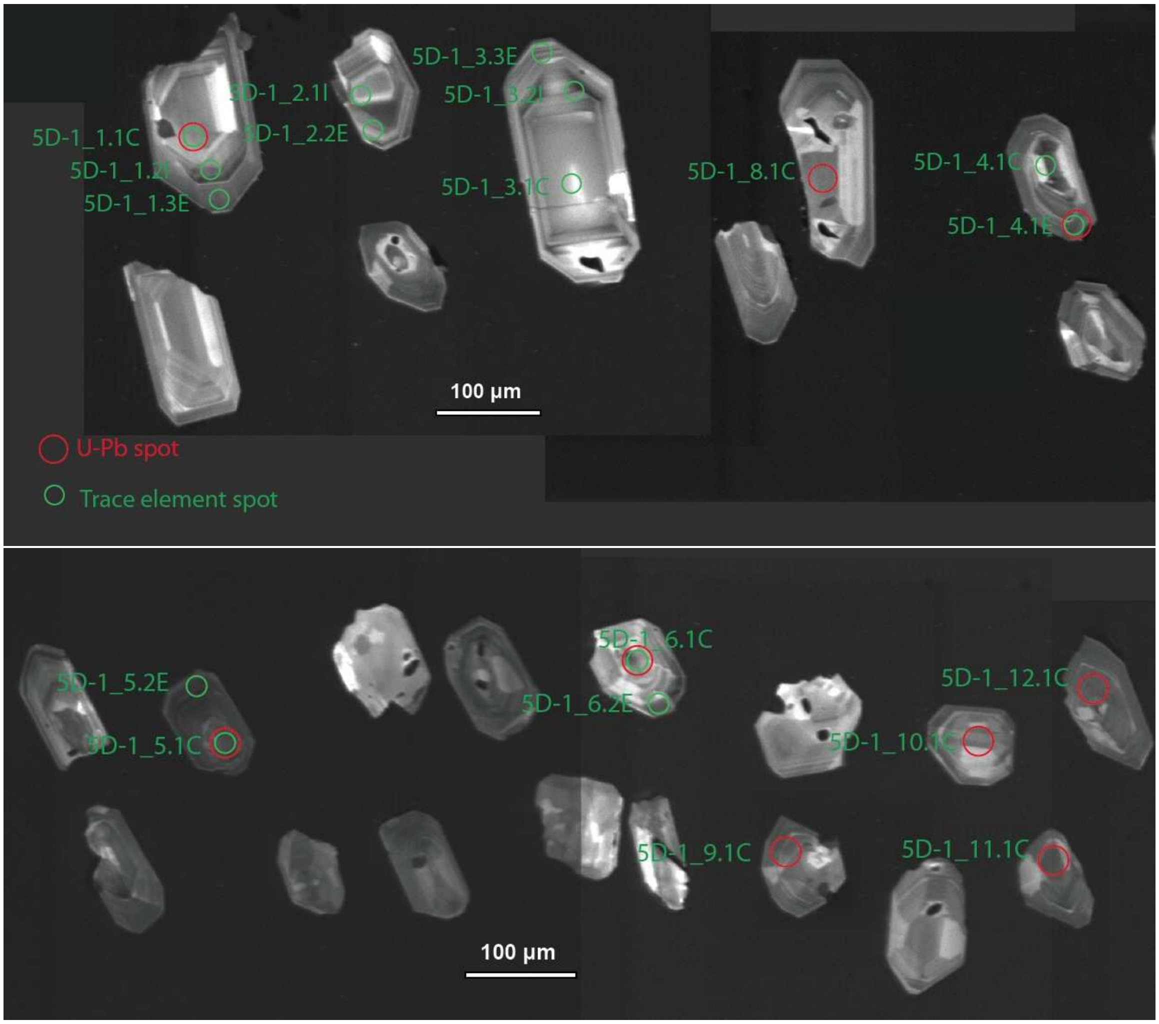

Figure D4. Cathodoluminescence mages from pumice sample 5d.

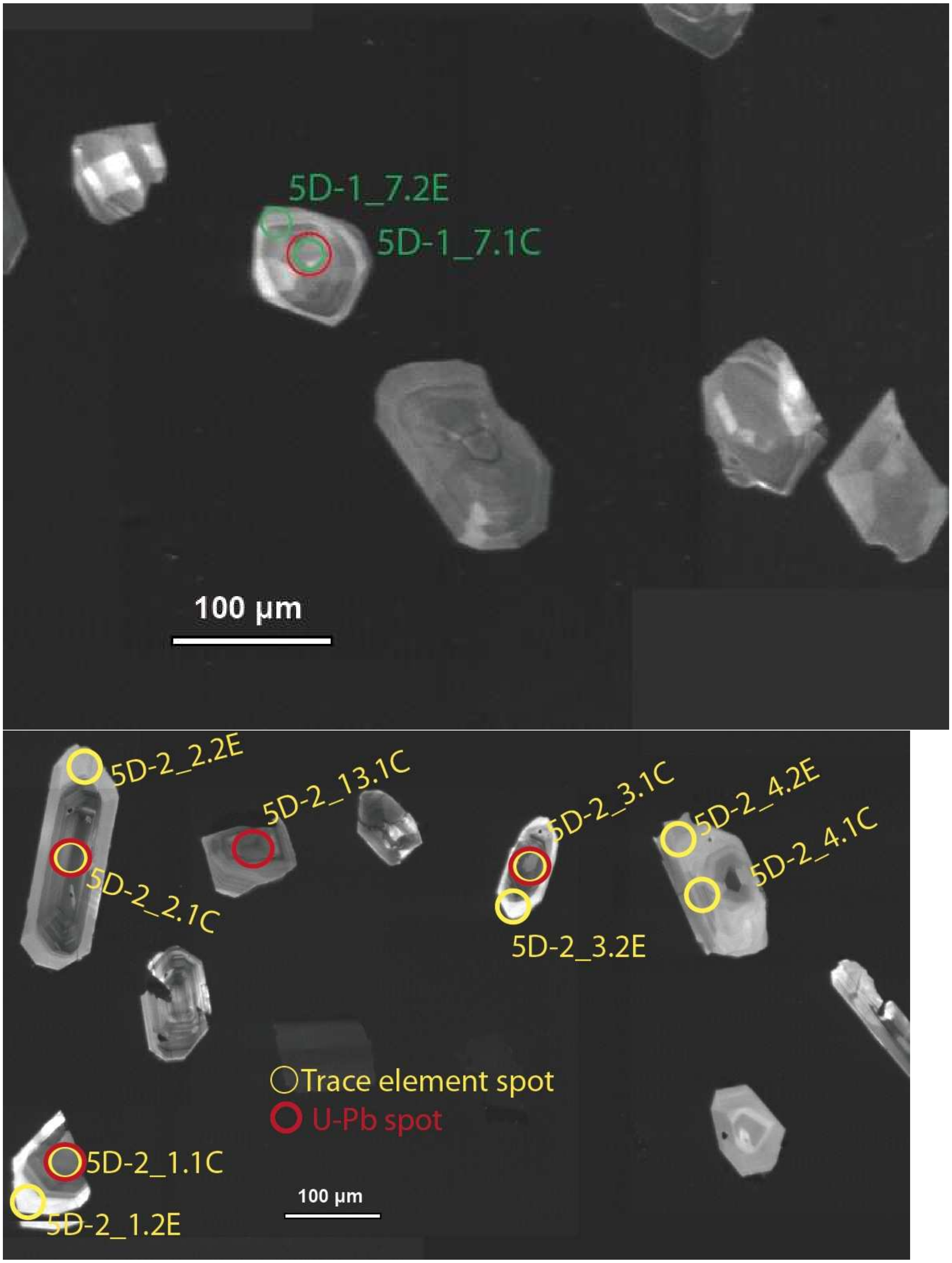

Figure D4. (continued)

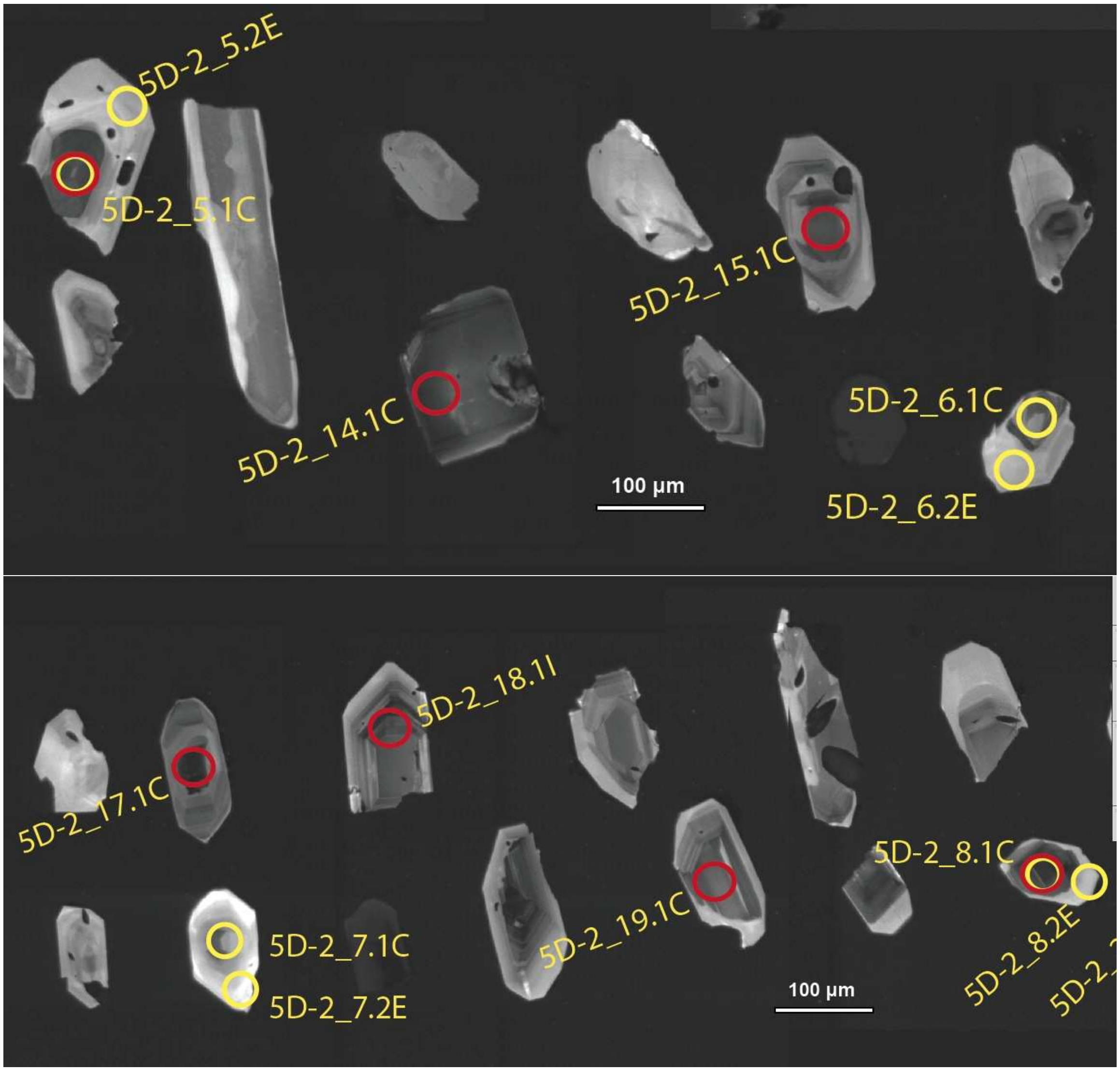

Figure D4. (continued)

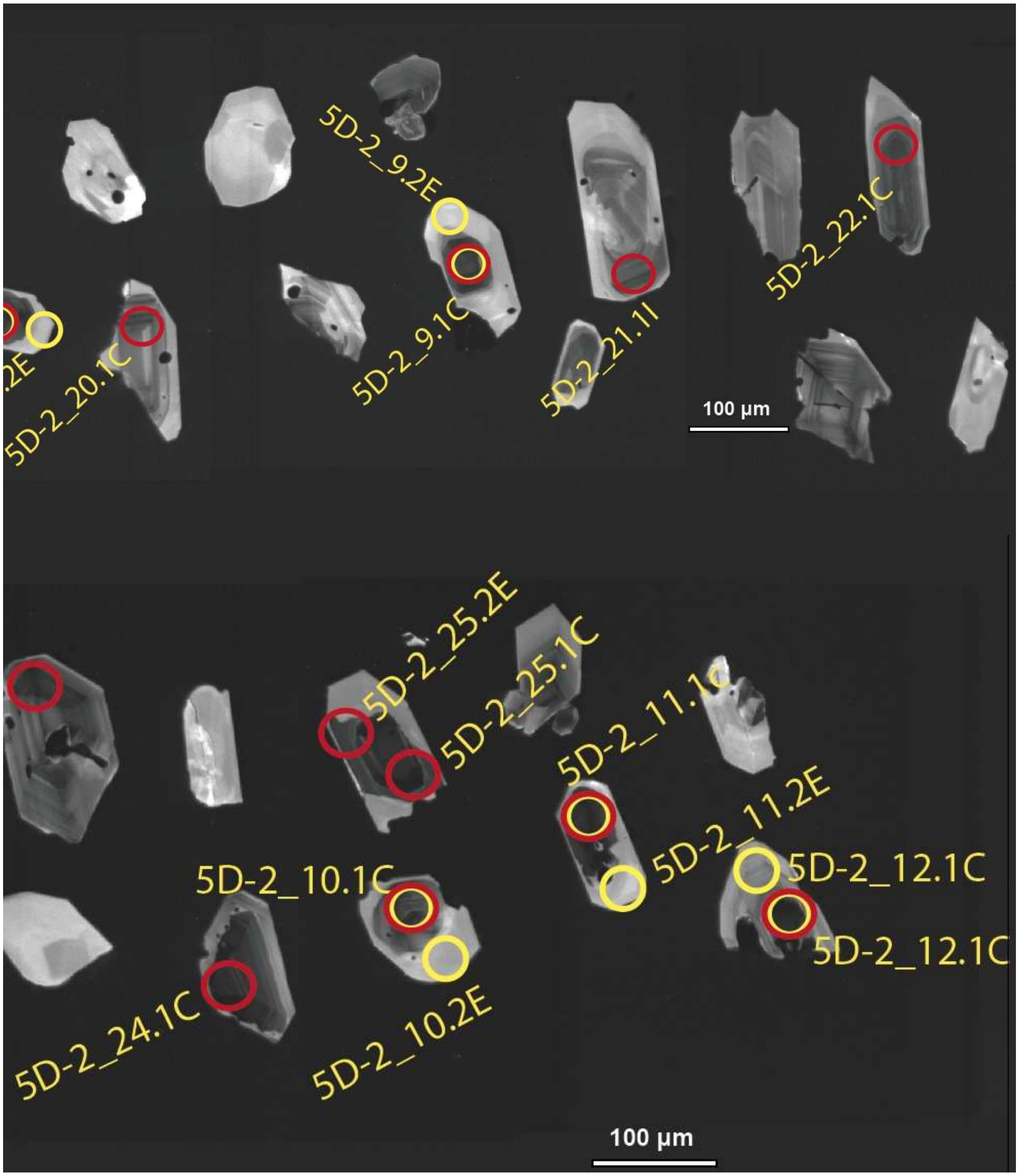

Figure D4. (continued)

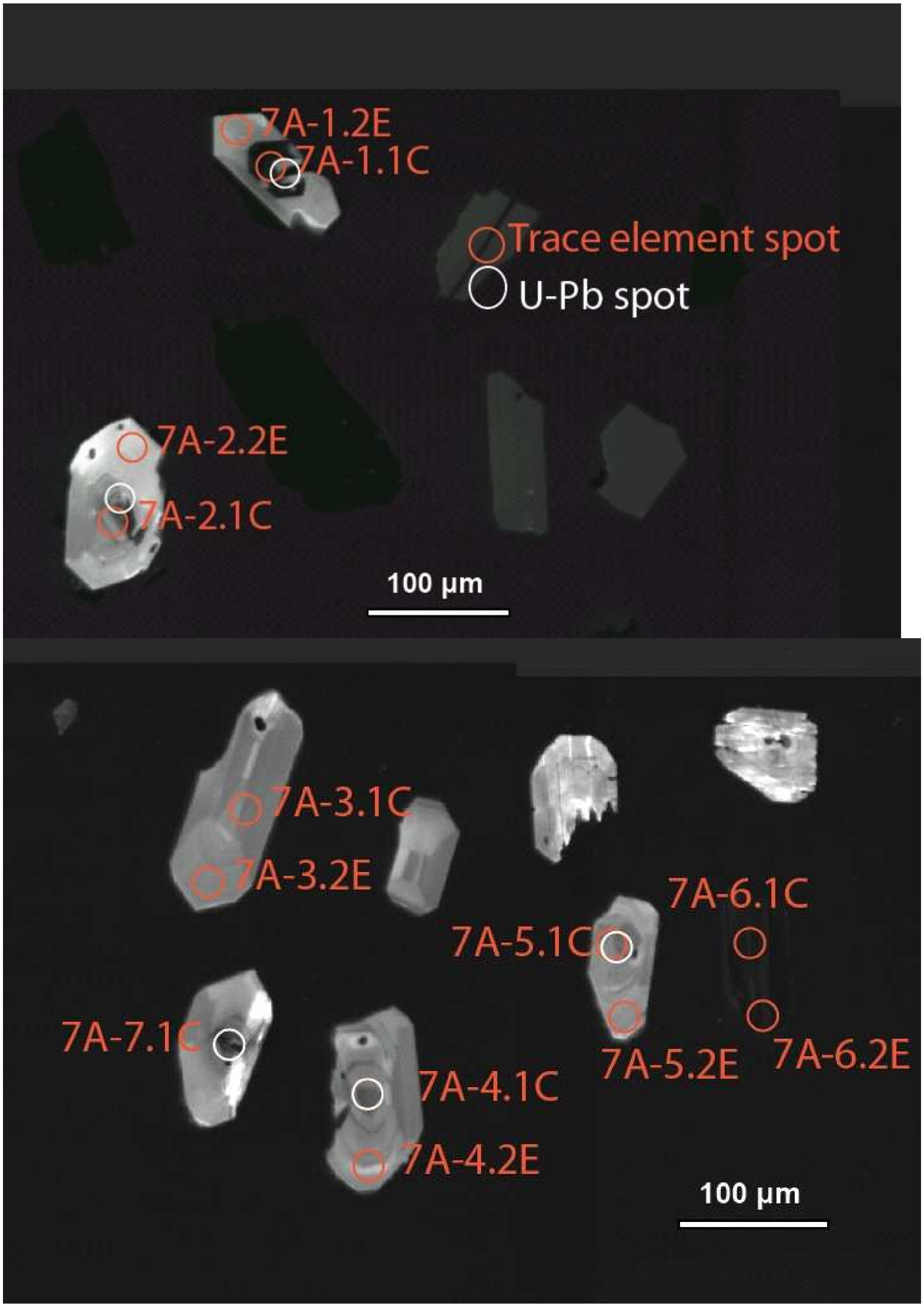

Figure D5. Cathodoluminescence mages from pumice sample 7a.

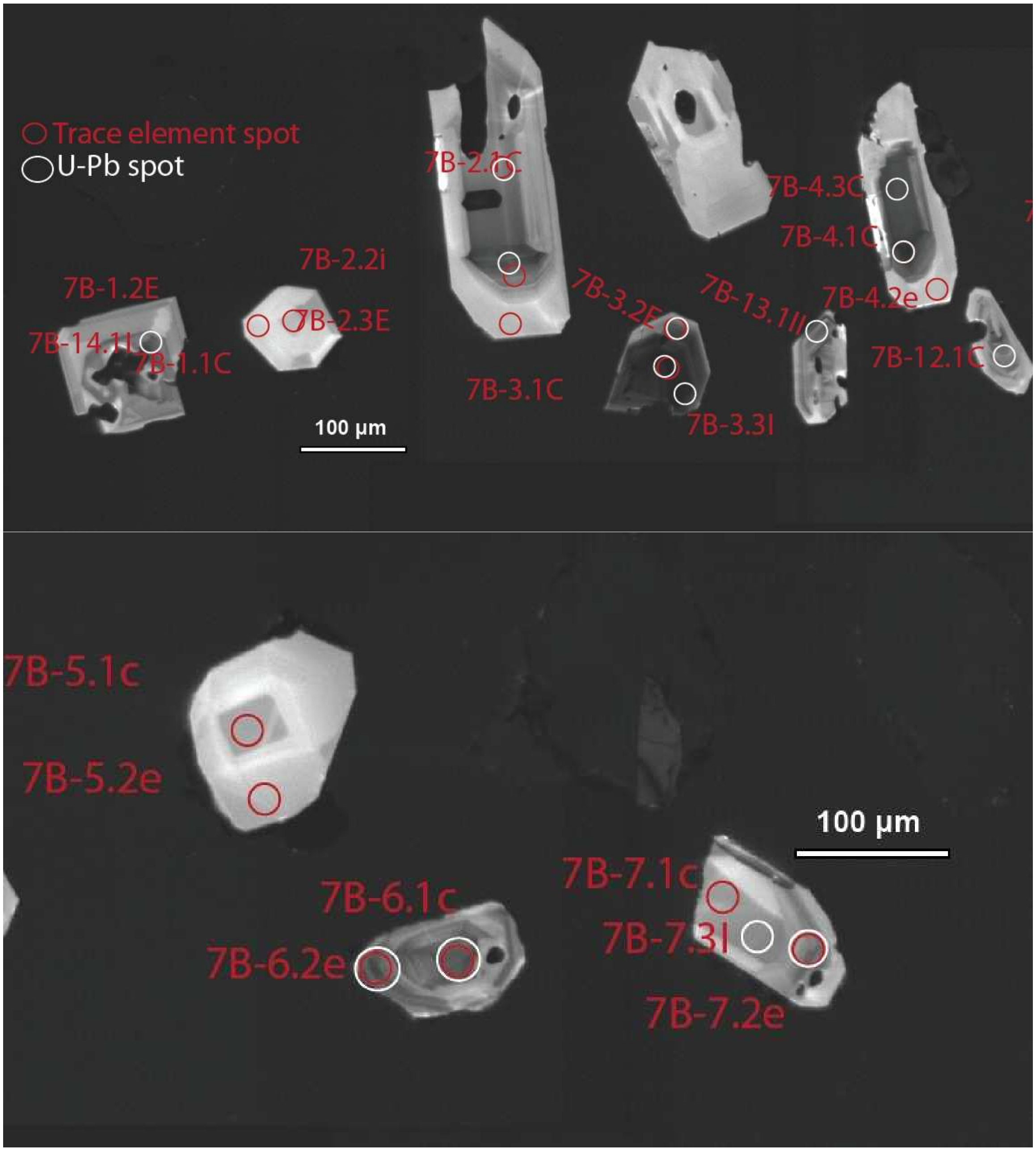

Figure D6. Cathodoluminescence mages from pumice sample 7b

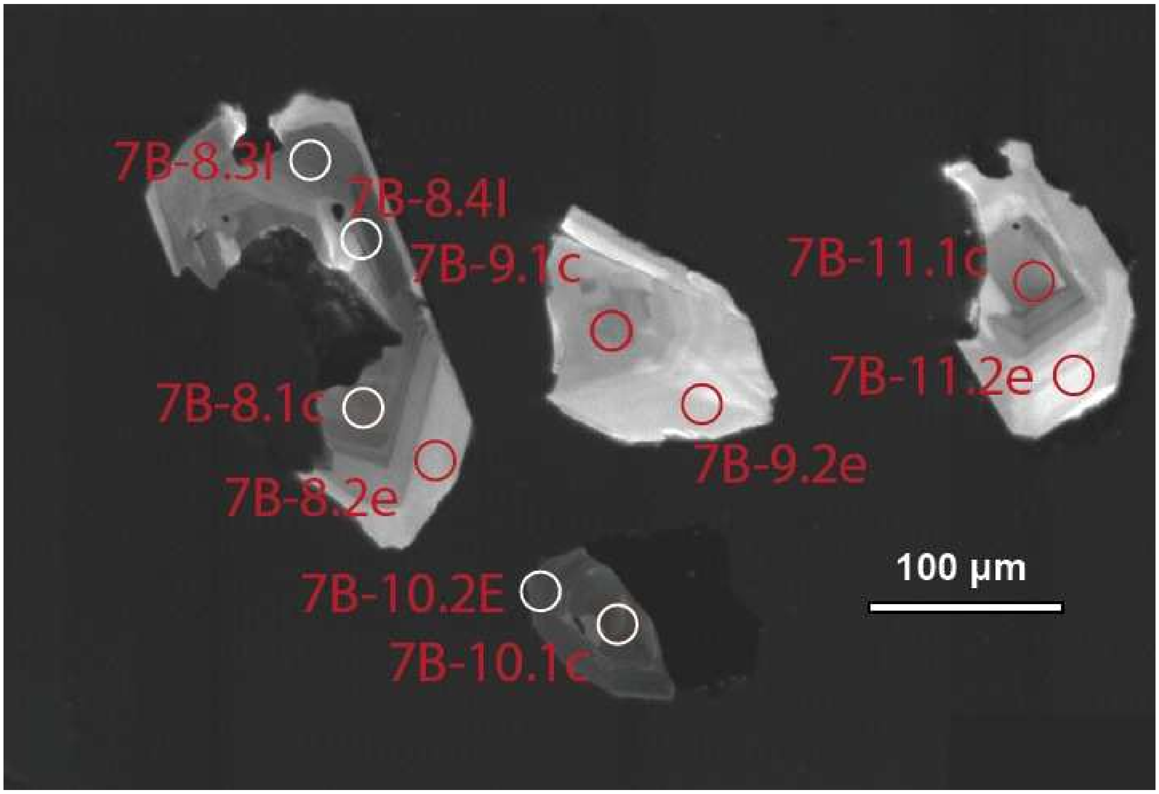

Figure D6. (continued)

APPENDIX E: PRE-CA SIMS MOUNT MAP AND ANALYSIS SPOT LOCATIONS

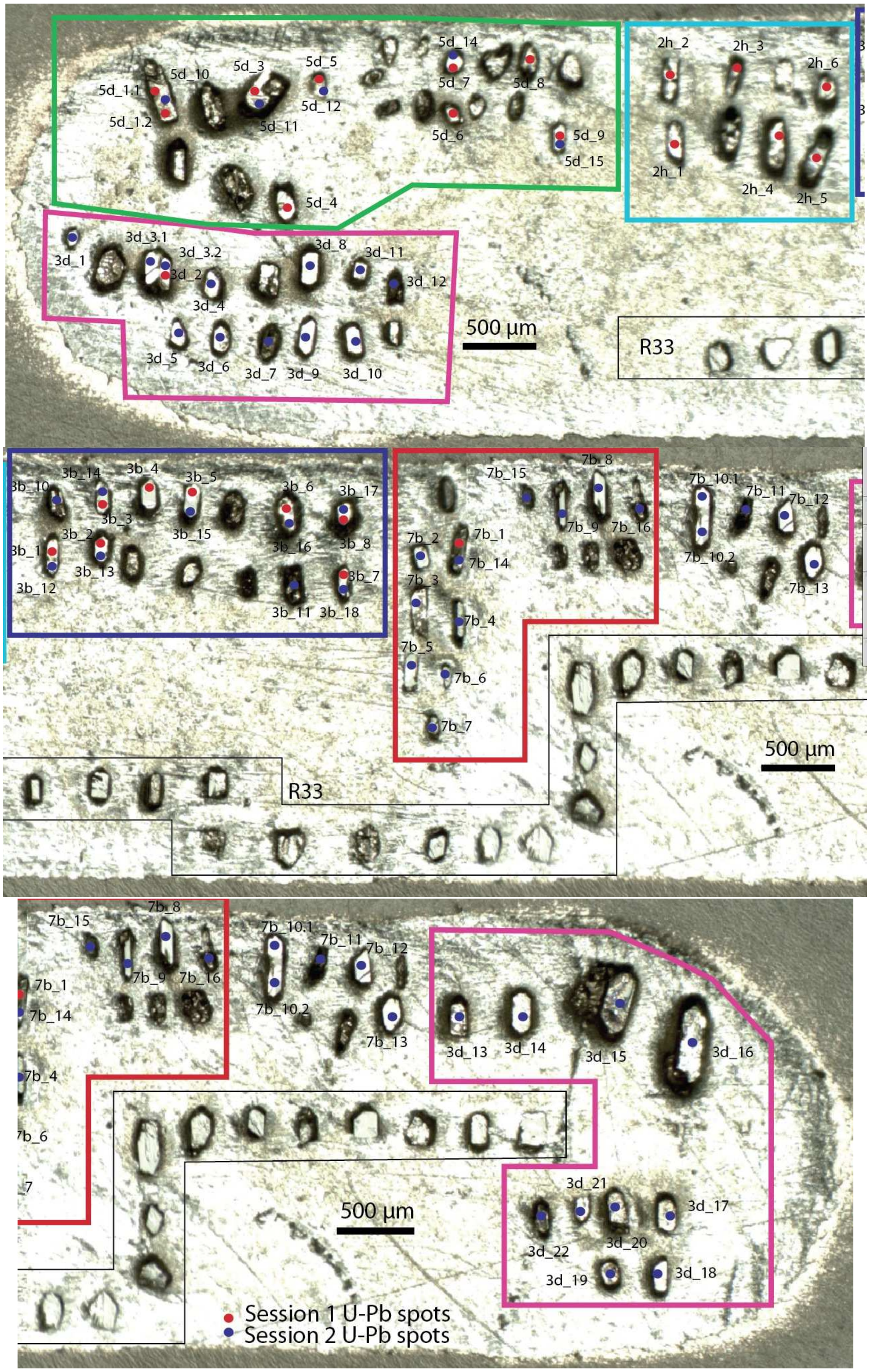

Figure E1. Pre-CA SIMS mount map and spot locations (mount# MLPT-3)

APPENDIX F: SECONDARY ELECTRON IMAGES OF CHEMICALLY ABRADED ZIRCON WITH ANALYZED CRYSTALS ANNOTATED

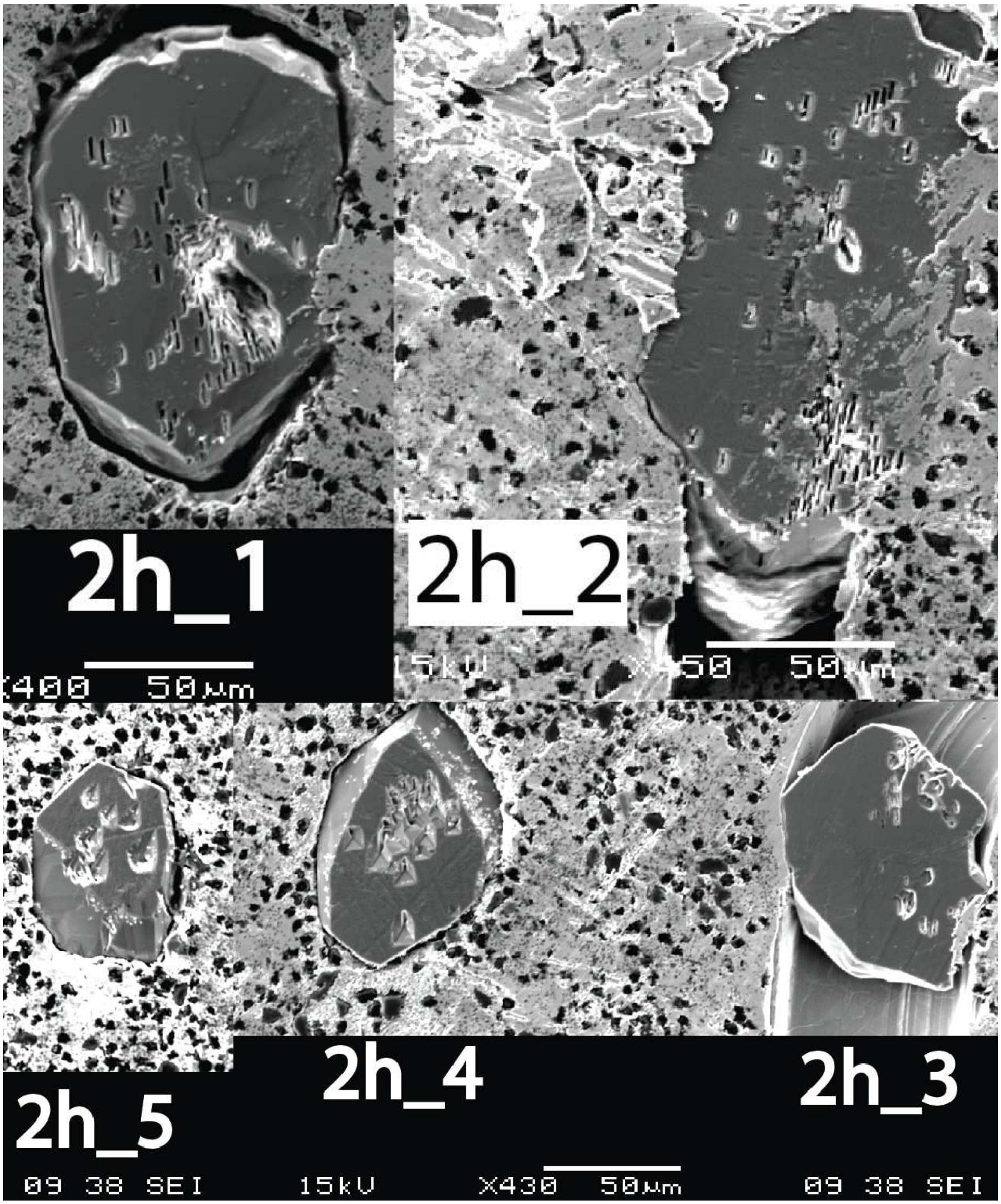

Figure F1. Secondary electron images of chemically abraded zircon from sample 2h.

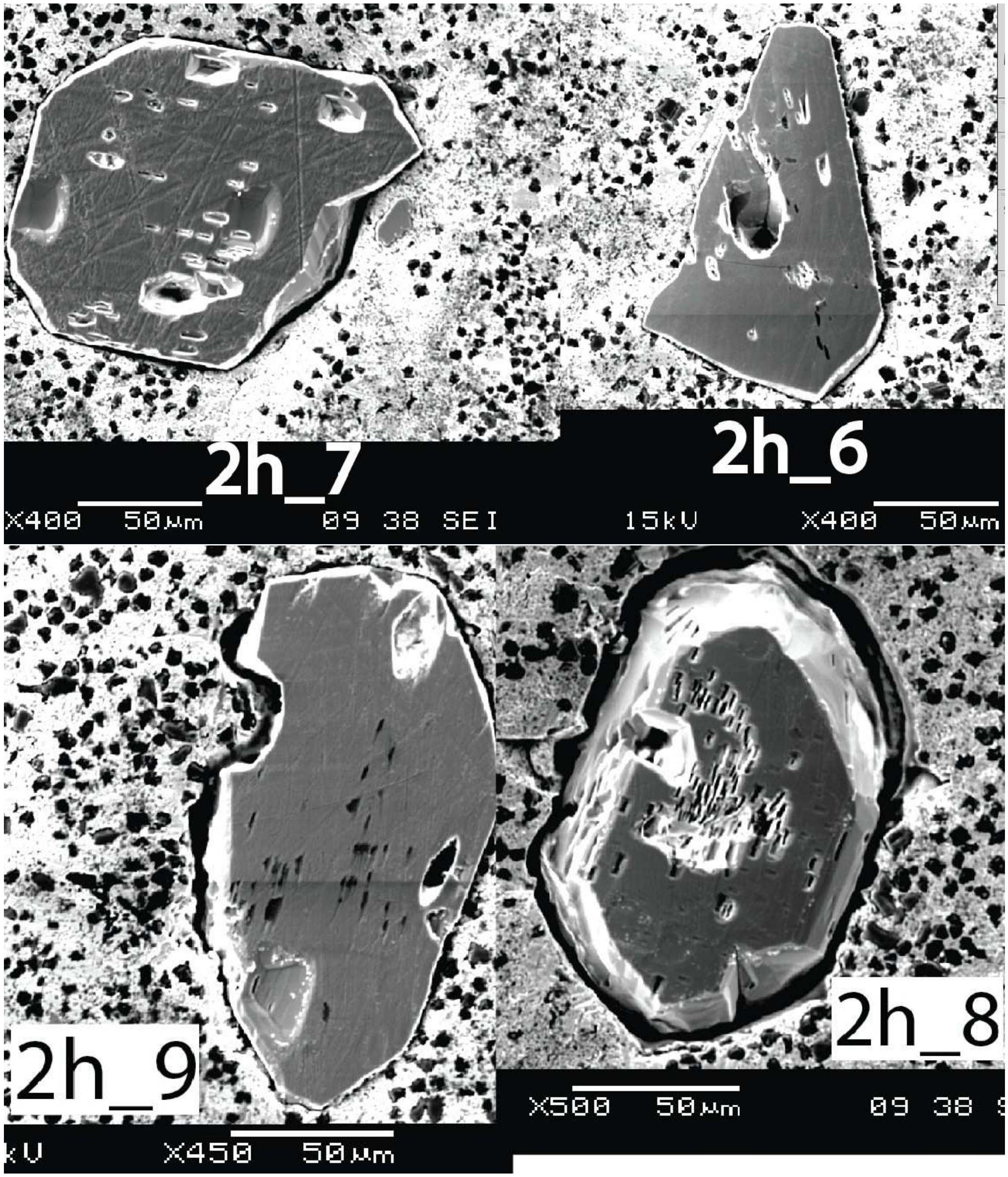

Figure F1. (continued)

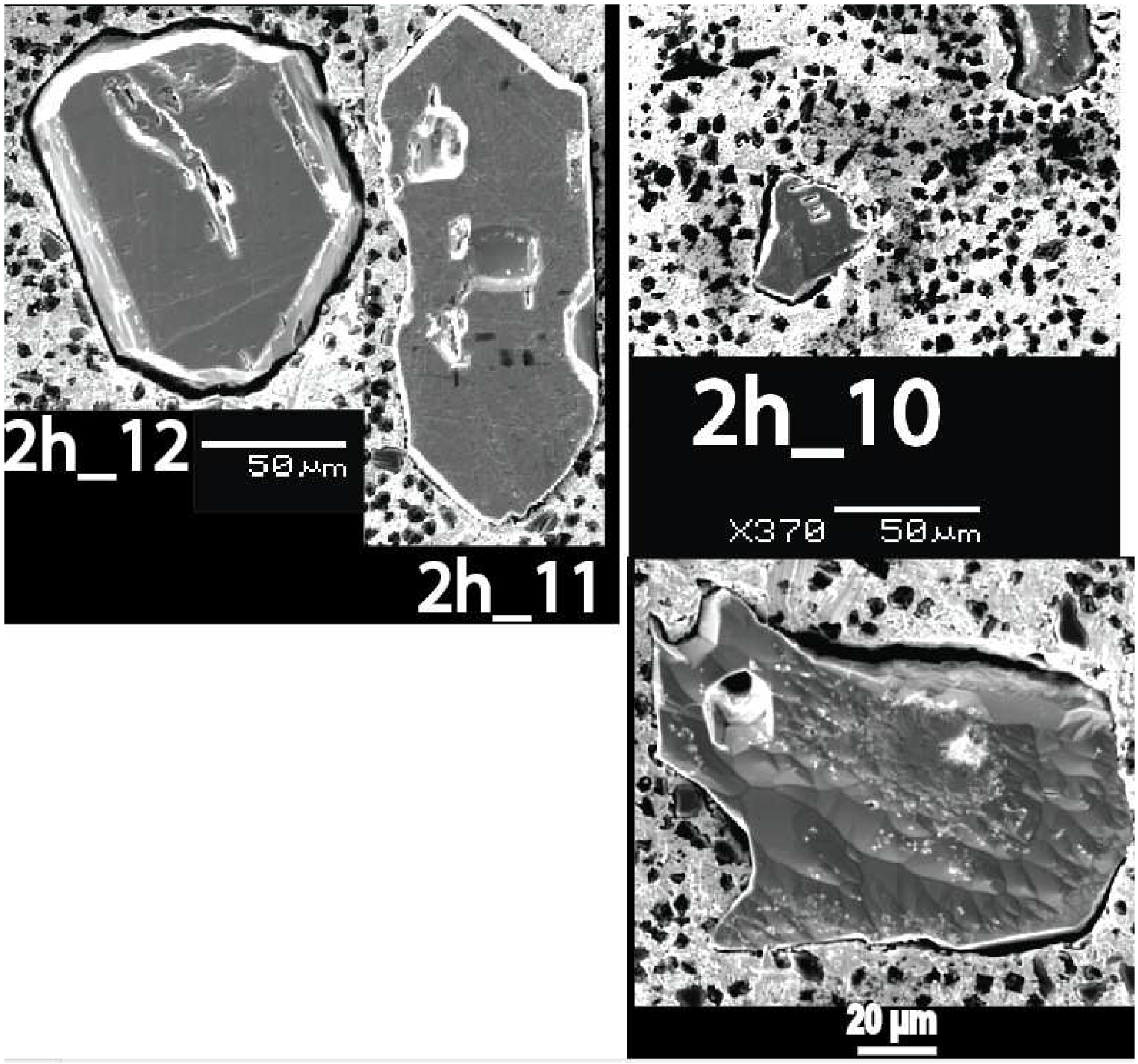

Figure F1. (continued)

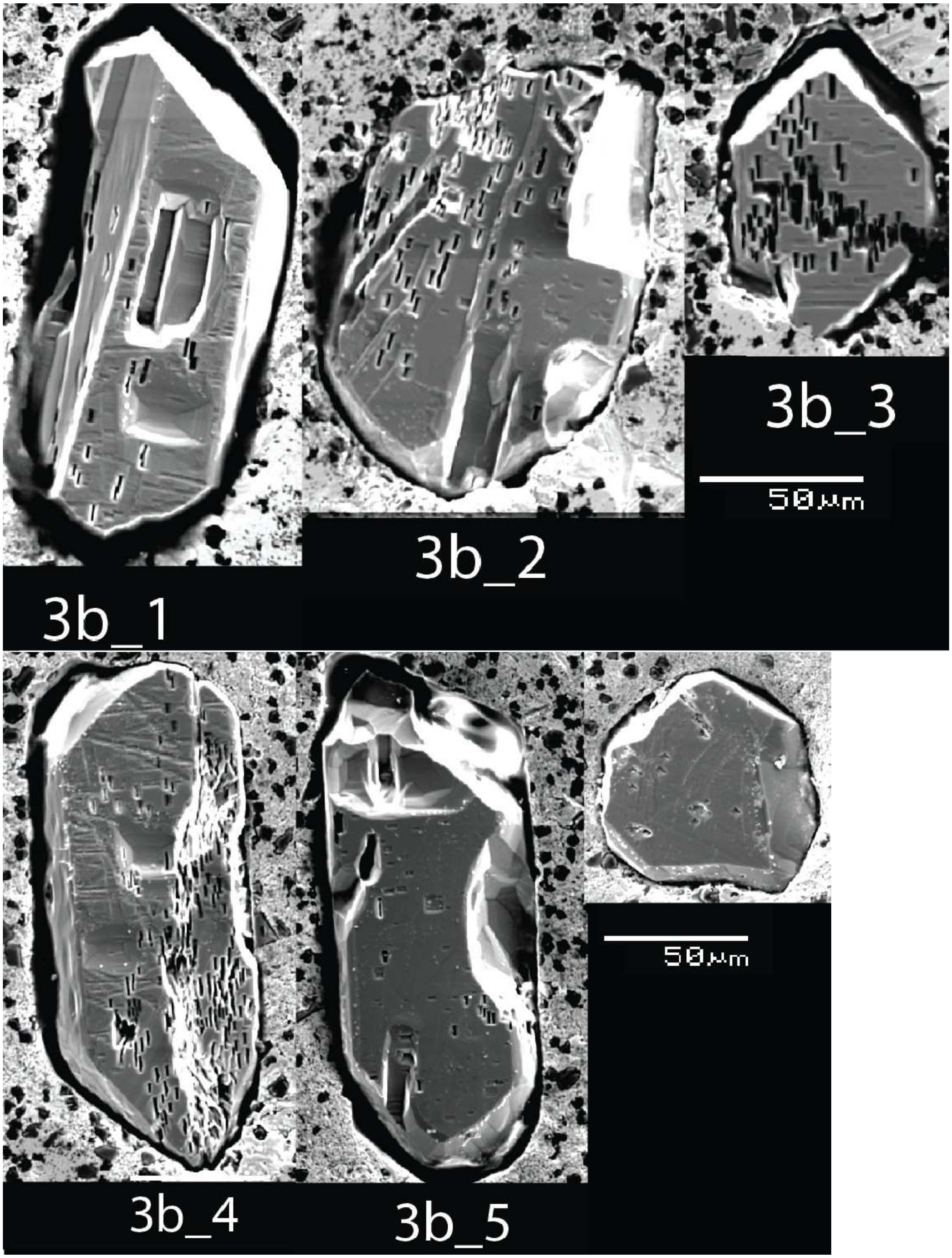

Figure F2. Secondary electron images of chemically abraded zircon from sample 3b.

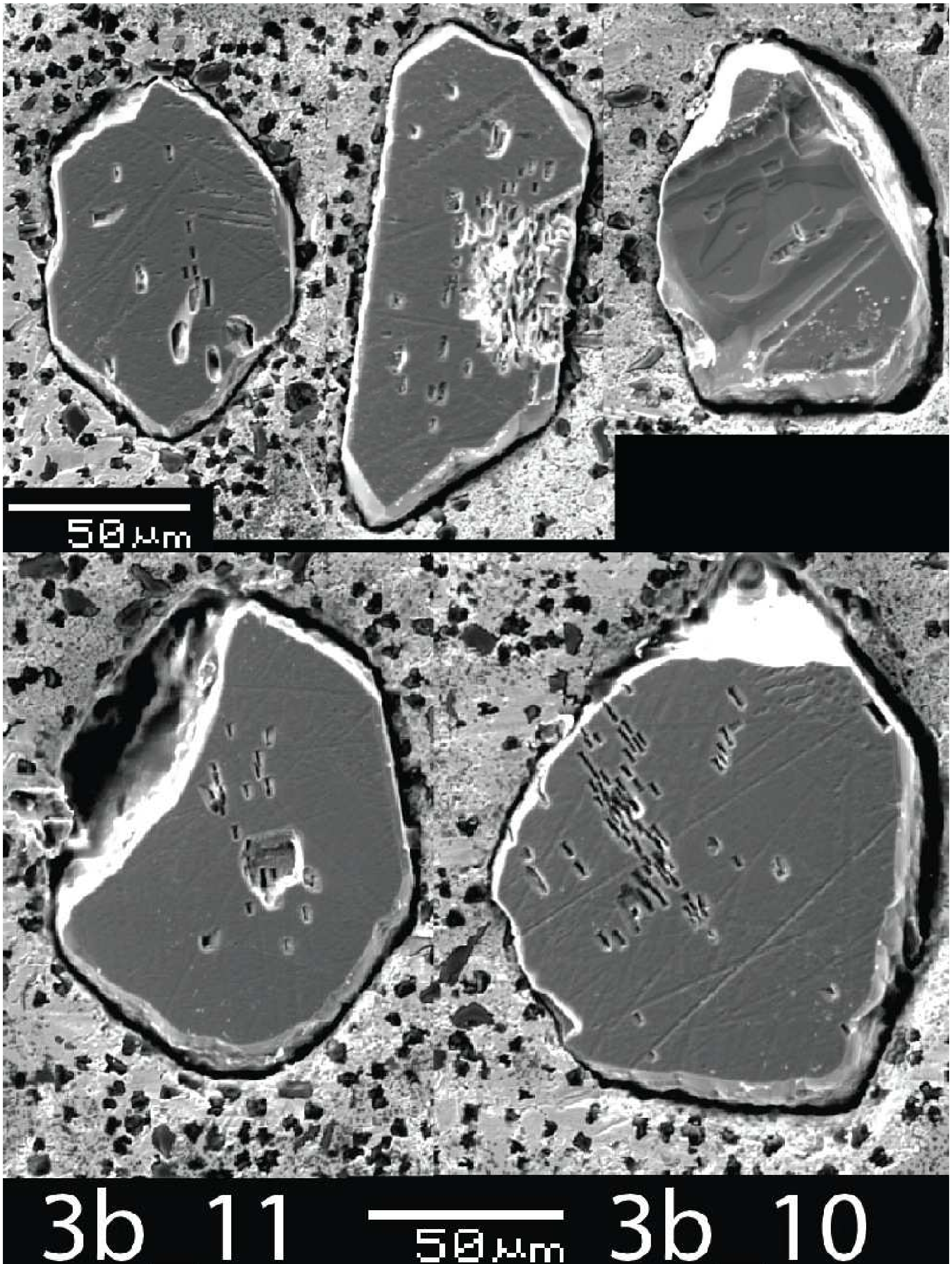

Figure F2. (continued)

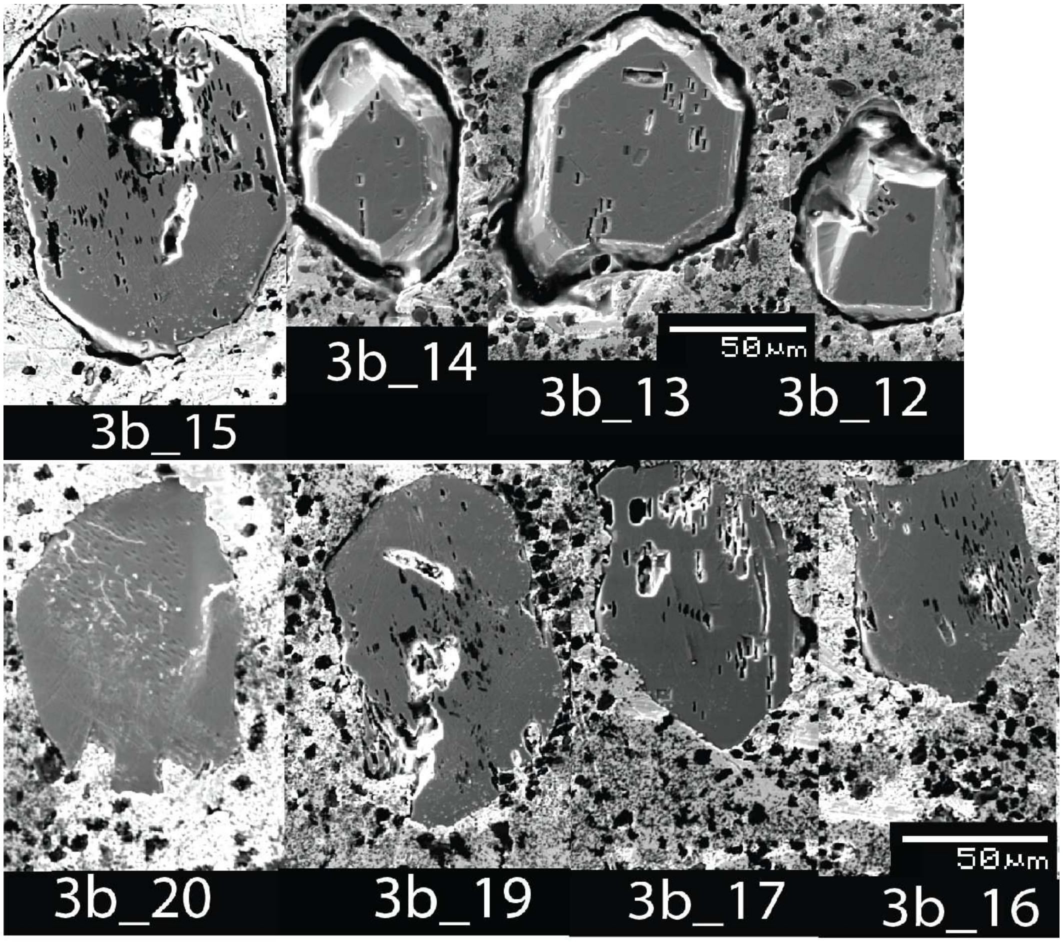

Figure F2. (continued)

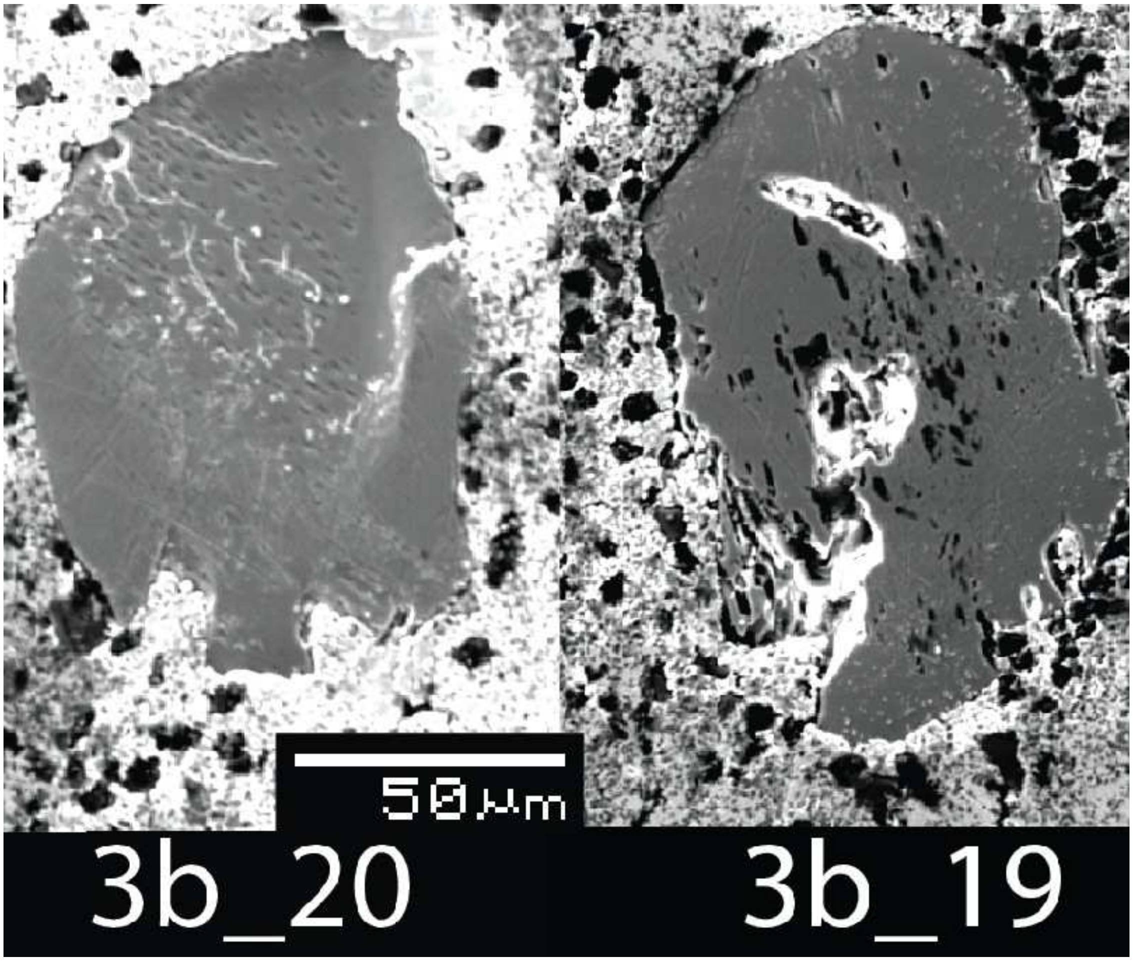

Figure F2. (continued)

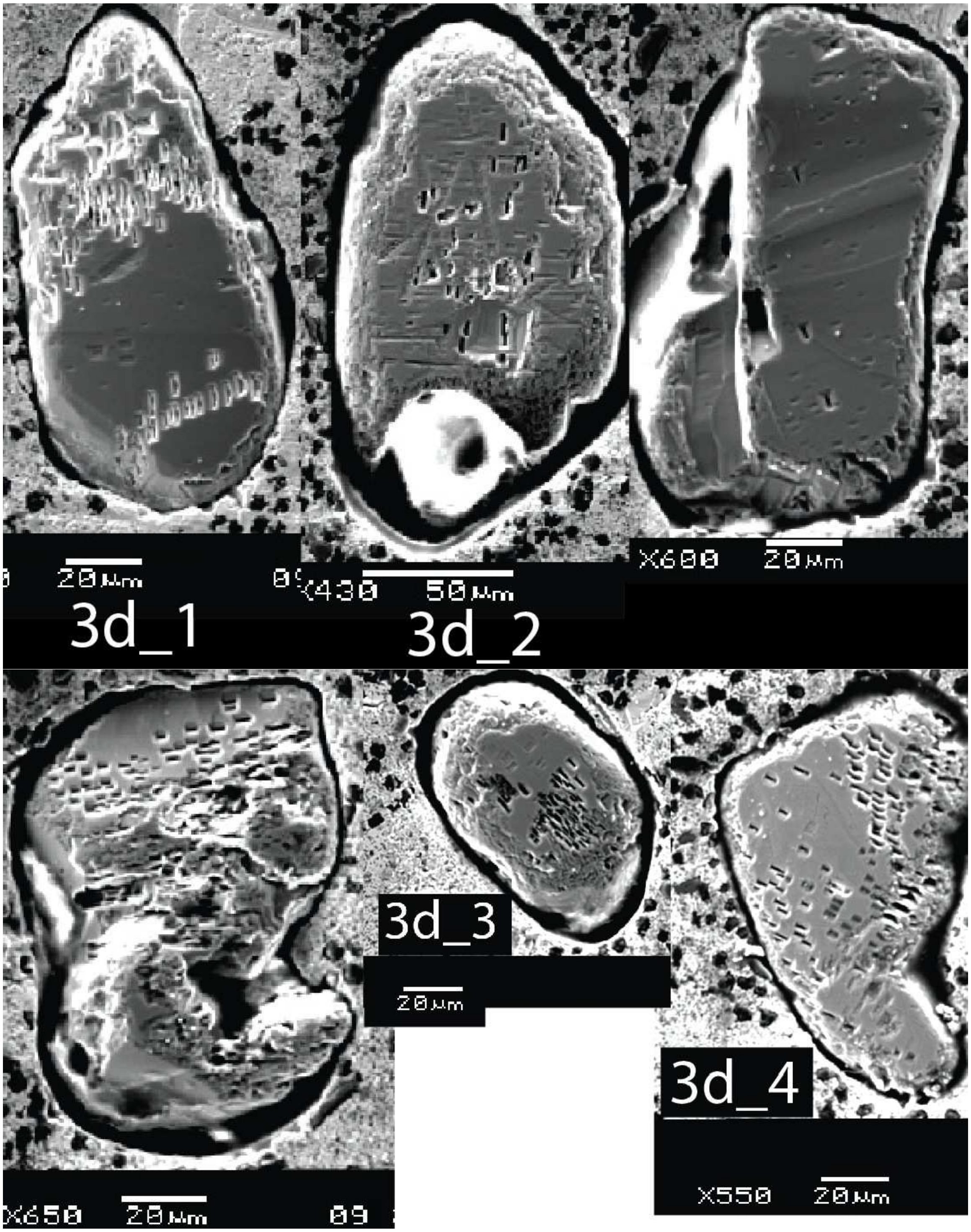

Figure F3. Secondary electron images of chemically abraded zircon from sample 3d.

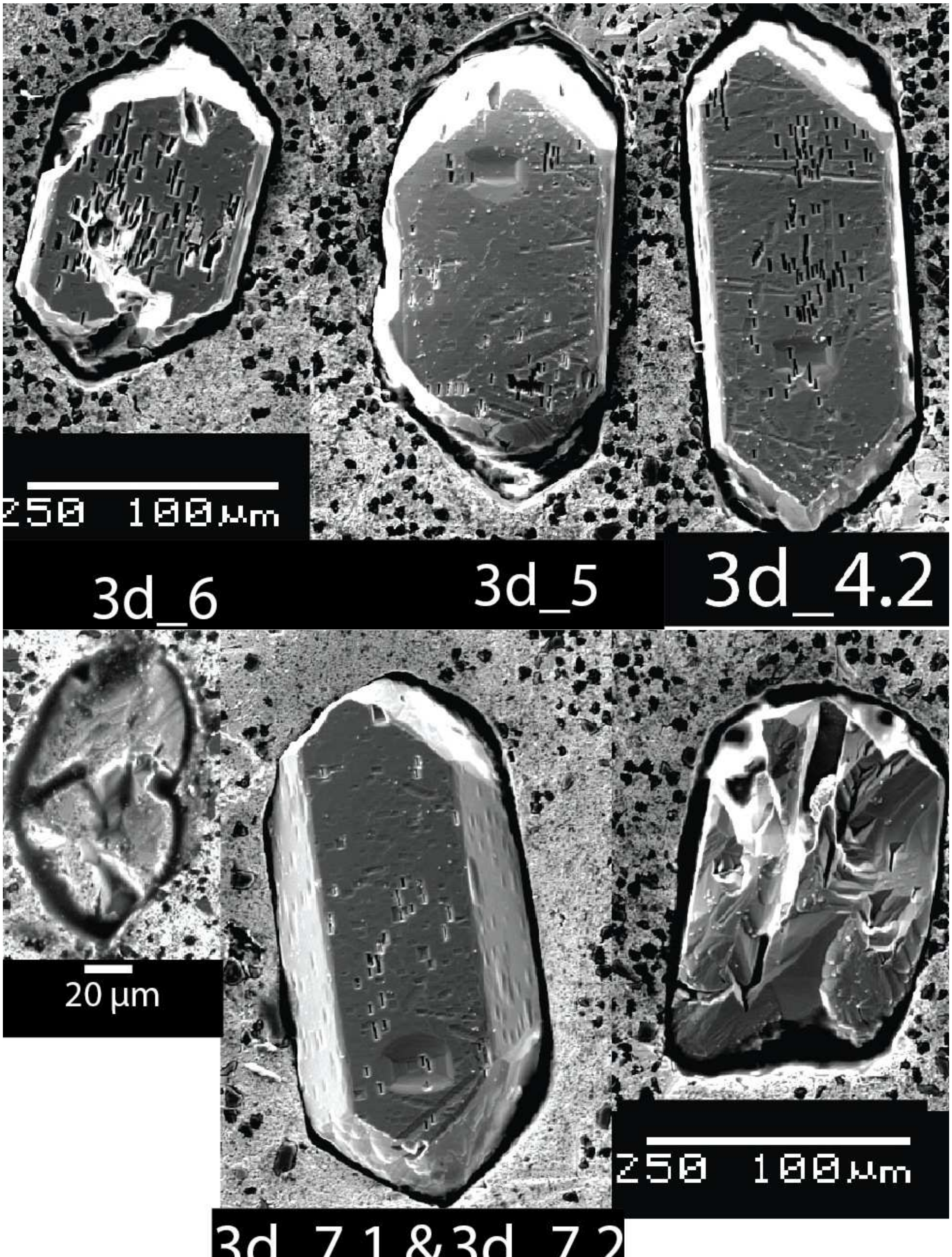

Figure F3. (continued)

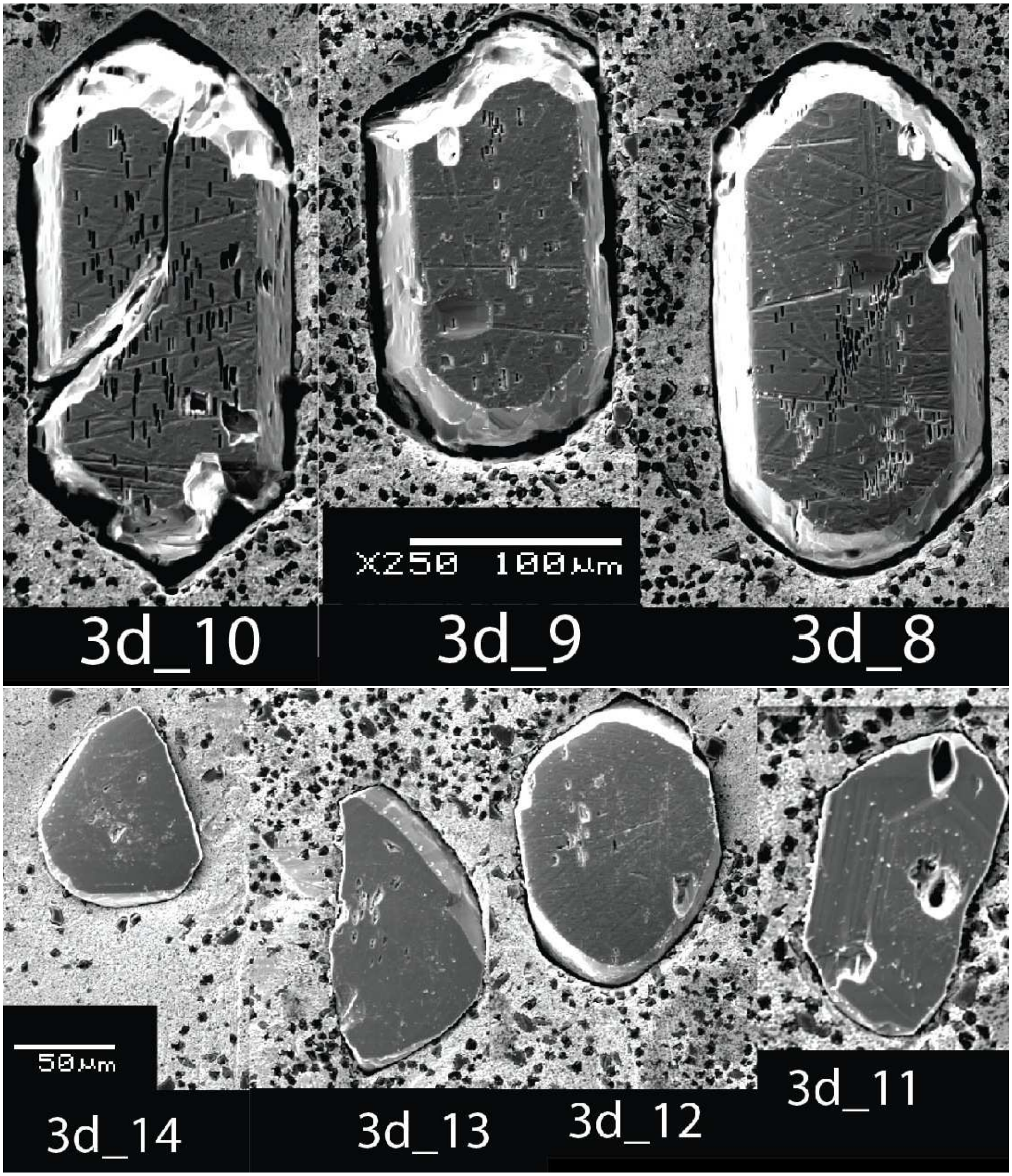

Figure F3. (continued)

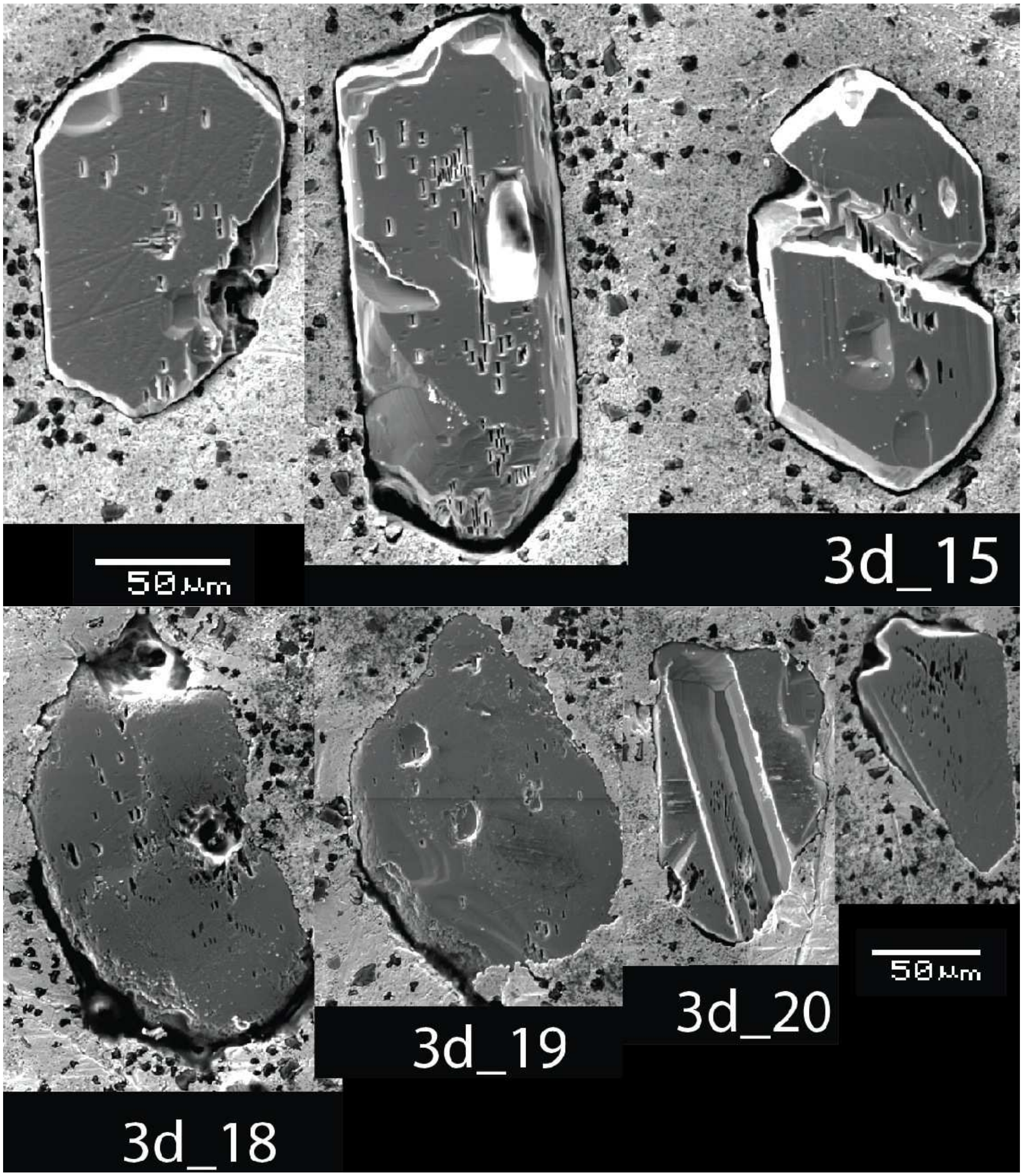

Figure F3. (continued)

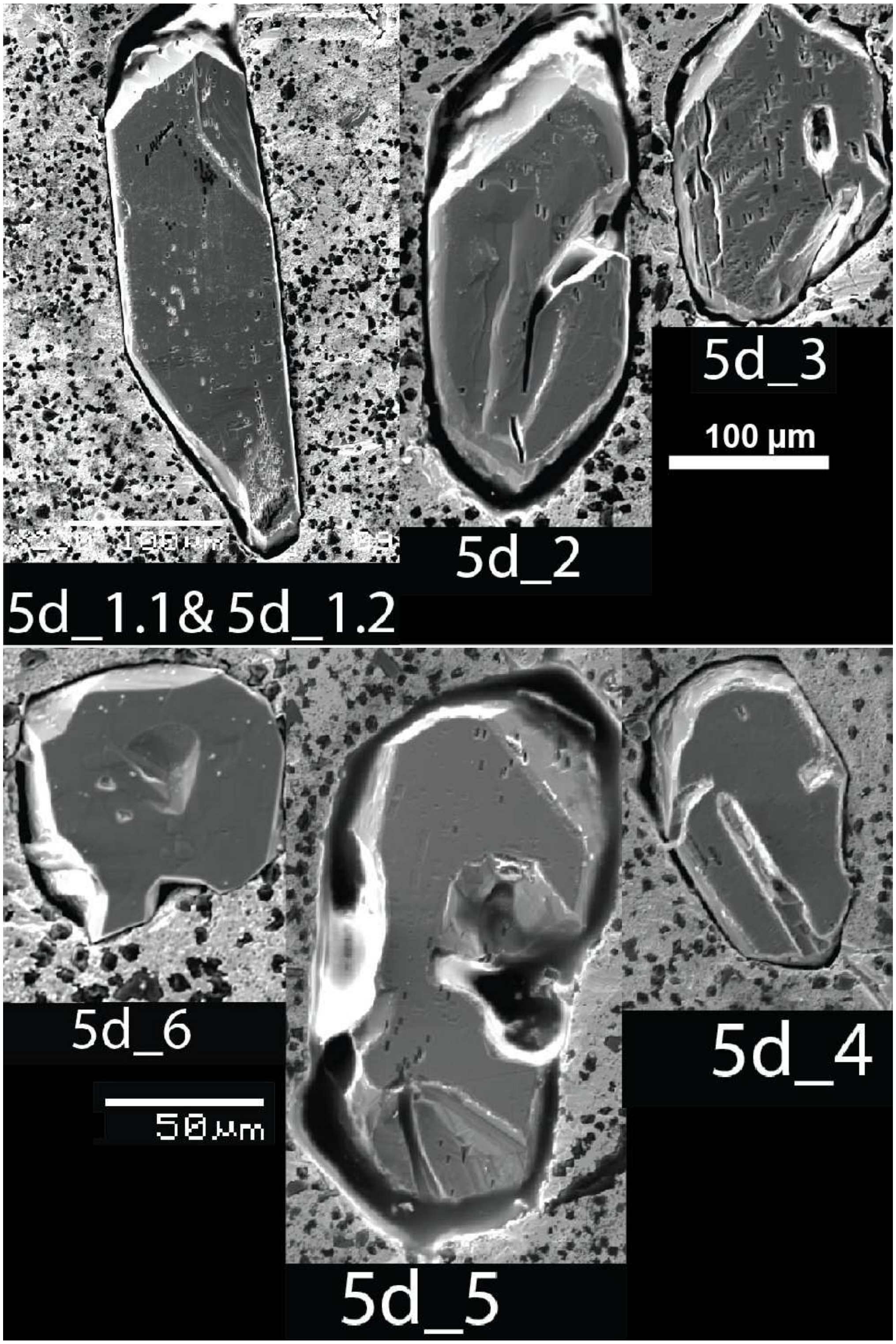

Figure F4. Secondary electron images of chemically abraded zircon from sample 5d.

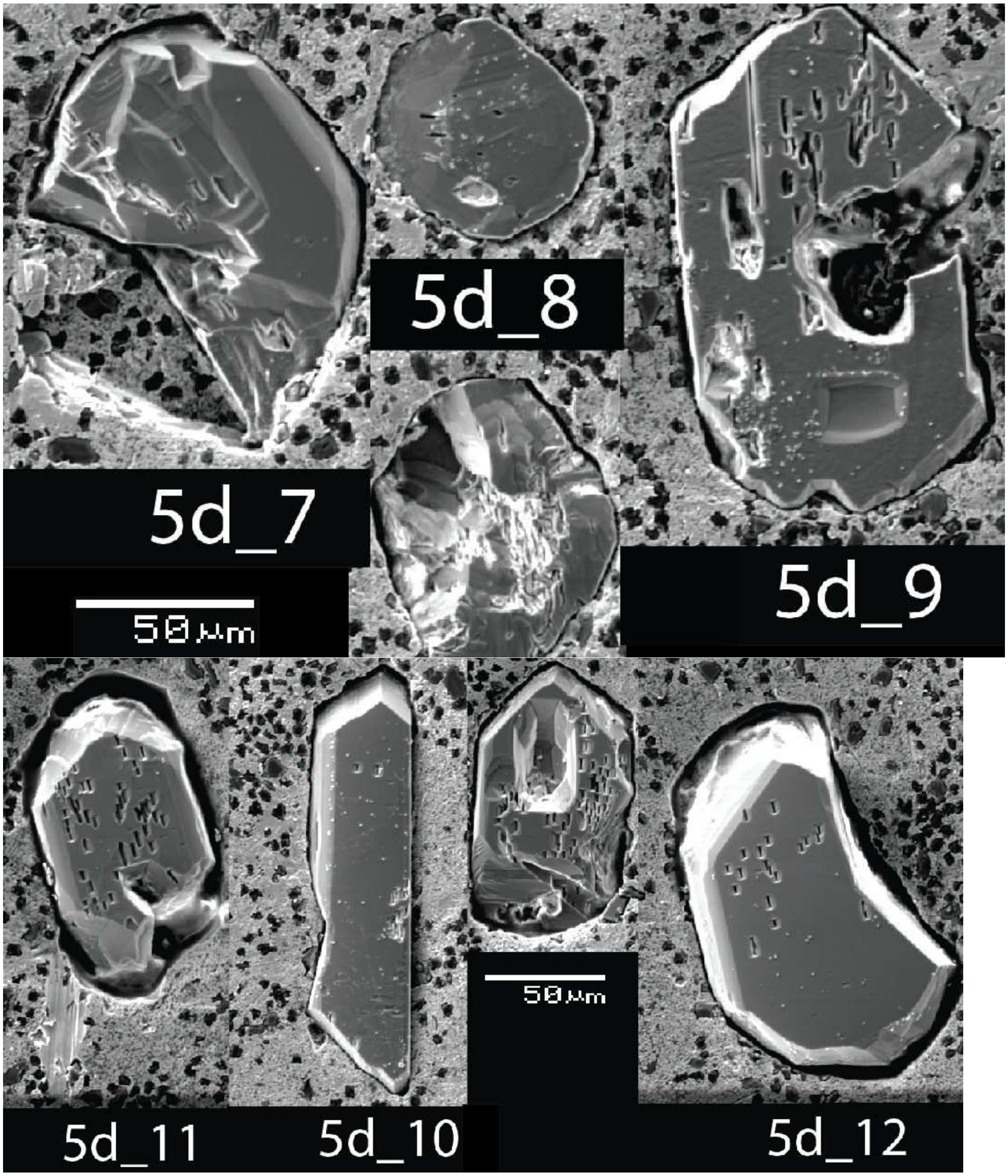

Figure F4. (continued)

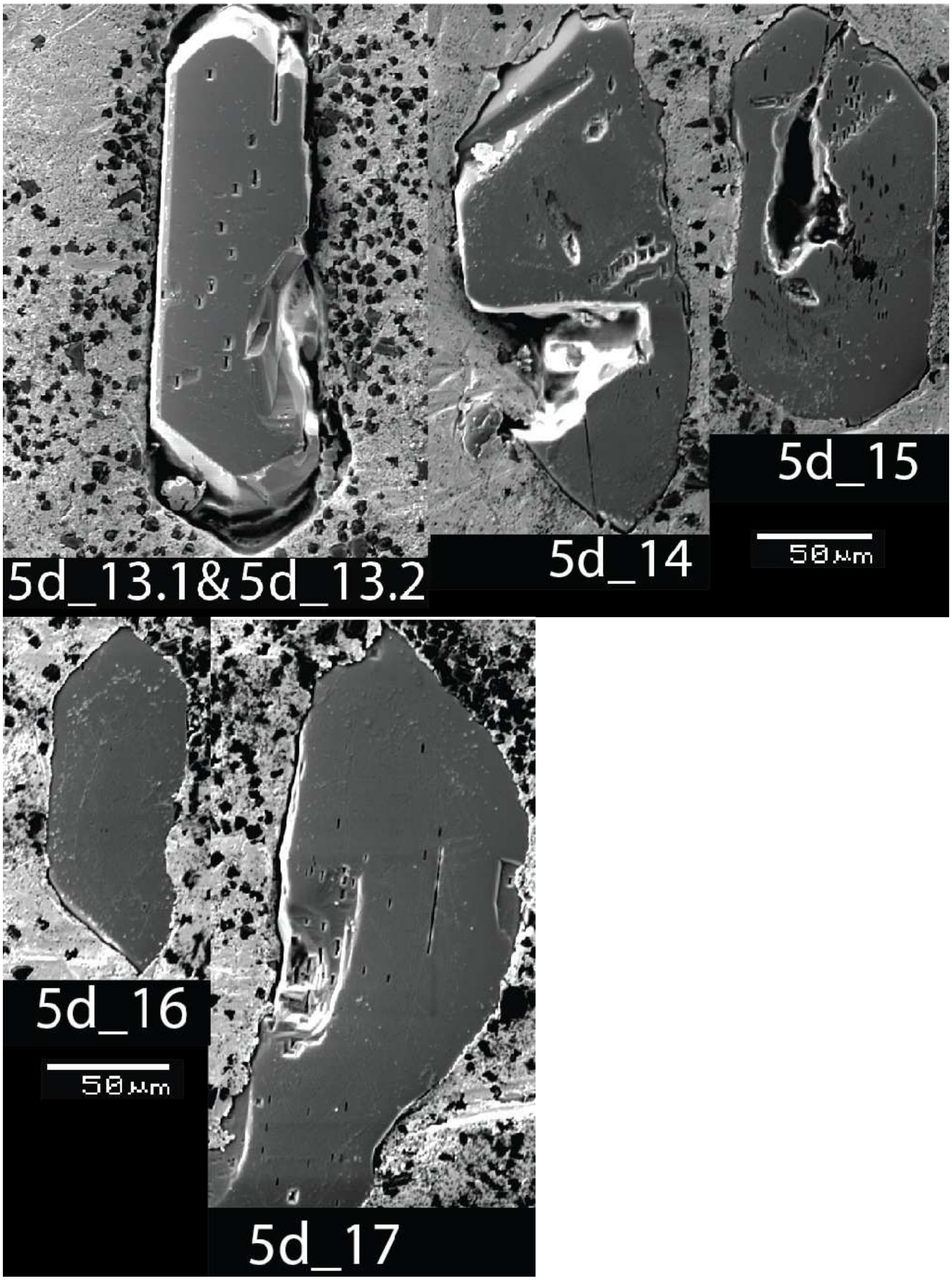

Figure F4. (continued)

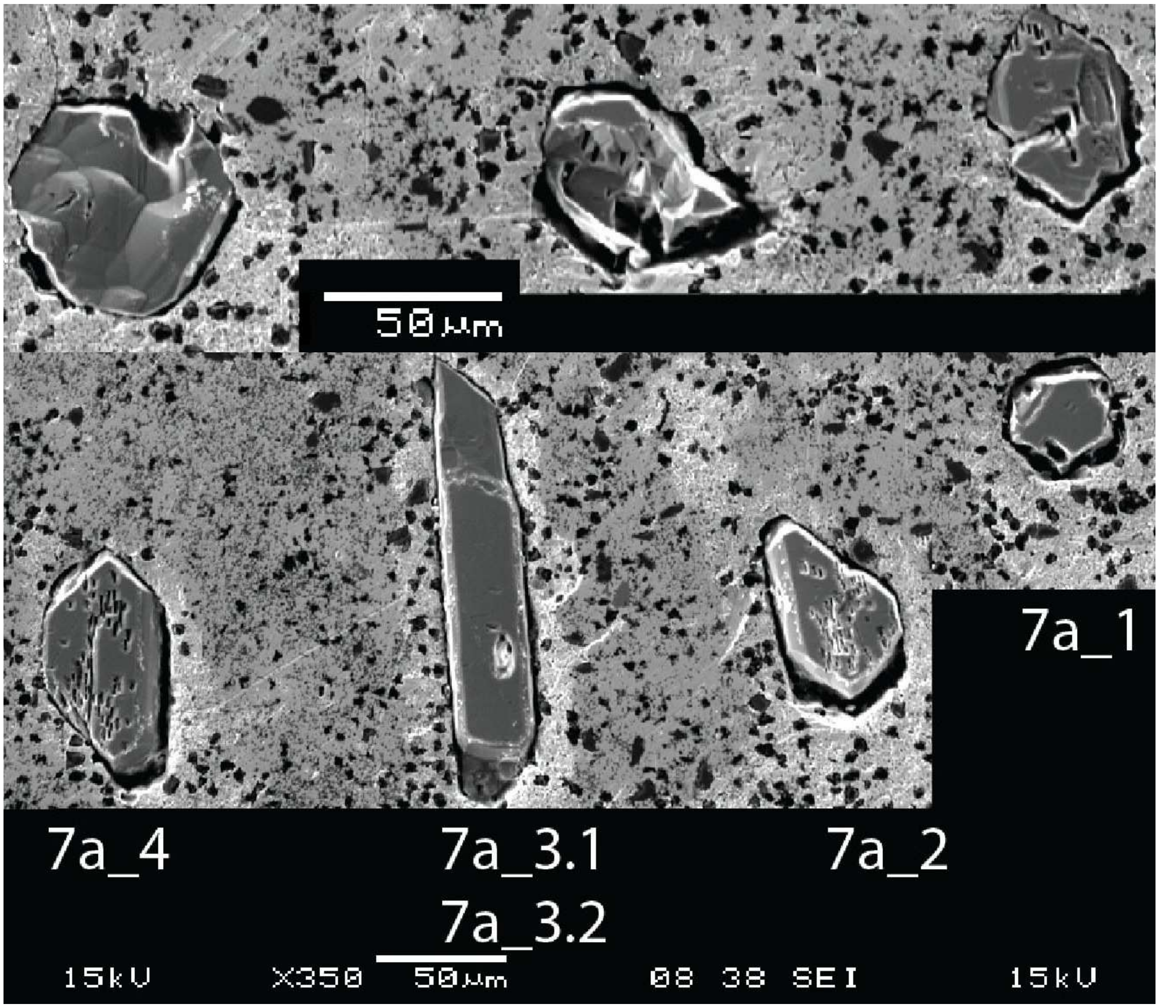

Figure F5. Secondary electron images of chemically abraded zircon from sample 7a.

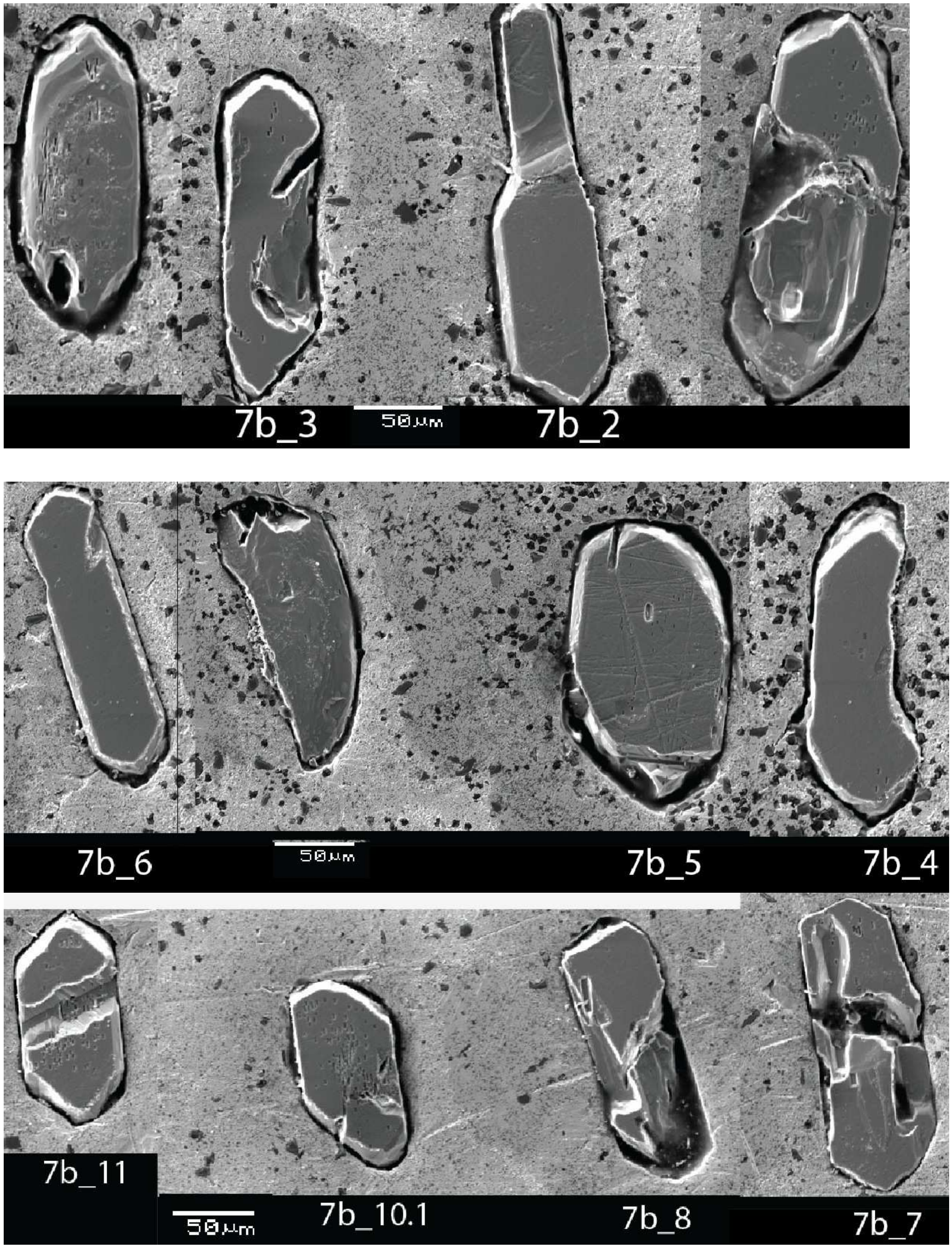

Figure F6. Secondary electron images of chemically abraded zircon from sample 7b.

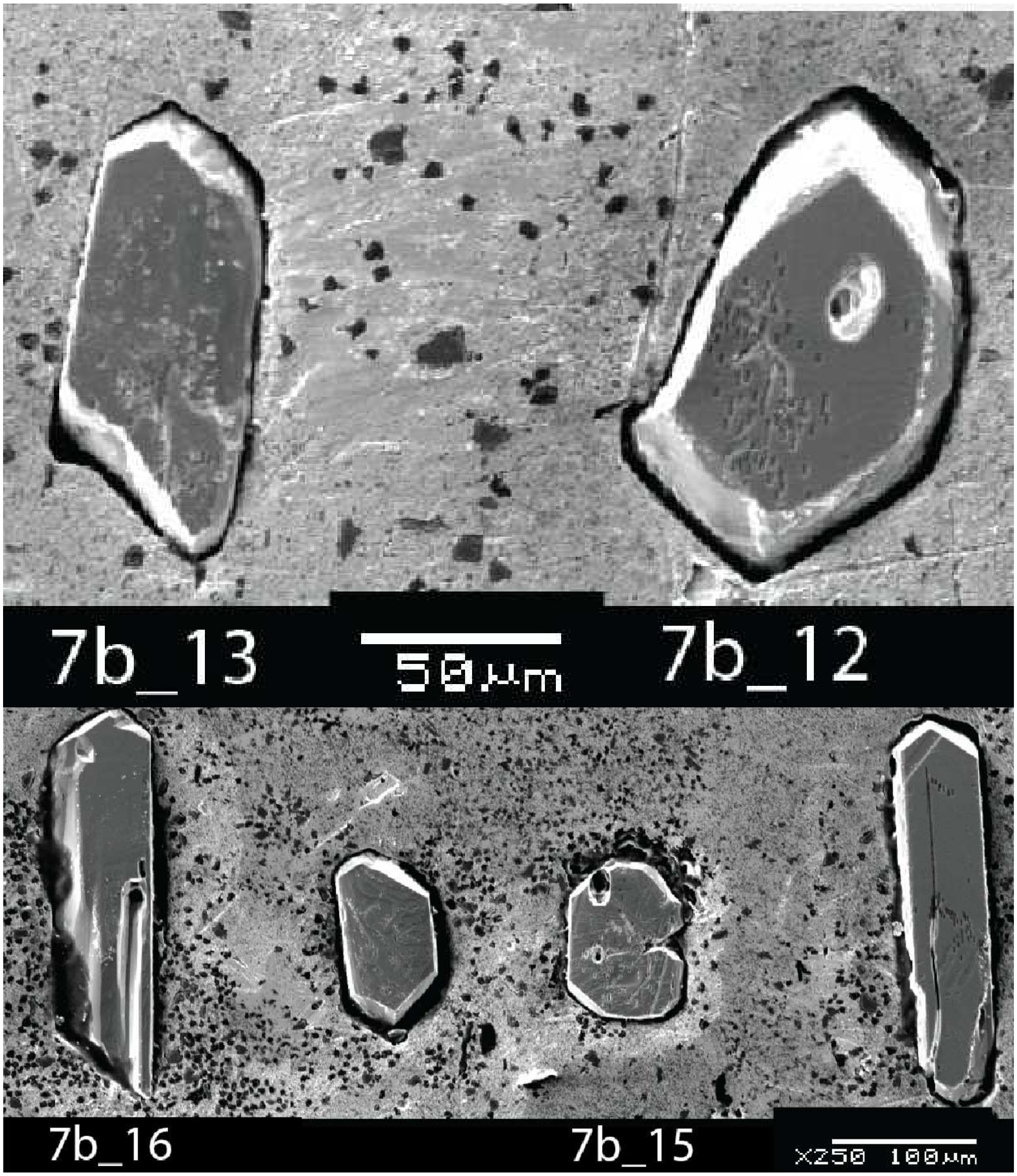

Figure F6. (continued)

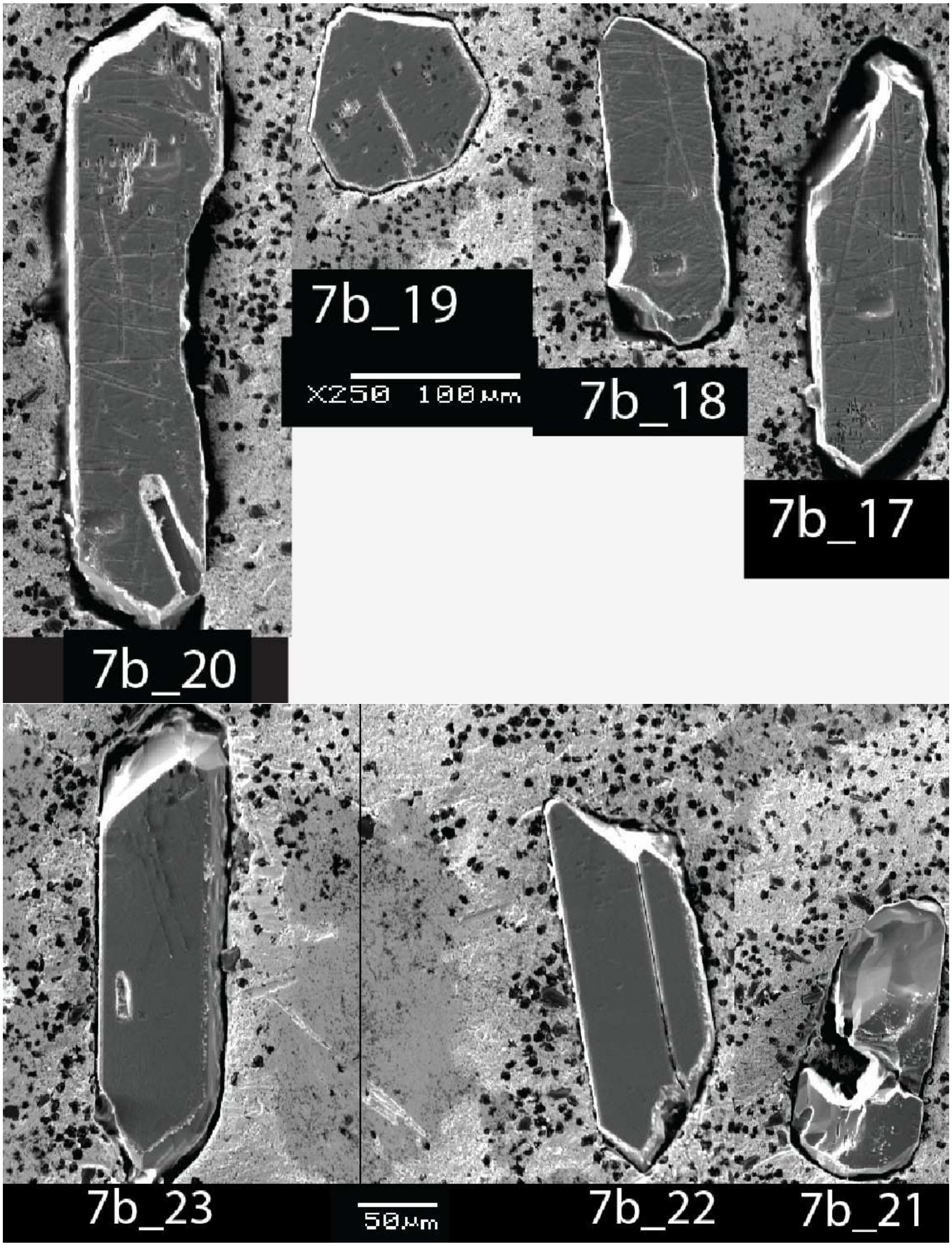

Figure F6. (continued)

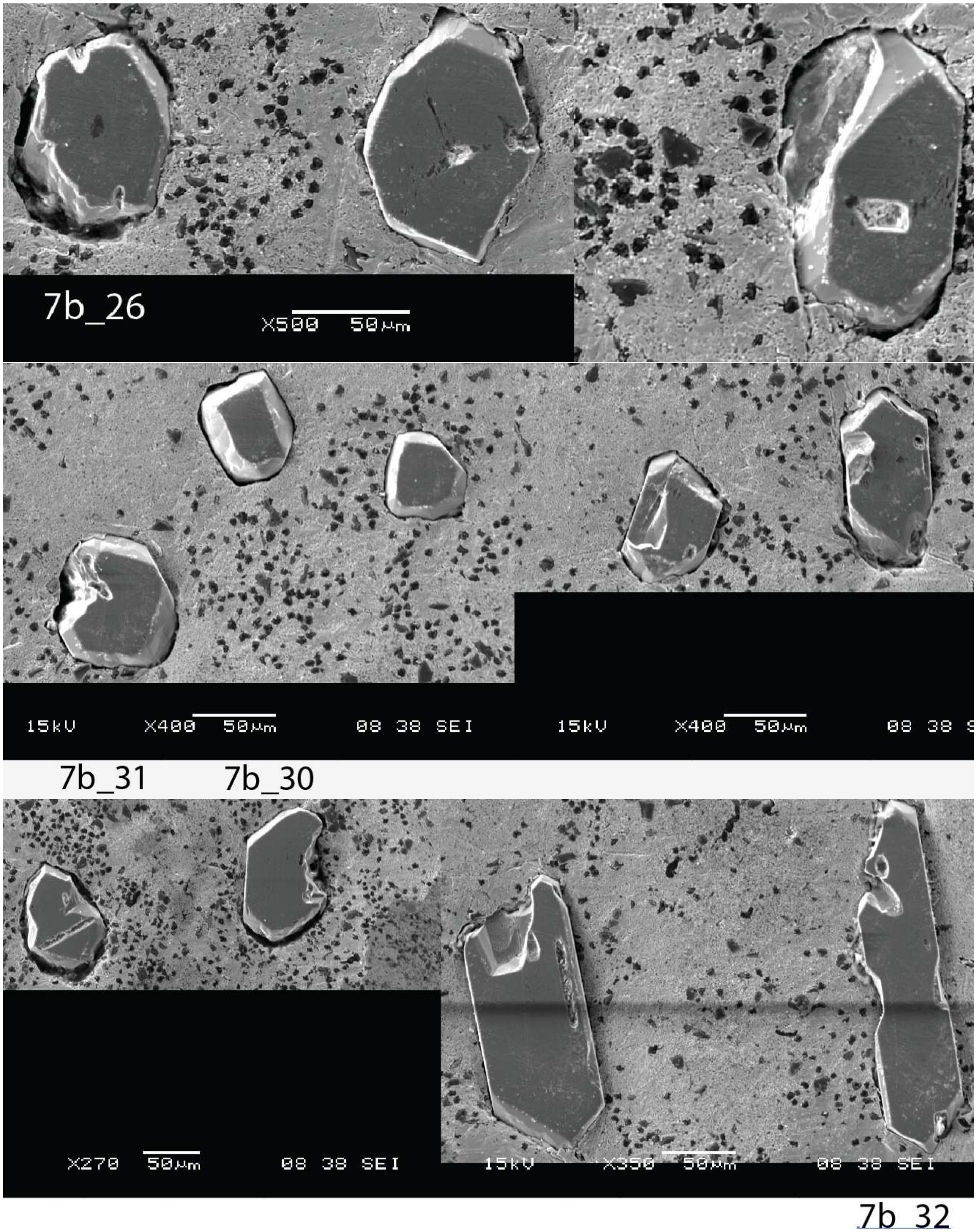

Figure F6. (continued)

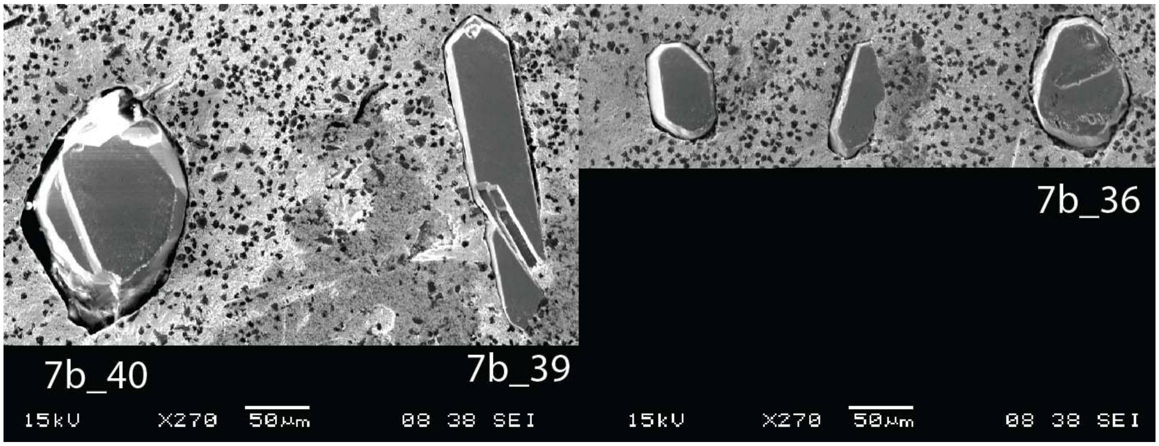

Figure F6. (continued)